CONTROL OF PORE STRUCTURE AND ACTIVITY OF PGM-ALUMINA EXHAUST CATALYSTS

Gerrit Coetzer, BSc., BSc.(Hons.), MSc.

Thesis submitted in fulfilment of the requirement for the degree Philosophiae Doctor to the Faculty of Engineering of the Potchefstroom University for Christian Higher Education.

Promotor: Prof J.C. Davidtz
Co-promotor: Dr P.J. Harris

Roodepoort
1995

ABSTRACT

Pore sizes in γ-alumina were controlled with additives (porogens) during formation of aluminium hydroxide. Porogens were active in the mesopore range with a sharply defined pore size distribution. Porogens that enhanced mesoporosity were diethylene glycol, glycerine, benzoic acid, ammonium tartrate and fatty acids/alcohol (stearic acid, palmitic acid and *cis*-oleic acid, oleyl alcohol, castor oil, olive oil and sunflower oil. These additives caused the formation of aggregates at the iso-electric point (pH 9) of aluminium hydroxide. Porogens that increased microporosity were tartaric acid, sebacic acid, lactic acid, citric acid and formic acid, 2-butanol, *n*-hexanol, propanol, 2-pentanol, ammonium formate and ammonium citrate. Pore sizes in the microporosity region were affected by alumina crystallite sizes, which, in turn, were determined by the inhibition effect of strong chelating agents on crystallite growth. Macroporosities were introduced by filler or spacer effects of additives, such as adipic acid, tartaric acid and fatty acids/alcohol, as well as ammonium tartrate and ammonium carbonate. All additives produced cylindrical-shaped pores, except fatty acids which produced ink-bottle pores.

Emulsified *cis*-oleic acid produced higher total pore, mesopore and macropore volumes as well as surface area, but smaller pore sizes than commercial alumina powder, which is being used in the automotive exhaust catalyst industry.

Sintering studies indicated that ceria (11 weight per cent) only stabilised the control samples to a certain degree, but it had no effect on fatty acid-derived alumina samples. Ceria crystallites sintered preferentially compared to γ-alumina, but it prevented the formation of θ-alumina during sintering at 1000 °C.

Two distinctive regions were observed when Knudsen effective diffusivity (KED (D^0)) (Carniglia adsorption method) and KED values were plotted as a function of tortuosity factor (TF). These were assigned to cylindrical (TF < 2.00 and KED (D^0) > 0.200 cm^2/s) and non-cylindrical (TF > 2.00) pores.

Uniform spherical spray-dried alumina powders were prepared from *cis*-oleic acid - aluminium hydroxide gel (COADA) after ageing of the hydroxide, flocculation and dispersion of the gel. This active, high surface area γ-alumina was applied as wash coat layers on monolithic cordierite supports. Factors such as purity of *cis*-oleic acid, milling time, peptisation (acetic acid), steam treatment and ceria amount (3 weight per cent and 11 weight per cent added or 3 weight per cent built into the structure of alumina prior to spray-drying) affected the properties of alumina spray-dried powders and wash coat layers. These also affected cracking and attrition resistance of wash coat layers. Coating of monoliths was facilitated by a charge neutralisation at the interface between monoliths and the alumina wash coat slurry at pH 3.

Activity evaluation of platinum impregnated catalysts showed that inhibition of the carbon monoxide oxidation reaction occurred in the temperature range between 68 to 150 °C depending on the catalyst.

Diffusion and effectiveness factors were determined for catalysts to ensure that intrinsic kinetics were measured. Effectiveness factors of unity (based on adsorption data) were obtained at 140 °C for all fresh catalysts (5 mm) comprising similar wash coat loadings. Therefore, pore diffusion was negligible for these catalysts. Experimental effectiveness factors (EEF) (based on intrinsic rate constants for lowest wash coat loading) higher than unity were obtained for 22 weight per cent and 38 weight per cent COADA catalysts. The 58 weight per cent commercial alumina powder catalyst had a low EEF which showed high pore diffusion restrictions.

Activation energies for fresh catalysts containing 11 weight per cent ceria increased in the order: commercial standard < commercial alumina powder = COADA = COADA containing 3 weight per cent ceria built in < COADA containing 3 weight per cent ceria.

Specific rate for fresh monolithic catalysts (5 mm) increased with increasing platinum crystallite size, which is due to the so-called size effect. Therefore, activity of a catalyst is not confined to the high surface area of the support, but to properties of active

platinum on the support material. Specific rates associated with certain platinum crystallite sizes correlated with the trends found for specific conversions and rates. This shows that the highest catalytic activity can be expected for the commercial alumina powder sample, followed by the COADA samples containing 11 weight per cent and 3 weight per cent ceria. This was also confirmed by T_{50} values of 60 mm monolithic catalysts.

High wash coat loading was detrimental to catalyst activity. COADA catalysts showed a reduced apparent activation energy with increasing thickness, which was consistent with measured diffusional restriction.

The effect of ageing 5 mm catalysts at 980 °C was a large decrease in activity for the commercial alumina powder catalyst, while the commercial monolith increased in activity. COADA catalysts containing 11 weight per cent ceria showed the highest activity after sintering compared to other COADA catalysts. Activation energy of the aged standard catalyst did not change significantly during sintering compared to its fresh counterpart, which indicates the high stability of this catalyst. This was also confirmed by T_{50} values of 60 mm catalysts. This stability was also observed for the commercial powder sample. Sintering caused severe platinum crystallite growth for aged COADA catalysts compared to fresh catalysts. Addition of 3 weight per cent and 11 weight per cent ceria resulted in a similar degree of platinum sintering for COADA catalysts. Thus, platinum was not stabilised by addition of ceria.

UITTREKSEL

Porie-groottes in γ-alumina is beheer met bymiddels (porievormende reagense) tydens die vorming van aluminiumhidroksied. Porievormende reagense was aktief in die mesoporie-gebied met 'n skerp gedefinieerde porie-grootte distribusie. Porievormende reagense wat mesoporositeit verhoog het, was dietileenglikol, gliserien, bensoësuur, ammonium wynsteensuursout en vetsure/alkohol (stearien, palmitiese en *cis*-oleïen sure, oleïelalkohol, kaster-, olyf-, en sonneblomolies). Hierdie bymiddels veroorsaak die vorming van aggregate van partikels by die iso-elektriese punt (pH 9) van aluminiumhidroksied. Porievormende reagense wat mikroporositeit verhoog het, was wynsteen-, sebasien-, melk-, sitriese - en mieresure, 2-butanol, *n*-heksanol, propanol, 2-pentanol, ammonium metanoaat en -sitraat. Porie-groottes in die mikroporositeitsgebied is beïnvloed deur alumina-kristallietgroottes, wat, op hulle beurt, bepaal is deur die onderdrukkings-effek van sterk chelerende reagense op kristalgroei. Makroporositeit is veroorsaak deur vuller- of spasieerder-effekte van bymiddels, soos adipiese, wynsteen- en vetsure/alkohol, asook ammonium wynsteensuursout en ammonium karbonaat. Alle bymiddels het silindries-vormige porieë gevorm, behalwe vetsure wat ink-bottel-vormige porieë tot gevolg gehad het.

Geëmulsifiseerde *cis*-oleïensuur het hoër totale porie, mesoporie- en makroporie-volume gevorm sowel as hoër oppervlakarea, maar die porie-groottes was kleiner as dié gevorm deur kommersiële alumina-poeier wat gebruik word in die outomobiel-uitlaatkatalis-industrie.

Sinterstudies het aangetoon dat seriumoksied (11 massapersentasie) slegs die kontrole monsters tot 'n sekere mate gestabiliseer het, maar dit het geen invloed op vetsuur-afgeleide alumina gehad nie. Seriumoksied-kristalliete het eerder gesinter as γ-alumina, maar dit het die vorming van θ-alumina voorkom tydens sintering by 1000 °C.

Twee kenmerkende gebiede is waargeneem wanneer Knudsen effektiewe diffusiwiteit KED (D^0) (Carniglia adsorpsiemetode) en KED waardes gestip is as 'n funksie van die

kronkelfaktor (TF). Hierdie gebiede is toegeskryf aan silindriese (TF < 2.00 en KED (D^0) > 0.200 cm^2/s) en nie-silindriese (TF > 2.00) porieë.

Uniforme, sferiese gesproeidroogde alumina-poeiers was berei vanaf *cis*-oleïensuur-aluminiumhidroksied jel (COADA) nadat die hidroksied verouder, geflokkuleer en gedispergeer is. Hierdie aktiewe, hoë oppervlakarea γ-alumina is aangewend as wasbedekkingslae op monolitiese kordiëriet-ondersteunstukke. Faktore soos suiwerheid van *cis*-oleïensuur, tyd van maling, peptisering (asynsuur), stoombehandeling en seriumoksied hoeveelhede (3 massapersentasie en 11 massapersentasie is bygevoeg of 3 massapersentasie is ingebou in die struktuur van alumina voor sproeidroging) het die eienskappe van gesproeidroogde aluminapoeiers en wasbedekkingslae beïnvloed. Dit het ook kraking en slytingsweerstand van die wasbedekkingslae beïnvloed. Bedekking van monoliete is vergemaklik gedurende 'n ladingsneutralisasie by die skeidingsvlak tussen monoliete en die alumina wasbedekkingsflodder by 'n pH van 3.

Aktiwiteits-evaluering van platinum geïmpregneerde kataliste het getoon dat onderdrukking van die CO oksidasiereaksie voorgekom het in die temperatuurgebied tussen 68 tot 150 °C afhangende van die katalis.

Diffusie- en effektiwiteitsfaktore is bepaal vir kataliste om te verseker dat intrinsieke kinetika gemeet is. Effektiwiteitsfaktore van een eenheid (gebaseer op adsorpsie data) is verkry by 140°C vir alle vars kataliste (5 mm) bestaande uit dieselfde wasbedekkingsbeladings. Om hierdie rede is porie-diffusie weglaatbaar klein vir hierdie kataliste. Eksperimentele effektiwiteitsfaktore (EEF) (gebaseer op intrinsieke tempokonstantes vir die laagste wasbedekkingsbelading) hoër as een is verkry vir 22 massapersentasie en 38 massapersentasie COADA-kataliste. Die 58 massapersentasie kommersiële alumina-poeier kataliste het 'n lae EEF gehad wat hoë poriediffusie-beperkings getoon het.

Aktiverings-energieë vir vars kataliste wat 11 massapersentasie seriumoksied bevat het, het toegeneem in die volgorde: kommersiële standaard < kommersiële alumina-poeier

= COADA = COADA wat 3 massapersentasie seriumoksied bevat wat ingebou is < COADA wat 3 massapersentasie seriumoksied bevat.

Die spesifieke tempo vir vars monolitiese kataliste (5 mm) het vermeerder met toenemende platinum kristalliet-grootte wat toe te skryf is aan die sogenaamde grootte-effek. Dus, aktiwiteit van 'n katalis is nie beperk tot die hoë oppervlakarea van die ondersteunstuk nie, maar tot eienskappe van aktiewe platinum op die ondersteuningsmateriaal. Spesifieke tempo's geassosieer met sekere platinum-kristallietgroottes het met die neigings ooreengestem soos gevind is met spesifieke omsettings en tempo's. Dit wys daarop dat die hoogste katalitiese aktiwiteit verwag kan word vir die kommersiële alumina-poeiermonster, gevolg deur die COADA-monster wat 11 en 3 massapersentasies seriumoksied bevat. Dit was ook bevestig deur T_{50} waardes van 60 mm monolitiese kataliste.

Hoë wasbedekkingsbelading was nadelig vir katalis-aktiwiteit. COADA-kataliste het 'n afnemende skynbare aktiverings-energie getoon met toenemende dikte en was konsekwent met gemete diffusiebeperking.

Veroudering van 5 mm kataliste by 980 °C het 'n groot vermindering in aktiwiteit vir die kommersiële alumina-poeier katalis veroorsaak, terwyl die kommersiële monoliet toegeneem het in aktiwiteit. COADA-kataliste wat 11 massapersentasie seriumoksied bevat het, het die hoogste aktiwiteit na sintering getoon wanneer dit vergelyk was met ander COADA-kataliste. Aktiverings-energie van die verouderde standaard katalis in vergelyking met vars katalis, het nie uitermate verander gedurende sintering nie. Dit dui op die hoë stabiliteit van hierdie katalis wat ook bevestig is met T_{50} waardes van 60 mm kataliste. Hierdie stabiliteit is ook waargeneem vir die kommersiële poeier monster. Sintering het uitermate platinum kristalliet-groei veroorsaak in verouderde COADA-kataliste vergelykende met vars kataliste. Byvoeging van 3 massapersentasie en 11 massapersentasie seriumoksied het gelei tot 'n soortgelyke graad van platinum kristalliet sintering vir COADA-kataliste. Dus, platinum is nie gestabiliseer deur die byvoeging van seriumoksied nie.

ACKNOWLEDGEMENTS

The author hereby wishes to express his sincere appreciation to the following people and companies:

To Mintek for their financial support and the opportunity to do this study full time.

To Dr L. Dry, former vice-president of Mintek, who initiated this project.

To Dr R. L. Paul, former director of the Process Chemistry Division of Mintek, for his interest in the project.

To Prof J. C. Davidtz, my supervisor in the Chemical Engineering Department of Potchefstroom University for Christian Higher Education, for his guidance, willingness to share his knowledge and for his inspiration.

To Dr P. J. Harris, my co-supervisor, for his guidance and interest in the project.

To Prof R. C. Everson, Head of the Chemical Engineering Department of Potchefstroom University for Christian Higher Education, where the project was done.

To Mr N. French, of Metchem (NCP) who arranged for the conversion of the platinum metal to hexachloroplatinic acid.

To Mr H. van Zyl and Mr H. Lombard, of the Chemical Engineering Department of the Potchefstroom University for Christian Higher Education, for building the reactor and for their assistance during the experimental stages of the project.

To Dr L. Tiedt, of the Electron Microscopy Department of the Potchefstroom University for Christian Higher Education, for the SEM analyses.

To Dr P. E. W. Blom, formerly of the Chemical Engineering Department of the Potchefstroom University for Christian Higher Education and currently at Mintek, for helpful discussions.

To Mr E. Erasmus, of the Biochemistry Department of the Potchefstroom University for Christian Higher Education, for analysis of the fatty acids.

To Miss C. van Sittert, of the Chemical Department of the Potchefstroom University for Christian Higher Education, for water analysis.

To Mr K. Coetzee, of the Soil Science Department of the Potchefstroom University for Christian Higher

Education, for TGA analysis.

To Mrs J. Harries, for the mammoth job she did, as well as Mr R. Mogoai and Dr S. Foster (currently at Chemserve) of Mintek, for characterising the samples.

To Miss M. M. Kruger and Miss K. T. Wintle, of Mintek for zeta potential analysis.

To Mr S. D. McCullough and Mr A. D. MacKenzie, of Mintek for XRD analysis.

To Mrs N. Ramphaleng and Miss M. M. Kruger, of Mintek for particle size distribution analysis.

To Mrs L. Nortman, of Mattek (CSIR) for supplying the zirconia beads.

To Drs K. C. Sole and J. S. Vaughan (currently at Sastech), of Mintek for editing the text.

To Impala Refineries, who donated the platinum group metals.

To Carst and Walker, for supplying the alumina sol (Bacosol 3C).

To Montan Chemicals, for supplying the anionic polyacrylamide flocculant.

To S & CI, for supplying the commercial fatty acids.

To the international company for supplying the alumina powder, coated and uncoated exhaust gas monolithic catalysts and supports.

To all the personnel of the Chemical Engineering Department of the Potchefstroom University for Christian Higher Education, for their hospitality and helpfulness.

To all my colleagues at Mintek for their support and helpful discussions.

To my wife, Linda, for her love, encouragement and support during this study.

To my parents, family and friends for their encouragement and support.

To my Creator - Soli Deo Gloria.

TABLE OF CONTENTS

LIST OF FIGURES

LIST OF TABLES

LIST OF MICROGRAPHS

LIST OF FLOW-CHARTS

LIST OF PLATES

LIST OF SYMBOLS AND ABBREVIATIONS

θ	x-ray diffraction angle (rad)
γ-Al_2O_3	gamma-alumina
$\in$	void fraction or porosity
Θ_{CO}	carbon monoxide coverage
λ	wavelength (Å)
η	effectiveness factor
ρ	bulk or nominal density (g/cm)
ρ_0	skeletal density (g/cm)
υ	gas phase volumetric flow rate (m^3/min)
τ	tortuosity factor
Υ	gas residence time (s)
[]	concentration (mol/m^3 or mol %)
A	pre-exponential factor (1/s)
A/F	air to fuel ratio
Amm	ammonia
BET SA	Brunauer, Emmett, Teller surface area (m^2/g)
BJH	Barrett, Joyner and Halenda method
C	concentration (mol/m^3 or mol %)
cat	catalyst
COADA	*cis*-oleic acid-derived γ-alumina
comm	commercial
comm pwd	commercial alumina powder
conc	concentration
cont	continued
D	crystallite diameter size (nm)
D_e or D_{eff}	effective diffusivity (cm^2/s)
D^0	mean $D_K(r_i)$ over all r_i
D_K	Knudsen diffusion coefficient (cm^2/s)
$D_{K,eff}$	effective Knudsen diffusion coefficient (cm^2/s)
deg C	degree celsius
E_a	activation energy (kJ/mol)
EKED	experimental Knudsen effective diffusion coefficient (cm^2/s)
EO	ethylene oxide
EtOH	ethanol
GHSV	gas hour space velocity (h^{-1})
iso-Pr	*iso*-propoxide
k_a	adsorption rate constant (1/mole% CO)
k_a^0	frequency factor for k_a
k_r	intrinsic rate constant (1/s)
k_s	rate constant per unit surface area (1/s)
K	reaction rate constant ($k[O_2]$)
KED	Knudsen effective diffusivities (cm^2/s)

M	molecular weight (g/mol)
n	slope of log-log plot of $D_K(r)$ versus r
NL	not linear
NO	not obtainable
P	pressure (kPa)
P	pyrolysis
PGM	platinum group metals
PSF	pore shape factor
r or r_e	pore radius (cm)
r_{CO}	carbon monoxide reaction rate (mol CO/(s m^3 catalyst))
R	gas constant (8.3441 J/mol/K)
$R(\theta)$	resistance term
R^2	linearity regression
SA	total BET surface area (m^2/g)
SEM	scanning electron microscopy
T	surface temperature (Kelvin)
T_{50}	temperature at 50% conversion or light-off temperature
TF	tortuosity factor
TGA	thermogravimetric analysis
U	urea
V	free catalyst volume (cm^3)
$V_{micro,meso,macro}$	cumulative volume of pores in micro-, macro-, mesopore region (cm^3/g)
V_s	total specific volume (cm^3/g)
wt%	weight per cent
X	conversion (%)
XRD	x-ray diffraction
y	pore shape factor (PSF)
Y_{A0}	initial mole fraction of A

CHAPTER 1. INTRODUCTION

South Africa is the world's largest producer of platinum-group metals (PGMs). The major industrial application is found in catalysts and, in particular, exhaust emission cordierite monolithic catalysts. Local technology and know-how concerning the manufacture and general characterisation of supported metal catalysts are therefore important. This study is the first ever done in South Africa regarding pore control in γ-alumina and its application in exhaust catalysis.

The monolithic cordierite structure is low in surface area (Young & Finlayson, 1974; Kummer, 1980; Lachman & McNally, 1985). Therefore, an active high surface area alumina (γ-alumina) is bonded to the support to enhance PGM dispersions and improve kinetics.

Effective control of pore sizes and their distributions is important in the design of supported catalysts. One method of producing pores involves porogens. These are organic and inorganic constituents that are used during pore formation.

The development of pores and surface areas in γ-alumina material with porogens are investigated to improve on their working and to study chemical and physical parameters that affect pores. Porogens investigated encompass organic compounds, such as ammonium salts of carboxylic acids, alcohols, glycols, mono-, di- and tricarboxylic acids, and fatty acids. Only limited information is available in the open literature concerning the pore-forming abilities of these organic additives, especially in γ-alumina material starting from aluminium nitrate and neutralising with ammonia.

Properties of γ-aluminas are described in terms of pore volume, surface area, pore size, bulk densities, porosities, tortuosity factors, pore shape factors, and effective Knudsen diffusivities. The latter is described in terms of carbon monoxide transfer at a preselected temperature.

The sintering behaviour of the most promising group of materials, based on the surface requirements needed for an exhaust gas catalyst material, are described in terms of the above properties. Ceria is built into the γ-alumina structure to evaluate sinter stability. One organic additive from this group is selected and spray-dried powders are prepared and applied as wash coat layers on monolithic cordierite supports. Peeling tests are also conducted on wash-coated monoliths to determine the adhesion of the alumina wash coat layer.

Differences caused by adding cerium nitrate to the wash coat slurries and where ceria was built into the structure of γ-alumina, before spray-drying and wash-coating, are evaluated to study the sinter stability of such a material. Commercially coated monolithic catalysts were used as standard reference catalysts, whereas commercial γ-alumina powder, currently being industrially employed to produce exhaust catalysts, was also used to produce reference wash coat catalysts.

The carbon monoxide oxidation reaction is studied to determine whether the above can be implemented to improve the system. Two different monolithic catalyst lengths are evaluated, *i.e.*, 5 mm and 60 mm lengths. The former monoliths are employed to determine kinetic parameters, while the latter are used for high conversion studies. The wash coat layers are impregnated with platinum and ceria. Some catalysts are aged before evaluation is carried out. The catalysts are evaluated in a laboratory-scale plug flow reactor for stability and activity. Platinum dispersion, platinum surface area and platinum crystallites are also evaluated. These properties are compared with activation energies, specific conversions, conversion rates, and specific rates. Diffusion and effectiveness factors are determined to ensure that intrinsic kinetics are measured. These latter data are obtained from the adsorption method of Carniglia and from experimental data.

A comprehensive study of the literature is conducted. This encompasses properties of catalyst supports, formation and properties of aluminium hydroxides and alumina, and factors controlling pore production in alumina. These factors include the following

effects:

- crystallinity of the gel,
- different phases and calcination temperature,
- pH,
- different ageing periods,
- washing of precipitates,
- drying,
- alumina precursors,
- different solvents, and
- different organic and inorganic additives.

A brief history and requirements of monolithic exhaust catalysts are also included. The requirements are divided into 1) ceramic monolith, 2) γ-alumina wash coat properties and application techniques, 3) the role of ceria, 4) impregnation of γ-alumina with hexachloroplatinic acid, 5) carbon monoxide oxidation and its kinetic reaction. The results of this study are reported hereafter.

CHAPTER 2. LITERATURE REVIEW

2.1 INTRODUCTION

Exhaust catalysts are used to limit polluting emissions of carbon monoxide and other gases from motor vehicles. These catalysts consist of a support material and active metals. Support materials consist of either a ceramic material or they are constructed from alloys. Cordierite is currently the most widely used ceramic support material. This material is constructed in a monolithic shape which is a thin-walled multi-channeled honeycomb. Ceramic walls between channels are the base support surfaces for the catalyst. Although they are porous, they are not the direct surface for the active metal. An intermediate alumina (γ-Al_2O_3) coating, called wash coat, provides a high surface area for the catalyst. Alumina is used because of its high thermal and chemical stability and it is robust, porous and relatively inexpensive (Dirksen, 1983).

Pore structural properties of alumina supports are usually controlled during the formation of aluminium hydroxide gels, followed by thermal treatments to decompose the gels to alumina. Important factors affecting pore production in aluminas are: preparation conditions and treatment of gel, alumina precursor used, precipitation reagents, and various additives present during gel formation.

Surface area, pore volume, pore sizes and their distributions, and density are important properties of catalyst carriers. They are intrinsic properties of catalyst carriers but they also affect mass transfer of reactants and products at the surface of a carrier material. The interrelationship of these properties is important in catalyst carrier design as well as in pore production in aluminium hydroxide gel and alumina.

2.2 PHYSICAL PROPERTIES OF CATALYST CARRIERS

Catalyst carrier materials and their physical properties are important in the activity,

selectivity, and stability of catalysts. The selection of a catalyst carrier is based on certain desirable properties. Principally, according to Satterfield (1980) and Stiles (1987), these are:

- purity,
- desirable mechanical properties, including attrition resistance, hardness, compressive strength, density, particle size and shape,
- stability under reaction and regeneration conditions,
- surface area,
- porosity, including average pore size, pore size distribution, and pore volume,
- low cost.

Properties to be controlled for proper performance of the catalyst or support are surface area, pore size, pore size distribution, and total pore volume. A high surface area is usually desirable in gas-phase reactions, whereas lower surface area is important in liquid-phase operations although there are exceptions. In this sense, a low surface area can be referred to that less than approximately 125 m^2/g, whereas a high surface area could be regarded to be greater than 125 m^2/g (Stiles, 1987).

Surface area and pore size are interrelated. A high surface area is mainly attributable to small pore sizes (micropores < 1.8 nm diameter and mesopore sizes between 1.8 and 30 nm diameter), while large pores (macropore sizes > 30 nm diameter) contribute little to the surface area (Hegedus, 1980). Pore sizes and shapes determine the accessibility of reactants to active catalyst sites as well as catalyst stability, resistance to fouling, and heat transfer (Misra, 1986a). Surface area is of major importance when the support is impregnated with a catalytic material. Large surface areas, which correspond to small pore diameters, could become blocked when filled with catalytic material. If this is an important consideration for catalytic activity then material with lower surface area, and hence larger pore diameter, is desirable.

Another requirement of a catalyst or catalyst support is the total pore volume, which is related to the porosity. The reactive area available is related to the total pore volume,

which comprises the support plus catalyst or support itself. Surface area and porosity can be varied independently, but only within a limited range. For the same surface area, different pore size distributions can be prepared (Misra, 1986a). From a catalyst point of view, pore size distribution should be such that larger pores permit easy mass transport of gases or liquids to smaller auxiliary pores where the major fraction of the reaction generally occurs (Stiles, 1987).

Stiles (1987) suggested an equilateral triangle to represent interrelationship of hardness, pore size, pore volume and density, as shown in Figure 2.1.

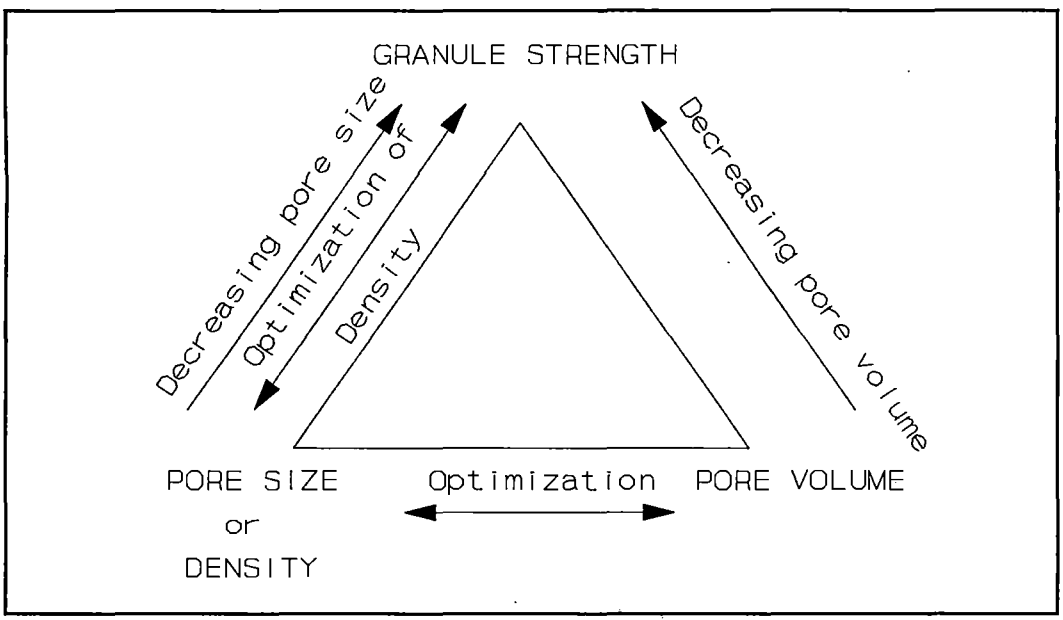

Figure 2.1 The interrelationship of the physical properties of a catalyst: granule strength, pore size (or density) and pore volume (after Stiles, 1987).

As hardness increases, pore volume and pore size decrease. As total pore volume increases, granule strength will decrease, but not necessarily pore size. Surface area and pore volume are closely related as shown in equation (1) (Hegedus, 1980):

$$\text{Surface area} = \frac{2\ \text{volume}_{\text{macro-}}}{\text{radius}_{\text{macro-}}} + \frac{2\ \text{volume}_{\text{meso-}}}{\text{radius}_{\text{meso-}}} + \frac{2\ \text{volume}_{\text{micropore}}}{\text{radius}_{\text{micropore}}} \quad \ldots\ldots\ldots \quad (1)$$

When typical numbers are substituted, the surface area is dominated by micropores.

Pore size can be replaced by density in Figure 2.1. As pore volume increases, density and hardness will decrease. As density increases to a maximum, pore volume decreases, but not necessarily hardness.

2.3 ALUMINIUM HYDROXIDES

Formation of aluminium hydroxide gels is the preliminary step in producing aluminas. The composition and properties of aluminium hydroxide gels depend largely on the method of preparation. Gelatinous hydroxides consist predominantly of x-ray insensitive (*i.e.*, amorphous) aluminium hydroxide or pseudoboehmite (Hudson *et al.*, 1985). The solubility of aluminium hydroxide gel as a function of the pH value is shown in Figure 2.2.

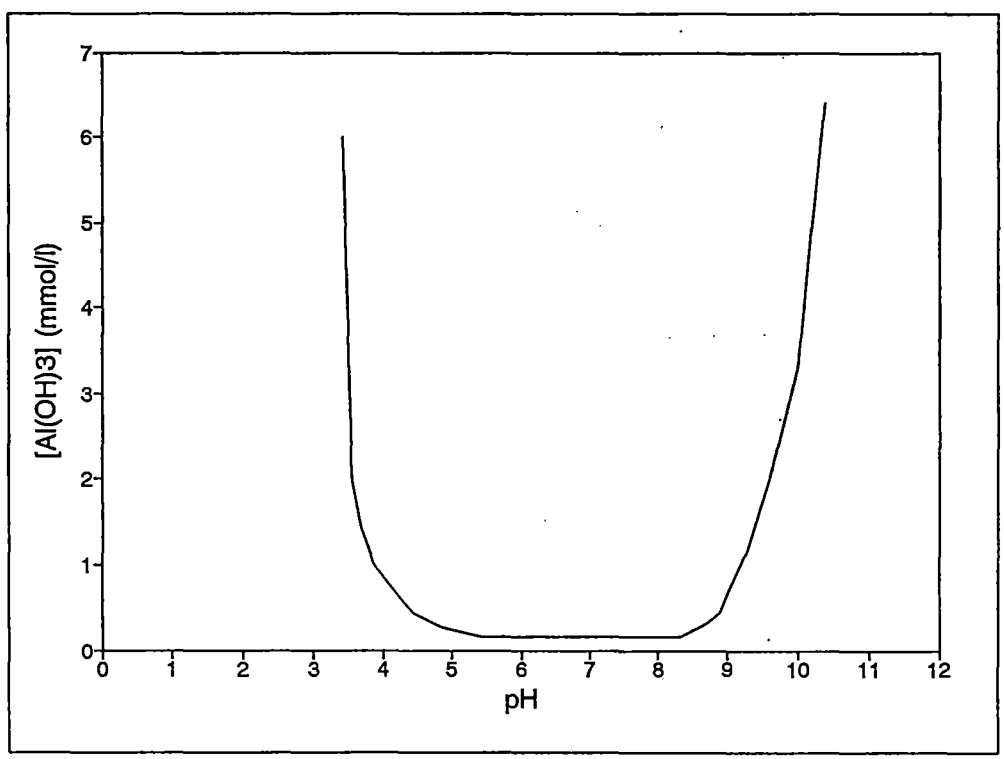

Figure 2.2 The solubility of $Al(OH)_3$ gel as a function of pH (after Misra, 1986b).

It can be seen from Figure 2.2 that the solubility is very low in the pH range of 5 to 8.

Aluminium hydroxide readily dissolves in strong acids and bases. A slight variation in pH, between pH 4 and 9, towards the neutral value can cause rapid and voluminous precipitation of colloidal hydroxides. Being hydrophilic, the colloidal precipitate readily coagulates to form a gel (Misra, 1986b). Aluminium hydroxide gels formed by neutralisation from either acidic or basic solutions contain excess water and variable amounts of anions. After prolonged drying at 100 - 110 °C, the water content of gels can be as high as 5 moles of water per mole of alumina. Water content, size of primary particles of precipitate, and specific surface area vary with precipitation conditions.

According to Misra (1986b), there are three general methods of preparation of gelatinous aluminium hydroxides:

1) neutralisation, either of aluminium salts with alkali or of alkali aluminates with CO_2 or acids;
2) decomposition (mostly by hydrolysis) of aluminium organic compounds such as aluminium methylate, ethylate, alcoholates, *iso*-propoxide and butoxide;
3) reaction of water with aluminium metal (usually activated by amalgamation).

During the preparation of gelatinous hydroxides, aluminium ions polymerise to form a series of gelatinous products. Baker and Pearson (1974) represented this hydrolytic polymerisation as a series of reactions:

$$Al(H_2O)_6^{3-} \rightarrow Al(H_2O)_5OH^{2-} + H^+ \quad \text{..... (2a)}$$

$$2\ Al(H_2O)_5OH^{2-} \rightarrow \left[(H_2O)_4Al\begin{matrix}OH\\OH\end{matrix}Al(H_2O)_4\right]^{4-} + 2\ H_2O \quad \text{..... (2b)}$$

fast $$\rightarrow \left[(H_2O)_4Al\begin{matrix}OH\\OH\end{matrix}(Al(H_2O)_2\begin{matrix}OH\\OH\end{matrix})_nAl(H_2O)_4\right]^{4(n-2)-} \quad \text{..... (2c)}$$

slow or ageing

$$\rightarrow Al_6O_3(OH)_9(H_2O)_{12}^{3-} \text{ or } Al_8O_4(OH)_{12}(H_2O)_{14}^{4-} \quad \text{..... (2d)}$$

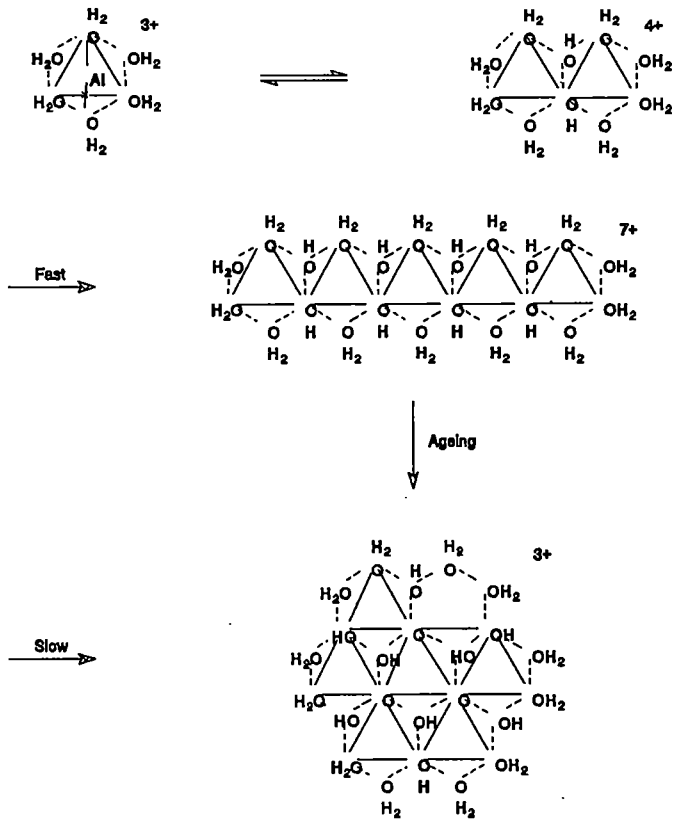

Figure 2.3 Polymerisation of aluminium hydroxides (after Baker & Pearson, 1974).

These transformations are depicted in Figure 2.3. The product of polymerisation described as 'fast' is similar to boehmite, and the 'slow' (or aged) ring structure is similarto bayerite or gibbsite. The product formed depends on the position of condensation of the octahedrons (location 1 - straight; location 2 - ring).

Figure 2.4 shows further three-dimensional polymerisation of the boehmite structure; two chains containing five aluminium atoms have condensed, and a third chain is starting in the third dimension, as represented by the shaded area.

A model was proposed by Baker and Pearson (1974) to determine where excess water resides in the pseudoboehmite structure. They concluded that constituent excess water is a function of the degree of polymerisation. To depict this, they show that the following

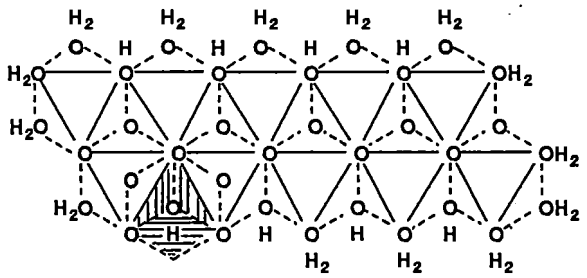

Figure 2.4 Continued chain-polymerisation in three dimensions (after Baker & Pearson, 1974).

chain has the theoretical stoichiometric AlO(OH) formulation of boehmite:

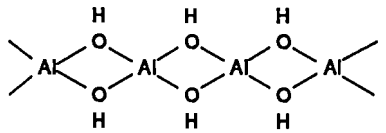

At the chain terminus, water molecules are attached as follows:

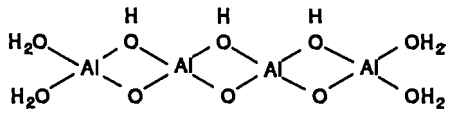

This yields a molecular total of four AlO(OH) groups plus four water groups. If additional AlO(OH) groups were present in the chain, the weight contributed by terminal water groups becomes less significant in comparison to the total weight of chain. Hence excess water in pseudoboehmite represents terminal water molecules. Therefore, the lower the degree of polymerisation, the smaller the crystallite size and larger the portion of excess (terminal) water.

2.4 ALUMINAS

According to MacZura *et al.* (1978), thermal decomposition of pseudoboehmite gives the

γ-alumina structure at 500 °C, followed, at higher temperatures, by δ-, θ- and α- phases. The decomposition sequence of pseudoboehmite and other aluminium hydroxides is given in Figure 2.5 and Table 2.1.

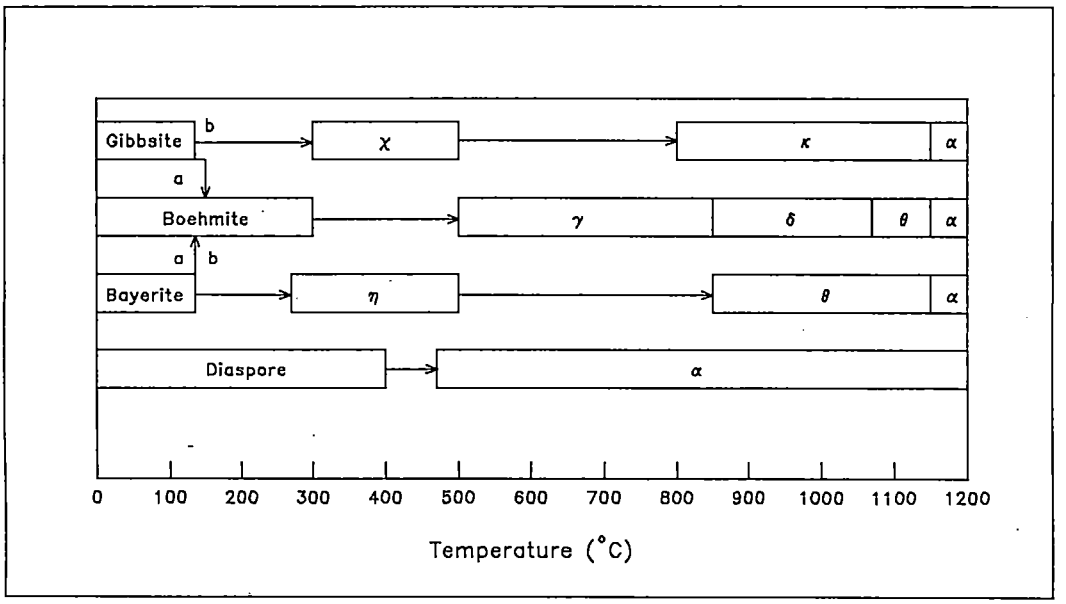

Figure 2.5 Decomposition sequence of various aluminium hydroxides (after MacZura *et al.*, 1978). [Enclosed area indicates range of occurrence; open area indicates range of transition.]

Table 2.1 Decomposition sequence of aluminium hydroxides.

Parameter	Conditions Path a	Conditions Path b
Pressure	> 1 atm	1 atm
Atmosphere	moist air	dry air
Heating rate	> 1 °C/min	< 1 °C/min
Particle size	> 100 μm	< 10 μm

γ-Alumina results from thermal dehydration of pseudoboehmite. Thermal dehydration procedures result in a highly porous structure of aluminium oxide which has a high surface area. The physical and chemical nature of the initial hydroxide and the thermal

history of the dehydration, influence the properties of the final product. γ-Aluminas generally have high surface area (typically 150 - 300 m^2/g) and comprise a large number of pores with diameters in the range 3.0 to 12.0 nm, and have pore volumes of 0.5 to greater than 1.0 cm^3/g (Oberlander, 1984).

Chen *et al.* (1989) proposed the following reaction mechanism for the thermal decomposition of aluminium hydroxides:

$$Al_n(OH)_{3n} \underset{k_{-1}}{\overset{k_1}{\rightarrow}} 2\ Al_{n/2}(OH)_{3n/2} \qquad \text{..... (3a)}$$

$$Al_{n/2}(OH)_{3n/2} \overset{k''}{\rightarrow} n/4\ Al_2O_3 + 3n/4\ H_2O\ (g) \qquad \text{..... (3b)}$$

where $n = 4m$, m being an arbitrary positive integer. These equilibrium reactions show simple homolytic fission to form $Al_{n/2}(OH)_{3n/2}$ from $Al_n(OH)_{3n}$, while $Al_{n/2}(OH)_{3n/2}$ may partly reverse by recombination and undergo homolytic fission continuously until the dehydration reaction occurs. In other words, the reaction mechanism suggests that dehydration reactions control the whole decomposition reaction, although other decomposition steps are at equilibrium and favour the forward direction of decomposition. Chen *et al.* (1989) have also found the apparent activation energy to be 30.6 kJ/mol, with a reaction order of 0.45 with respect to aluminium hydroxide.

Oxygen ions in γ-alumina are cubic close packed, almost identical to those of a spinel (Schuit & Gates, 1973). This packing is characterised by a slightly different type of stacking of close packed oxygen layers, *i.e.*, 1-2-3-1-2-3. In addition, there is a change in Al^{3+} ion distribution; instead of being confined to octahedral interstices, some cations are positioned in tetrahedral sites, hence they are tetrahedrally surrounded by O^{2-} ions. In a cubic close packing of anions there is one octahedral and two tetrahedral sites per anion. In spinels like $MgAl_2O_4$, Al^{3+} ions occur in octahedral sites and Mg^{2+} ions in tetrahedral sites. When compared to spinels, one third of the cations are missing in alumina (Lippens & Steggerada, 1970). Cation vacancies in alumina can be distributed

in different ways among cation sites normally occupied in a spinel so that the formula can be written as: $Al_{2/3+x}[]_{1/3-x}(Al_{2-x}[]_x)O_4$ with $0 \leq x \leq 1/3$, where [] denotes vacant sites. Indications are that x is close to 2/9, so that the fraction of Al^{3+} in tetrahedral sites is about 1/3. The total sum of octahedral and tetrahedral holes per formula unit of Al_2O_4 is nine, only two of which are filled. This renders γ-alumina susceptible to cation diffusion (Pott & Stork, 1976). Schuit and Gates (1973) represented aluminas by the general formula $[Al_{2/3}]_t[Al]_oO_4$ where $[Al]_t$ and $[Al]_o$ are tetrahedral and octahedral aluminium sites, respectively.

Soled (1983) described γ-alumina as a defective oxyhydroxide of stoichiometry $Al_{2.5}[]_{0.5}O_{3.5}(OH)_{0.5}$, where OH groups are considered to be located on the surface of microcrystallites. He concluded from this stoichiometry that γ-alumina should consist of particles which have the shape of octahedra and are terminated by the most densely packed (111) faces. This model predicted an idealised particle to have an edge length of 11.5 nm, a surface area of about 200 m^2/g, and pore volumes ranging between 0.04 and 1.30 cm^3/g, which is in fair agreement with textural data of typical aluminas.

2.5 FACTORS AFFECTING PORE PRODUCTION IN ALUMINAS

Various processing factors affect pore properties of aluminium hydroxide gels and aluminas. These factors include:

1) crystallinity of gels;
2) crystalline allotropy of aluminas and calcination temperature;
3) pH of solution;
4) ageing period;
5) washing of gel precipitates;
6) drying of gels;
7) aluminium precursors;
8) solvent type, and
9) nature of additives used.

2.5.1 Effect of crystallinity of gel

Lippens and Steggerada (1970) studied the crystallinity and surface area (as measured by the method of Brunauer, Emmett and Teller (BET) method) of pseudoboehmite gels. Their results are summarised in Table 2.2.

Table 2.2 shows that the initial surface area of gelatinous hydroxides decreases with increasing crystallinity. However, dehydration produces a smaller increase in surface area the less crystalline the material. In extreme cases of highly amorphous products, a decrease in surface area is observed with dehydration. This reduction in surface area is due, almost completely, to loss of water, which causes a shrinkage of particles. No new internal pores are formed, nor do particles sinter together to any appreciable extent (Lippens & Steggerada, 1970). In crystalline or partly crystalline products, the number of new pores which are produced by dehydration depends on the crystallinity of the original hydroxide.

Table 2.2 BET surface area of hydroxides of different crystallinity and their dehydration products (after Lippens & Steggerada, 1970).

Type of boehmite	Surface area (m^2/g) Dried at 120 °C	Surface area (m^2/g) Dehydrated at 500 °C	Surface area change (m^2/g)
Well crystallised	1.3	65	+64
Microcrystalline	64	100	+36
Microcrystalline	68	99	+31
Microcrystalline	100	101	+1
Microcrystalline	201	180	-21
Microcrystalline	255	208	-47
Gelatinous	395	257	-138
Gelatinous	490	316	-174
Gelatinous	609	398	-211

2.5.2 Effect of crystalline allotropy of aluminas and calcination temperature

Table 2.3 lists crystal phases and the BET surface areas of aluminium oxides after heat treatment of prepared aluminium hydroxides, as studied by Al-Mashta *et al.* (1988). With increasing temperature, water is driven off and it is transformed first to a monohydrate and then to a succession of nearly anhydrous crystalline forms. As heating is continued above 400 °C, crystal growth sets in, with concomitant decrease in surface area.

Huang *et al.* (1989) found that increasing the calcination time at constant temperature increased the pore volume while decreasing the surface area of alumina due to the formation of larger pores as a result of sintering. Maximum pore volume was obtained by calcining at 600 °C. The mean pore radius of alumina was found to increase slightly with calcination time and temperature.

Table 2.3 Crystal phases and surface areas of aluminium oxides after heat treatment of prepared aluminium hydroxides (after Al-Mashta *et al.*, 1988).

Temperature[a] (°C)	Oxide form	BET surface area (m^2/g)
200	Nordstrandite & Bayerite	310
300	γ-alumina & Gibbsite	289
400	Poorly crystallised η- & χ-phases	269
500	γ-phase	173
600	γ- & trace of δ-phase	154
700	γ- & δ-phases	149
800	Poorly crystallised θ-phase	118
900	Well ordered θ-phase	85
1000	Well ordered θ-phase	50

[a] Precipitates were dried at 120 °C for 50 h and then calcined for 24 h at the temperatures indicated.

2.5.3 Effect of pH

Huang and co-workers (1989) studied the effect of pH during the precipitation of aluminium hydroxide gel from aluminium nitrate and ammonia, on the resulting surface area and pore volume (Table 2.4). These authors found that aluminas prepared by calcination of precipitates formed at pH < 9 have unimodal pore size distributions (attributed to pseudoboehmite) with pores approximately 3.6 to 8 nm in diameter. Precipitates formed at pH 10 and pH 10.8 produced aluminas with bimodal pore size distributions, with the smaller pores less than 10 nm in diameter while the larger pores measured 30 to 200 nm for precipitation at pH 10 and 100 to 2000 nm for pH 10.8. According to Huang *et al.* (1989), the larger pores are due to the presence of bayerite in these precipitates.

Table 2.4 Effect of precipitation pH on properties of alumina (after Huang *et al.*, 1989).

pH	BET surface area[b] (m^2/g)	Pore volume[b] (cm^3/g) 3.6 - 20 nm diameter	Pore volume (cm^3/g) 20 - 10 000 nm diameter
5.9	237	0.16	0.02
7.0	232	0.22	0.02
8.0	250	0.23	0.01
8.3	221	0.34	0.02
9.0	248 ± 20	0.26	0.01
10.0	310	0.17	0.20
10.8	330 ± 10	0.10	0.67

[b] Refers to alumina prepared from precipitate, aged 24 h (without washing or drying) and calcined at 500 °C for 5 h.

Huang and co-workers (1989) also found that the surface area of products precipitated between pH values 5.9 and 9.0 remained fairly constant, as indicated in Table 2.4. The contribution to pore volumes by small pores reached a maximum at about pH 8.3. Pore volumes and surface areas in the 20 to 10 000 nm diameter range increased with pH

value.

2.5.4 Effect of ageing period

The ageing period affects both the surface area and pore volume of aluminium hydroxide precipitates. Huang *et al.* (1989) reported that the pore volume of small pores of aluminas prepared at pH 8, increased with ageing (Table 2.5). This is attributed to the transformation of amorphous material into pseudoboehmite during ageing, which results in an increase in surface area. Ageing at pH 10 resulted in aluminas with bimodal pore size distributions. Conversion of pseudoboehmite to bayerite during ageing tended to decrease pore volumes in the 3.6 to 20 nm diameter range, while the volume of pores larger than 30 nm in diameter increased with ageing time.

Table 2.5 Effect of ageing time on properties of alumina (after Huang *et al.*, 1989).

pH	Ageing time (day)	Surface area[c] (m^2/g)	Pore volume[c] (cm^3/g) 3.6 - 100 nm	Pore volume (cm^3/g) 100 - 10 000 nm
8	1	269	0.23	0.01
8	23	247	0.24	0.01
8	44	276	0.28	0.01
8	65	245	0.33	0.01
10	1	310	0.17	0.20
10	10	325	0.08	0.42
10	20	331	0.09	0.43
10	30	328	0.10	0.58
11	1	320	0.11	0.45
11	12	342	0.08	0.45
11	23	375	0.08	0.50
11	33	369	0.06	0.52

[c] Refers to alumina obtained from precipitates (without washing or drying) after calcining at 500 °C for 5 h.

Variation in pore volume is greater for ageing at pH 10 than pH 11 and Huang *et al.* (1989) ascribed this to the increased rate of conversion of pseudoboehmite to bayerite which occurs with increasing pH. As a result, the formation of bayerite in precipitates produced at pH 11 is essentially complete after one day and ageing effects beyond this time are less pronounced.

These workers also found that the surface area of alumina prepared from precipitate and aged at pH 8 remained essentially constant with time (Table 2.5). As a consequence of the opposing effects of pseudoboehmite crystallite growth and amorphous-to-pseudoboehmite transformation, little net change in surface area of the aluminas was observed. At pH 10 and 11, the surface area of alumina appears to increase during the first few days of ageing and then remain constant.

2.5.5 Effect of washing gel precipitates

The effect of washing gel precipitates with different solvents before calcination is shown in Table 2.6.

White *et al.* (1989) found that washing with water, butanol, and mixtures of propanol and water had no significant effect on pore volume or surface area, although both increased slightly. Washing with propanol, ethanol or acetone gave a large increase in surface area and pore volume and changed the pore size distribution significantly. Washing preformed precipitates can only affect the texture (White *et al.*, 1989) within the limited time after washing and prior to drying/calcination, or during the latter two operations. Replacement of water by alcohol or acetone probably leads to a reduction of surface tension and to less pore collapse on calcination (White *et al.*, 1989). Solubility decreases as the homologous series is ascended and the absence of an effect with butanol is probably due to a lack of displacement of water during washing. The increase in pore volume in the 3.6 to 1000 nm diameter range observed with propanol is attributed by White and co-workers to the onset of pore size control by a 'pore filling-removal' mechanism.

Table 2.6 Effect of using different washing liquors prior to calcination on properties of precipitated aluminas (after White *et al.*, 1989).

Additive	Surface area[d] (m^2/g)	Pore volume[d] (cm^3/g) 3.6 - 100 nm	Pore volume (cm^3/g) 3.6 - 500 nm	Pore volume (cm^3/g) 3.6 - 1000 nm
None	245	0.27	0.27	0.27
Water	283	0.34	0.36	0.36
Acetone	302	0.72	1.20	1.20
Ethanol	353	0.36	1.20	1.30
Propanol	375	0.50	1.46	1.73
25% Propanol/H_2O	254	0.28	0.29	0.29
50% Propanol/H_2O	265	0.35	0.36	0.36
Propanol, then water	258	0.35	0.36	0.36
Butanol	242	0.29	0.30	0.31

[d] Precipitates prepared without additives, filtered and washed with 500 ml additive. Calcined at 500 °C for 5 h.

2.5.6 Effect of drying of gels

Huang and co-workers (1989) found that predrying precipitates after precipitation affected the pore size distribution of the alumina after calcination. Maximum pore volume was obtained by drying the precipitate at 150 °C for the range of drying temperatures indicated in Table 2.7 (105 to 175 °C). No trend in variation of surface area with drying temperature was observed.

2.5.7 Effect of different alumina precursors

By using different aluminium precursors and neutralisation agents, various surface areas and pore volumes of precipitated aluminas were obtained by Kotanigawa and co-workers (1981), as shown in Table 2.8.

Table 2.7 Effect of drying and calcination conditions on properties of aluminas (after Huang *et al.*, 1989).

Drying temp.[e] (°C)	Calcination time (h)	Calcination temp. (°C)	Surface area (m^2/g)	Pore volume (cm^3/g)	Mean pore diameter (nm)
105	5	500	268	0.29	6.4
120	5	500	273	0.32	5.6
150	5	500	235	0.35	5.7
175	5	500	260	0.28	5.1

[e] Precipitates dried before calcining.

Table 2.8 Pore dimensions obtained from various Al_2O_3 precursors (after Kotanigawa *et al.*, 1981).

Alumina	BET surface area[f] (m^2/g)	Pore volume[f] (cm^3/g)	Particle[g] size (μm)	Crystallite size (nm)
Cl-NH_3	230	0.434	14.5	4.0
NO_3-NH_3[h]	295	0.955	8.7	7.2
SO_4-NH_3	254	0.901	31.6	7.1
iso-Pr-P[i]	264	0.674	12.4	5.5
NO_3-P	134	0.188	30.6	-
Cl-P	66	1.299	12.3	-
Na-Al-CO_2	240	0.651	2.4	6.5
SO_4-U[j]	-	-	1.7	-
Cl-U	158	0.669	15.5	6.9
Br-U	260	2.092	1.0	6.5
NO_3-U	158	1.739	19.6	6.6

[f] Samples dried at 120 °C for one day and calcined at 550 °C for 10 h.
[g] By scanning electron microscopy.
[h] pH adjusted to 10.4 and aged at 90 °C for 2 h.
[i] P = pyrolysis
[j] U = urea

Kotanigawa *et al.* (1981) reported that aluminas prepared using aqueous ammonia as the

precipitating agent exhibited a single pore size of about 2 nm radius. Similar structures were found for products from CO_2 neutralisation of sodium aluminate and pyrolysis (P) of aluminium nitrate. Products from urea (U) neutralisation and aluminium *iso*-propoxide (*iso*-Pr) decomposition, showed a bimodal pore size distribution with radii of about 2 and 5 nm. From adsorption and desorption experiments and scanning electron microscopy (SEM) observations, it was concluded that the unimodal distribution of 2 nm is composed of tabular or ink bottle-shaped pores formed between individual cubic particles or cubic particles built in layers with platelike particles. The smaller 2 nm pores were slit-shaped and formed as spaces between plate structures, whereas the larger 5 nm pores were tabular or ink-bottle shaped, formed as spaces between cubic particles that are composites of layered plate structures. Kotanigawa and co-workers (1981) also showed that aluminium precursor salts, with the exception of nitrate, contained impurities of that precursor in the final alumina product. These impurities are undesirable and therefore a nitrate salt is the preferred precursor.

Addition of ammonium bicarbonate or carbonate to a boehmite gel, formed from aluminium nitrate and ammonia at pH 8 before calcination, resulted in development of a pore structure which had a well-defined maximum in the 2 to 15 nm range of radii (Vogel *et al.*, 1984). These authors attributed this result to formation of intermediate complex salts of the type $[(NH_4)_2Al_6OH_{14}(CO)_3 \cdot xH_2O]$, for which an x-ray diffraction pattern is reported. It was suggested that the pore structure was formed by removal of NH_4^+ and CO_3^{2-} ions during calcination.

Marcantonio (1987) prepared an ammonium aluminium hydroxycarbonate precursor with the molecular formula $NH_4Al(OH)_2CO_3 \cdot H_2O$ at pH values between 10 and 11. At 250 °C and slow heating rates for 8 h, these aluminium hydroxides possessed BET surface areas of 700 to 800 m^2/g. Rapid heating rates for 3 h had adverse effects on the surface area.

Sivaraj and co-workers (1986) showed that aluminium succinate resulted in aluminas which had higher surface areas and pore volumes than those from bayerite.

2.5.8 Effect of solvent type and mechanistic behaviour

Cormack and co-workers (1980) studied the effect of different solvents used during the preparation of aluminium hydroxide gels, as summarised in Table 2.9. These gels were prepared by passing gaseous ammonia into solutions of aluminium nitrate in various alcohols at room temperature, followed by washing with methanol, drying under vacuum for 3 h at 45 °C, and then in air for 3 days at 110 °C.

Significant differences were noted in both the total pore volume and pore size distribution for gels prepared in these alcohols. Gel prepared in 2-methyl-2-butanol had the largest overall total pore volume, whereas gel prepared in heptanol had the largest volume in the 750 to 7500 nm radius range (macropores). Gels prepared in ethanol and in propanol had smaller total pore volumes than gel prepared in pure water, whereas gels prepared in other alcohols had larger total pore volumes. According to Cormack *et al.* (1980), this is due to the ability of ethanol to reduce the 'solvent barrier' (*i.e.*, breaking of the interface between liquid and solid due to the lowering of the surface tension on the surface of the gel), thus allowing bridging to occur around the particle-particle contact (*i.e.*, mechanism of aggregation-cementation).

Cormack *et al.* (1980) concluded that alcohols play a double role in influencing changes in pore structures by:

- interfering with the crystallite ordering by replacing water at the solid-liquid interface, thus promoting aggregation-cementation and the development of a well-defined mesopore structure due to the formation of loosely packed particles. Alternatively, the formation of large irregularly shaped particles occurs to form agglomerates leaving pores (voidage) between the particles (Trimm & Stanislaus, 1986); and,

- decreasing the solubility, thereby reducing the rate of Ostwald ripening, *i.e.*, growth of larger particles in a suspension at the expense of smaller ones which

Table 2.9 Pore volumes and surface areas, measured by mercury porosimetry, of gels prepared in different solvents (after Cormack *et al.*, 1980).

Solvent	Total pore volume (cm^3/g)	Pore volume 3.75 - 25 nm radius (cm^3/g)	Pore volume 25 - 750 nm radius (cm^3/g)	Pore volume 750 - 7500 nm radius (cm^3/g)	Surface area (m^2/g)
Water	0.70	0.06	0.14	0.49	20
Ethanol	0.35	0.15	0.09	0.11	51
Propanol	0.64	0.54	0.11	0.00	135
Butanol	0.85	0.11	0.16	0.60	36
Heptanol	0.98	0.04	0.16	0.78	12
2-propanol	0.94	0.71	0.22	0.00	175
2-butanol	1.25	0.25	1.00	0.00	70
2-methyl-2-propanol	1.03	0.73	0.30	0.00	157
2-methyl-2-butanol	1.82	0.07	1.51	0.24	31

redissolve (Schwertmann & Cornell, 1991). Under these conditions, particle bridging is encouraged, which in turn tends to stabilise surface area due to the formation of small regular particles which are loosely packed leaving low voidage (Trimm & Stanislaus, 1986), *i.e.*, decreasing the extent of mesoporosity but increasing the microporosity of the material.

Cormack and co-workers (1980) also indicated that by increasing the proportion of alcohol, the development of mesopore structures is favoured. Mesoporosity is especially well-defined in gels obtained from propanol and propan-2-ol and it seems that these solvents promote aggregation-cementation. On the other hand, the results in Table 2.9 indicate that a more open pore structure is produced in certain other solvents, *i.e.*, butanol and heptanol, and it would appear that these solvents favour particle growth rather than aggregation-cementation.

2.5.9 Effect of different additives and their mechanistic behaviour

White and co-workers (1989) investigated the effect of addition of various additives during neutralisation of aluminium nitrate with ammonia, as shown in Table 2.10.

Table 2.10 Physical properties of aluminas precipitated in the presence of additives (after White *et al.*, 1989).

Additive	Molar ratio additive : Al^{3+}	BET surface area[k] (m^2/g)	Pore volume[k] (cm^3/g) 3.6 - 10 000 nm
None	0.00	247	0.27
Acetone	8.48	230	0.26
Methanol	15.90	239	0.26
Ethanol	10.10	221	0.29
Propanol	8.94	228	0.29
Butanol	6.06	261	0.16
Phthalic anhydride	0.14	275	0.10
Propanoic acid	0.14	242	0.27
Succinic acid	0.12	240	0.15
Benzoic acid	0.03	208	0.28
Benzoic acid	0.16	261	0.29
Benzoic acid	0.17	272	0.31
Ethylene glycol	13.28	237	0.46

[k] Samples aged for 24 h at room temperature and calcined at 500 °C for 5 h.

Alcohols added before precipitation (Table 2.10) had little effect on the resulting surface area with the exception of butanol, where pore volume was approximately halved. However, the higher surface area indicates that significant microporosity developed in this alumina. White *et al.* (1989) attributed this to the higher adsorption potential of butanol, which favours replacement of water at the solid-liquid interface as the precipitate is formed, which in turn favours higher surface area. This probably leads to formation of a series of smaller crystallites surrounded by butanol. As a result,

microporosity was enhanced as shown by the higher surface areas.

Addition of different organic acids before precipitation was also examined by White *et al.* (1989) and indicated in Table 2.10. Propanoic acid had little effect on surface area or pore volume and benzoic acid only had an effect at high concentration. Succinic acid and phthalic anhydride were found to reduce pore volume. Surface areas remained about the same, or increased slightly, which may indicate the development of microporosity.

White *et al.* (1989) explained these phenomena as follows. With two functional groups (phthalic anhydride and succinic acid), the chance of particle-particle bridging is enhanced, giving a structured precipitate of lower mesoporosity in which the surface area of each particle is available. These two additives showed the expected effect of low pore volume and high surface area. With one functional group (propanoic acid and benzoic acid), the water 'solvent barrier' would be replaced by an organic group surface coating, and bridging would be expected to be less favoured. The latter two additives showed some increase in surface area (higher microporosity) but no decrease in mesoporosity. The authors argued that the acids were acting more as a filler additive than butanol, and hence maintained the mesoporosity.

The interaction of additives, based on their chelating behaviour, with aluminium or aluminium hydroxide is also reported by various investigators. According to Kwong and Huang (1975, 1979), Violante and Violante (1978, 1980), Violante and Huang (1985), Nagai *et al.* (1991), and Tayaa and co-workers (1992), complexing agents, such as carboxylic acids, can influence crystallisation of $Al(OH)_3$, and finally alumina phases, by displacing hydroxide and H_2O groups. Nagai *et al.* (1991) described this chelating process as follows: the pH value at which precipitation starts is determined by complex formation between the additive and the Al^{3+}-carrying ion. As the pH increases, Al^{3+} aqua ions become polynuclear complex ions by olation (M-OH + M-OH_2 → M-OH-M + H_2O (M: metal ion)) and oxolation (M-OH + M-OH → M-OH-M + H_2O) and finally precipitate by the condensation of the polynuclear complex ions as aluminium hydroxide (see Section 2.3).

Kwong and Huang (1975, 1979) and Violante and Violante (1980) demonstrated that the stronger the chelating power of organic anions, the easier was the formation of pseudoboehmite or amorphous material and the more stable should be their occupation of the coordination sites of aluminium and therefore the greater should be their disruptive influence on hydrolysis of terminal groups of aluminium ions (see Section 2.3) and subsequent precipitation of aluminium. The authors also found that the higher the organic acid concentration or the greater the affinity of chelating anions for aluminium, the greater their capacity to occupy the coordination sites of aluminium and distort the arrangement of the unit layers. Violante and Violante (1980) reported that the effectiveness of an organic anion increased with increasing concentration and decrease in pH value. However, according to Bailar (1956), stabilisation due to chelation decreases rapidly as the chain of the ligand is lengthened. According to Parfitt (1978), organic ions are specifically adsorbed on aluminium hydroxides, and the sorption of these anions could be described by a sorption-pK_a-pH-relationship.

Violante and Huang (1985) demonstrated that the effectiveness of chelating ligands in promoting formation of noncrystalline products over crystalline aluminium hydroxide polymorphs at pH $\leq$ 9, was found to increase in the following order:

succinic < oxalic < citrate < tartaric acids.

These workers concluded that polydentate (such as tartaric acid) and large ligands were more inhibitive than those with fewer functional groups or of smaller size. Violante and Huang (1992) have demonstrated that polydentate ligands in certain concentration ranges inhibited the growth of crystals and, thus, increased the surface area. At higher concentrations these ligands promoted aggregation of the particles of the precipitates and consequently decreased the apparent surface area. These workers also found that aggregation of the particles, initially promoted by organic ligands, still remained after combustion of the ligand.

The greater influence of oxalic acid than succinic acid was explained by Violante and

Huang (1985) by considering that chelate 5- or 6-membered rings (oxalic acid) are more stable than larger ones (succinic acid forms unstable 7-membered rings with aluminium), so that the closer the carbonyl groups, the more active is the bicarboxylate anion. Earl and co-workers (1979) demonstrated that tartaric acid is more strongly adsorbed by aluminous materials or more easily coprecipitates with aluminium than citric acid, whereas citric acid showed a much stronger influence on solubilising aluminium than tartaric acid.

Nagai *et al.* (1991) found that the presence of formic and acetic acid during the formation of aluminium hydroxide gel, resulted in rapid precipitation of the gel and the formation of ultrafine non-spherical particles. According to Bailar (1956), anions such as these can form strong bonds with metals and they often bind two metal atoms together, each oxygen of the carboxyl group linking to a different metal atom. Oxalic and citric acid resulted in slow precipitation and slow particle growth and the formation of spherical particles, or aggregates of spherical particles. The authors concluded that spherical particle formation was due to stabilisation of the Al^{3+} ion by the strong complexing behaviour of these acids. Tayaa *et al.* (1992) observed that a strong complexing agent, such as triethanolamine (chelating through either oxygen or nitrogen (Bailar, 1956)), resulted in amorphous to fine crystalline phases, whereas weak complexing agents, such as acetic acid, resulted in the formation of large crystals. Different experimental conditions used by Tayaa *et al.* (1992) probably explain why the latter findings differ from those found by Nagai *et al.* (1991).

According to Trimm and Stanislaus (1986), an additive can react in two ways. A given additive may possess a particular functional group which influences pore size by, for example, reacting with alumina or aluminium hydroxides as described above. The same additive (or a different material) may also possess bulky functional groups which change pore size merely by the physical separation of particles — the 'steric' or 'space filling' factor. Examples of these mechanisms are found, for instance, with acids and polymers. The effect of acids, which resulted in controlling small pore sizes, is due to peptisation where particles are assembled into aggregates on addition of the acid after formation of

the gel. As a result of this, according to Trimm and Stanislaus (1986), there is a degree of long-term order in the deposit and larger pores are minimised. The pore produced is characteristic of the interparticle space and good agreement is observed with pore sizes produced at about 2 to 7 nm in the absence of additives. One exception involves polycarboxylic acids, where the size of the group attached to the acid function is sufficient to introduce some larger pores by a 'space filling' mechanism.

'Space filling' can also be expected by using water-soluble polymeric additives (Trimm & Stanislaus, 1986). This was found, for example, with methyl cellulose ethers which produced changes in pore size as a result of 'space-filling' effects. According to Trimm and Stanislaus (1986), polymers can prevent the collapse of gel structure under surface tension forces produced during drying. The main role of polymers is to stabilise and flocculate colloidal suspensions. These suspensions are stable because of repulsive interactions between similarly charged electrical double layers, or as a result of particle-solvent affinity. Additions to such systems can have different effects.

Apart from the polymers, other materials, such as carbon (Lim *et al.*, 1982), sawdust, cotton linters, linters from various types of synthetic fibres such as polyimids, polyesters and polyacrylonitriles, and mixtures of tall oil[1] (Stiles, 1987), vegetable stearine and starch (Sanford *et al.*, 1976), and humic acid (Slaugh, 1985) have been incorporated into aluminium hydroxide during its preparation. Pores formed by burnouts are usually orders of magnitude larger than pores formed by dehydroxylation. Hot spots can alter the properties of the material (Stiles, 1987), which imposes restrictions on their use.

Methods such as extrusion, molding, disc pelletisation, oil drop procedures, and spray drying can produce other shapes. The first two methods usually produce cylindrical shapes, whereas spheres are made by the latter three procedures (Oberlander, 1984).

[1] According to Niesen (1940), tall oil consists of mixtures of *cis*-oleic (15 - 22.7%), linoleic (71.3 - 79%) and linolenic acids (6%).

Trimm and Stanislaus (1986) have compiled a list (Table 2.11) of effects of various additives on the gel and pore structure of alumina formed by calcination. They suggested which additives to use to control pore size in alumina as indicated in Table 2.12. It is, therefore, apparent that additives influence either (i) crystallinity, as well as packing thereof, of formed aluminium hydroxides, which, in turn, determine the size of pores formed especially in the mesopore and micropore size range, or (ii) act as space-fillers which influence macroporosity. As an overall result, the interaction of these additives will determine the surface area and overall porosity of the material.

2.6 EXHAUST CATALYSTS

2.6.1 History

E. J. Houdry (1956) pioneered the monolith support to oxidise exhaust fumes from waste gas. His catalytic unit consisted of an array of ceramic (porcelain) rods and discs with drilled holes, which had a high surface area alumina coating containing a small amount of dispersed platinum metal. Legislation in the USA in 1970 required automobiles to be equipped with catalytic mufflers or converters. The most successful designs are the ceramic monolithic honeycomb structure, γ-alumina wash coat material, and Pt-Rh-(Pd)/CeO_2/γ-Al_2O_3 catalyst[2].

2.6.2 Construction of monolithic exhaust catalysts

2.6.2.1 Ceramic monolith

Currently, the ceramic monolith, produced from cordierite ($2MgO\text{-}2Al_2O_3\text{-}5SiO_2$), is the most popular commercial product. A cellular design provides the following benefits (Kummer, 1980; Bensalem & Ernst, 1982; Taylor, 1984; Lachman & McNally, 1985; Howitt, 1987; Kainer & Reh, 1991):

[2] Palladium is sometimes included together with the other two metals.

Table 2.11 Effect of additives to the gel on the pore structure of alumina formed by calcination (after Trimm & Stanislaus, 1986).

Additive	Concentration	Effect on pore radius in alumina
Nil	-	2 - 7 nm depending on particle agglomeration and shape
ACIDS various peptising nitric acid polycarboxylic acid containing 2 - 22 C atoms	various > 5% 0.1 - 15 wt%	monodisperse 5 nm monodisperse 5 nm elimination of most pores > 10 nm plus creation of some macropores
ALKALI ammonium bicarbonate ammonium carbonate or bicarbonate	HCO_3^-/ Al_2O_3 = 0 - 6 15 - 22%	mean value increases from 2.4 to 13.4 nm 70% of volume in 2 - 15 nm range
POLYMERS polyethylene oxides polyethylene glycols	40 wt%	All polymer additives may show some increase in macroporosity as a result of 'space filling' effects. Other effects observed are: low molecular weight polymers cause pores in the range 20 - 1000 nm radius to disappear and pores in the range 2 - 20 nm to increase; high molecular weight polymers cause size broadening in the range 5 - 1000 nm range.
polyethylene glycols polypropylene glycols polyethylene amines (2-4 monomer units)	polymer:alumina= 0.5 - 4	increase in 5 - 50 nm
ethylene oxide (EO)	EO:Al halide =1.5 - 2.0	maximum in pore size distribution at 5 - 14 nm or 5 - 10 nm
polyacrylamide polyvinyl alcohols	*ca.* 10%	increase in radii over the range 5 - 1000 nm large increase in pore volume
methyl cellulose ethers	< 40 wt%	marked increase in pore radii > *ca.* 8000 nm
mixture of polyethylene glycol and methyl cellulose	*ca.* 50%	additive as per the two additives individually increase in 2 - 100 nm pores and in 8000 nm pores

- adaptability to the extrusion process;
- thermal shock fracture resistance through an inherently low thermal expansion coefficient of 8 - 12×10^{-7} $°C^{-1}$. [The material exhibits a directed linear thermal expansion which is due to the fact that the *c*-axis of cordierite modifications may even exhibit a negative expansion, whereas the *a*- and *b*-axes remain positive (Lachman *et al.*, 1981)];

Table 2.12 Control of pore size in alumina (after Trimm & Stanislaus, 1986).

Pore properties required in alumina. Values of range of pore radius	Nature of control step in preparation procedure
PORES UP TO 50 nm monodisperse 2 - 7 nm	carefully control precipitation and ageing using ammonia as precipitant
bidisperse 2 and 5 nm with some larger pores	as above using urea as precipitant
monodisperse 2 - 30 nm narrow pore size distribution	swing pH during ageing
minimise pores ca. > 10 nm maintain pores 2 - 10 nm	a) peptise boehmite using one of many organic or inorganic acids before calcination b) add low molecular weight polyethylene oxides or glycols to boehmite
as above, but also introduce some macropores	add polycarboxylic acids to boehmite
monodisperse 5 - 15 nm	add ethylene oxide to boehmite
monodisperse 13 - 15 nm	add ammonium bicarbonate to boehmite
increase pore size over 5 - 1000 nm	a) add high molecular weight polyethylene oxides or glycols to boehmite b) add polyacrylamide or polyvinyl alcohol to boehmite c) sinter alumina by controlled calcination
PORES > 50 nm control size	use methyl cellulose ethers or melamine. Expect pore size to be the same as particle size of filler material. Other additives may be used with care.

- a melting point of 1460 °C;
- porosity and pore size distribution for catalyst coating application (30 - 35% open porosity and 4 - 15 μm median pore size). [It is important that a large fraction of the porosity has relatively large pores (10 μm) to ensure good adhesion of a high surface area wash coat to the monolith (Houdry, 1956; DeLuca & Campbell, 1977), otherwise the catalytic film may flake off];
- sufficient crush strength and low vibration attrition for assembly into the converter containers and to endure the rigours of automotive use, respectively;
- raw materials are (a) economical, (b) readily available, (c) have acceptable firing properties;
- inertness to catalysts and to oxide coatings used with it;
- fast heat up;

- honeycomb structures guarantee uniform distribution of gas flow through catalyst module;
- low back pressure, which reduces power loss from engine in comparison with packed-bed reactors;
- resistance to corrosion; and
- resistance to deposition of carbon and dust.

The main drawback is the risk of melting or breaking which occur at high temperature.

Ceramic honeycomb monoliths have been produced in various cell densities and geometries (Howitt, 1987). The square cell shape with 64 cells/cm^2 is the most widely used monolithic shape. Geometric properties of this shape are given in Table 2.13.

Table 2.13 Geometric properties of a square honeycomb monolith with 64 cells/cm^2 (after Howitt, 1987).

Web thickness (mm)	0.165
Hole size (mm)	1.105
Geometric surface area (cm^2/cm^3)	165.35
Density (g/cm^3)	0.411
Open area (%)	76

The internal surface area of the substrate is relatively low (5 - 10 m^2/g) and, therefore, a wash coat of a catalyst dispersed on activated γ-alumina is deposited on the substrate (Young & Finlayson, 1974).

2.6.2.2 γ-Alumina wash coat properties and application techniques

According to Nortier and Soustelle (1987), the following catalyst properties are required for improved mass transfer from a gas stream to the catalytic material surface:

- a high degree of macroporosity (diameter > 0.1 μm) facilitates intraparticular diffusion, whereas micropores (diameter < 20 nm) are necessary to develop a high surface area;
- increasing the porous volume by addition of macropores is also an advantage for cold start efficiency. This decreases the total heat capacity of the catalytic bed and enables the catalyst to attain its lightoff temperature (*i.e.*, temperature needed to reach 50% conversion or T_{50}) more quickly.

Pereira *et al.* (1988a) recommended the following wash coat properties:

- a thickness in the range 30 to 80 μm;
- a total pore volume in the range 0.60 to 1.80 cm^3/g wash coat;
- a micropore volume in the range 0.35 to 0.60 cm^3/g wash coat;
- a micropore radius below 6 nm and preferably above 3 nm; and
- a surface area between 125 to 250 m^2/g wash coat.

Coating of the honeycomb involves either dipping it into a slurry or dispersion of the precursor alumina (Kummer, 1980; Oberlander, 1984; Nortier & Soustelle, 1987; Blachou *et al.*, 1992), or using a vacuum method to draw up a predetermined amount of slurry into one half of the skeletal structure then inverting the structure and coating the other half (Shimrock *et al.*, 1985). Reed *et al.* (1980) recommended an alternative vacuum method to draw the slurry through the monolith. Larger scale commercial coating processes are described by Hoyer *et al.* (1976), Reed *et al.* (1980), and Shimrock *et al.* (1985).

The amount of alumina which can be deposited on the honeycomb is a function of the slurry concentration and viscosity and the surface texture and porosity of the honeycomb material itself (Oberlander, 1984; Pereira *et al.*, 1988b; Blachou *et al.*, 1992; Philippopoulos, 1992). Texture and porosity properties can promote bonding of alumina and substrate. Control of viscosity is important; if it is too low, insufficient alumina will be deposited on the honeycomb, whereas if it is too high, excess alumina may be deposited and clog some of the channels. The suggested viscosities are 200 to 1000 cP.

The pH of the slurry should preferably be acidic (pH < 5) and is obtained by the use of either organic acid (acetic) or inorganic acids (hydrochloric or nitric) (Hindin & Dettling, 1979; Blachou *et al.*, 1992). Low pH values cause alumina to peptise more readily (Retallick, 1988). Aluminium nitrate also promotes bonding to the substrate. Alumina sol is also used as a binder for adhesion (Kato *et al.*, 1980).

The amount of alumina wash coat added is usually 15 - 30% by weight of the honeycomb and the overall BET surface area is 15 - 30 m^2/g (Gandhi & Shelef, 1987; Larsson *et al.*, 1987), whereas typical solids in the slurry comprise 30 - 45 wt% (Rhodes, 1978; Hindin & Dettling, 1979; Retallick, 1988). A typical specification for wash coats is given in Table 2.14.

Table 2.14 Typical specification for wash coats (after Anon., 1988).

Compound or property	Mass %
Al_2O_3	70.7
Loss on ignition	29.3
C	0.3
SiO_2	0.005
Fe_2O_3	0.004
Na_2O	0.004
TiO_2	0.14

Retallick (1988) described a number of wash coat formulations: (i) alumina composite and (ii) ceria (which acted as stabiliser and promoter - see Section 2.6.2.3). The composition of these two types of formulation is listed in Tables 2.15 and 2.16. Two important design properties of the alumina wash coat layer are the prevention of (a) cracking, and (b) peeling off, of the wash coat layer. Cooper (1983) found that calcination of the wash coat structure resulted in severe cracking with potential loss of the catalyst layer from the underlying substrate. Structural stabilisers, such as ceria and/or BaO, La_2O_3 and ZrO_2, therefore have to be incorporated into wash coats to prevent these effects.

Table 2.15 Alumina compositions used by Retallick (1988).

Compound	Parts by weight
Al_2O_3 calcined at 400 - 500 °C	20
Al_2O_3 calcined at 700 - 900 °C	80
Nitric acid (concentrated)	7
Water	120

Table 2.16 Ceria/Al_2O_3 compositions used by Retallick (1988).

Compound	Weight (g)
γ-Al_2O_3	48
Alumina made by calcining alumina sol at 400 °C	17
Cerium oxide	21
Nitric acid (concentrated)	6
Water	50

Plate 2.1 shows a typical monolith carrier and catalytic substrate at various stages of preparation.

2.6.2.3 Role of ceria

According to Kummer (1980), Su *et al.* (1985), Diwell *et al.* (1991), and Yamada *et al.* (1993) ceria acts as an oxygen storage component, which is manifested in the ability of ceria-containing catalysts to store oxygen under lean operating conditions and release it under rich conditions, during air to fuel (A/F) ratio variations, by reaction with CO, H_2 and hydrocarbons. An enhanced oxygen-storage capacity can be generated by an increase in the ceria dispersion on alumina, achieved by precious metal addition (Miki *et al.*, 1990).

According to Ozawa and Kimura (1990) and Church *et al.* (1993), addition of ceria

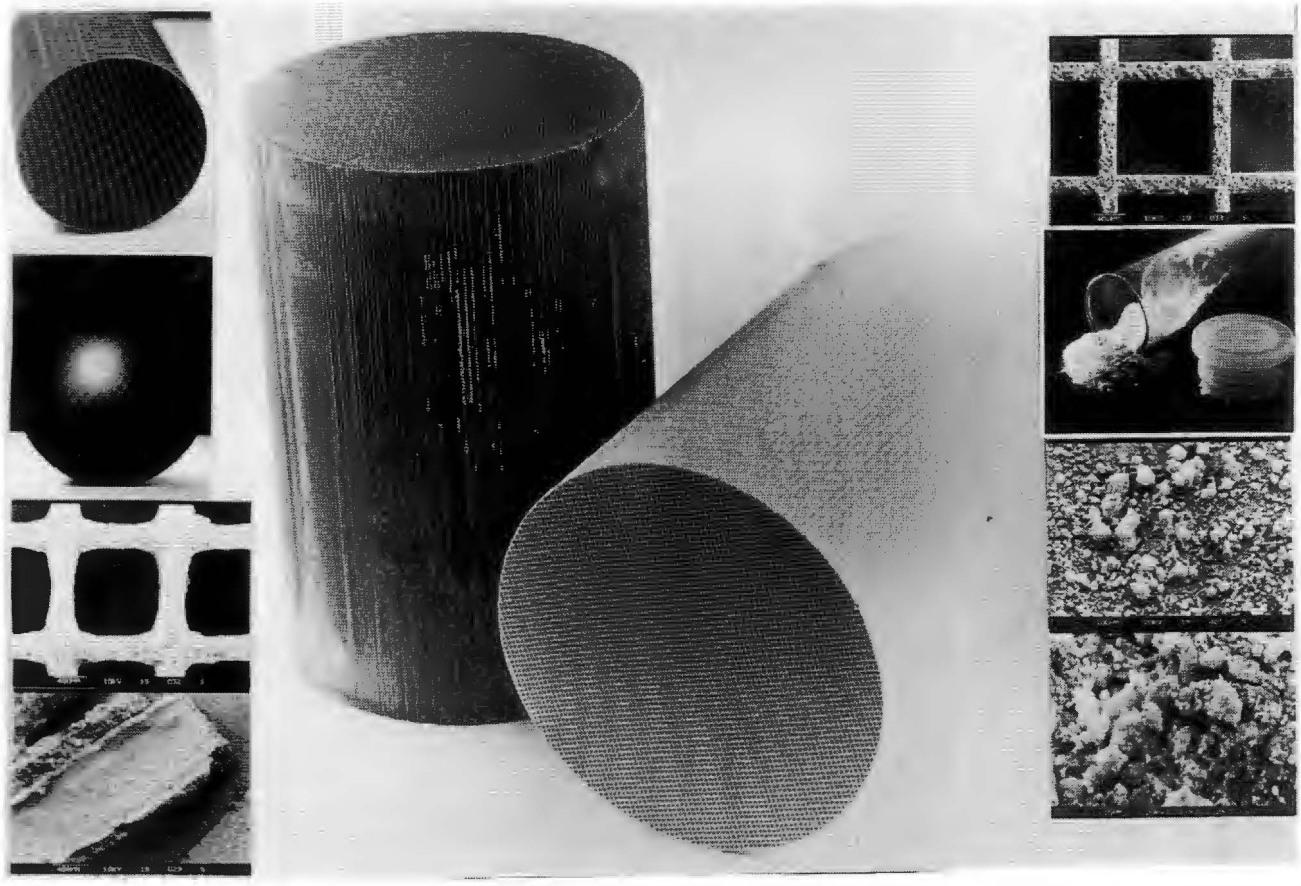

Plate 2.1 Monolith carrier and catalytic substrate at various stages of preparation.

stabilises the alumina support against sintering. It reduces grain growth of active alumina at high temperatures (1000 to 1200 °C) and decreases the rate of transformation to α-Al_2O_3. Overloading of cerium decreases the surface area of the alumina because of the growth of CeO_2 particles. Kolbrecka *et al.* (1995) have shown that the addition of ceria during coprecipitation of hydroxides from solutions of Ce and Al salts results in the most effective thermal stability of alumina. Other rare earth oxides such as lanthana and baria have even higher stabilization effects on alumina compared with ceria (Harrison *et al.* (1988), Church *et al.* (1993)).

Ceria also stabilises noble metal dispersion. According to Diwell *et al.* (1991), addition of ceria resulted in stabilisation of Pt dispersion up to temperatures of 700 to 800 °C, indicating significant Pt-CeO_2 interaction, most probably through the formation of a

surface complex involving Pt^{2+}-O^{2-}-Ce^{4+}. Structural stabilisation of Pt by ceria is due to a stronger interaction than that which exists between Pt and Al_2O_3. This was also confirmed by Raman studies by Brogan and co-workers (1994). According to Nunan *et al.* (1992), the degree of Pt/Ce interaction, and thus activity after catalyst activation, is controllable by varying the CeO_2 crystallite size. Decreasing the CeO_2 crystallite size results in greater Pt/Ce interaction and greater activity for both fresh and aged catalysts. For fresh Pt catalysts, metal dispersions decreased with increasing CeO_2 content (Summers & Ausen, 1979). Fresh Pt catalysts prepared by Summers and Ausen exhibited average Pt particle diameters ranging from 1.1 to 2.8 nm as CeO_2 loading increased from 0 to 13 wt%. The extent of Pt-oxygen bonding of the Pt and the support is a strong function of Pt dispersion. Katzer and Sayers (1978) have shown that when Pt is highly dispersed ($\approx$100%) on Al_2O_3, the Pt is electron deficient, *i.e.* oxidized. At larger particle sizes ($\approx$2 nm) the Pt is present primarily as the bulk metal. In the presence of a powerful oxidizing agent such as CeO_2, even large particles of Pt ($\geq$ 2 nm) might be oxidized. The oxidation of CO occurs via the donation of oxygen from surface oxide ions from ceria and the oxygen is replaced via oxidized Pt (Golunski *et al.*, 1995).

Small quantities of ceria (0.6 - 1.3 wt%) enhance oxidation of CO over fresh Pt catalysts (Kummer, 1980), whereas Summers and Ausen (1979) found that CO conversion activity greatly deteriorates with increasing ceria quantities. According to Yao (1984) and Lööf *et al.* (1991), ceria lowers the activation energy of the CO oxidation reaction. According to Yao and Kummer (1987), 3 wt% ceria causes a $Pt/CeO_2/Al_2O_3$ catalyst to exhibit a higher T_{50} during CO oxidation than with 10 wt% ceria.

2.6.2.4 Impregnation of γ-Al_2O_3 with platinum salt

Hexachloroplatinic acid adsorbs strongly onto γ-alumina at pH < 3.5. Several investigators (Heise & Schwarz, 1985; Ruckenstein & Karpe, 1989) determined the effect of pH, ionic strength and coimpregnants during impregnation of hexachloroplatinic acid onto γ-Al_2O_3.

Santacesaria and co-workers (1977) showed that adsorption of hexachloroplatinic acid proceeded by an acid attack of alumina (due to a highly acidic solution of hexachloroplatinic acid), with dissolution of some surface aluminium ions:

$$Al_2O_3 + 6\ H^+ \rightarrow 2\ Al^{3+} + 3\ H_2O \qquad \text{..... (4)}$$

The Al^{3+} ion is easily readsorbed by alumina, but the $PtCl_6^{2-}$ anion is not exchanged, and H_2PtCl_6 is not adsorbed by alumina. The platinum hexachloride ion is adsorbed only after dissolution of Al^{3+}, its partial hydrolysis with formation of $Al(OH)^{2+}$, and readsorption probably through exchange of an OH^- group. The platinum hexachloride ion is adsorbed together with the aluminium cation. The proposed mechanism is given as:

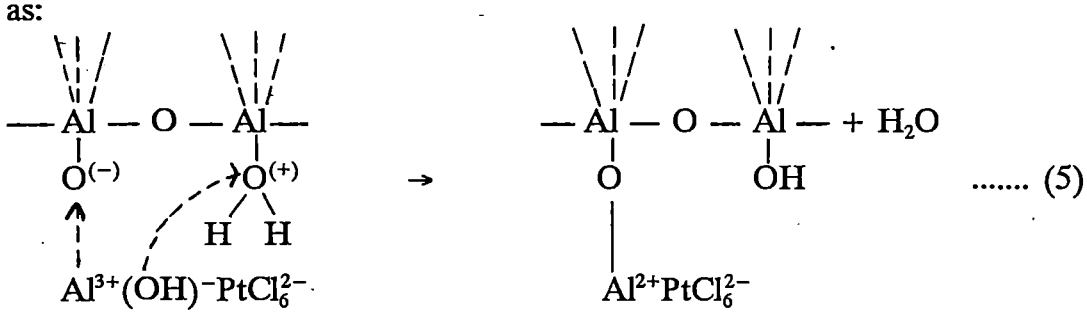

..... (5)

Immobilisation of adsorbed species is accomplished by reduction of platinum hexachloride to metallic platinum.

2.6.3 Carbon monoxide oxidation

Platinum readily oxidises CO to carbon dioxide. Purification of CO is a kinetic problem and therefore catalysts that enhance reaction rates and decrease activation energies are preferable.

According to Wei (1975), Morrison (1977), Ertl (1983), Harold and Luss (1987), oxygen must be adsorbed for the oxidation of CO on platinum. Yoshinobu and Kawai (1995) have found that thermal excitation of adsorbed oxygen species initiate CO oxidation on Pt (111). As soon as CO coverage exceeds a critical value, the sticking coefficient for

oxygen drops steeply and the catalytic reaction practically ceases. For this reason, a temperature of ≥ 147 °C is necessary in order to establish a low enough CO coverage through the adsorption-desorption equilibrium of this species. If CO is adsorbed first to a coverage Θ_{CO} = 1/3, oxygen adsorption is inhibited. The oxidation process is dominated by an interaction between coadsorbed species with CO coverage less than Θ_{CO} = 1/3. This is described by a Langmuir-Hinshelwood adsorption mechanism, especially at low temperatures and high CO concentrations. According to this mechanism, it is the adsorbed oxygen atom, bonded weakly to CO-free portions of the platinum surface, which is the active site for the oxidation reaction and controls the rate of reaction and subsequent catalytic activity. The Langmuir-Hinshelwood mechanism dominates at CO concentrations of approximately > 1%, which correspond to a rich automotive exhaust.

According to Madey *et al.* (1976), the Eley-Rideal mechanism may become more important at high temperatures and low CO concentrations (< ± 1%). This mechanism requires that only one reactant has to be firmly adsorbed on the catalyst surface, while the other has to strike the adsorbate from the gas phase in order to form a bond between them:

$$O\ (adsorbed) + CO\ (gas) \rightarrow CO_2\ (gas) + M, \qquad \ldots\ldots\ (6)$$

where M represents a bare site on the surface.

The oxidation of CO is an exothermic reaction with ΔH°_{298} = -282.6 kJ/mole and practically irreversible up to 1227 °C with a ΔG°_{298} value of -256.7 kJ/mole (Meunier *et al.*, 1987). A competitive backdonation model was proposed by Chang and Huang (1995) which illustrates the mechanism of the light-off phenomenon of CO oxidation over platinum catalysts. According to the orbital theory of CO and O_2 adsorption on a metal surface, the competitive model of charge transfer was proposed. Thus, CO and O_2 molecules simultaneously compete to get Pt dπ electrons for adsorption. The O^{2-} ion was identified as the primary adsorbed oxygen species at temperatures above 200 °C. As the O^{2-} ion carries saturated two-valence electrons, Pt must provide more electrons to form

an O^{2-} ion than other forms of oxygen species. Hence, when the temperature is over 200 °C, Pt backdonates most of its $d\pi$ electrons to the adsorbed oxygen for forming O^{2-} ions. This result will cause the probability of Pt $d\pi$ backdonation to the CO $2\pi^*$ orbital to be dramatically decreased. This decreases the adsorption of CO on the Pt surface so that the Pt surface can provide enough active sites for oxygen adsorption for CO oxidation to proceed. Through this competitive backdonation model, the reaction barrier, *i.e.*, oxygen adsorption is overcome so that the CO oxidation rate dramatically increases.

Various workers, for example Ertl (1983), Gasser (1985), Cameron *et al.* (1986), Razon and Schmitz (1986) and Kaukonen and Nieminen (1989), have studied the interaction reactions between adsorbed and desorbed CO and O_2 on surface sites of Pt during inhibition, instabilities and the oxidation of CO to CO_2. These workers have taken effects such as diffusion, reactant depletion as well as infinite reaction probability into account on the equilibrium window where steady CO_2 formation occurs.

2.6.4 CO oxidation kinetics

Voltz and co-workers (1973) expressed the oxidation kinetics of CO on a Pt/Al_2O_3 catalyst in terms of Hougen-Watson kinetics, which accounted for the fact that high CO concentrations led to inhibition of the oxidation reaction. The reaction rate exhibits a negative first-order dependence on reactant concentration of the form:

$$r_{CO} = -k_r[CO][O_2]/R(\theta) \qquad \text{..... (7)}$$

where k_r is the intrinsic rate constant (1/s), [CO] and $[O_2]$ are the CO and O_2 concentrations (mole%), respectively, and $R(\theta)$ is a resistance term which includes the inhibition effect on the reaction rate.

According to Wei and Becker (1975), when oxygen is in stoichiometric excess, its concentration can be included in a parameter K, where K is a reaction rate constant (1/s) $= k[O_2]$.

The resistance term $R(\theta)$ (Voltz *et al.*, 1973) is given by:

$$R(\theta) = [1+k_a[CO]]^2, \quad \text{..... (8)}$$

where k_a is an adsorption rate constant (1/mole% CO) for CO and its temperature dependence is expressed by the Arrhenius equation:

$$k_a = k_a^0 e^{[-(E_a/R)/(T)]}, \quad \text{..... (9)}$$

where k_a^0 is a frequency factor for k_a, and T is the catalyst surface temperature (K). Typical values for these parameters were determined by Voltz and co-workers (1973), Koberstein and Wannemacher (1987), and Hegedus *et al.* (1977) and are given in Table 2.17 for the temperature range from 200 to 500 °C.

Voltz and co-workers (1973) also indicated that the oxidation rate of CO increases with increasing temperature, whereas the adsorption constants decrease with increasing temperature. This means that inhibition effects decrease with increasing temperature.

Table 2.17 Typical inhibition kinetic parameters for CO oxidation, as determined by various investigators.

Parameter	Voltz *et al.* (1973)	Koberstein & Wannemacher (1987)	Hegedus *et al.* (1977)
k_a^0 (m^3/mol)	0.655	0.36	0.45
E_a (J/mol)	7990	16000	8368
Temperature range (°C)	200 - 500	< 250	< 500

CHAPTER 3. EFFECTS OF ADDITIVES USED TO CONTROL THE PORE SIZE DISTRIBUTION OF γ-ALUMINA SUPPORTS

3.1 INTRODUCTION

Controlling pores in γ-alumina is pivotal to the design of catalyst carrier materials. One method of generating pores is by means of additives and their subsequent removal during calcination of the intermediate aluminium hydroxide. The literature is not clear concerning the effect of organic additives on the porosity and surface area of γ-alumina prepared from aluminium nitrate, ammonia and organic additives. In this chapter, an attempt is made to correlate surface properties of γ-alumina with properties of the additives.

Compounds used as additives include (i) ammonium salts of certain organic acids, (ii) alcohols (containing one OH-group), (iii) glycols or polyols (containing more than one OH-group), (iv) monocarboxylic acids (containing one acid group (COOH)), (v) di- and tricarboxylic acids (containing two or three acid groups), (vi) hydroxycarboxylic acids and (vii) certain fatty acids (comprising long hydrocarbons of chain lengths C_{16} - C_{18}). *The γ-alumina prepared from these additives will be compared to standard γ-alumina prepared from aluminium nitrate and ammonium hydroxide.*

Since these additives differ in size, shape and structure of the molecule and in the number of carbonyl and hydroxyl groups available for bonding with the aluminium cation or the aluminium hydroxide gel, it can be expected that they will influence pore formation in a different manner. Many of these agents have previously been evaluated by other workers in this field (Cormack *et al.* (1980), Kotanigawa *et al.* (1981), Violante & Huang (1985), Huang *et al.* (1989), White *et al.* (1989)). The major differences between this work and those reported in the obtainable literature are primarily the experimental conditions, *viz.* drying temperature and period, final pH and amount of

various organic materials added, and the aluminium precursor used to generate pores in alumina materials.

The specific objectives in using the above additives were:

- To systematize pore-creating effects with those listed in the literature. The pH was maintained at 9, which is close to the iso-electric point of aluminium hydroxide (Kwong & Huang (1979), Dudeney *et al.* (1991)).

- To determine their effects on porosity, surface area, pore volume and pore size, and to compare these properties with those of a standard commercial γ-alumina exhaust catalyst carrier material.

- To evaluate the stabilizing effect of ceria on selected γ-alumina samples.

- To consider pore-forming mechanisms, as described, for instance, by Cormack *et al.* (1980) and White *et al.* (1989), and pore-forming abilities of certain functional groups of organic additives for several additives.

Flow-chart 3.1 gives a layout of the contents of this chapter.

3.2 EXPERIMENTAL METHODS

Aluminium nitrate was used as an aluminium source because the decomposition products are volatile upon calcination. The different organic channel-directing agents (porogens) were added at 30 wt%, unless otherwise stated, of the final alumina present. All additives were mixed with aluminium nitrate solution (37.5 g aluminium nitrate in 100 ml deionised water) prior to neutralisation with aqueous ammonia (25% solution) and controlled to a pH value of 9.0 $\pm$ 0.2. Additives (see Appendix A for purity) which were

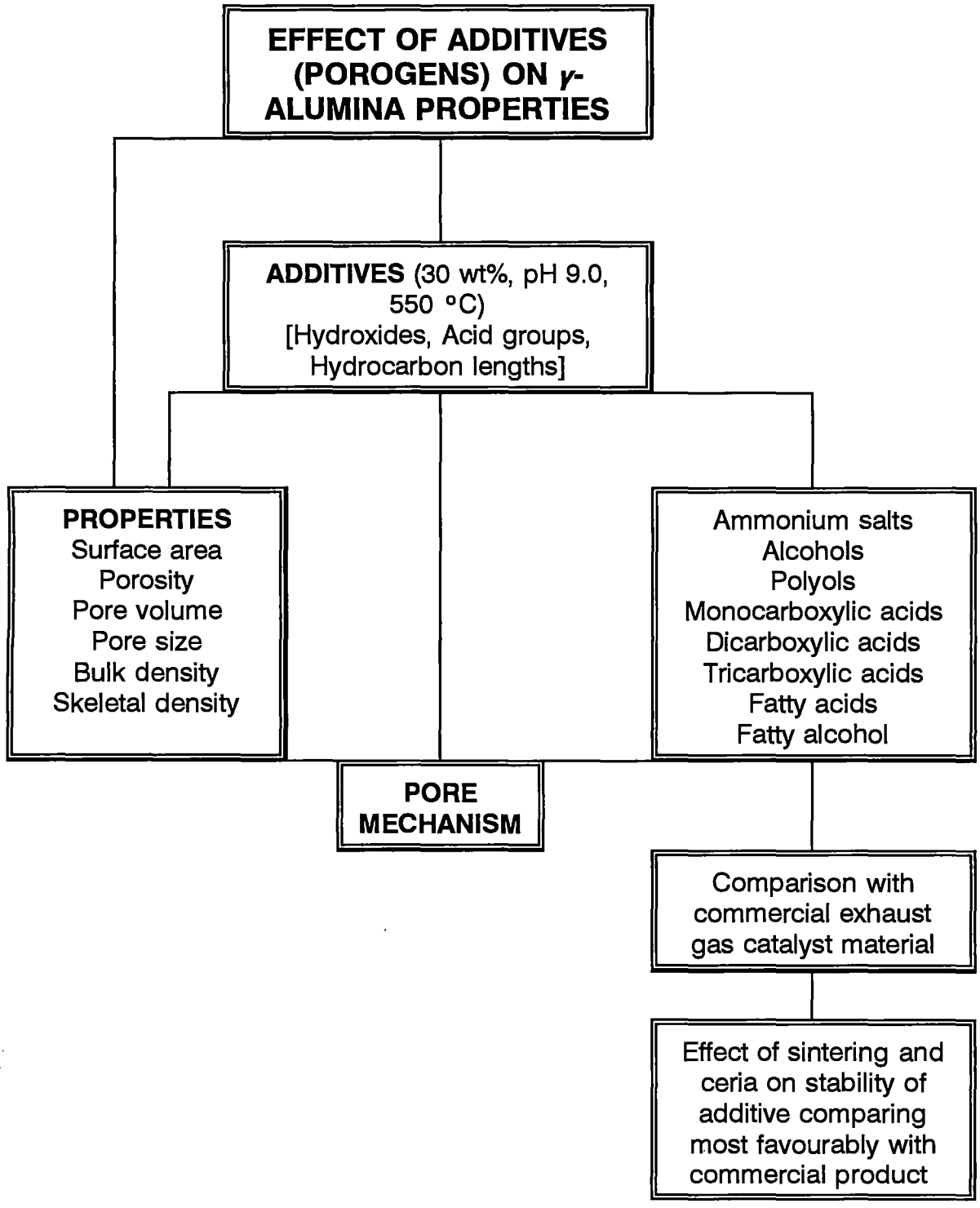

Flow-chart 3.1 Contents of chapter.

not water soluble were dissolved in either 40 ml ethanol[1], diethyl ether or acetone before mixing with aluminium nitrate solution. The aluminium hydroxide gel formed was filtered and washed with 200 ml deionised water to minimise occlusion of ammonium nitrate (byproduct) within the gel. The products were transferred to steel containers and aged at 75 °C for 2 hours. The products were then dried at 120 °C for 4 hours before sintering at 550 °C for 2 hours. Samples were step-heated to 550 °C, as indicated in Table 3.1.

Fatty-acid derived samples were also sintered at 700, 800, 900 and 1000 °C for 2 hours. The respective heating rates were 100 °C/h, 114 °C/h, 129 °C/h and 143 °C/h. Fatty-acid derived gels containing 3 and 11 wt% ceria were prepared by emulsifying the fatty acids with cerium nitrate and aluminium nitrate solutions, followed by neutralisation to pH 9 with ammonium hydroxide. The gels were then processed as described above and calcined at the appropriate temperature.

Additives studied are listed in Table 3.2. Molecular dimensions were calculated by means of the program Hyperchem (© Autodesk, Inc.). The geometric energies of the molecular structures were minimised using the molecular mechanics module MM+.

Pore size distributions were obtained by mercury intrusion using a Quantachrome Autoscan porosimeter and the well-known Washburn equation. A contact angle of 140° was assumed. Pore size distributions were divided into three regions:

$V_{macro} = \Sigma(V_{30}$ to $V_{5000})$, *i.e.*, cumulative volume of pores with radii from 30 to 5000 nm,

$V_{meso} = \Sigma(V_{1.8}$ to $V_{30})$, *i.e.*, cumulative volume of pores with radii from 1.8 to 30 nm,

$V_{micro} = V_t - V_{macro} - V_{meso}$,

[1]Ethanolic, acetone or diethyl ether solutions facilitated emulsion formation during mixing with aqueous aluminium nitrate solution, which was advantageous for homogeneous mixing.

Table 3.1 Step heating during calcining of samples to a final temperature of 550 °C.

Temperature (°C)	Period (h)
25 - 270	1
270 - 370	1
370 - 450	1
450 - 480	1
480 - 520	1
520 - 540	1
540 - 550	0.5
550	2
Cool	± 6

where V_t represents total pore volume measured. This was obtained by subtracting the true volume of the solid, *i.e.*, the reciprocal of true density (measured with a Quantachrome helium stereopycnometer), from the volume of solid and pores. The latter value was obtained from the mercury displacement volume of the sample plus pores, assuming no intrusion of mercury into the pores at atmospheric pressure. Bulk densities were calculated as the inverse of the specific volume of solid and pores as determined by mercury porosimetry. Porosity fractions were calculated as the product of bulk density and total specific pore volume.

Extrapolation was used to estimate pore size distributions in cases where pore sizes, which extended into the micropore size range, were cut off below 1.8 nm due to limitations of the mercury porosimeter. For this purpose, the curves were considered to possess either Gaussian, Lorentzian or a log-normal pore size distribution in the mesopore and micropore interfacial region. Appendix B shows examples of the various types of distribution curves used.

Table 3.2 Properties of additives studied.

Ammonium salts	Monocarboxylic acids	Di- and tricarboxylic acids	Alcohols
formate [1][a] (63, 0.42, 0.25)[b]	formic [1] (46, 0.30, 0.35)	-	methanol [1] (32, 0.28, 0.50)
acetate [2] (77, 0.52, 0.21)	acetic [2] (60, 0.39, 0.27)	-	ethanol [2] (46, 0.41, 0.35)
-	propionic [3] (74, 0.48, 0.22)	-	propanol [3] (60, 0.54, 0.27)
-	-	-	*n*-butanol [4] (74, 0.66, 0.22, EtOH)
-	iso-butyric [4] (88, 0.49, 0.18, EtOH)	succinic [4] (118, 0.67, 0.14, EtOH)	*iso*-butanol [4] (74, 0.54, 0.22, EtOH)
-	-	-	*sec*-butanol [4] (74, 0.57, 0.22, EtOH)
oxalate [2] (142, 0.76, 0.11)	-	oxalic [2] (90, 0.49, 0.18)	-
tartrate [4] (184, 0.91, 0.09)	-	tartaric [4] (150, 0.69, 0.11)	-
citrate [6] (226, 1.00, 0.07)	-	citric [6] (192, 0.69, 0.08)	-
Other: carbonate (96, 0.70, 0.33)	lactic [3] (90, 0.49, 0.18)	maleic [4] (116, 0.68, 0.14)	2-pentanol [5] (88, 0.63, 0.18, EtOH)
	benzoic [6] (122, 0.70, 0.13, EtOH)	adipic [6] (146, 0.89, 0.11)	*n*-hexanol [6] (102, 0.92, 0.16, EtOH)
		sebacic [10] (202, 1.37, 0.08, EtOH)	

Polyols	Fatty acids
glycerine [3] (92, 0.63, 0.17)	palmitic [16] (256, 2.12, 0.06, EtOH)
diethylene glycol [4] (106, 0.87, 0.15)	oleyl alcohol [18] (268, 2.28, 0.06, EtOH)
triethanolamine [6] (149, 0.84, 0.11, EtOH)	*cis*-oleic acid [18] (282, 1.26, 0.06, EtOH)
glucose [6] (180, 0.60, 0.09)	stearic [18] (285, 2.37, 0.06, diethylene ether)
mannitol [6] (182, 1.02, 0.09)	castor oil [18][c] (298, 1.82, 0.05, EtOH)
sucrose [12] (342, 1.03, 0.05)	sunflower oil[c] (266, 1.30, acetone)
	olive oil[c] (282, 1.26, acetone)

Notes:

[a] Value in square brackets presents the carbon number.

[b] First figure in brackets presents the molecular mass in g/mol, while the second figure gives the largest diameter of the molecule in nm. The third figure presents the additive to aluminium molar ratio. Additives that were not water soluble were solubilised with solvents as indicated after the molar ratio.

[c] The properties of the most abundant molecule are cited in the case of mixtures [see Appendix A].

Surface areas were determined by mercury porosimetry at 25 °C and by nitrogen adsorption at -196 °C. A Micromeritics ASAP 2000 surface area analyzer was used to determine the BET 5-point surface area. The samples were degassed at 150 °C for 4 hours before BET analysis was performed.

Scanning electron microscopy (SEM) micrographs were recorded with a Cambridge Stereoscan 250. Samples were mounted and coated with gold-palladium to increase the electronic conductance of the surface before recording of the surface of samples.

X-ray diffraction patterns were obtained using a Siemens powder x-ray diffractometer at 35 kV and 25 mA with Cu-K_α radiation. The samples were pulverised prior to XRD analysis. Crystallite diameter sizes (D) in nm were determined by applying the Scherrer formula (Ganesan *et al.*, 1978), namely

$$D_{\text{half-breadth}} = K\lambda/\beta_D\cos\theta, \qquad \text{..... (1)}$$

where β_D is the half-breadth of the profile in radians corrected for instrumental broadening by using silica as the standard ($\beta_D^2 = \beta_{D_{\text{apparent}}}^2 - \beta_{D_{\text{instrument}}}^2$), λ is the wavelength in Ångstrom, θ is the diffraction angle in radians, and K is a constant close to 0.9.

3.3 RESULTS

It is important to differentiate between micropores that are totally irregular in geometry and micropores that occur in materials such as zeolites. Although micropores in materials that are amorphous to x-ray diffraction, but catalytically similar to ZSM 5, have been reported (Manton & Davidtz (1979), Derouane *et al.* (1981)), this investigation does not attempt to test whether the synthesized materials have controlled regular pore systems or not. Differences in bulk physical properties such as porosity are very small in different molecular sieves, so small effects of porogens on physical properties will not be obvious and channel properties such as configurational diffusion (Weisz, 1973) will not be detected even though they may be present. The micropore region is difficult to

describe quantitatively, however small differences in porogen structures can have subtle differences on support geometries. Although this study is eventually directed towards CO oxidation, where pore geometry is less critical than in organic reactions, it should be borne in mind that no attempts have been made to investigate any differences that sterically controlled reactions may have. The objective here is to produce an improved automotive catalyst support.

3.3.1 Reproducibility of properties

To evaluate reproducibility of preparative procedures (Section 3.2), the samples prepared with organic additives were compared to a standard produced from aluminium nitrate and ammonium hydroxide. γ-Alumina properties were also compared with those obtained by various investigators.

3.3.1.1 Reproducibility of control samples

The physical properties obtained for several γ-alumina samples are given in Table 3.3. With the exception of micro- and macropore volumes, reproducibility of all properties was found to be acceptable[2] after calcination at 550 °C for 2 hours. Variation of micro- and macropore volume is due to limitations of the mercury porosimeter in the micropore region[3]. In the high pressure mode, the porosimeter technique cannot distinguish between voids and true macropores in the macropore region (> 30 nm to $\pm$ 5 μm pore radius, by definition) and therefore treats these as macropores. This is probably more pronounced for particles of < 250 μm diameter.

[2]A correlation coefficient (standard deviation divided by average value) of 5% or less indicates a high confidence in that value. Generally, a 5% correlation coefficient is accepted as falling within experimental error range.

[3]Cut-off point for the high-pressure mercury porosimeter occurs at 1.8 nm, which corresponds to a pressure of 60 000 psi. No attempt was made to utilise the low-pressure mercury porosimeter to obtain properties for larger macropores. Pore sizes up to 20 μm radius can be measured with this latter technique.

Table 3.3 Properties of γ-alumina samples prepared from aluminium nitrate and ammonia.

Sample	Total pore volume (cm^3/g)	Meso= pore volume (cm^3/g)	Micro= pore volume (cm^3/g)	Macro= pore volume (cm^3/g)	ϵ^*	Median pore diameter (nm)	Hg surface area (m^2/g)	N_2 surface area (m^2/g)	Bulk density (g/cm^3)	Skeletal density (g/cm^3)
1	0.336	0.288	0.032	0.016	0.52	5.36	220	217	1.54	3.19
2	0.327	0.275	0.039	0.013	0.51	4.82	233	218	1.55	3.15
3	0.319	0.270	0.034	0.015	0.50	4.97	221	234	1.57	3.13
4	0.332	0.319	0.004	0.009	0.52	5.72	224	235	1.56	3.21
5	0.290	0.277	0.007	0.006	0.47	5.37	216	232	1.64	3.12
Average	0.321	0.286	0.023	0.012	0.50	5.25	223	227	1.57	3.16
Standard deviation	0.016	0.018	0.015	0.004	0.02	0.32	5.7	8.0	0.04	0.03
Correlation coefficient (%)	5.1	6.2	63	32	3.7	6.1	2.6	3.5	2.3	1.1

* porosity fraction

Macropore and mesopore volumes were used to calculate micropore volumes from the skeletal (true) density value (see Section 3.2). These values are therefore approximate and the range of accuracy is acceptable. In general, voids, *i.e.*, unfilled spaces between packed particles, can be considered to occur in the pore size region of > 2000 nm or 2 μm. SEM studies were used to supplement the macropore region data.

The average BET surface area of the alumina samples was 227 ± 8 m^2/g, and the observable total pore volume was concentrated in the 4.8 - 5.7 nm diameter pore size (mesopores, see Figure 3.1), with a value of 0.32 ± 0.02 cm^3/g, representing an overall porosity of 0.50[4] and skeletal and bulk densities of 3.16 and 1.57 g/cm^3, respectively. The skeletal density value corresponded favourably with the value reported by MacZura *et al.* (1978) for γ-alumina, *viz.* 3.2 g/cm^3. Skeletal density values are not discussed further since they were used only as a control that indicated that the same type of alumina was prepared (MacZura *et al.*, 1978); in this case, γ-alumina as confirmed by XRD[5]. Deviations from the value of 3.16 may indicate serious experimental errors.

A high correlation was obtained between mercury porosimeter and N_2 BET surface areas (see Table 3.3), indicating that limited microporosity is present and that pore size distribution curves obtained with the porosimeter are true values. Deviation of this is observed due to either the presence of microporosity or formation of ink-bottle pores.

In Table 3.4 properties of γ-alumina samples prepared by various investigators are listed. Values obtained in this work compared favourably with those obtained by White and co-workers (1989). The differences compared to results of other investigators cited in the table probably arise from different precipitation preparations, as indicated in Section 2.5.

[4]These average values are used when compared with cases where additives were utilised.

[5]Checks were made periodically to confirm the formation of a γ-alumina phase.

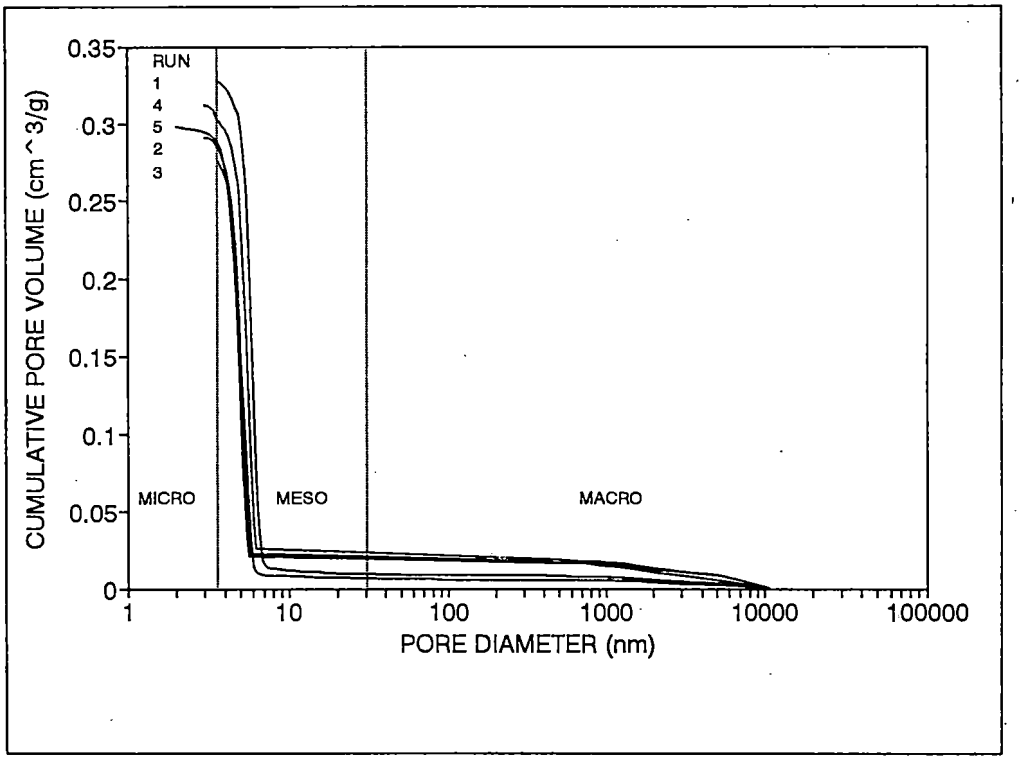

Figure 3.1 Pore size distributions of γ-alumina samples prepared from aluminium nitrate and ammonia [Calcined at 550 °C for 2 h].

3.3.1.2 Reproducibility of samples prepared from selected organic additives

Although the concentrations of additives used by White and co-workers (1989) differ from those used in this study, there are no significant differences between properties obtained with methanol, ethanol, propanol and propionic acid (Table 3.5).

Significant differences are, however, apparent between the sets of *n*-butanol, benzoic acid and succinic acid. The differences probably arise from the different amounts of additives used by the various investigators. Considering this, it is not clear why no differences were observed between the other additives (methanol, ethanol, propanol and propionic acid).

Table 3.4 Physical properties of γ-alumina samples prepared by various investigators.

Investigator(s)	BET surface area (m^2/g)	Total pore volume (cm^3/g)	Pore diameter (nm)	Remarks
Kotanigawa *et al.* (1981)	295	0.96	-	pH 10.4, aged in mother liquor at 90 °C for 2 h, dried at 120 °C for 12 h and calcined at 550 °C for 10 h
Vogel *et al.* (1984)	302	0.32	-	pH 8, dried for 20 h at 120 °C and calcined for 10 h at 500 °C
White *et al.* (1989)	248 ± 6	0.27 ± 0.01	4.8	pH 9, aged 24 h in mother liquor and calcined for 5 h at 500 °C
This work	227 ± 8	0.32 ± 0.02	5.25	pH 9, aged at 75 °C for 2 h then dried 4 h at 120 °C, calcined at 550 °C for 2 h

Table 3.5 Effect of additives on properties of γ-alumina samples as studied by various investigators.

Additive	Surface area (m^2/g)		Mesopore volume (cm^3/g)		Molar ratio additive/Al^{3+}	
	White *et al.*	This work	White *et al.*	This work	White *et al.*	This work
Methanol	239	247	0.26	0.25	15.9	0.50
Ethanol	221	210	0.29	0.25	10.1	0.35
Propanol	228	231	0.29	0.28	8.9	0.27
n-Butanol	261	221	0.16	0.29	6.0	0.22
Propionic acid	239	245	0.27	0.31	0.14	0.43
Benzoic acid	272	236	0.31	0.33	0.17	0.26
Succinic acid	240	265	0.15	0.30	0.12	0.27

It must be borne in mind that, during this investigation, in both cases emulsions were formed when benzoic acid and succinic acid, which were dissolved in ethanol, were introduced into aluminium nitrate solution. This set of data clearly demonstrates that preparation procedures used during the formation history of γ-alumina will influence the final obtainable properties.

3.3.2 Effect of additives on γ-alumina properties

Pore size distributions and surface areas are the main theme of this section, and include all additives with the exception of fatty acids. These will be discussed separately in Section 3.3.2.5. Appendix C contains all data. For the purpose of discussion, those additives that significantly influenced pore properties, together with their corresponding data, are reported in Tables 3.6 and 3.7. Table 3.7 schematically summarises differences in correlation coefficients. For quantitative comparisons relative to the standard, the horizontal arrows indicate no effect, while upward and downward arrows indicate increasing and decreasing mesopore volumes, respectively. The presence of micropores is described in terms of surface area differences. In the description of macropores, mercury porosimetry and scanning electron micrographs are employed.

In general, the porosity is dominated by pore sizes in the mesopore volume range with a sharply defined pore size distribution in this region (see Table 3.8). The discussion will therefore centre on the mesopore volume with the control samples as reference (see Table 3.3).

3.3.2.1 Constant mesopore volume

The first part of Table 3.7 highlights those additives that had no significant effect on mesopore volume. It is concluded that these additives all caused a considerable increase in microporosity and macroporosity and, therefore, total pore volume. In this particular case, macropore volumes are underestimated and, therefore, microporosity overestimated. According to Shields and Lowell (1983), a close agreement between surface areas measured by nitrogen adsorption (BET) and mercury intrusion indicates no micropores (< 3.6 nm in diameter) to be present, and that meso- and macropores are cylindrical in shape. Therefore, the large differences observed between the surface area values of ammonium carbonate and ammonium citrate indicate the presence of micropores (see Table 3.7). An increase in micropore volume will inevitably result in an

Table 3.6 Effect of additives on properties of γ-alumina samples.

Sample	Total pore volume (cm^3/g)	Meso= pore volume (cm^3/g)	Micro= pore volume (cm^3/g)	Macro= pore volume (cm^3/g)	ϵ^*	Median pore diameter (nm)	Hg surface area (m^2/g)	N_2 surface area (m^2/g)	Bulk density (g/cm^3)	Skeletal density (g/cm^3)
Control	0.321	0.286	0.023	0.012	0.50	5.25	223	227	1.57	3.16
Saturated alcohols										
sec-Butanol	0.318	0.218	0.072	0.028	0.50	5.17	184	207	1.59	3.21
2-Pentanol[d]	0.446	0.254	0.094	0.098	0.58	4.62	245	271	1.30	3.07
n-Hexanol	0.346	0.242	0.030	0.074	0.52	4.75	216	245	1.51	3.14
Glycols										
Diethylene glycol[e]	0.381	0.338	0.027	0.016	0.54	5.57	247	260	1.42	3.08
Glycerine[f]	0.368	0.335	0.018	0.015	0.54	5.50	243	248	1.46	3.14
Triethanolamine[g**]	0.517	0.316	0.089	0.112	0.62	5.48	237	249	1.19	3.13
Mannitol[h]	0.429	0.317	0.060	0.053	0.57	5.31	246	241	1.34	3.13
Monocarboxylic acids										
Formic acid	0.299	0.245	0.046	0.008	0.49	3.78	227	253	1.62	3.15
iso-Butyric acid[i]	0.385	0.312	0.038	0.035	0.54	5.14	251	279	1.41	3.09
Lactic acid[j]	0.415	0.250	0.121	0.044	0.56	4.33	243	299	1.34	3.02
Benzoic acid[k]	0.387	0.332	0.018	0.037	0.54	5.66	236	236	1.40	3.05

** Not a true glycol but added as a comparison

continued overleaf

Table 3.6 cont.

Sample	Total pore volume (cm^3/g)	Meso= pore volume (cm^3/g)	Micro= pore volume (cm^3/g)	Macro= pore volume (cm^3/g)	ϵ^*	Median pore diameter (nm)	Hg surface area (m^2/g)	N_2 surface area (m^2/g)	Bulk density (g/cm^3)	Skeletal density (g/cm^3)
Ammonium salts										
Amm. Formate	0.290	0.250	0.039	0.001	0.48	4.88	206	223	1.66	3.19
Amm. Carbonate	0.686	0.283	0.094	0.309	0.67	4.86	204	236	0.98	3.02
Amm. Oxalate	0.364	0.319	0.040	0.005	0.53	5.09	249	244	1.47	3.15
Amm. Tartrate	0.511	0.362	0.069	0.080	0.61	5.58	265	282	1.20	3.12
Amm. Citrate	0.416	0.298	0.062	0.056	0.57	5.20	227	276	1.36	3.15
Di-and tricarboxylics										
Oxalic acid[l]	0.315	0.304	0.006	0.005	0.48	4.86	253	268	1.52	2.92
Maleic acid[m]	0.421	0.291	0.067	0.063	0.57	4.93	248	245	1.34	3.09
Succinic acid[n]	0.480	0.295	0.083	0.102	0.60	4.98	256	265	1.25	3.15
Adipic acid[o]	0.406	0.301	0.037	0.068	0.56	5.22	231	242	1.38	3.14
Tartaric acid[p]	0.545	0.103	0.202	0.240	0.63	3.76	130	223	1.16	3.16
Citric acid[q]	0.404	0.232	0.107	0.065	0.56	4.76	201	275	1.39	3.17
Sebacic acid[r]	0.514	0.185	0.151	0.178	0.60	4.22	181	232	1.17	2.93

[d] $CH_3CH_2CH_2CH(OH)CH_3$
[e] $HOCH_2CH_2OCH_2CH_2OH$
[f] $HOCH_2CH(OH)CH_2OH$
[g] $(HOCH_2CH_2)_3N$
[h] $HOCH_2[CH(OH)]_4CH_2OH$
[i] $(CH_3)_2CHCOOH$
[j] $CH_3CH(OH)COOH$
[k] ϕ-COOH
[l] HOOCCOOH
[m] HOOCCH=CHCOOH
[n] $HOOCCH_2CH_2COOH$
[o] $HOOC(CH_2)_4COOH$
[p] HOOCCH(OH)CH(OH)COOH
[q] $HOOCCH_2C(OH)(COOH)CH_2COOH$
[r] $HOOC(CH_2)_8COOH$
* porosity fraction

Table 3.7 Effect of additives on mesoporosity compared to the control sample.

Sample	Additive: Al^{3+} molar ratio	Total pore volume	Micro= pore volume	Macro= pore volume	ϵ^*	Median pore diameter	N_2 surface area	Bulk density
Unchanged mesopore volume 2-Pentanol	0.18	↑↑	↑↑↑↑	↑↑↑↑	↑	↓	↑	↓
Triethanolamine	0.11	↑↑↑	↑↑↑↑	↑↑↑↑	↑↑	↔	↔	↓↓
Mannitol	0.09	↑↑	↑↑↑↑	↑↑↑↑	↑	↔	↔	↓
iso-Butyric acid	0.18	↑	↑↑↑	↑↑↑↑	↔	↔	↑↑	↓
Oxalic acid	0.18	↔	↓↓↓↓	↔	↔	↔	↔	↔
Maleic acid	0.14	↑↑	↑↑↑↑	↑↑↑↑	↑	↔	↔	↓
Succinic acid	0.14	↑↑	↑↑↑↑	↑↑↑↑	↑	↔	↑	↓↓
Adipic acid	0.11	↑↑	↑↑↑	↑↑↑↑	↑	↔	↔	↓
Amm. Carbonate	0.33	↑↑↑↑	↑↑↑↑	↑↑↑↑	↑↑	↔	↔	↓↓↓
Amm. Oxalate	0.11	↑	↑↑↑	↔	↔	↔	↔	↔
Amm. Citrate	0.07	↑↑	↑↑↑↑	↑↑↑↑	↑	↔	↑	↓

continued overleaf

Table 3.7 cont.

Sample	Additive: Al^{3+} molar ratio	Total pore volume	Meso= pore volume	Micro= pore volume	Macro= pore volume	ϵ^*	Median pore diameter	N_2 surface area	Bulk density
Decreased mesopore volume									
sec-Butanol	0.22	↔	↓↓	↑↑↑↑	↑↑↑↑	↔	↔	↔	↔
n-Hexanol	0.16	↔	↓	↑↑	↑↑↑↑	↔	↔	↔	↔
Formic acid	0.35	↔	↓	↑↑↑↑	↔	↔	↓↓	↔	↔
Amm. Formate	0.25	↓	↓	↑↑↑	↓↓↓↓	↔	↔	↔	↔
Lactic acid	0.18	↑↑	↓	↑↑↑↑	↑↑↑↑	↑	↓	↑↑	↓
Tartaric acid	0.11	↑↑↑	↓↓↓↓	↑↑↑↑	↑↑↑↑	↑↑	↓↓	↔	↓↓
Citric acid	0.08	↑↑	↓	↑↑↑↑	↑↑↑↑	↑	↔	↑	↓
Sebacic acid	0.08	↑↑↑	↓↓↓	↑↑↑↑	↑↑↑↑	↑	↓↓	↔	↓↓
Increased mesopore volume									
Diethylene glycol	0.15	↑	↑	↔	↔	↔	↔	↑	↔
Glycerine	0.17	↑	↑	↔	↔	↔	↔	↔	↔
Benzoic acid	0.13	↑	↑	↔	↑↑↑↑	↔	↔	↔	↓
Amm. Tartrate	0.09	↑↑↑	↑↑	↑↑↑↑	↑↑↑↑	↑	↔	↑↑	↓↓

KEY: Differences in correlation coefficients

↔:	≤ 5% (no difference)	↑↑↑ or ↓↓↓:	> 20% ≤ 30%
↑ or ↓:	> 5% ≤ 10%	↑↑↑↑ or ↓↓↓↓:	> 30%
↑↑ or ↓↓:	> 10% ≤ 20%	* porosity fraction	

increase in surface area (Hegedus, 1980), such as obtained for 2-pentanol, succinic acid and ammonium citrate. Contrary to this is the higher surface area obtained with *iso*-butyric acid.

In general, to conclude, the decreasing bulk densities observed correlated well with increasing micropore and macropore volumes. The increasing porosity fraction ($\in$) supported this contention. Pore size distributions obtained with these additives are shown in Figure 3.2.

3.3.2.2 Decreasing mesopore volume

The second part of Table 3.7 shows those additives that decreased the mesopore volume. It is again noted that these additives caused a significant increase in microporosity and macroporosity. The only exception is ammonium formate which decreased the macroporosity and consequently total pore volume. Tartaric and sebacic acids, as well as 2-butanol to a lesser degree, caused a considerable reduction in mesoporosity. The former acids also reduced the median pore diameter and decreasing bulk densities correlated well with increasing micropore and macropore volumes. The increasing porosity fractions again supported this contention. Surface areas of these two acids remained the same despite the considerable reduction in median pore diameter. The latter were also observed with formic acid.

Surface area increased but median pore diameter decreased with lactic acid. The presence of microporosity induced with lactic, citric, tartaric and sebacic acids is supported by the higher surface areas obtained with the BET method than with mercury porosimetry. Considering this, microporosity observed with 2-butanol, *n*-hexanol, formic acid and ammonium formate was overestimated. Pore size distributions are shown in Figure 3.3.

Table 3.8 Order of increasing pore sizes.

Additive	Additive: Al^{3+} molar ratio	Additive molecular size (nm)	Pore diameter (nm)	Additive	Additive: Al^{3+} molar ratio	Additive molecular size (nm)	Pore diameter (nm)
Tartaric acid	0.11	0.69	3.76	Control	-	-	5.25
Formic acid	0.35	0.30	3.78	Mannitol	0.09	1.02	5.31
Sebacic acid	0.08	1.37	4.22	Propanol	0.27	0.54	5.31
Lactic acid	0.18	0.49	4.33	Ethanol	0.35	0.41	5.32
2-Pentanol	0.18	0.63	4.62	Sucrose	0.05	1.03	5.34
n-Hexanol	0.16	0.92	4.75	*n*-Butanol	0.22	0.66	5.37
Citric acid	0.08	0.69	4.76	Amm. Acetate	0.21	0.52	5.37
Amm. Carbonate	0.33	0.70	4.86	Triethan= olamine	0.11	0.84	5.48
Oxalic acid	0.18	0.49	4.86	Glycerine	0.17	0.63	5.50
Amm. Formate	0.25	0.42	4.88	Glucose	0.09	0.60	5.51
Maleic acid	0.14	0.68	4.93	Propionic acid	0.22	0.48	5.52
Succinic acid	0.14	0.67	4.98	Diethy= lene glycol	0.15	0.87	5.57
Acetic acid	0.21	0.39	5.06	Amm. Tartrate	0.09	0.91	5.58
Stearic acid	0.06	2.37	5.08	Benzoic acid	0.13	0.70	5.66
Amm. Oxalate	0.11	0.76	5.09	Oleyl alcohol	0.06	2.28	5.71
Methanol	0.50	0.28	5.11	Olive oil	0.05	1.26	6.26
iso-Butyric acid	0.18	0.49	5.14	Sunflower oil	0.05	1.30	6.45
sec-Butanol	0.22	0.57	5.17	Castor oil	0.05	1.82	6.60
iso-Butanol	0.22	0.54	5.19	Palmitic acid	0.06	2.12	7.02
Amm. Citrate	0.07	1.00	5.20	*cis*-Oleic acid	0.06	1.26	7.12
Adipic acid	0.11	0.89	5.22				

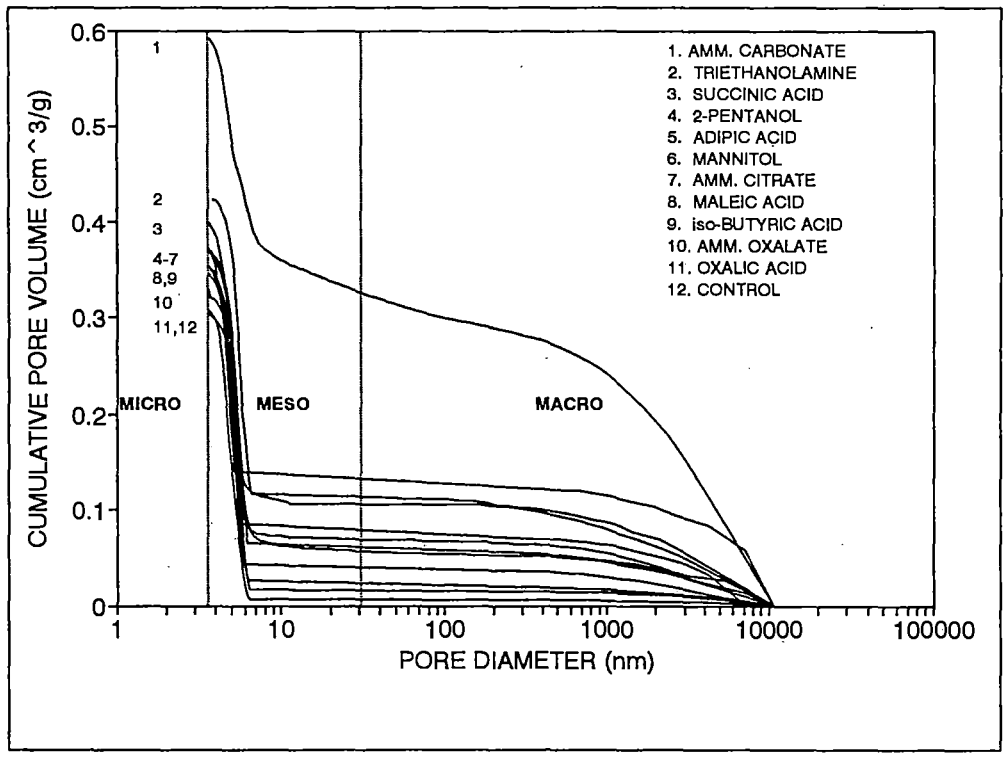

Figure 3.2 Pore size distributions of γ-alumina samples prepared in the presence of additives which resulted in constant mesopore volume.

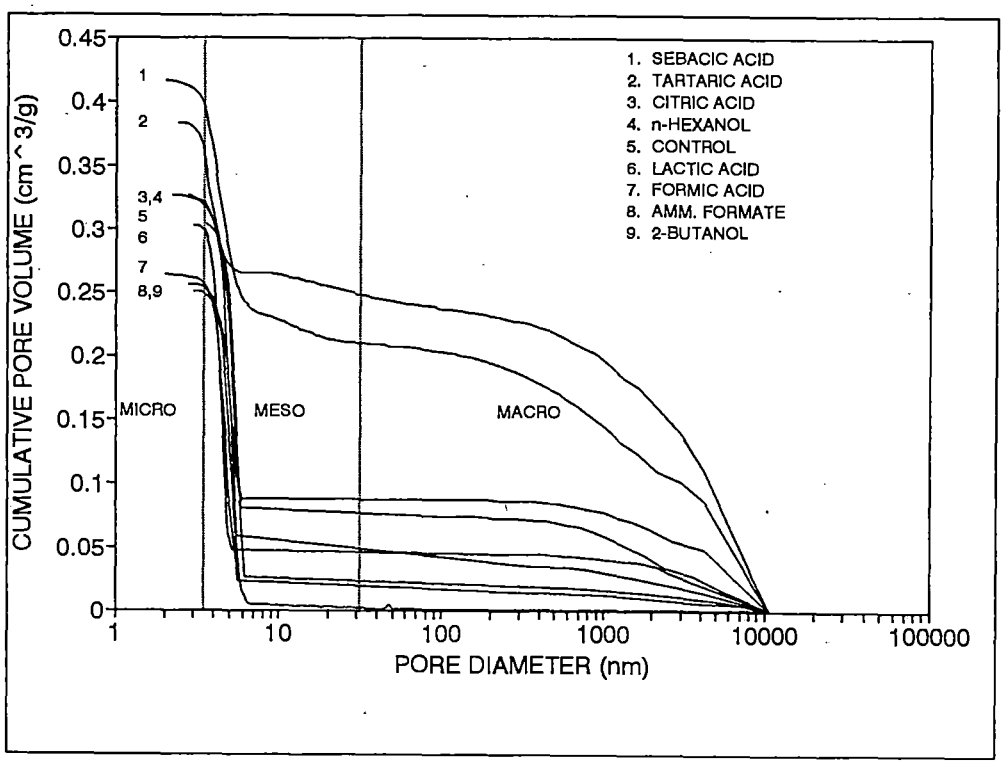

Figure 3.3 Pore size distributions of γ-alumina samples prepared in the presence of additives which resulted in a decrease of mesopore volume.

3.3.2.3 Increasing mesopore volume

Mesoporosity was enhanced with diethylene glycol, glycerine, benzoic acid and ammonium tartrate as shown in Table 3.7. The highest mesopore volume was obtained with ammonium tartrate. This caused the surface area to increase since no significant micropores were detected. All these additives produced cylindrical shaped pores and their pore size distributions are shown in Figure 3.4.

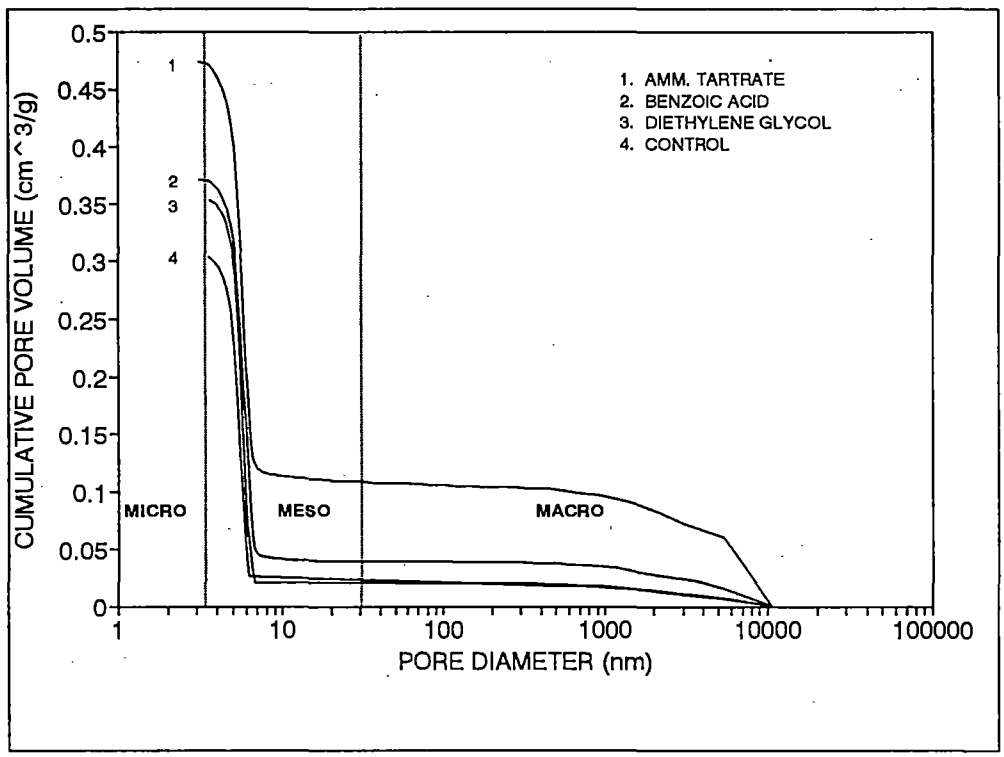

Figure 3.4 Pore size distributions of γ-alumina samples prepared in the presence of additives which resulted in an increase in mesopore volume.

3.3.2.4 Related chemical additive effects on properties of γ-alumina

The additives were grouped into five major classes: (1) acids and their ammonium salts, (2) acids and their related alcohols, (3) dibasic acids with and without double bonds, (4) normal and branched butanols and (5) lactic and propionic acids and propanol.

There were, in general, no major porogenic differences detected within the class of ammonium salts and their homologue acids (specifically ammonium citrate/citric acid, ammonium oxalate/oxalic acid and ammonium acetate/acetic acid) (see Tables 3.6, 3.7 and 3.8). Therefore, their interaction with the alumina gel and the resultant physical properties of the product were similar. Exceptions are, however, ammonium tartrate/tartaric acid and ammonium formate/formic acid. In the former case, significant differences are observed, especially between mesopore, micropore and macropore volumes, pore sizes and surface areas, although their addition molar ratios were similar, *i.e.*, 0.09 and 0.11, respectively. In the latter case, formic acid also caused a significantly lower pore size than ammonium formate, but their addition molar ratios differ, *i.e.*, 0.35 and 0.25, respectively. These latter two sets of additives clearly indicate a difference between pore-forming mechanisms involved for these additives. This will be discussed further in Section 3.4.

Short chain acids are compared with their homologue alcohols (formic acid/methanol, acetic acid/ethanol, propionic acid/propanol and *iso*-butyric acid/*iso*-butanol) in Table 3.9. All surface properties were similar. One exception is the smaller pore size observed with formic acid compared to methanol. Another exception is the significantly higher mesopore volume, total pore volume and surface area observed with *iso*-butyric acid compared to its homologue alcohol.

All surface properties were similar when comparing short chain organic acids with and without double bonds, such as maleic and succinic acids, respectively, with the exception of a slight difference in surface area.

Properties obtained with straight chain butanol differed slightly from branched butanols. When comparing properties obtained with *n*-, *iso*- and *sec*(2)-butanol, it follows from Table 3.9 that most properties were similar except for mesoporosity, which decreased, and macroporosity, which increased, within this order. Although these alcohols had no

Table 3.9 Effect of alcohols and acids on properties of γ-alumina.

Sample	Total pore volume (cm^3/g)	Meso= pore volume (cm^3/g)	Micro= pore volume (cm^3/g)	Macro= pore volume (cm^3/g)	∈	Median pore diameter (nm)	Hg surface area (m^2/g)	N_2 surface area (m^2/g)	Bulk density (g/cm^3)	Skeletal density (g/cm^3)
Methanol	0.334	0.245	0.077	0.012	0.52	5.11	227	247	1.54	3.18
Formic acid	0.299	0.245	0.046	0.008	0.49	3.78	227	253	1.62	3.15
Ethanol	0.321	0.249	0.045	0.027	0.50	5.32	196	210	1.57	3.15
Acetic acid	0.328	0.273	0.046	0.009	0.51	5.06	224	232	1.55	3.14
Propanol	0.307	0.276	0.020	0.011	0.49	5.31	210	231	1.58	3.07
Propionic acid	0.332	0.310	0.015	0.007	0.50	5.52	228	245	1.52	3.06
Lactic acid	0.415	0.250	0.121	0.044	0.56	4.33	243	299	1.34	3.02
iso-Butyric acid	0.385	0.312	0.038	0.035	0.54	5.14	251	279	1.41	3.09
iso-Butanol	0.307	0.259	0.035	0.013	0.49	5.19	206	220	1.60	3.14
n-Butanol	0.341	0.293	0.048	-	0.52	5.37	221	221	1.54	3.22
sec(2)-Butanol	0.318	0.218	0.072	0.028	0.50	5.17	184	207	1.59	3.21

macroscopic differences with a higher degree of branching, it does not mean that there were no microscopic differences (Manton & Davidtz, 1979).

Lactic acid, which contains both a hydroxide and acid functional group, compared to propanol (one hydroxide group) and propionic acid (one acid group), caused a significant increase in total pore, micropore and macropore volumes, porosity fraction and surface area, while other properties decreased (see Table 3.9). The properties obtained with lactic acid compared favourably with those obtained with the tricarboxylic citric acid.

3.3.2.5 Fatty acids and a fatty alcohol

Fatty acids are those organic acids with hydrocarbon chain lengths of 16 or 18 carbons (see Table 3.2). Kaganova and Shakhova (1959) patented a method whereby *cis*-oleic acid was used as a porogen in aluminium silicate gel. Dudeney *et al.* (1991) used *cis*-oleic acid as a surfactant to separate aluminium hydroxide gel from bulk water and dissolved salts.

When water-immiscible fatty acids were dissolved in solvents and mixed with aluminium nitrate solution, emulsions formed (Al-Mamun, 1982). Therefore, small oily globules, depending on their sizes, would influence formation of porosities over the spectrum of pore sizes. No attempt was made to control or measure globule sizes. Most fatty acids were dissolved in 40 ml ethanol and mixed with aluminium nitrate solution before neutralisation with ammonia. Stearic acid and olive oil were dissolved in diethylene ether and acetone, respectively. Sunflower oil was dissolved in acetone.

Table 3.10 shows the detrimental effect of 40 ml ethanol on properties of alumina when compared to those of the control sample. Therefore, a net effect is observed when fatty acids were dissolved in ethanol.

Table 3.10 Effect of 40 ml ethanol on properties of γ-alumina.

Sample	Total pore volume (cm^3/g)	Meso= pore volume (cm^3/g)	Micro= pore volume (cm^3/g)	Macro= pore volume (cm^3/g)	ϵ^*	Median pore diameter (nm)	Hg surface area (m^2/g)	N_2 surface area (m^2/g)	Bulk density (g/cm^3)	Skeletal density (g/cm^3)
Control	0.321	0.286	0.023	0.012	0.50	5.25	223	227	1.57	3.16
Ethanol	0.275	0.225	0.008	0.042	0.43	4.81	208	266	1.55	2.90

Table 3.11 Properties of γ-alumina samples obtained in the presence of 30 wt% *cis*-oleic acid.

Sample	Total pore volume (cm^3/g)	Meso= pore volume (cm^3/g)	Micro= pore volume (cm^3/g)	Macro= pore volume (cm^3/g)	ϵ^*	Median pore diameter (nm)	Hg surface area (m^2/g)	N_2 surface area (m^2/g)	Bulk density (g/cm^3)	Skeletal density (g/cm^3)
1	0.889	0.620	0.039	0.230	0.73	6.44	371	317	0.82	3.06
2	0.914	0.600	0.021	0.293	0.74	7.38	310	296	0.81	3.16
3	0.931	0.631	0.058	0.242	0.74	7.55	328	292	0.80	3.06
Average	0.911	0.617	0.039	0.255	0.74	7.12	336	302	0.81	3.09
Standard deviation	0.017	0.012	0.015	0.027	-	0.49	26	11	0.01	0.05
Correlation coefficient (%)	1.9	2.1	38.4	10.7	0.6	6.9	7.6	3.6	1.0	1.5

* porosity fraction

The reproducibility of properties obtained with a fatty acid, for example *cis*-oleic acid, is illustrated in Table 3.11 and cumulative pore size distributions are presented in Figure 3.5. The reproducibility is acceptable for most properties. The variation in micro- and macroporosities could have been due to a variation in globule sizes formed during emulsification of the *cis*-oleic acid/aluminium nitrate mixture. Average values obtained with *cis*-oleic acid are used in further comparisons with other fatty acids.

The following points are noted from the data shown in Table 3.12 and the cumulative pore size distribution curves in Figure 3.6 where the control was described in Section 3.3.1.1:

1) Fatty acids induced porosity in the mesopore volume range, but a large amount of macropore volume was also generated with these additives.

2) These porogens also induced a considerable increase in porosity fraction, median pore diameter, as well as BET surface area.

3) Properties of these samples compared favourably with those of the commercial powder. The latter material is currently being used as carrier material in CO oxidation automobile exhaust catalysts.

4) Properties of *cis*-oleic acid-derived samples compared most favourably with those of the commercial powder. *cis*-Oleic acid produced higher total pore volume, mesopore and micropore volumes as well as surface area than the commercial powder, while porosity fractions and bulk densities were similar. The *cis*-oleic acid-derived sample showed the presence of ink-bottle pores as indicated by the higher surface area obtained with a mercury porosimeter than with the BET method (Shields & Lowell, 1983). This was also observed with palmitic acid, sunflower oil and olive oil.

5) The very high macroporosity obtained with the commercial powder is also shown in Figure 3.6, but since this sample is a powder it is doubtful if all macropore volumes

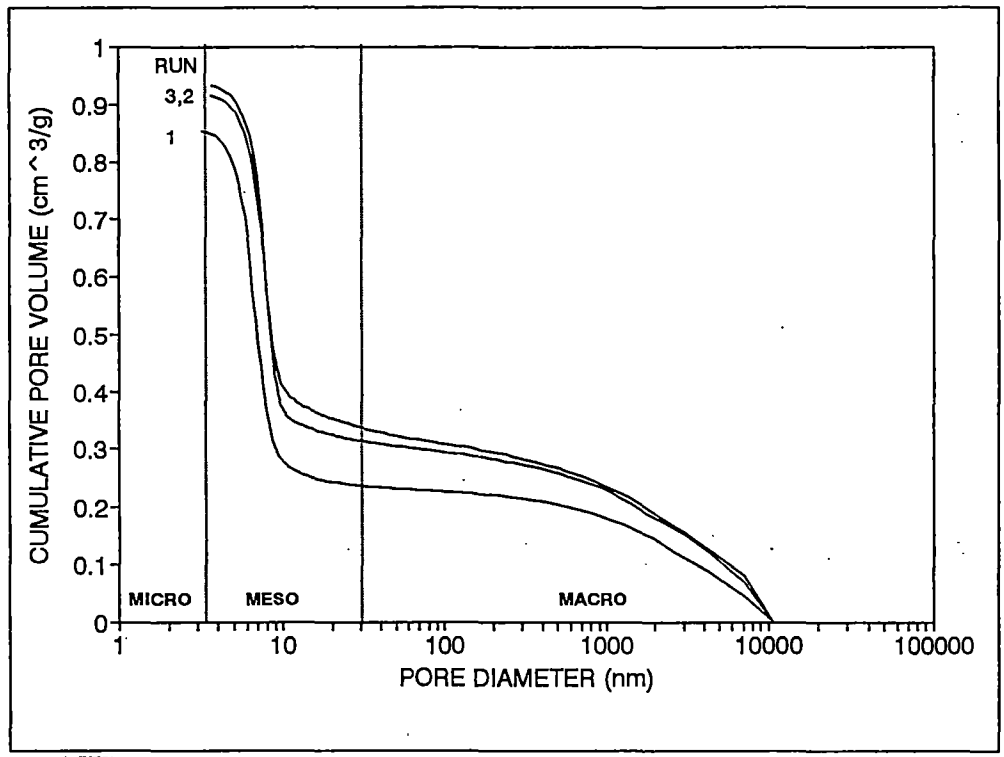

Figure 3.5 Cumulative pore size distribution curves of γ-alumina samples prepared in the presence of 30 wt% *cis*-oleic acid.

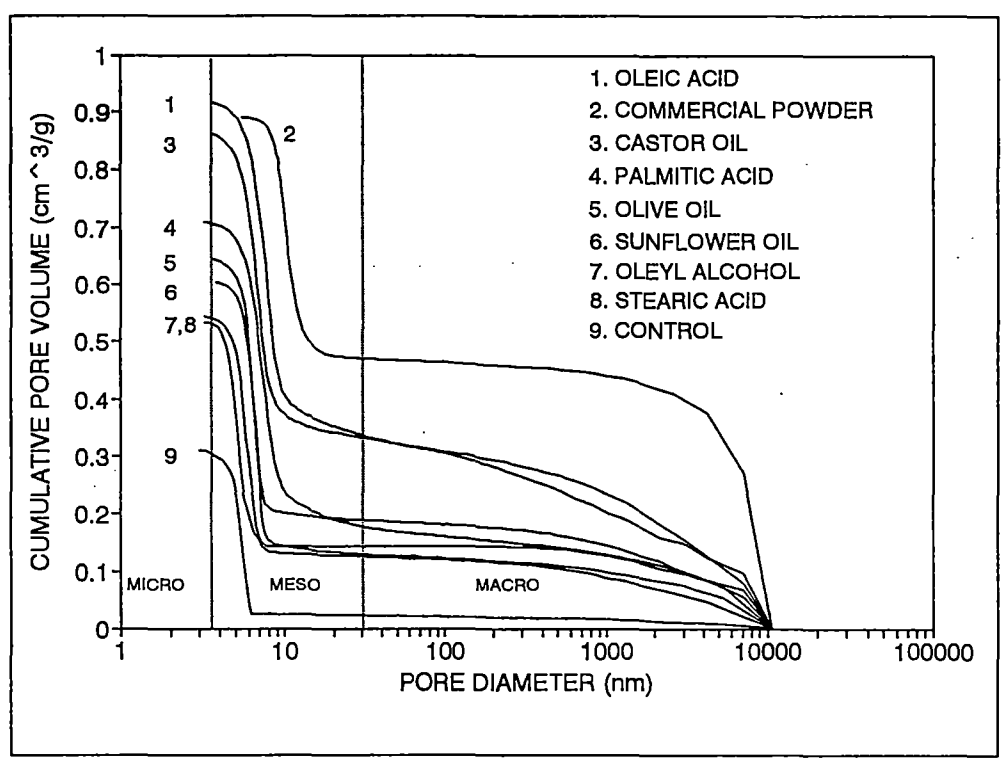

Figure 3.6 Cumulative pore size distribution curves of γ-alumina samples prepared in the presence of various fatty acids and a fatty alcohol.

Table 3.12 Effect of fatty acids and a fatty alcohol on properties of γ-alumina samples.

Sample	Total pore volume (cm^3/g)	Meso= pore volume (cm^3/g)	Micro= pore volume (cm^3/g)	Macro= pore volume (cm^3/g)	ϵ	Median pore diameter (nm)	Hg surface area (m^2/g)	N_2 surface area (m^2/g)	Bulk density (g/cm^3)	Skeletal density (g/cm^3)
Commercial powder	0.890	0.415	-	0.475	0.75	10.20	160	149	0.84	3.33
Control	0.321	0.286	0.023	0.012	0.50	5.25	223	227	1.57	3.16
Ethanol - 40 ml	0.275	0.225	0.008	0.042	0.43	4.81	208	266	1.55	2.90
Palmitic acid[s]	0.727	0.540	0.061	0.126	0.69	7.02	291	255	0.96	3.13
Oleyl alcohol[t]	0.552	0.413	0.041	0.098	0.62	5.71	316	293	1.12	2.96
cis-Oleic acid[u]	0.911	0.617	0.039	0.255	0.74	7.12	336	302	0.81	3.09
Stearic acid[v]	0.575	0.392	0.111	0.072	0.64	5.08	307	324	1.12	3.13
Castor oil[w]	0.875	0.543	0.063	0.269	0.73	6.60	296	296	0.83	3.09
Sunflower oil[x]	0.603	0.479	0.032	0.092	0.66	6.45	295	271	1.09	3.20
Olive oil[y]	0.645	0.459	0.002	0.184	0.67	6.26	290	264	1.04	3.20

[s] $CH_3(CH_2)_{14}COOH$ [t] $CH_3(CH_2)_7CH{=}CH(CH_2)_7CH_2OH$ [u] $CH_3(CH_2)_7CH{=}CH(CH_2)_7COOH$

[v] $CH_3(CH_2)_{16}COOH$ [w] $CH_3(CH_2)_5CH(OH)CH_2CH{=}CH(CH_2)_7COOH$ (Major)

[x] $CH_3(CH_2)_4CH{=}CHCH{=}CH(CH_2)_7COOH$ (Major) [y] Major component is [u] - see Appendix I

obtained are true because voids are most probably also included in the macroporosity value listed in Table 3.12. From a catalytic point of view, macropores are advantageous.

6) Stearic acid, which consists of a slightly longer hydrocarbon chain than palmitic acid, *i.e.*, 2.37 nm and 2.12 nm diameter, respectively, caused considerably smaller pore diameters and mesopore volume, but a significantly higher microporosity and surface area than obtained with palmitic acid. The high surface area found with stearic acid was due to the smaller pore sizes since no micropores were present as indicated by similar mercury porosimetry and BET surface areas. Different solvents used could have obscured obtainable properties induced by these porogens.

7) Lower property values were obtained with oleyl alcohol than with *cis*-oleic acid, except for bulk density. These results are in accordance with those found with other alcohol/acid pairs.

8) Properties obtained for similar hydrocarbon chain length fatty acid/alcohol pairs followed the order: *cis*-oleic acid (COOH group) > castor oil (OH and COOH group) > oleyl alcohol (OH group). This is also in accordance with results found above (see point (7)). These results, however, differ from those found with propanol/propionic acid/lactic acid (Section 3.3.2.5).

According to Stiles (1987), a carrier material possessing the highest porosity and surface area as well as the lowest bulk density is most favoured in an optimum catalyst support system. Samples prepared in the presence of *cis*-oleic acid fulfilled these prerequisites.

3.3.2.6 Effect of cis-oleic acid concentration on properties of γ-alumina

To optimise the amount of *cis*-oleic acid, concentrations were varied. Results in Table 3.13 summarise the effect of various amounts of *cis*-oleic acid and Figure 3.7 shows cumulative pore size distribution curves.

All surface properties, except for bulk density, increased with increasing amounts of *cis*-oleic acid from 0.5 to 60 wt%. Up to 60 wt%, there was a linear increase in these properties. The smaller pore sizes occurring with low amounts of *cis*-oleic acid (0.5 and 1.6 wt%) were probably due to the relatively high amounts of ethanol, which was the dominating pore forming additive present as indicated in Table 3.10. A high addition of 60 wt% *cis*-oleic acid did not increase surface area despite the significant increase in mesoporosity, which was probably due to larger pores created.

For further investigations, additions of 30 wt% were selected because properties introduced by this amount of *cis*-oleic acid compared most favourably with the commercial powder.

3.3.2.7 Sintering and ceria stabilisation of fatty acid-derived γ-alumina

Sintering and stability behaviour of selected fatty acid-derived γ-aluminas were also investigated. The effect of various ceria additions (3 and 11 wt% based on the weight of alumina) on stability of properties as a function of calcination temperature (550 - 1000 °C) was also investigated. The results are given in Appendix D.

Surface areas decreased and pore sizes increased significantly with increased calcination temperature for all samples under consideration. The effect is a growth of pore sizes at the expense of surface area due to coalescence of smaller pores. The highest overall surface areas and largest pore sizes were obtained with *cis*-oleic acid. Differences between BET and mercury porosimeter surface area measurements indicated the

Table 3.13 Effect of various concentrations of *cis*-oleic acid on properties of γ-alumina samples.

Sample (wt%)	Total pore volume (cm^3/g)	Meso= pore volume (cm^3/g)	Micro= pore volume (cm^3/g)	Macro= pore volume (cm^3/g)	ϵ	Median pore diameter (nm)	Hg surface area (m^2/g)	N_2 surface area (m^2/g)	Bulk density (g/cm^3)	Skeletal density (g/cm^3)
Commercial powder	0.890	0.415	-	0.475	0.75	10.20	160	149	0.84	3.33
Control	0.321	0.286	0.023	0.012	0.50	5.25	223	227	1.57	3.16
0.5	0.343	0.305	0.027	0.011	0.52	4.79	238	261	1.51	3.15
1.6	0.369	0.304	0.027	0.038	0.54	4.96	243	265	1.46	3.16
15	0.677	0.392	0.058	0.227	0.67	5.81	262	276	0.99	3.01
30*	0.911	0.617	0.039	0.255	0.74	7.12	336	302	0.81	3.09
60	1.057	0.663	0.069	0.325	0.77	7.86	306	303	0.73	3.11
R^2 linearity (%)	90	90	70	83	83	94	82	67	80	-

* average values from Table 3.11.

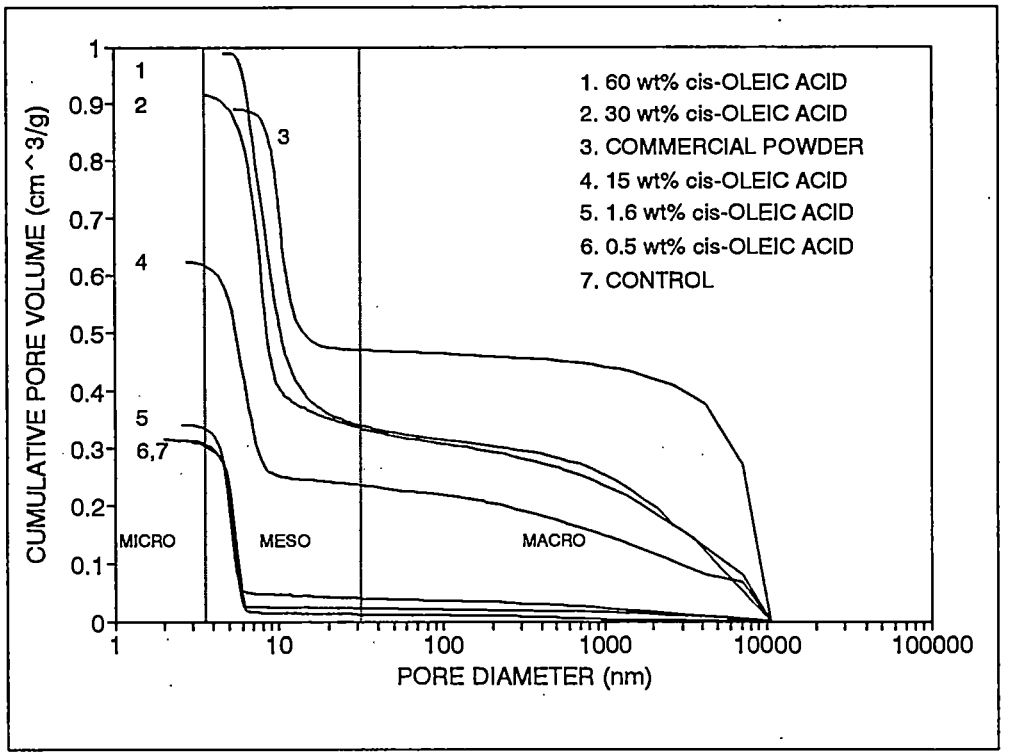

Figure 3.7 Cumulative pore size distribution curves of γ-alumina samples prepared in the presence of various concentrations of *cis*-oleic acid.

development of some ink-bottle shaped pores. This was more pronounced at high (> 800 °C) calcination temperatures.

Addition of 3 wt% ceria resulted in slightly higher BET surface areas compared with 11 wt% additions. The latter amount, in the case of *cis*-oleic acid-derived alumina, resulted in the largest pore sizes for all calcination temperatures, while the opposite, in general, was found for the control and all other fatty acids. High calcination temperatures and various ceria additions had no significant effect on porosities. Ink-bottle pores also were obtained for samples containing ceria, but these were less prominent in sunflower and olive oil samples.

It is difficult to assess the influence of ceria from all available data on the stabilisation of properties of γ-alumina. Therefore, the changes in values of properties as a function

of calcination temperature were estimated from the slopes of the linear curves. These values are summarised in Table 3.14. An asterisk indicates that one data point was omitted because of possible experimental errors, while a negative sign shows that a specific property decreased with increasing temperature.

Linear sintering relationships were obtained for all surface properties under consideration. Linear (R^2) sintering relationships with the surface areas and pore sizes of the control samples were significantly lower compared to those of the fatty acids. These relationships indicate that ceria only stabilised the control samples to a certain degree, but it had no significant effect on fatty acid samples. However, 11 wt% ceria additions tended, in general, to increase pore size and skeletal density sintering relationships.

The influence of ceria (hkl 311) was also evaluated by determining specific crystallite sizes with x-ray line broadening (see Section 3.2 equation 1) of *cis*-oleic acid-derived alumina (hkl 400) and control samples that were sintered at 1000 °C (Table 3.15 and Appendix E). Addition of 3 wt% ceria caused γ-alumina crystallite sizes to decrease for both samples under consideration. At 3 wt% ceria, crystallites appear to sinter preferentially in comparison to γ-alumina crystallites; 11 wt% ceria did not decrease alumina crystallite sizes for the control sample, but restricted γ-alumina growth in *cis*-oleic acid samples. δ- and γ-alumina phases were detected when ceria was present, while θ-alumina was detected when ceria was absent. Similar results were also obtained by Ozawa and Kimura (1990). The former two phases were also present at sintering temperatures of 700 °C.

3.3.2.8 Scanning electron micrographs

Scanning electron micrographs were used to give a qualitative description of the macroporosity and structures of prepared γ-alumina material. Four different macropore structures were observed (Micrographs 3.1 to 3.4):

Table 3.14 Slopes and linearity of various sample properties as a function of ceria content and calcination temperature.

Sample	Surface area (m^2/g °C)	Pore size 10^2 (nm/°C)	Bulk density 10^3 (g/cm^3 °C)	Skeletal density 10^3 (g/cm^3 °C)	Total pore volume 10^3 (cm^3/g °C)
Control	-0.24 (0.84)**	0.93 (0.95)	0.51 (0.83)	0.69 (1.00)	NL
Control + 3 wt% ceria	-0.13 (0.90)	0.94 (0.95)	0.85 (0.83)	0.52 (0.93)	-2.86 (0.79)
Control + 11 wt% ceria	-0.14 (0.95)	1.35 (0.83)*	0.64 (0.94)	0.68 (0.99)	-0.15 (0.95)
Palmitic acid	-0.38 (0.94)	0.79 (0.75)*	0.54 (0.99)*	0.84 (0.93)	-0.81 (0.91)*
Palmitic acid + 3 wt% ceria	-0.38 (0.99)	2.01 (1.00)*	0.40 (1.00)*	NL	-0.60 (1.00)*
Palmitic acid + 11 wt% ceria	-0.36 (0.99)	1.86 (0.99)	0.35 (1.00)*	0.45 (0.91)	-1.13 (1.00)*
Castor oil	-0.38 (0.95)	1.20 (0.99)	0.27 (0.94)	0.75 (0.97)	-0.27 (0.89)
Castor oil + 3 wt% ceria	-0.30 (0.94)	0.36 (1.00)*	1.20 (0.78)	0.50 (0.89)	-1.15 (0.80)
Castor oil + 11 wt% ceria	-0.34 (0.92)	NL	0.25 (1.00)*	NL	-0.25 (1.00)*
Sunflower oil	-0.37 (0.90)	NL	0.18 (0.78)*	0.40 (0.93)	NL
Sunflower oil + 3 wt% ceria	-0.36 (1.00)	1.28 (1.00)*	0.05 (1.00)*	0.25 (0.99)	-0.02 (1.00)*
Sunflower oil + 11 wt% ceria	-0.26 (0.99)	2.20 (0.83)	0.80 (1.00)*	1.10 (0.82)	-0.48 (1.00)*
Olive oil	-0.35 (1.00)	1.50 (0.92)	NL	0.45 (0.93)	NL
Olive oil + 3 wt% ceria	-0.32 (0.97)	1.70 (0.99)	0.10 (1.00)*	0.45 (0.75)	-0.25 (0.85)
Olive oil + 11 wt% ceria	-0.29 (0.83)	2.30 (0.95)	0.80 (1.00)*	0.80 (0.75)	-0.39 (1.00)*
cis-Oleic acid	-0.36 (0.96)	1.30 (0.96)	NL	NL	NL
cis-Oleic acid + 3 wt% ceria	-0.34 (0.98)	1.30 (1.00)	NL	0.37 (0.97)	NL
cis-Oleic acid + 11 wt% ceria	-0.37 (0.99)	1.60 (0.97)	NL	0.82 (0.80)	-1.42 (0.93)*

NL = not linear/varied too much * One data point omitted ** R^2 linearity in brackets

Table 3.15 γ-Alumina and ceria crystallite sizes after sintering at 1000 °C.

Sample	γ-Alumina crystallite size (nm)	Ceria crystallite size (nm)
Control	12.4	-
Control + 3 wt% ceria	10.8	13.9
Control + 11 wt% ceria	13.4	21.3
cis-Oleic acid	13.5	-
cis-Oleic acid + 3 wt% ceria	11.6	16.8
cis-Oleic acid + 11 wt% ceria	13.5	24.7

1) Micrograph 3.1 shows a typical surface structure obtained for control samples. The large channel-like structure probably originated from either air trapped in the gel during its formation or a cavity that was not closed during gel formation.

2) Macroporosity obtained with ammonium citrate can be attributed to void volume between blocky agglomerates, shown in Micrograph 3.2.

3) Micrograph 3.3 shows a close-up of a macropore where different channels/pores are sprouting deeper into the structure of the sample. It can be concluded that an alumina film formed at surfaces which seemed to screen off the internal pore network.

4) Micrograph 3.4 shows the typical crater-type structures obtained with fatty acids. Macroporosity generated with these additives are quite homogeneously distributed throughout the structure. This can be attributed to emulsion formation induced with fatty acids.

It is concluded that these macropores were not reflected in measurements of pore size distribution by mercury porosimetry.

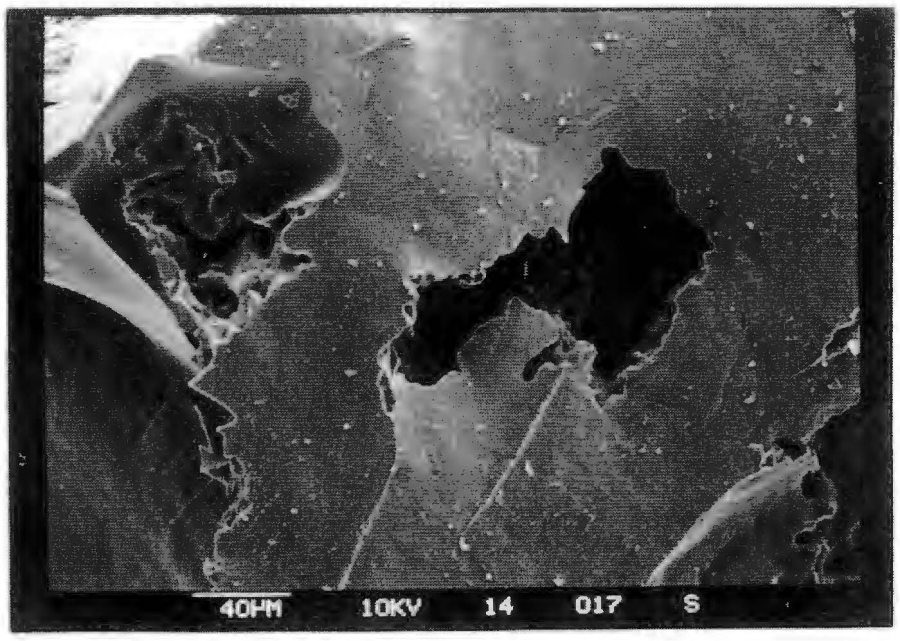

Micrograph 3.1 Macroporosity due to air entrapment in control sample.

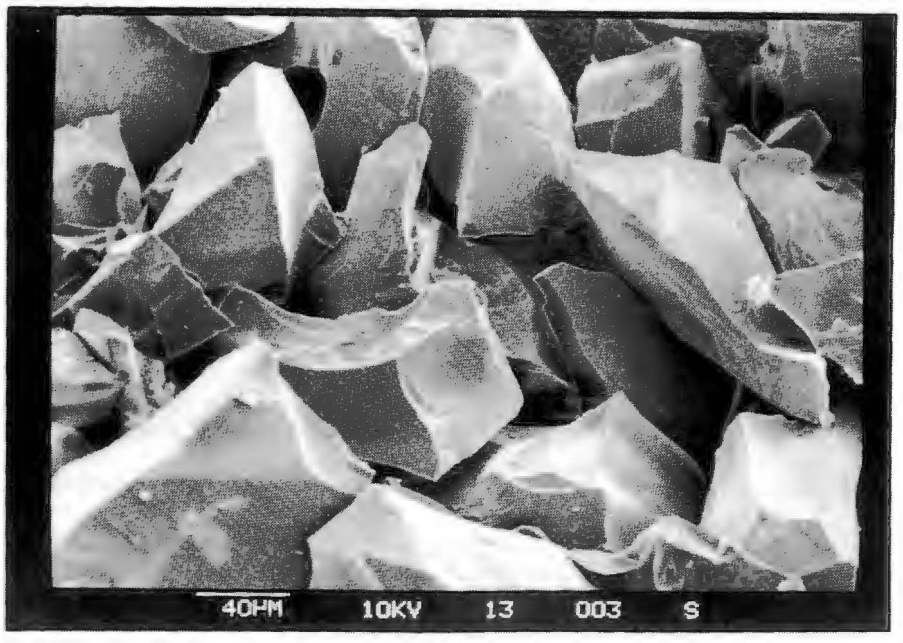

Micrograph 3.2 Macroporosity due to blocky structures obtained with ammonium citrate-derived γ-alumina.

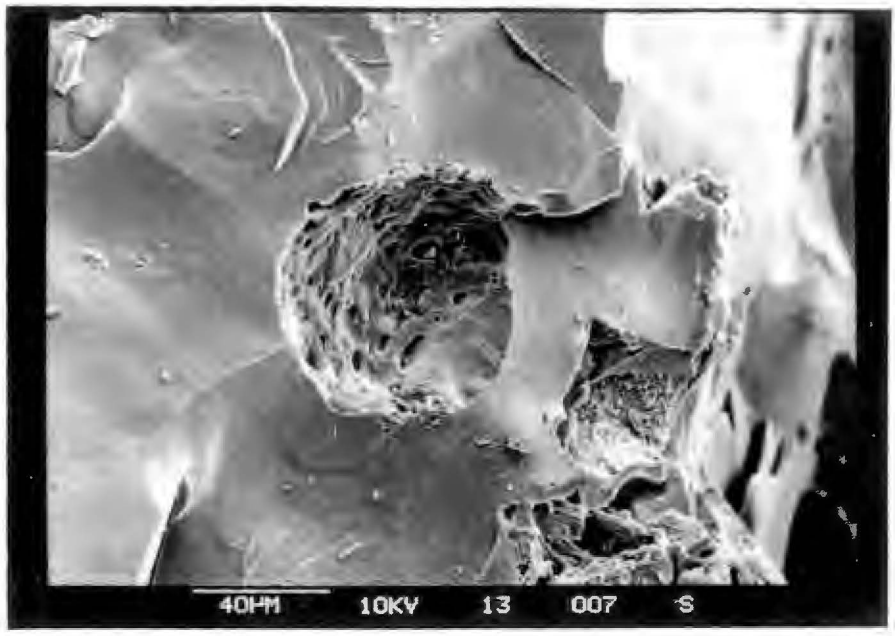

Micrograph 3.3 Macroporosity screened off with film formation for *iso*-butyric acid-derived γ-alumina.

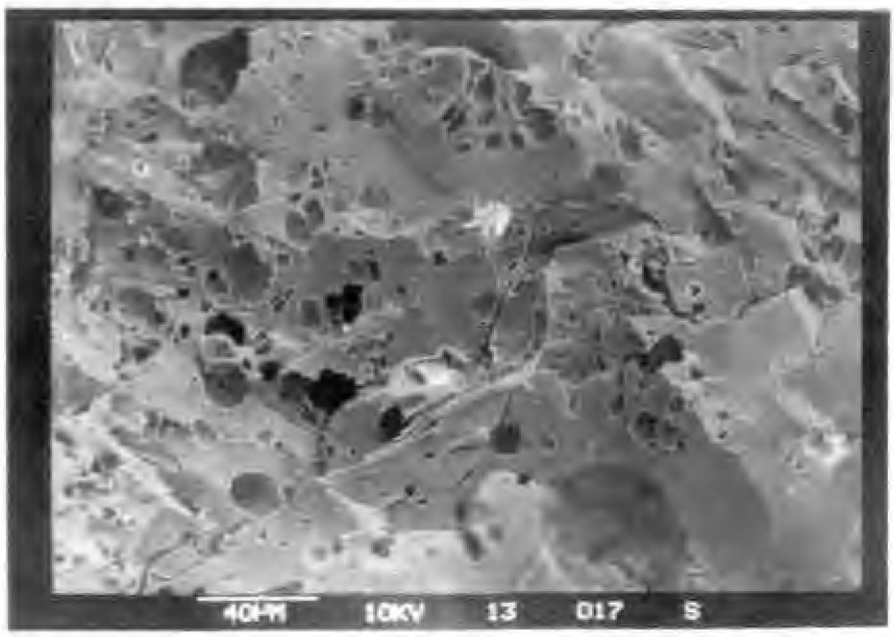

Micrograph 3.4 Macroporosity due to emulsion formation obtained with fatty acids.

3.4 DISCUSSION

Table 3.16 summarises the effect of the porogens investigated on the various porosity regions. Porosities increased from top to bottom within each column, and mesoporosities also decreased from top to bottom. Constant mesoporosity and macroporosity indicated that those porogens had no effect on changing porosity in those regions under consideration. From a mechanistic point of view this is difficult to explain, but it is possible that the concentration of these porogens was too low to have any effect.

3.4.1 Relationship between pore and crystallite size (Microporosity)

To evaluate the relationship between crystallite size and pore volume, three samples were selected from Table 3.6. They were the extremes in pore size (tartaric acid smallest and *cis*-oleic acid largest) and an intermediate (citric acid). The results are reported in Table 3.17 and Appendix E.

Pore sizes followed the same sequence of crystallite sizes. The Scherrer method of determining crystallite sizes is valid, since crystallite sizes are larger than 2 nm and, consequently, crystallite strain was ignored (Wanke & Flynn (1975), Langford (1979)). Therefore, it can be concluded that crystallite size affects porosity especially in the micropore range. This was also the contention of Trimm and Stanislaus (1986).

The addition of chelating agents to inhibit crystallite growth is common practice in the preparation of aluminate solutions (Lindsay & Willey, 1944). It is, therefore, possible that when once a small crystallite has formed, the surface reaction with chelating groups could inhibit further growth, with a resultant smaller crystallite being the product. Therefore, citric, lactic, sebacic and tartaric acids were expected to favour particle-bridging. Pore sizes obtained with these acids are considerably smaller than the control sample and followed the reversed order of the microporosity.

Table 3.16 Effect of porogens on porosity.

Mesoporosity			Microporosity	Macroporosity	
Increased	**Constant**	**Decreased**	**Increased**	**Increased** (most significant)	**Constant**
Benzoic acid	2-Pentanol	Amm. formate	Propanol	Adipic acid	Formic acid
Glycerine	Triethanolamine	Lactic acid	*n*-Hexanol	Stearic acid	Amm. formate
Diethylene glycol	Mannitol	Formic acid	*iso*-Butyric acid	*n*-Hexanol	Oxalic acid
Amm. tartrate	*iso*-Butyric acid	*n*-Hexanol	Formic acid	Amm. tartrate	Methanol
Stearic acid	Oxalic acid	Citric acid	Amm. citrate	Sunflower oil	Acetic acid
Oleyl alcohol	Maleic acid	2-Butanol	2-Butanol	2-Pentanol	Propanol
Olive oil	Succinic acid	Sebacic acid	Amm. carbonate	Oleyl alcohol	Propionic acid
Sunflower oil	Adipic acid	Tartaric acid	2-Pentanol	Succinic acid	*iso*-Butanol
Palmitic acid	Amm. carbonate		Citric acid	Triethanolamine	
Castor oil	Amm. oxalate		Lactic acid	Palmitic acid	
cis-Oleic acid	Amm. citrate		Sebacic acid	Sebacic acid	
	iso-Butanol		Tartaric acid	Olive oil	
	Propanol, *n*-Butanol			Tartaric acid	
	Methanol, Ethanol			*cis*-Oleic acid	
	Acetic acid			Castor oil	
	Propionic acid			Amm. carbonate	

Table 3.17 Relationship between pore size and crystallite size.

Sample	Pore diameter (nm)	Crystallite diameter size (nm)
Tartaric acid	3.76	5.33
Citric acid	4.76	6.84
cis-Oleic acid	7.12	6.89

The pore size order obtained for the carboxylic acids under consideration followed the sequence:

citric > lactic > sebacic > tartaric acid,

which is a similar order obtained for increasing microporosities. However, there is no simple relationship between bridging functional groups and porosity. This former order is similar to that reported by Violante and Violante (1980).

Lactic acid resulted in a smaller pore size than citric acid. According to Cornell and Schwertmann (1979), citric acid has stronger complexing abilities with aluminium than lactic acid (lack of a second group for bridging), and therefore citric acid was expected to cause smaller pore sizes than lactic acid. Citric acid also has a lower dissociation constant than lactic acid. The performance of lactic acid is attributable to the relatively higher concentration used, *i.e.*, 0.012 moles COOH and OH compared to 0.007 moles COOH and OH for citric acid.

No detectable microporosity was obtained with succinic, maleic, oxalic and adipic acids although they contain two functional groups. Succinic acid complexes weakly with aluminium ions by forming unstable 7-membered rings (Violante & Violante (1980)), which explains the lack of any effect. A lack of influence observed with maleic and oxalic acids compared to hydroxycarboxylic acids was also reported by Cornell and Schwertmann (1979) for ferrihydrite at high pH. According to these authors and

Violante and Huang (1985), higher dicarboxylic acid concentrations than for hydroxy-carboxylic acids are necessary to show similar effects.

Microporosities caused with formic acid and *iso*-butyric acid were due to relatively high concentrations, *i.e.*, 0.034 and 0.538 moles COOH and OH for the acids, respectively. The latter high value is due to the presence of ethanol which was used as a solvent. Violante and Violante (1980) reported the same effect of high concentration.

Increased microporosities were also observed with alcohols, such as propanol, *n*-hexanol, 2-butanol and 2-pentanol. This suggests bridging as the pore-forming mechanism. Microporosities, obtained with these alcohols, also increased with decreased pore sizes, with 2-pentanol having the most significant effect. Increased microporosities were obtained for an addition of 6.86 ethanol-to-Al^{3+} molar ratio (Table 3.9). This implies that microporosities obtained with these alcohols were due to the combined effects of alcohols.

It is not clear why certain ammonium salts influenced microporosities and the others not. The ammonium salts acted as co-precipitants, which changed the pH rapidly during precipitation of aluminum gel. This would have most probably inhibited growth of crystallites resulting in the observed microporosities obtained with ammonium citrate and carbonate.

3.4.2 Packing of particles (Mesoporosity)

At a final neutralisation pH of 9, which is close to the iso-electric point of aluminium hydroxide (pH 8.5 - 9.6 (Violante & Huang (1985), Lee & Hench (1987))), formation of aggregates was most probably enhanced by packing of particles. This effect is observed as a rise in mesoporosity (Cormack *et al.*, 1980). The formation of large, irregularly shaped particles also results in formation of agglomerates leaving pores (voidage) between particles (Trimm & Stanislaus, 1986). Increased mesoporosities were especially observed with fatty acids/alcohol, *i.e.*, stearic acid, oleyl alcohol, olive and sunflower oil,

palmitic acid, castor oil and *cis*-oleic acid. The latter showed the highest mesoporosity with crystallite sizes of 6.89 nm in diameter (Table 3.17). The process of adsorption of fatty acids on the surface of aluminium hydroxide gel is favoured to occur, evidenced by the flocculation of the latter with *cis*-oleic acid as demonstrated by Dudeney *et al.* (1991). Polyols such as glycerine and diethylene glycol, as well as benzoic acid and ammonium tartrate, similarly increased mesoporosity.

3.4.3 Filler effects (Macroporosity)

Most porogens also affected macroporosity, which implies that they acted as fillers or "spacers". The most significant macroporosities obtained are listed in Table 3.16. These macroporosities can be attributed to emulsion formation and removal of the porogen during calcination. Coiling and dimer formation of fatty acids (Iwahashi *et al.*, 1991) cannot be eliminated as factors which play a role during macropore formation. The following fatty acids are known to have coiled molecules: *cis*-oleic acid, *cis*-ricinoleic acid (major component in castor oil) and *cis*-linoleic acid (major component in sunflower oil). Ammonium carbonate also showed significant filler effects. Macroporosities obtained with small molecules, such as adipic and tartaric acids as well as ammonium tartrate, are probably due to other effects such as air entrapment and/or void volumes between blocky agglomerates.

3.4.4 Effect of molecular size

An attempt was made to relate pore properties to the molecular size of the porogen. No relationship was observed between molecular size of porogens and surface properties obtained with porogens.

3.5 CONCLUSIONS

1) Porogens were largely effective in the mesopore volume range with sharply defined pore size distributions.

2) *Mesoporosity*. Porogens that enhanced mesoporosity significantly were: diethylene glycol, glycerine, benzoic acid, ammonium tartrate and fatty acids/alcohol such as stearic, palmitic and *cis*-oleic acids, oleyl alcohol, olive, castor and sunflower oils. These additives caused the formation of aggregates by packing of particles at the iso-electric point (pH 9) of aluminium hydroxide.

3) *Microporosity*. Tartaric and sebacic acids and 2-butanol reduced mesoporosity due to their increased effects on microporosity. Other porogens that also increased microporosity were lactic, citric and formic acids, *n*-hexanol, propanol, 2-pentanol, ammonium formate and ammonium citrate. Pore sizes in the microporosity region were affected by alumina crystallite sizes, which, in turn, were determined by the inhibition effect of strong chelating agents, mentioned above, on crystallite growth. The formerly above-mentioned acids were expected to favour particle-bridging and pore sizes obtained with these acids are considerably smaller than the control sample and followed the reversed order of the microporosity.

No detectable microporosity was obtained with succinic, maleic, oxalic and adipic acids although they contain two functional groups. This confirmed that higher dicarboxylic acid concentrations than for hydroxycarboxylic acids are necessary to show similar effects.

4) *Macroporosity*. Macroporosity was underestimated for most samples due to limitations of the high pressure mercury porosimeter. Macroporosity was obtained by i) entrapped air in the gel during its formation, or ii) a cavity that was not closed during gel formation, or iii) void volume between blocky agglomerates, or iv) formation of different channels/pores which are sprouting deeper into the internal pore network of the structure of the sample, but were screened off by an alumina film formed at surfaces or v) crater-type structures obtained with fatty acids. These macroporosities were introduced by filler or spacer effects of additives due to i) emulsion formation, ii) removal of the porigen during

calcination, or iii) coiling and dimer formation of fatty acids. Ammonium carbonate also showed significant filler effects. Macroporosities obtained with small molecules, such as adipic tartaric and fatty acids as well as ammonium tartrate, are probably due to air entrapment and/or void volumes between blocky agglomerates.

5) *Concentration of additive.* The concentration of additives used affected properties of prepared γ-alumina. Properties obtained for *cis*-oleic acid-derived γ-alumina increased linearly up to 60 wt% addition. Relatively high concentrations of formic acid enhanced microporosity and decreased pore sizes, while those of ethanol enhanced surface area but reduced pore sizes and mesoporosity. Surface area increased with *iso*-butyric acid. Lactic acid resulted in a smaller pore size than citric acid due to a higher concentration despite of the stronger complexing abilities of the latter with aluminium hydroxide.

6) *Pore shapes.* All additives produced cylindrical-shaped pores, except fatty acids. The latter showed the presence of ink-bottle pores as indicated by the higher surface area obtained with a mercury porosimeter than with the BET adsorption method. This was observed with *cis*-oleic and palmitic acid, sunflower and olive oil. The development of ink-bottle pores in fatty acid-derived alumina was especially evidenced at high (> 800 °C) calcination temperatures. Ink-bottle pores also were obtained for sintered samples containing ceria, but these were less prominent in sunflower and olive oil samples.

7) *cis*-Oleic acid produced higher total pore volume, mesopore and micropore volumes as well as surface area, but smaller pore size than the commercial alumina powder, which is being used in the automotive exhaust catalyst industry, while porosity fractions and bulk densities are similar.

8) Surface properties obtained for similar hydrocarbon chain length fatty acid/alcohol pairs followed the order: *cis*-oleic acid (COOH group) > castor oil

(OH and COOH group) > oleyl alcohol (OH group). These results, however, differ from those found with propanol/propionic acid/lactic acid.

9) *Sintering and ceria.* After sintering at 1000 °C, *cis*-oleic acid resulted in the highest overall surface area and largest pore size in alumina amongst the fatty acids investigated. Linear sintering relationships were obtained for all surface properties under consideration. Sintering relationships indicate that ceria only stabilised the control samples to a certain degree, but it had no significant effect on fatty acid-derived alumina samples. However, 11 wt% ceria additions tended, in general, to increase pore size and skeletal density sintering relationships. Addition of 3 wt% ceria caused γ-alumina crystallite sizes to decrease for both control and *cis*-oleic acid-derived alumina samples after sintering. Therefore, ceria crystallites sinter preferentially in comparison with γ-alumina crystallites. Addition of 11 wt% ceria did not decrease alumina crystallite sizes for the control sample, but restricted growth in *cis*-oleic acid samples.

10) *Alumina phases.* After sintering of alumina samples at 1000 °C for 2 hours, δ- and γ-alumina phases were detected when ceria was present, while θ-alumina was detected when ceria was absent. The former two phases were also present at sintering temperatures of 700 °C. Thus, ceria prevented phase transformation in alumina.

CHAPTER 4. TORTUOSITY FACTOR AND KNUDSEN EFFECTIVE DIFFUSIVITY OF PREPARED γ-ALUMINAS

4.1 INTRODUCTION

Many reaction processes of industrial importance occur in porous solids (catalysis, electrolysis, *etc.*) (Bell, 1991). Access to the interior of the solid is by diffusional transport and the transport of mass is usually described by Fick's law for diffusional flux (Satterfield & Sherwood, 1963; Froment & Bischoff, 1979). According to Fogler (1986), in a heterogeneous reaction sequence, mass transfer of reactants first takes place from the bulk gas to the external surface of a catalyst support material. The reactants then diffuse from the external surface into and through the pores within the support material, with reaction taking place only on the catalytic surface of the pores. Materials having relatively high surface areas and porosities will promote diffusion and mass transport of the reacting gas and product(s) in and out of the catalyst support material.

The parameter describing the ease of mass transport or diffusion in these supports requires information on the pore size distribution and the tortuosity of the porous catalyst (Satterfield & Sherwood, 1963; Froment & Bischoff, 1979; Fogler, 1986). This parameter is known as the effective diffusivity and is defined as:

$$D_e = D_K \in / \tau, \qquad \text{..... (1)}$$

where D_K is the Knudsen diffusion coefficient[1], which is valid for pores with radii between 1 and 100 nm, and includes most catalyst carriers. For Knudsen diffusion, molecules approach collision frequency with pore walls because the radii

[1] According to Weisz (1973) and Fogler (1986), diffusional fluxes in the Knudsen region range from 10^{-6} to 10^{-1} cm^2/s and for the bulk or regular diffusion region they range from 0.01 to 1 cm^2/s. For configurational diffusion, fluxes may vary from 10^{-6} to 10^{-14} cm^2/s.

of the pores are equal to the mean free path of the molecules (Hines & Maddox, 1985);

$\in$ is the void fraction or total connected pore volume fraction or porosity fraction; and,

τ is the tortuosity factor related to the path of the molecule, which includes both the effect of altered diffusion path length as well as changing cross-sectional areas in constrictions.

Knudsen diffusion coefficient, D_K, in a straight round pore (unimodal pore size distribution) is defined by Satterfield and Sherwood (1963) as:

$$D_K = 9700\, r_e \sqrt{(T/M)} \quad (\text{cm}^2/\text{s}) \qquad \ldots\ldots\ldots (2)$$

where r_e is pore radius (cm) of a cylindrical pore;

T is temperature (K);

M is molecular weight of the diffusing gas molecule.

Mean radius, r_e, of a cylindrical pore is defined as

$$r_e = 2\in/(SA\rho), \qquad \ldots\ldots\ldots (3)$$

where SA is total BET surface area of porous solid (cm^2/g);

ρ is bulk density of the solid particle (g/cm^3), defined as

$$\rho = 1/(V_s + 1/\rho_0), \qquad \ldots\ldots\ldots (4)$$

where V_s is total specific connected pore volume of catalyst support (cm^3/g);

ρ_0 is skeletal density, *i.e.*, density of the solid between pores (g/cm^3).

Thus, the effective Knudsen diffusion coefficient for a unimodal porous solid becomes:

$$D_{K,eff} = D_K \in /\tau = 19400 \in^2/(\tau\, SA\, \rho)\sqrt{(T/M)}. \quad \text{..... (5)}$$

Various investigators have proposed models and methods to determine the tortuosity factor. Diffusion measurements made by Wakao and Smith (1962) resulted in a deduction that tortuosity is given as

$$\tau = 1/\in. \quad \text{..... (6)}$$

Froment and Bischoff (1979) also reported this relationship, while Cheng *et al.* (1987) approximated the tortuosity as $3\in$. Doğu and Doğu (1991) proposed a grain model to calculate the tortuosity factor based on the porosity of micropores and macropores.

Carniglia (1986) developed a 'construction method', which allows prediction of tortuosity from detailed mercury porosimeter pore size distribution data together with BET surface area values. This method caters for both cylindrical and non-cylindrical pores. Effective Knudsen diffusivities for a multimodal pore size distribution can be predicted from these tortuosity factors from properties of the overall porous structure of a catalyst support material. The major restriction is that this method cannot be applied to microporosity regions unless mercury porosimetry data is extended to this region.

4.2 COMPUTATION OF TORTUOSITY FACTOR AND EFFECTIVE DIFFUSIVITIES BASED ON THE 'CONSTRUCTION METHOD' OF CARNIGLIA

The following steps were used to determine the tortuosity factor, τ, and effective diffusivity for a catalyst support:

Step (1):

A critical tortuosity factor was determined from the following relationship:

$$\tau_c = 2.23 - 1.13\in = x, \qquad \text{..... (7)}$$

(valid for $(0.05 \leq V_s\rho \leq 0.95)$)[2]

with $\in = V_s\rho$.

Equation (7) is applicable to any pore size distribution with cylindrical diffusion paths as mathematically constructed by Carniglia (1986) from properties of connected porosity.

Step (2):

From raw mercury porosimeter data, the median of a narrow radius interval as indicated by the mercury porosimeter was determined, *i.e.*, of 'throats' in the pore network defined as:

$$(1/r)_t = \sum(\Delta V_i/r_{ti})/V_s \qquad \text{..... (8)}$$

with ΔV_i = specific pore volume of all porosity of the ith size group (radius r_i) in a body, and

r_{ti} = median of a narrow radius interval as indicated by the mercury porosimeter.

Step (3):

Total specific pore volume, BET surface area, and $(1/r)_t$ were used in equation (9) to obtain the pore shape factor, y:

$$y = (2/SA)V_s(1/r)_t \qquad \text{..... (9)}$$

If $y < 1.1$, but > 1.0, then the tortuosity factor is defined by $\tau = x$ for cylindrical pores. A value below unity has no geometrical meaning, but it indicates that the BET surface area and the corresponding porosimeter data are inconsistent under the pore geometry model described (Carniglia, 1994).

[2] This range brackets all solid catalysts of practical interest.

Step (4):

If $y > 1.1$ (for non-cylindrical pores), from the $D_K(r)$ (diffusivity) *vs.* r curve for every r_{ti} of the porosimetry data was used in equation (10) to obtain D^0 (mean of $D_K(r_i)$ over all r_i)

$$D^0 = \Sigma \Delta V_i D_K(y r_{ti}) / V_s \quad \text{..... (10)}$$

Similarly, D^0 was also estimated for cylindrical pores where the pore shape factor, y, is unity.

Step (5):

D^0 was entered on a log-log plot of $D_K(r)$ (equation 2) vs r and the slope, n, was obtained.

Step (6):

Tortuosity factors for non-cylindrical pores were determined by entering x, y and n into equation (11):

$$\tau = x\,(0.92\,y)^{1+n} = (2.23 - 1.13\,V_s\rho)(0.92\,y)^{1+n} \quad \text{..... (11)}$$

Step (7):

Knudsen effective diffusivities (D^0-based) were calculated from the following relationship:

$$D_{K,eff} = D^0 \in / \tau. \quad \text{..... (12)}$$

In order to apply the method of Carniglia to determine tortuosity factors, certain mercury pore size distribution curves were extrapolated into the microporous region[3] as described in Section 3.2. An attempt was also made to correlate BET surface areas

[3] According to Carniglia (1986), another way of overcoming this problem is to calcine the sample to cause coalescence of the micropores and to move the pore size distribution curve to higher radii.

and the corresponding porosimeter data as proposed by Carniglia (1994). This depends on the modelled pore size distribution curve which extends into the microporous region. A reaction temperature of 111 °C (384 K)[4] was selected, which corresponds to a low CO oxidation conversion obtained for fresh 5 mm catalysts indicated in Section 6.5.1.1, to estimate Knudsen effective diffusivities. Carbon monoxide was used as the diffusing gas that was also used in reactor studies described in Section 6.

The tortuosity factors, pore shape factors, and Knudsen effective diffusivities were calculated for samples prepared in the presence of various additives (see Chapter 3) and those sintered at different temperatures with and without the presence of ceria.

4.3 RESULTS AND DISCUSSION

Tables 4.1 to 4.10 represent the tortuosity factors (TF), pore shape factors (PSF) and Knudsen effective diffusivities (KED) as obtained from the mercury pore size distribution data and BET surface area determinations for all additives reported in Chapter 3. Two different tortuosity factors are reported, *i.e.*, those based on the methods of Wakao and Smith (1962) and Carniglia (1986). Two different Knudsen effective diffusivities are reported, those described by Satterfield and Sherwood (1963) and those described by Carniglia (1986) (Equations (5) and (12), respectively). Tortuosity factors defined by Carniglia were used to estimate these parameters.

4.3.1 Relationship between various tortuosity factors

Figure 4.1 shows the relationship between the various tortuosity factors, as estimated for the different methods described by Wakao and Smith (1962) and Carniglia (1986). The effect of different pore shape factors as a function of porosity is also included. There is a close resemblance between the tortuosity factors for these three methods, especially for porosity factors greater than 0.60. Tortuosity factors for the cylindrical and non-

[4] Any other reaction temperature would also be applicable and the trends will be similar.

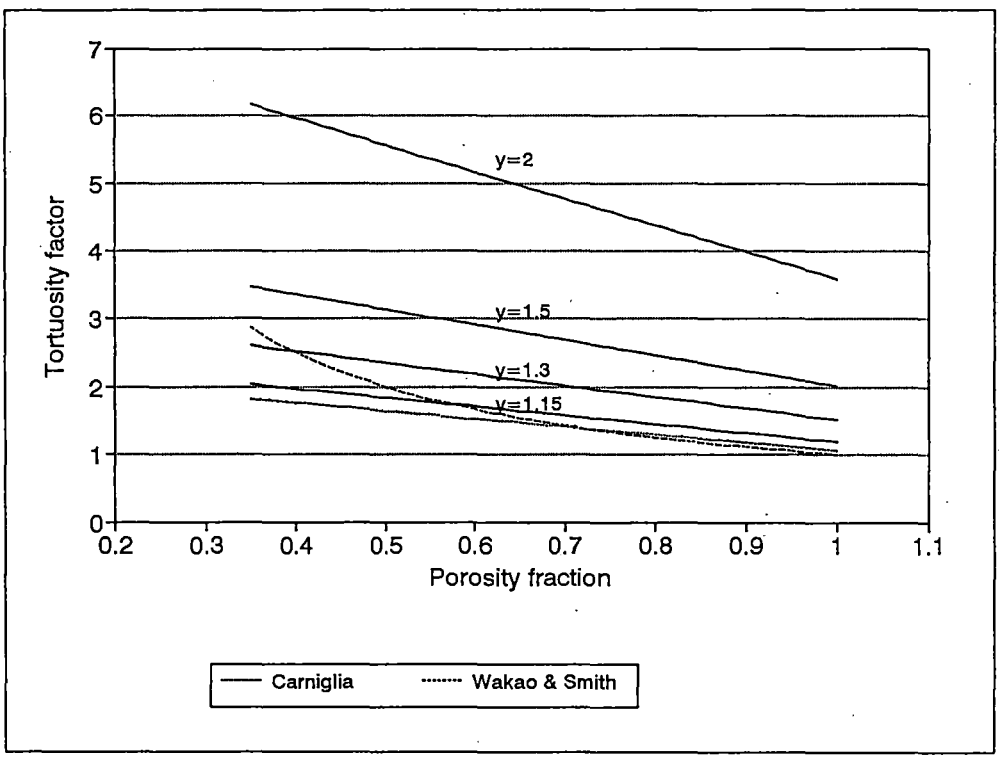

Figure 4.1 Relationship between various tortuosity factors.

cylindrical diffusion paths, equations (7) and (11) respectively, coincide for the case where the pore shape factor (y) equals 1.1 for the non-cylindrical path.

4.3.2 Repeatability of TF and KED values for γ-alumina samples

Table 4.1 shows that γ-aluminas prepared in the absence of additives have average tortuosity factors of 1.66 ± 0.02 and 1.99 ± 0.06, respectively, for the two methods. These values were linked to a porosity fraction of 0.50 ± 0.02. These parameters have acceptable correlation coefficients. Although not indicated, a pore shape factor of 1 was obtained, which indicated the presence of cylindrical pores. KED values of 0.0031 ± 0.0003 cm^2/s and 0.0671 ± 0.0265 cm^2/s (D^0-based) were obtained for the respective

Table 4.1 Tortuosity factor and Knudsen effective diffusivities for γ-alumina prepared in the absence of additives.

Sample	$\in$ [a]	$\tau_{Carniglia}$ [b]	$\tau_{Wakao\&Smith}$ [b]	$D_{K,eff,384K}$ (cm^2/s)	$D_{K,eff,384K}$ D^0-based (cm^2/s)
1	0.52	1.65	1.93	0.0035	0.0763
2	0.51	1.66	1.97	0.0033	0.1012
3	0.50	1.67	2.00	0.0029	0.0837
4	0.52	1.65	1.94	0.0032	0.0474
5	0.47	1.69	2.11	0.0025	0.0271
Average	0.50	1.66	1.99	0.0031	0.0671
Standard deviation	0.02	0.02	0.06	0.0003	0.0265
Correlation coefficient	3.68	0.90	3.26	11	39

[a] Porosity
[b] Tortuosity factor

diffusion estimate methods. The former KED value corresponds favourably with values estimated by Conner *et al.* (1991) for γ-alumina based on the method of Satterfield and Sherwood (1963), namely 0.003 cm^2/s. Higher KED (D^0) values based on the method of Carniglia (1986) can be expected, since this method accounts for the effective diffusion over the whole pore size distribution range. Therefore, these KED values can be considered as the more representative values. A difficulty in controlling the actual pore size distribution was suggested, as indicated by the high correlation coefficient of the KED (D^0) values. Similar repeatability trends were obtained for *cis*-oleic acid γ-alumina as found for the control samples (Table 4.2) and the correlation coefficients improved significantly.

Table 4.2 Tortuosity factor and Knudsen effective diffusivities for γ-alumina prepared in the presence of *cis*-oleic acid.

Sample	$\in$ [a]	$\tau_{Carniglia}$ [b]	$\tau_{Wakao\&Smith}$ [b]	$D_{K,eff,384K}$ (cm^2/s)	$D_{K,eff,384K}$ D^0-based (cm^2/s)
1	0.73	1.40	1.37	0.0105	0.3398
2	0.74	1.39	1.35	0.0119	0.6441
3	0.74	1.39	1.35	0.0122	0.4750
Average	0.74	1.39	1.36	0.0115	0.4863
Standard deviation	0.005	0.005	0.009	0.0007	0.1245
Correlation coefficient	0.64	0.34	0.69	6.42	25.60

[a] Porosity
[b] Tortuosity factor

4.3.3 TF, PSF and KED values for γ-alumina prepared in the presence of various additives

The effects of various porogens on TF, PSF and KED values are shown in Table 4.3. Data was sorted into descending order of KED (D^0) values. Where the PSF values (y) exceeded 1.1, plots of $D_K(r)$ versus radii at D^0 yielded slopes of unity for n.

The following points are noted from the data shown in Table 4.3:

1) Materials having relatively high porosity are, in general, associated with high KED (D^0) values, although no linear relationship is evident.

2) KED (D^0) values obtained with ammonium carbonate- and 2-pentanol-derived γ-alumina approached those for molecular diffusion.

3) The shorter members of porogens investigated, for example ethanol/acetic acid/ammonium acetate, resulted in the lowest KED (D^0)

Table 4.3 Tortuosity factor and Knudsen effective diffusivities for γ-alumina prepared in the presence of various porogens.

Sample	Additive: Al^{3+} molar ratio	ϵ^a	y^c	$\tau_{Carniglia}{}^b$	$\tau_{Wakao\&Smith}{}^b$	$D_{K,eff,384K}$ (cm^2/s)	$D_{K,eff,384K}$ D^0-based (cm^2/s)
Amm. carbonate	0.33	0.67	-	1.47	1.49	0.0096	0.9103
2-Pentanol	0.18	0.58	-	1.58	1.72	0.0043	0.7344
Castor oil	0.05	0.73	-	1.40	1.37	0.0110	0.5714
Olive oil	0.05	0.67	-	1.47	1.49	0.0081	0.5117
cis-Oleic acid	0.06	0.74	-	1.39	1.36	0.0115	0.4863
Stearic acid	0.06	0.64	-	1.50	1.56	0.0055	0.4271
Tartaric acid	0.11	0.63	-	1.52	1.59	0.0073	0.4233
Sunflower oil	0.05	0.66	-	1.49	1.52	0.0071	0.3683
Citric acid	0.08	0.56	-	1.60	1.79	0.0037	0.3474
Amm. citrate	0.07	0.57	-	1.59	1.75	0.0039	0.3171
Succinic acid	0.14	0.60	-	1.55	1.67	0.0050	0.2855
Maleic acid	0.14	0.57	-	1.59	1.75	0.0044	0.2602
Sebacic acid	0.08	0.60	-	1.55	1.67	0.0062	0.2509
Amm. tartrate	0.09	0.61	-	1.54	1.64	0.0052	0.2385
n-Hexanol	0.16	0.52	-	1.64	1.92	0.0032	0.2378
Adipic acid	0.11	0.56	-	1.60	1.79	0.0042	0.2209
Palmitic acid	0.06	0.69	-	1.45	1.45	0.0098	0.2167
Oleyl alcohol	0.06	0.62	-	1.53	1.61	0.0055	0.2150
Mannitol	0.09	0.57	-	1.58	1.75	0.0046	0.2079
Triethanolamine	0.11	0.62	-	1.63	1.61	0.0060	0.2024
Ethanol	0.35	0.50	-	1.66	2.00	0.0033	0.1583
Lactic acid	0.18	0.56	-	1.60	1.79	0.0035	0.1582
Benzoic acid	0.13	0.54	-	1.62	1.85	0.0040	0.1255
sec-Butanol	0.22	0.50	-	1.66	2.00	0.0034	0.1210
Formic acid	0.35	0.49	1.21	2.08	2.04	0.0020	0.0980
iso-Butyric acid	0.18	0.54	-	1.62	1.85	0.0033	0.0927
Methanol	0.50	0.52	-	1.65	1.92	0.0030	0.0808

continued overleaf

Table 4.3 cont.

Sample	Additive: Al^{3+} molar ratio	$\in^a$	y^c	$\tau_{Carniglia}{}^b$	$\tau_{Wakao\&Smith}{}^b$	$D_{K,eff,384K}$ (cm^2/s)	$D_{K,eff,384K}$ D^0-based (cm^2/s)
Amm. oxalate	0.11	0.53	-	1.63	1.89	0.0035	0.0719
Control	-	0.50	-	1.66	1.99	0.0031	0.0671
Sucrose	0.05	0.51	-	1.65	1.96	0.0034	0.0658
Diethylene glycol	0.15	0.54	1.38	2.61	1.85	0.0022	0.0601
Glucose	0.09	0.52	2.08	6.05	1.92	0.0009	0.0570
Acetic acid	0.27	0.51	1.88	4.96	1.96	0.0010	0.0533
iso-Butanol	0.22	0.49	1.44	2.95	2.04	0.0017	0.0457
Glycerine	0.17	0.54	1.56	3.36	1.85	0.0017	0.0377
n-Butanol	0.22	0.52	-	1.64	1.92	0.0035	0.0355
Propanol	0.27	0.49	1.56	3.47	2.04	0.0013	0.0318
Oxalic acid	0.18	0.48	-	1..69	2.08	0.0024	0.0264
Propionic acid	0.22	0.50	1.56	3.40	2.00	0.0014	0.0164
Amm. acetate	0.21	0.48	1.20	2.06	2.08	0.0022	0.0105
Amm. formate	0.25	0.48	-	1.69	2.08	0.0027	0.0013

[a] Porosity
[b] Tortuosity factor
[c] Pore shape factor

values. The development of non-cylindrical pores in γ-alumina was also evidenced at these low values.

4) The highest KED (D^0) values were obtained for the fatty acids as a group of porogens.

5) No correlation was found between KED and KED (D^0) values.

6) No relationship was noted between KED (D^0) values and additive-to-Al^{3+} molar ratios.

4.3.4 TF and KED values as obtained for γ-alumina prepared in the presence of various amounts of *cis*-oleic acid

Increased additions of *cis*-oleic acid resulted in increased γ-alumina porosities with a concomitant decrease in TF values with R^2 linearity of 83 and 84 - 86%, respectively (Table 4.4). This increase also resulted in increasing KED values with R^2 linearities of 92 and 90%, respectively, for the two KED properties under consideration. The increases in KED values are most likely due to the higher macroporosity and mesoporosity as well as larger pore sizes, which favour higher gas diffusion and therefore a higher diffusion flux, as indicated in Table 3.12 and 4.4, respectively.

4.3.5 Effect of ceria on TF and KED values of fatty acid-derived γ-alumina as a function of calcination temperature

Tables 4.5 to 4.10 give the TF and KED results obtained as a function of calcination temperature for various fatty acids/oils with and without the presence of ceria. The following points are noteworthy:

1) No change in tortuosity factors were observed because calcination temperature had, in general, no effect on porosity.

2) The KED (D^0) values were, in general, relatively constant during calcination for each type of fatty acid-derived γ-alumina. The variation in these values probably indicated the difficulty in controlling pore size distributions. Average KED (D^0) values were estimated and it was concluded that for all calcination temperatures and ceria additions these values increased in the order:
control < palmitic acid < *cis*-oleic acid < sunflower oil < olive oil < castor oil.

Similar averages were estimated for KED values, but the sequence was:
control < sunflower oil < olive oil < palmitic acid < castor oil < *cis*-oleic acid.

Table 4.4 Tortuosity factor and Knudsen effective diffusivities for γ-alumina prepared in the presence of various amounts of *cis*-oleic acid.

Sample (wt%)	ϵ [a]	$\tau_{Carniglia}$ [b]	$\tau_{Wakao\&Smith}$ [b]	$D_{K,eff,384K}$ (cm^2/s)	$D_{K,eff,384K}$ D^0-based (cm^2/s)
Control	0.50	1.66	1.99	0.0031	0.0671
0.5	0.52	1.64	1.92	0.0030	0.0233
1.6	0.54	1.62	1.46	0.0033	0.1175
15	0.68	1.46	1.47	0.0080	0.0128
30[d]	0.74	1.39	1.36	0.0115	0.4863
60	0.77	1.36	1.30	0.0141	0.8660
R^2 linearity (%)	83	84	86	92	90

[a] Porosity
[b] Tortuosity factor
[d] Average values from Table 4.2.

3) No correlation was obtained between KED (D^0) values, calcination temperature, and various ceria additions. KED values, however, increased with calcination temperature for all samples under consideration. In general, similar KED values were obtained for samples containing various ceria additions.

4.3.6 Relationship between KED (D^0) and TF values

Figure 4.2 illustrates the relationship between KED (D^0) and TF values for all additives investigated. Two distinctive regions were observed. It follows from this figure that most of the KED (D^0) values were concentrated above 0.200 cm^2/s and TF values below 2.00. This region was ascribed to cylindrical pores, while non-cylindrical pores are found in the TF region above 2.00. No linear correlations were obtained for either region. Similar trends were observed for KED and TF values. The sunflower oil-derived sample having a KED (D^0) value of 0.47 cm^2/s and a TF value of 3.38 was most probably an artefact caused by experimental errors.

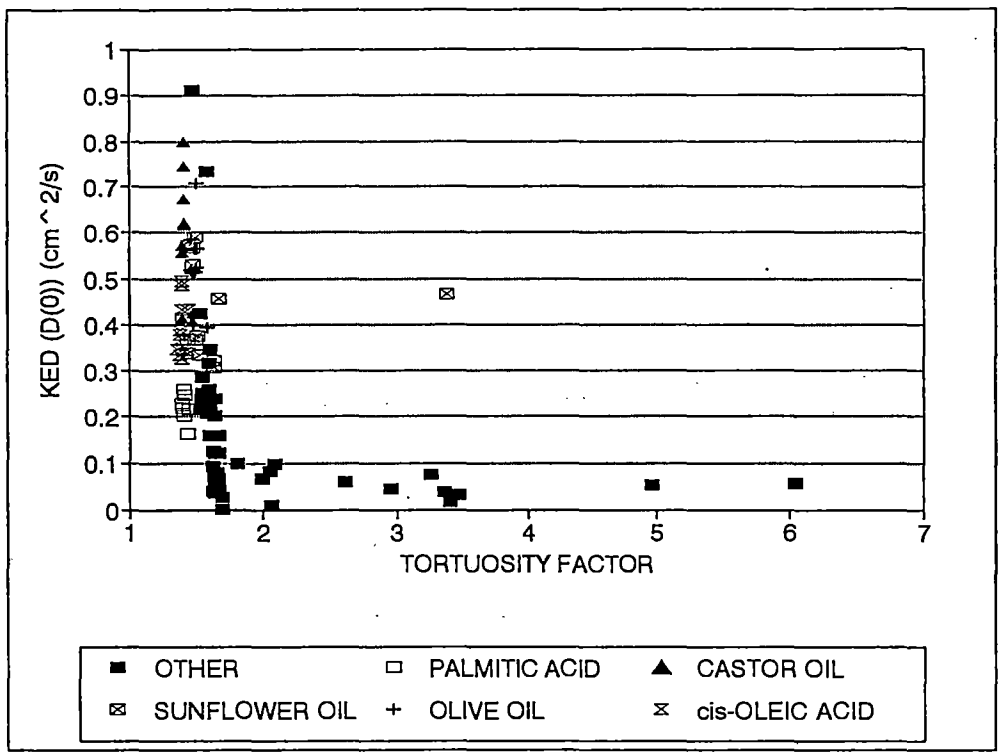

Figure 4.2 Relationship between KED (D^0) and TF values.

4.4 CONCLUSIONS

It is concluded that:

1) A close resemblance exists between the TF values determined by the methods of Wakao and Smith (1963) and Carniglia (1986) at porosity fractions greater than 0.60.

2) The KED value of 0.0031 cm^2/s obtained for γ-alumina (control) corresponds favourably with values listed in the literature.

3) Significantly higher KED (D^0) values were obtained when the method of Carniglia was employed. This method accounts for the effective gas diffusion over the whole pore size distribution range, and so can be considered as more representative values than those obtained from the method of Satterfield and Sherwood.

4) Materials having relatively high porosity are associated with high KED (D^0) values, although no linear relationship existed.

5) KED (D^0) values obtained with ammonium carbonate- and 2-pentanol- derived γ-alumina approached those for molecular diffusion.

6) The shorter members of porogens investigated, for example ethanol/acetic acid/ammonium acetate, resulted in the lowest KED (D^0) values. The development of non-cylindrical pores in γ-alumina is also evidenced at these low values.

7) The highest KED (D^0) values were obtained for the fatty acids as a group of porogens.

8) No correlation was found between KED and KED (D^0) values.

9) No relationship was noted between KED (D^0) values and additive-to-Al^{3+} molar ratios.

10) Increased additions of *cis*-oleic acid resulted in increased γ-alumina porosities with a concomitant decrease in TF values, while both types of KED values increased. This was most likely due to higher macro- and mesoporosity as well as to larger pore sizes which favour higher gas diffusional fluxes.

11) TF values of γ-aluminas were not affected by various calcination temperatures because the porosities were constant throughout.

12) KED (D^0) values were relatively constant during calcination for each type of fatty acid-derived γ-alumina. The variation in these values is ascribed to the difficulty in controlling pore size distributions.

13) No correlation was found between KED (D^0) values, calcination temperature, and various ceria additions, but KED values increased with calcination temperature for all samples investigated. Similar KED values were obtained for samples containing ceria additions.

14) Average KED (D^0) values increased for fatty acid-derived γ-alumina for all calcination temperatures and ceria additions. The order was:
control < palmitic acid < *cis*-oleic acid < sunflower oil < olive oil < castor oil.

For KED values, the sequence was:
control < sunflower oil < olive oil < palmitic acid < castor oil < *cis*-oleic acid.

15) Two distinctive regions were observed when KED (D^0) and KED were plotted as a function of TF. These were assigned to cylindrical (TF < 2.00 and KED (D^0) > 0.200 cm^2/s) and non-cylindrical (TF > 2.00) pores.

Table 4.5 Tortuosity factors and Knudsen effective diffusivities for γ-alumina samples prepared in the absence of additives and in the presence of ceria and calcined at various temperatures.

Sample	ϵ	y	$\tau_{Carniglia}$	$\tau_{Wakao\&Smith}$	$D_{K,eff,384K}$ (cm^2/s)	$D_{K,eff,384K}$ D^0-based (cm^2/s)
550	0.50	-	1.66	1.99	0.0031	0.0671
700	0.54	-	1.62	1.85	0.0037	0.0397
800	0.51	1.21	2.05	1.96	0.0042	0.0831
900	0.51	-	1.65	1.94	0.0055	0.0735
1000	0.50	-	1.67	2.00	0.0061	0.0422
700 + 3 wt% ceria	0.56	-	1.81	1.78	0.0058	0.0995
700 + 11 wt% ceria	0.53	1.11	3.26	1.89	0.0027	0.0752
800 + 3 wt% ceria	0.52	-	1.65	1.92	0.0057	0.0445
800 + 11 wt% ceria	0.52	-	1.64	1.92	0.0055	0.1228
900 + 3 wt% ceria	0.52	-	1.64	1.92	0.0054	0.0607
900 + 11 wt% ceria	0.52	-	1.64	1.92	0.0043	0.0471
1000 + 3 wt% ceria	0.50	-	1.66	2.00	0.0057	0.0538
1000 + 11 wt% ceria	0.50	-	1.66	2.00	0.0062	0.0497

Table 4.6 Tortuosity factors and Knudsen effective diffusivities for γ-alumina samples prepared in the presence of palmitic acid and ceria and calcined at various temperatures.

Sample	ϵ	$\tau_{Carniglia}$	$\tau_{Wakao\&Smith}$	$D_{K,eff,384K}$ (cm^2/s)	$D_{K,eff,384K}$ D^0-based (cm^2/s)
550	0.69	1.45	1.44	0.0098	0.2167
700	0.73	1.40	1.36	0.0143	0.4161
800	0.73	1.41	1.37	0.0183	0.2589
900	0.71	1.43	1.42	0.0195	0.3700
700 + 3 wt% ceria	0.73	1.41	1.38	0.0137	0.2024
700 + 11 wt% ceria	0.72	1.42	1.38	0.0129	0.2475
800 + 3 wt% ceria	0.74	1.39	1.35	0.0178	0.2301
800 + 11 wt% ceria	0.74	1.40	1.36	0.0179	0.2178
900 + 3 wt% ceria	0.68	1.44	1.43	0.0179	0.5703
900 + 11 wt% ceria	0.71	1.43	1.41	0.0175	0.1632

Table 4.7 Tortuosity factors and Knudsen effective diffusivities for γ-alumina samples prepared in the presence of castor oil and ceria and calcined at various temperatures.

Sample	ϵ	$\tau_{Carniglia}$	$\tau_{Wakao\&Smith}$	$D_{K,eff,384K}$ (cm^2/s)	$D_{K,eff,384K}$ D^0-based (cm^2/s)
550	0.73	1.40	1.37	0.0110	0.5714
700	0.74	1.39	1.35	0.0148	0.4144
800	0.73	1.40	1.37	0.0156	0.5549
900	0.72	1.41	1.38	0.0184	0.6192
700 + 3 wt% ceria	0.73	1.41	1.37	0.0142	0.7996
700 + 11 wt% ceria	0.73	1.41	1.37	0.0136	0.7454
800 + 3 wt% ceria	0.73	1.41	1.38	0.0151	0.6717
800 + 11 wt% ceria	0.67	1.47	1.50	0.0117	0.4073
900 + 3 wt% ceria	0.67	1.48	1.50	0.0123	0.4233
900 + 11 wt% ceria	0.72	1.41	1.38	0.0183	0.6143

Table 4.8 Tortuosity factors and Knudsen effective diffusivities for γ-alumina samples prepared in the presence of sunflower oil and ceria and calcined at various temperatures.

Sample	ϵ	y	$\tau_{Carniglia}$	$\tau_{Wakao\&Smith}$	$D_{K,eff,384K}$ (cm^2/s)	$D_{K,eff,384K}$ D^0-based (cm^2/s)
550	0.66	-	1.49	1.52	0.0071	0.3683
700	0.53	-	1.63	1.87	0.0048	0.3218
800	0.66	-	1.48	1.51	0.0111	0.5303
900	0.65	-	1.49	1.53	0.0132	0.5897
700 + 3 wt% ceria	0.63	1.62	3.38	1.59	0.0033	0.4671
700 + 11 wt% ceria	0.53	-	1.63	1.88	0.0042	0.3067
800 + 3 wt% ceria	0.50	-	1.67	2.01	0.0036	0.4581
800 + 11 wt% ceria	0.66	-	1.48	1.52	0.0108	0.5662
900 + 3 wt% ceria	0.63	-	1.52	1.59	0.0110	0.3342
900 + 11 wt% ceria	0.64	-	1.51	1.56	0.0109	0.3754

Table 4.9 Tortuosity factors and Knudsen effective diffusivities for γ-alumina samples prepared in the presence of olive oil and ceria and calcined at various temperatures.

Sample	ϵ	$\tau_{Carniglia}$	$\tau_{Wakao\&Smith}$	$D_{K,eff,384K}$ (cm^2/s)	$D_{K,eff,384K}$ D^0-based (cm^2/s)
550	0.67	1.47	1.48	0.0081	0.5117
700	0.65	1.50	1.54	0.0089	0.7081
800	0.69	1.46	1.46	0.0128	0.5852
900	0.68	1.46	1.47	0.0147	0.5185
700 + 3 wt% ceria	0.64	1.51	1.57	0.0077	0.5644
700 + 11 wt% ceria	0.58	1.58	1.73	0.0058	0.3946
800 + 3 wt% ceria	0.65	1.49	1.53	0.0108	0.5147
800 + 11 wt% ceria	0.65	1.49	1.54	0.0096	0.5656
900 + 3 wt% ceria	0.66	1.48	1.51	0.0127	0.3978
900 + 11 wt% ceria	0.64	1.50	1.55	0.0123	0.5236

Table 4.10 Tortuosity factors and Knudsen effective diffusivities for γ-alumina samples prepared in the presence of *cis*-oleic acid and ceria and calcined at various temperatures.

Sample	ϵ	$\tau_{Carniglia}$	$\tau_{Wakao\&Smith}$	$D_{K,eff,384K}$ (cm^2/s)	$D_{K,eff,384K}$ D^0-based (cm^2/s)
550	0.74	1.39	1.36	0.0115	0.4863
700	0.75	1.38	1.33	0.0157	0.3890
800	0.74	1.39	1.35	0.0163	0.4937
900	0.74	1.39	1.35	0.0176	0.4329
1000	0.70	1.44	1.44	0.0179	0.4338
700 + 3 wt% ceria	0.75	1.39	1.34	0.0140	0.3251
700 + 11 wt% ceria	0.74	1.39	1.35	0.0146	0.3698
800 + 3 wt% ceria	0.75	1.38	1.33	0.0173	0.3788
800 + 11 wt% ceria	0.77	1.36	1.30	0.0215	0.3486
900 + 3 wt% ceria	0.74	1.39	1.34	0.0184	0.3452
900 + 11 wt% ceria	0.75	1.38	1.33	0.0216	0.3347
1000 + 3 wt% ceria	0.70	1.44	1.43	0.0178	0.3399
1000 + 11 wt% ceria	0.70	1.43	1.42	0.0207	0.3459

CHAPTER 5. SPRAY-DRIED POWDERS AND WASH COAT COMPOSITES

5.1 INTRODUCTION

Preparation procedures for an effective cordierite wash coat eventually determine the mechanical and physical properties of the final product. The steps involved consist of spray-drying γ-alumina gels and redispersion of the spray-dried particles with an alumina sol which also serves as a final binder of the particles.

Because of promising results obtained with *cis*-oleic acid as a porogen, this was used during the preparation of spray-dried powders. Two commercial grades, with different *cis*-oleic acid concentrations, were also evaluated and compared with surface properties obtained for pure *cis*-oleic acid prepared in Section 3.2 and a commercial γ-alumina powder used to produce automobile exhaust catalysts. The effect of ceria placement into the alumina structure prior to calcination was also investigated.

Flow-chart 5.1 gives an outline of the contents of this chapter.

5.2 EXPERIMENTAL PROCEDURES

5.2.1 Spray-drying of aluminium hydroxide gels

Batches of aluminium hydroxide gels were produced from 368 g aluminium nitrate nonahydrate dissolved in one litre deionised water. This was followed by the addition of 15 g *cis*-oleic acid dissolved in 120 ml ethanol, which is equivalent to 30 wt% of dry product. The white-to-yellow emulsion was immediately neutralised with 265 $\pm$ 15 ml ammonia solution (25%) to a final pH of 9.0 $\pm$ 0.2. In the case where 3 wt% ceria (based on formed γ-alumina) was built into the structure, 3.8 g cerium nitrate hexahydrate was added. This was allowed to dissolve in the aluminium nitrate solution

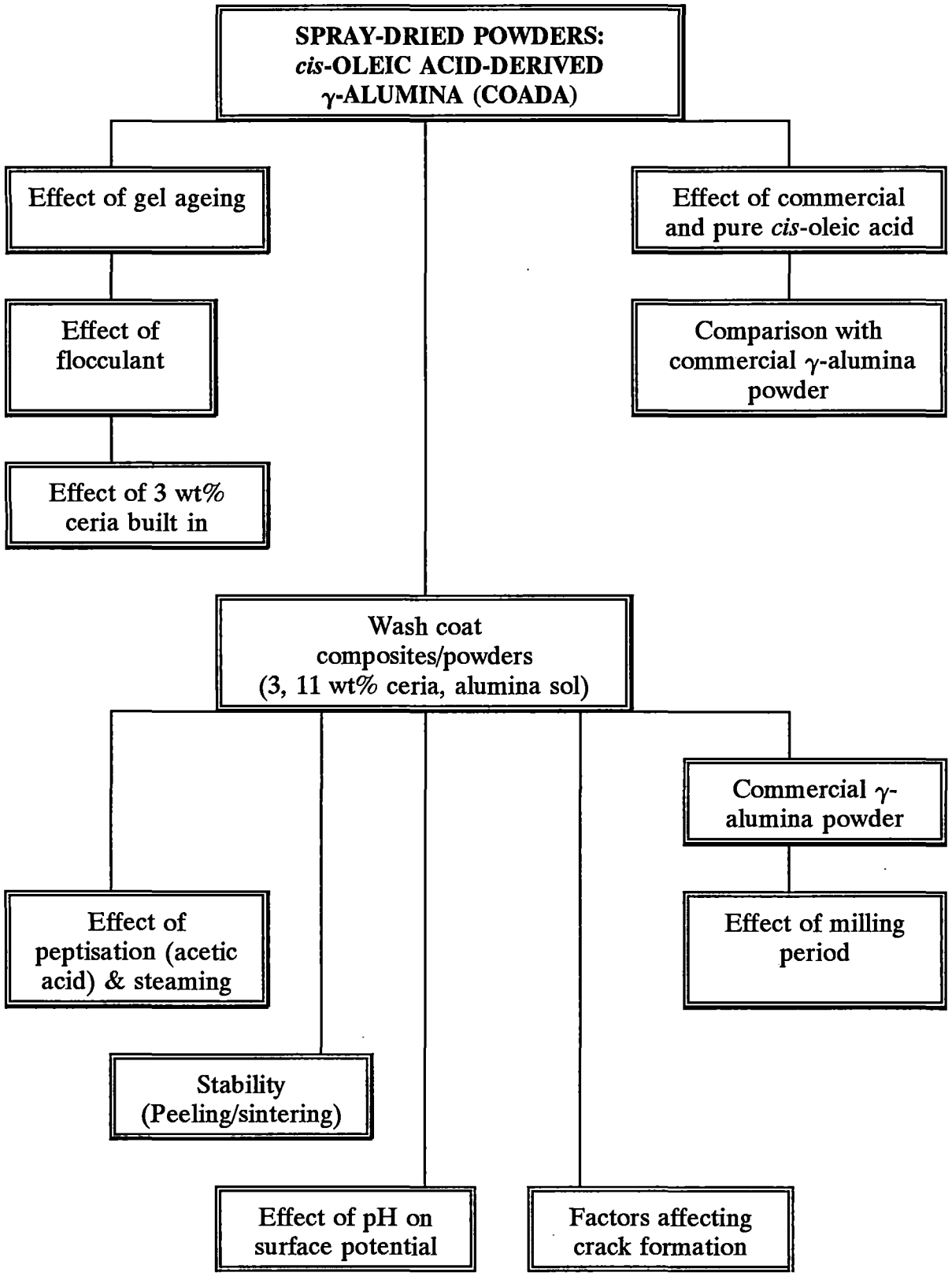

Flow-chart 5.1 Contents of chapter.

prior to addition of ethanolic *cis*-oleic acid and neutralisation with ammonia. The slurry was agitated for 10 minutes at 100 rpm. The resultant gel was aged for 12 h at 90 °C in a water bath. The product was a thick gel and final pH value of the mother liquor was 8.0 $\pm$ 0.3.

The gel was flocculated with a commercially available low anionic polyacrylamide flocculant, with a molecular mass of 6 - 7 million. This flocculant was added in amounts of 0.25 g/kg of formed gel and water. The mother liquor was then decanted and mixed with one litre deionised water. This latter step was repeated until a nitrate-free (Waters Anion chromatograph) level of <100 ppm was obtained. The gel was redispersed by the addition of 0.36% sodium metasilicate, which was based on the weight of dry product. Viscosities were determined with a Sheen rotary viscometer at 200 rpm. Slurries were spray-dried in a laboratory-scale rotating disc Niro atomizer with a one kg/h capacity. The spray-drying conditions used are given in Table 5.1.

Table 5.1 Spray-drying conditions of aluminium hydroxide gels.

Inlet pressure (kg/cm^2)	4.2 - 7.6
Inlet air temperature (°C)	225 - 240
Outlet air temperature (°C)	120 - 140
Feed rate of slurry (ml/min)	20 - 25
Viscosity of feed (cP)	200 - 300

After spray-drying, the resultant powders were calcined at 700 °C for 2 h for small batches ($\pm$ 50 g) and 3 h for larger batches (300 - 350 g). Two commercial *cis*-oleic acid samples, namely Priolene 6921 and 6952 (see Appendix A), were also used to produce small batches of γ-alumina spray-dried powders. These powders were used for wash-coating monoliths.

5.2.2 Monolith wash-coating

Four different types of wash coat slurries were prepared:

1) A commercial γ-alumina (see Appendix F for composition and surface properties) to which 11 wt% ceria was added.

2) *Cis*-oleic acid-derived γ-alumina (COADA) spray-dried powder containing 3 wt% ceria built in subsequent to calcination.

3) *Cis*-oleic acid-derived γ-alumina (COADA) spray-dried powder containing 11 wt% ceria built in subsequent to calcination.

4) COADA spray-dried powder containing 3 wt% ceria that was built into the structure prior to calcination.

Table 5.2 summarises the compositions and preparation conditions used for various wash coat slurries.

Table 5.2 Slurry compositions and wash coat conditions.

Parts by weight	Commercial powder + 11 wt% ceria	*cis*-Oleic acid + 11 wt% ceria	*cis*-Oleic acid + 3 wt% ceria	*cis*-Oleic acid + 3 wt% ceria built-in
γ-alumina	79	79	79	82
Alumina sol[a]	57	58	59	59
Aluminium nitrate solution (40%)	13	13	15	13
Acetic acid conc.	10	10	10	10
Cerium nitrate	27	27	7	-
Water	79	136	130	152
Solids (%)	40	33	33	32
Slurry density (g/cm^3)	1.55	1.42	1.40	1.36
pH	2.99 - 3.25	3.17 - 3.42	3.41 - 3.48	3.78 - 3.87
Milling time[b] (h)	12	1	1	1.5

[a] See Appendix G for specifications.

[b] Slurries were milled in a 100 ml glass container, containing 200 g ZrO_2 2 mm beads, that was suspended on rollers.

Monoliths of 5 and 60 mm lengths, consisting of 144 square channels cut from a commercial monolith comprising 64 cells/cm^2, were coated. Two different coating techniques were used:

1) The 5 mm samples were dip-coated for 20 seconds. Excess suspension was removed by blowing the entrained excess solution out with compressed air.

2) For 60 mm samples, surfaces were coated with a slurry amount capable of coating 60 - 70% of the inner surface by drawing the suspension up into the monolith channels at 50 mm water pressure for the first minute, followed by 300 mm water pressure for another minute. The monolith was inverted through 180° and the previous step was repeated. The final amount used was such that the weight contributed by the wash-coated layers after calcination was between 20 - 30% of the total weight of the coated monoliths. Excess slurry was also removed with compressed air.

The coated monoliths were suspended on a wire mesh and aged for 24 h in a closed vessel filled one third with water. This was followed by steam drying at 125 °C for 4 h, followed by calcination at 700 °C for 2 h to fix the wash coat layers.

Properties of calcined products (powders and 5 mm coated monoliths) were determined by similar techniques as described before (Sections 3.2 and 4.2). Particle size analysis was carried out with a Malvern particle size analyzer. Peeling tests were carried out with 60 mm samples in an ultrasonic water bath. Each sample was subjected to ultrasound for 30 minutes and dried at 125 °C for 2 h. Stability tests were also performed on similarly coated 60 mm monoliths. These were sintered at 980 °C for 4 h in static air. These monoliths were then subjected to peeling tests. Zeta potentials of uncoated monoliths and various alumina powders were measured on a Malvern Zetasizer 2C in a 5 x 10^{-3} M $NaClO_4$ medium, after conditioning the samples for 30 minutes in this medium.

5.3 RESULTS AND DISCUSSION

5.3.1 Properties of spray-dried powders

Table 5.3 summarises all surface properties obtained for various spray-dried *cis*-oleic acid-derived γ-alumina (COADA) and commercial alumina powders. The COADA samples were flocculated, washed, and spray-dried and these included:

1) pure and commercial *cis*-oleic acid-derived γ-alumina samples,

2) aged and non-aged aluminium hydroxide gel samples,

3) samples containing 3 wt% ceria that was built into the structure of γ-alumina, followed by ageing, and

4) samples prepared in the absence of *cis*-oleic acid (control), but aged.

These results were compared to properties obtained for commercial alumina powder, while those results obtained for *cis*-oleic acid in Sections 3.2 and 4.2 were also compared to *cis*-oleic acid samples prepared in this section.

5.3.1.1 Factors affecting pore properties

Factors that affected pore properties were:

1) Ageing of *cis*-oleic acid-derived aluminium hydroxide gels. This procedure (compare samples B and C) enhanced total, meso- and macropore volumes, pore diameter size and surface area. Chertov and Okopnaya (1975) also observed an increase in surface area for chromium hydroxide after ageing at 100 °C. Ageing, however, decreased KED and KED (D^0) values as well as bulk density.

2) Flocculation. When a flocculant (samples A and B) was employed in the presence of *cis*-oleic acid there was an increase in total and macropore volumes as well as $\in$ and KED values, but pore diameter size and TF values decreased.

Table 5.3 Properties of spray-dried *cis*-oleic acid and commercial alumina powder.

Sample	Total pore volume (cm^3/g)	Meso-pore volume (cm^3/g)	Macro-pore volume (cm^3/g)	ϵ^a	Median pore diam. (nm)	Hg surface area (m^2/g)	N_2 surface area (m^2/g)	Bulk density (g/cm^3)	Skeletal density (g/cm^3)	τ^d	τ^e	$D_{Knud,eff,384K}$ D^0-based (cm^2/s)	$D_{Knud,eff,384K}$ (cm^2/s)
cis-oleic acid (A)[f]	0.911	0.617	0.255	0.74	7.12	336	302	0.81	3.09	1.39	1.36	0.4863	0.0115
Control[g]	1.024	0.536	0.636	0.76	6.22	349	289	0.75	3.04	1.38	1.32	0.8171	0.0215
Non-aged gel, flocculated *cis*-oleic acid (B)[h]	1.264	0.322	0.788	0.80	6.26	190	190	0.64	3.26	1.32	1.25	0.4349	0.0292
Gel aged, flocculated *cis*-oleic acid (C)[i]	1.482	0.496	0.986	0.82	9.76	204	277	0.56	3.15	1.30	1.21	0.4189	0.0233
cis-oleic acid (D)[j]	0.905	0.673	0.232	0.75	10.29	265	226	0.83	3.34	1.38	1.33	0.3890	0.0157
3 wt% ceria built-in *cis*-oleic acid[i]	1.227	0.521	0.706	0.79	6.91	303	266	0.65	3.10	1.34	1.27	0.3374	0.0196
Commercial cis-oleic acid Priolene 6921[k]	1.195	0.447	0.744	0.79	6.85	164	265	0.66	3.13	1.34	1.27	0.6082	0.0191
Priolene 6952[k]	1.302	0.498	0.803	0.80	7.67	264	262	0.62	3.09	1.32	1.25	0.5372	0.0216
Commercial powder Fresh[l]	0.888	0.421	0.468	0.75	10.20	160	149	0.84	3.33	1.39	1.33	0.8697	0.0231
Calcined[m]	0.877	0.415	0.462	0.74	10.47	154	154	0.85	3.28	1.39	1.35	0.5699	0.0218

continued overleaf

Table 5.3 cont.

[c] Porosity fraction.

[d] Tortuosity factor based on method of Carniglia (1986).

[e] Tortuosity factor based on method of Wakao & Smith (1962).

[f] From Tables 3.12 and 4.2.

[g] Prepared in absence of *cis*-oleic acid, washed in presence of flocculant, spray-dried and calcined at 550 °C for 2 h.

[h] Gel not aged, washed in presence of flocculant, spray-dried and calcined at 550 °C for 2 h.

[i] Gel aged for 12 h in water bath, washed in presence of flocculant, spray-dried and calcined at 700 °C for 3 h.

[j] Gel calcined at 700 °C for 2 h without washing or spray-drying.

[k] Processed as (i) above, but calcined at 700 °C for 2 h.

[l] As received.

[m] Powder calcined at 700 °C for 3 h.

In the absence of *cis*-oleic acid (control), the flocculant caused all physical properties to increase, except for the TF values.

3) *Cis*-oleic acid. This porogen (samples B and control) enhanced the total and macropore volumes as well as KED values, but mesopore volume and BET surface areas decreased.

4) Built-in ceria. Where 3 wt% ceria was built into the γ-alumina structure, all properties decreased compared to *cis*-oleic acid sample C. The most significant change was the drop in mesopore size and KED value.

5) Commercial *cis*-oleic acids. The pure *cis*-oleic acid sample (93%) (sample C) differed from the commercial grade mixtures. Lower physical properties were obtained with Priolene 6921 (88% *cis*-oleic acid) and Priolene 6952 (62% *cis*-oleic acid) (see Appendix A) than for pure COADA samples. Most notable were lower total and macropore volumes, smaller pore diameter and lower KED values, but higher KED (D^0) values.

6) Fresh and calcined (700 °C) commercial alumina powders had lower total, meso- and macropore volumes, $\in$ and surface areas than the COADA samples, although no differences occurred between the former samples after calcination.

7) The combined effect of *cis*-oleic acid, ageing, flocculation and spray-drying (samples C and D) enhanced BET surface area, porosity fraction and KED values. However, mesopore volume, pore diameter size and TF values decreased.

5.3.1.2 Scanning electron micrographs

Micrographs 5.1, 5.2 and 5.3 show the morphology of spray-dried COADA and commercial γ-alumina powders. A more uniform particle size distribution was seen with Micrograph 5.1 than 5.3 (see also Figure 5.1). Higher magnification of the COADA

sample revealed well-developed macropore structures.

5.3.1.3 Pore size distribution

The cumulative pore volume distribution in Figure 5.2 demonstrates the high amount of macroporosity (30 - 10 000 nm) as well as mesoporosity (± 10 nm) present in these samples.

5.3.2 Properties of wash coat composites/powders

Micrographs were employed to study different wash coat procedures. Micrographs 5.4 to 5.10 illustrate textures obtained for different wash coat slurries, while Table 5.4 summarises their physical properties.

5.3.2.1 Wash-coating with commercial alumina powder

Certain preparative procedures are required before bonding of the spray-dried material. One of these procedures is milling of the spray-dried material. A distribution of particle sizes results in a more dense and harder calcined matrix. The effect of milling for 24 h and 12 h, respectively, is seen in Micrographs 5.4 and 5.5. Stresses and strains in the matrix during cutting resulted in the cracks seen in Micrograph 5.4.

Uncontrolled preparative procedures, such as milling time, peptisation (double layer effects) and steaming, can give rise to undesirable structures and an example of a poor product is given in Micrograph 5.6. The commercial alumina sample that was peptised with acetic acid and steam treated resulted in the product shown in Micrograph 5.7. The enhanced KED and KED (D^0) values (Table 5.4) were also desirable properties of this preparation.

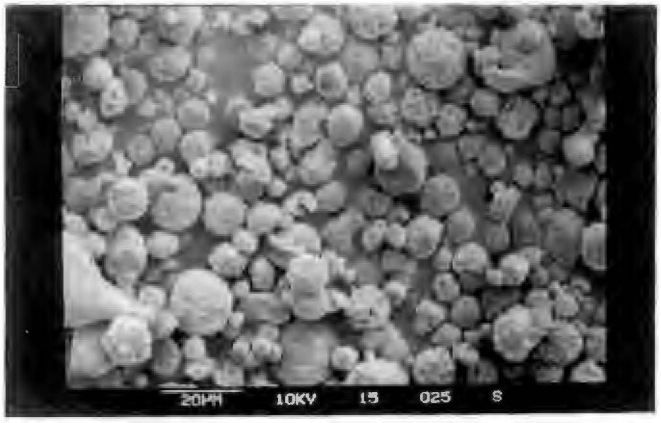

Micrograph 5.1 COADA spray-dried powder.

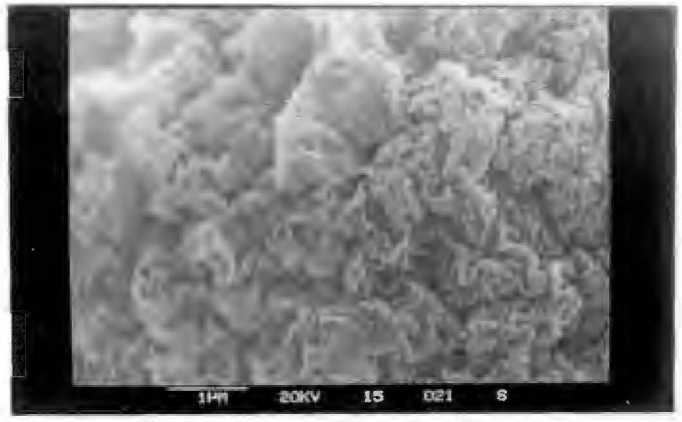

Micrograph 5.2 COADA spray-dried powder.

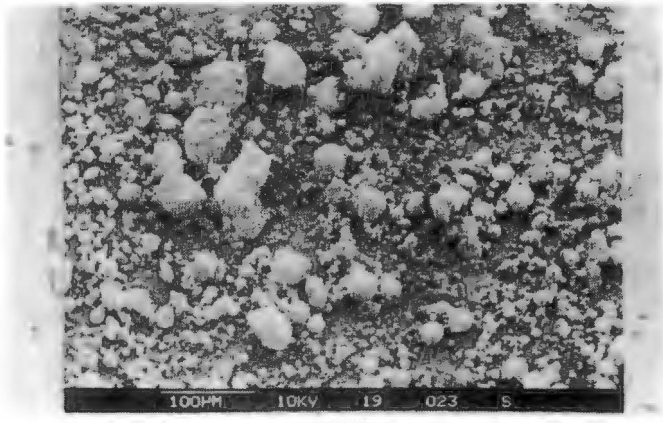

Micrograph 5.3 Commercial γ-alumina powder.

5.3.2.2 Wash-coating with COADA powder

Electron micrographs of monoliths coated with the commercial γ-alumina powder (Micrographs 5.7 and 5.8) can be compared with monoliths coated with COADA powder (Micrographs 5.9 and 5.10), respectively. These surface properties correspond to pore size distribution curves 1 and 5 in Figure 5.3, respectively. In Figure 5.3 commercial samples 1 and 2 differed in that the first was peptised with acetic acid and the second with nitric acid. The *cis*-oleic acid samples 3, 4 and 5 in Figure 5.3 differed in that sample 3 had 3 wt% ceria built into the crystallites of γ-alumina, whereas 4 and 5 contained 3 and 11 wt% ceria, respectively, added subsequent to wash-coating. Increased amounts of ceria increased mesoporosity, KED and KED (D^0) values, and these were significantly higher than the commercial alumina samples; macroporosity correspondingly decreased.

Micrographs 5.8 and 5.10 differ primarily in particle size distribution. From Figure 5.2 it can be seen that commercial γ-alumina powder had a wider distribution of particle sizes and there was a greater fraction of particle sizes less than 1 μm. These differences are due to different milling periods employed. For equivalent amounts of ceria added, the sample containing ceria built into the crystallite had a larger fraction of meso- and macropores.

Higher KED and KED (D^0) values were obtained for the COADA wash coat composites compared to their respective spray-dried powders. This is an indication of the packing of particles during preparation of the wash coat composite. This is in contrast with the lower KED and KED (D^0) values obtained for the commercial alumina powder composite, thereby demonstrating the advantage of employing COADA material.

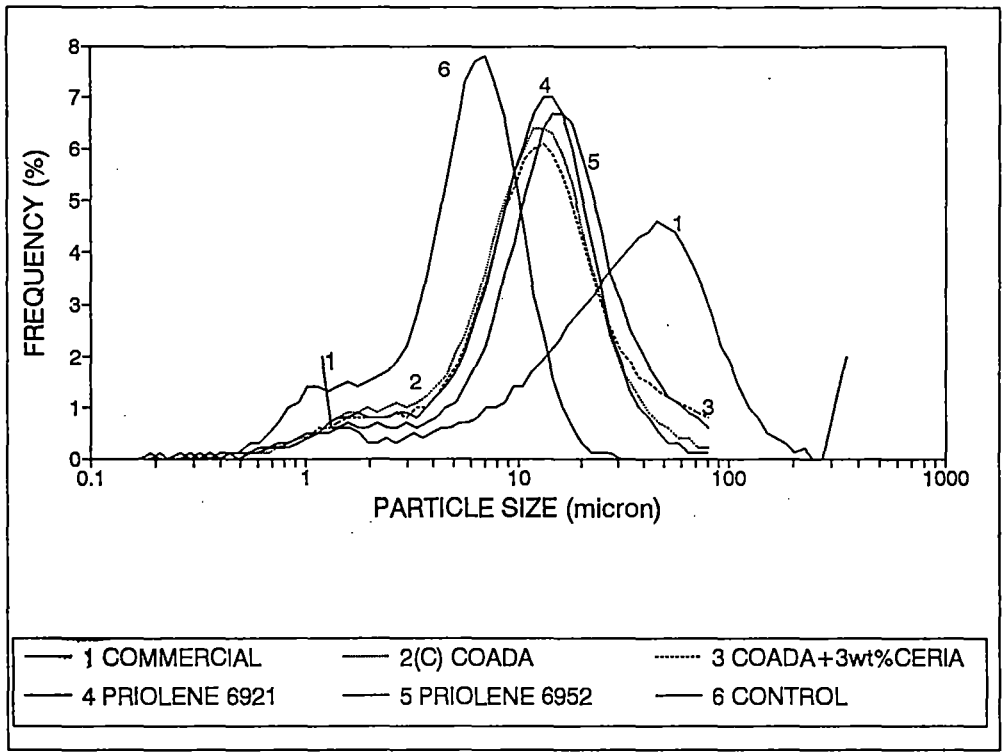

Figure 5.1 Particle size distributions of spray-dried powders.

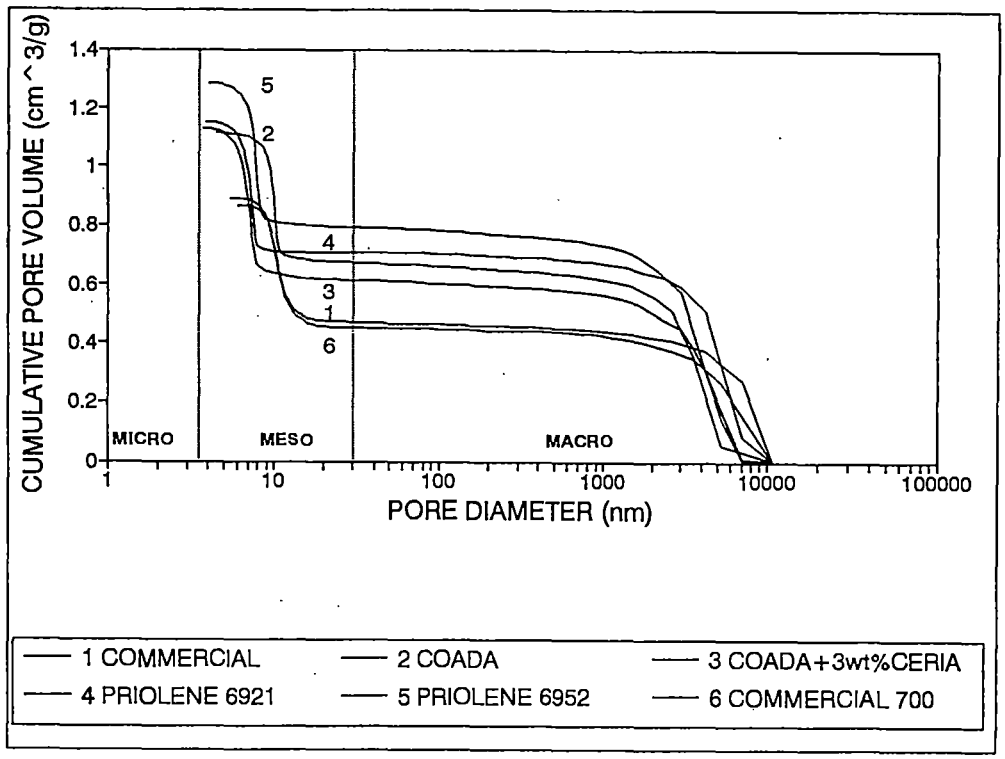

Figure 5.2 Cumulative pore volume distributions of spray-dried powders as a function of pore diameter.

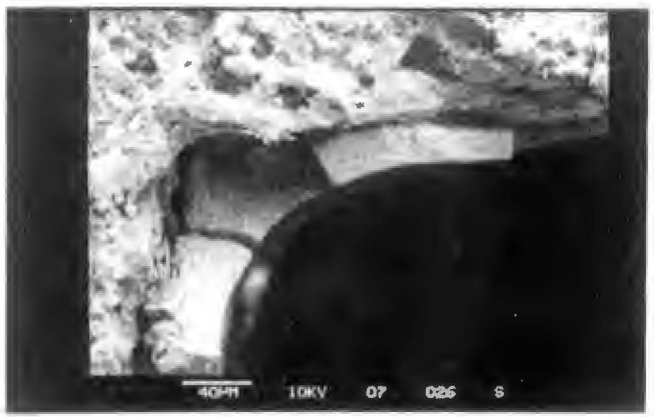

Micrograph 5.4 Sections of wash-coated commercial powder milled for 24 h.

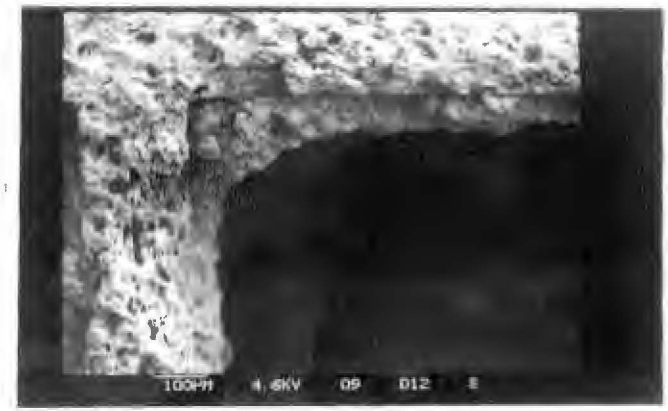

Micrograph 5.5 Sections of wash-coated commercial powder milled for 12 h.

Micrograph 5.6 Typical poor coating with commercial alumina powder.

Micrograph 5.7 Monolith wash-coated with commercial powder milled for 12 h.

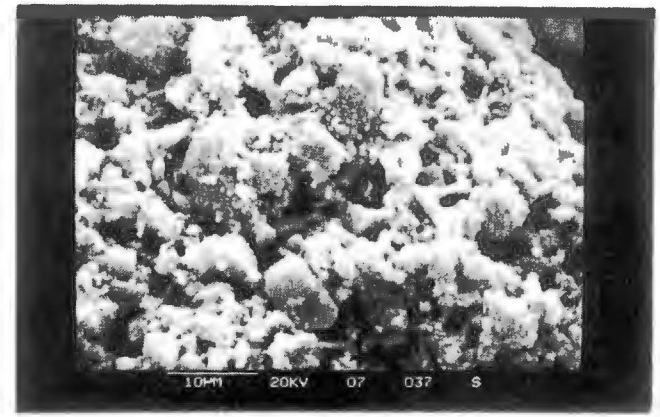

Micrograph 5.8 Surface of monolith wash-coated with commercial powder.

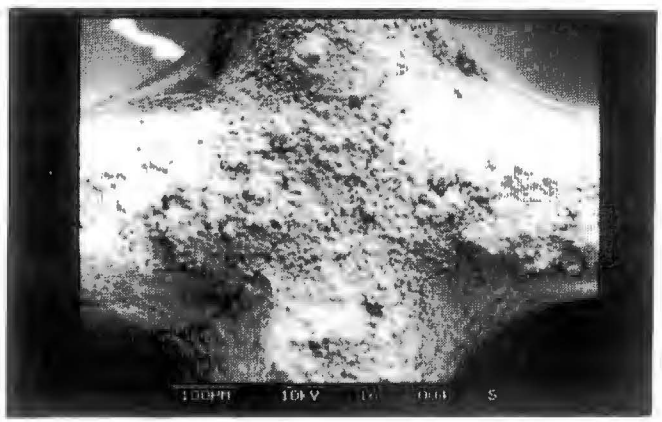

Micrograph 5.9 Monolith wash-coated with COADA powder.

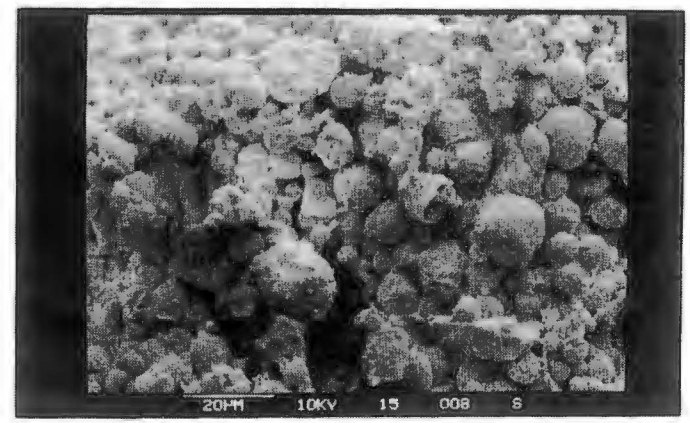

Micrograph 5.10 Surface of monolith wash-coated with COADA powder.

Table 5.4 Properties of wash coat composites. [Calcined at 700 °C for 2 h.]

Sample	Total pore volume (cm^3/g)	Meso-pore volume (cm^3/g)	Macro-pore volume (cm^3/g)	ϵ^c	Median pore diam. (nm)	Hg surface area (m^2/g)	N_2 surface area (m^2/g)	Bulk density (g/cm^3)	Skeletal density (g/cm^3)	τ^d	τ^e	$D_{Knud,eff,384K}$ (cm^2/s)	$D_{Knud,eff,384K}$ D^0-based (cm^2/s)
Commercial powder nitric acid + 11 wt% ceria	0.431	0.331	0.100	0.59	10.06	120	158	1.38	3.41	3.84	1.68	0.0030	0.1229
acetic acid + 11 wt% ceria	0.401	0.326	0.076	0.57	10.39	114	139	1.43	3.34	1.58	1.75	0.0075	0.1821
COADA powder 3 wt% ceria built-in	1.073	0.518	0.555	0.77	9.18	226	191	0.72	3.13	1.36	1.30	0.0228	0.6389
3 wt% ceria added	1.164	0.432	0.732	0.78	9.92	175	186	0.67	3.10	1.35	1.28	0.0262	0.4395
11 wt% ceria added	1.057	0.455	0.602	0.78	10.49	176	168	0.73	3.27	1.35	1.29	0.0259	1.0006

[c] porosity fraction

[d] tortuosity factor based on method of Carniglia.

[e] tortuosity factor based on method of Wakao & Smith.

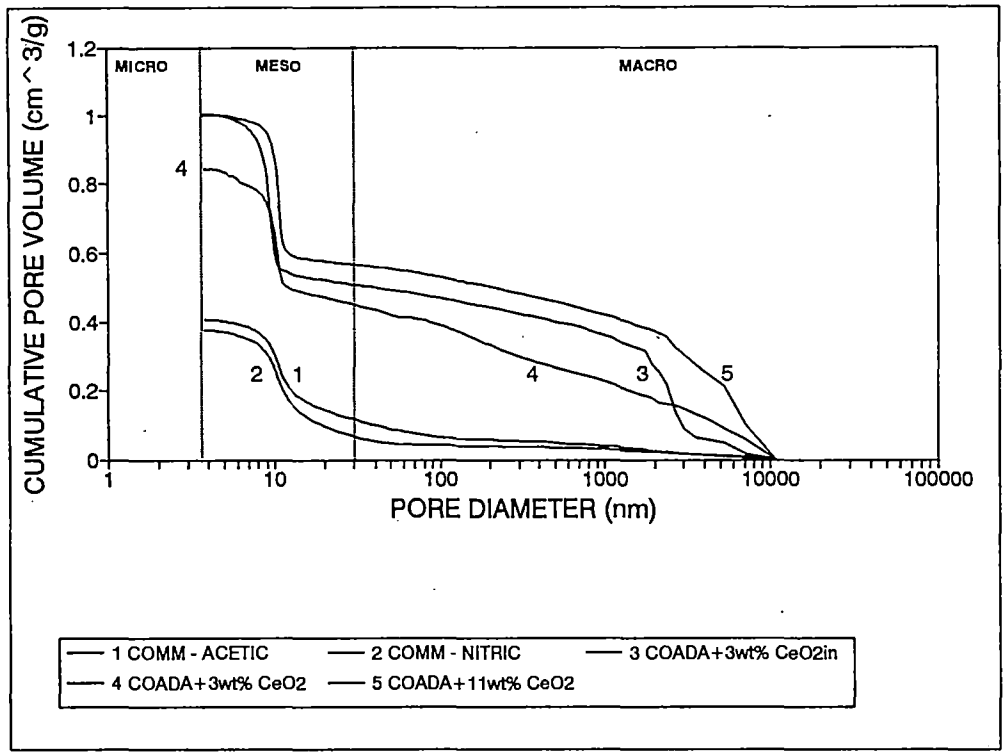

Figure 5.3 Cumulative pore volume distributions of wash coat composites.

5.3.2.3 Stability of wash coat layers

Table 5.5 gives weight losses after peeling and sintering tests of wash coat layers for different coated monoliths. In this attrition test, there was no difference whether the 3 wt% ceria was added or built into the crystallites. Weight losses of these samples were relatively high (29%) due to a certain lack of extra stickiness or bonding induced by this low ceria addition. The addition of 11 wt% ceria, however, significantly improved attrition resistance. Wash coats prepared with the commercial powder in the presence of nitric acid resulted in higher weight losses in comparison with the case where acetic acid was present.

Table 5.5 also shows the results obtained for the commercially coated monolith. The 3.59 wt% loss was obtained on a sawn-out sample from a commercial monolith. The high loss on peeling after sintering on COADA samples was a negative result.

Table 5.5 Peeling and sintering results of wash-coated monoliths.

Sample	Loss on peeling (wt%)	Loss on sintering (wt%)	Loss on peeling after sintering (wt%)
COADA - 3 wt% ceria built-in	28.8	2.76	92.5
COADA - 3 wt% ceria added	29.1	2.01	96.3
COADA - 11 wt% ceria added	1.33	1.93	72.1
Commercial powder - 11 wt% ceria - acetic acid	0.71	1.12	22.4
Commercial powder - 11 wt% ceria - nitric acid	3.04	-	-
Commercial monolith	3.59	0.26	11.3

5.3.2.4 Effect of pH on surface potential of cordierite and γ-alumina

Kolb *et al.* (1993) described the mechanism of the wash-coating process at a channel level on the basis of a physico-mechanical model. This model is described in terms of wetting or filling of the channels with the slurry and cleaning of the channels by forcing air through them. These authors stated that the rheological behaviour of the slurries is governed by the solids content of the wash coat slurry, as well as its pH, zeta potential, and viscosity, although no data are given to substantiate these effects.

An attempt was, therefore, made to clarify this mechanism. Zeta potential measurements as a function of pH for commercial γ-alumina powder sintered at 700 °C, a wash coat slurry prepared from this powder containing 11 wt% ceria, and uncoated cordierite monoliths are illustrated in Figure 5.4. The commercial alumina powder possessed a high positively charged surface at the pH range under consideration, and addition of ceria increased the zeta potential. Uncoated monoliths possessed a negatively charged surface at pH values between 3 and 4.5 as well as at pH values above 5.5, but the surface was positively charged at pH values between 4.5 and 5.5. Most wash-coating processes were completed at pH values below 4 (see Table 5.2), and especially in the vicinity of pH 3, where the viscosity of a typical wash coat slurry was the lowest (Blachou *et al.*, 1992). This latter property allowed for easy handling of the wash coat slurry. Therefore, one important mechanism during the coating of the monoliths was this charge neutralisation

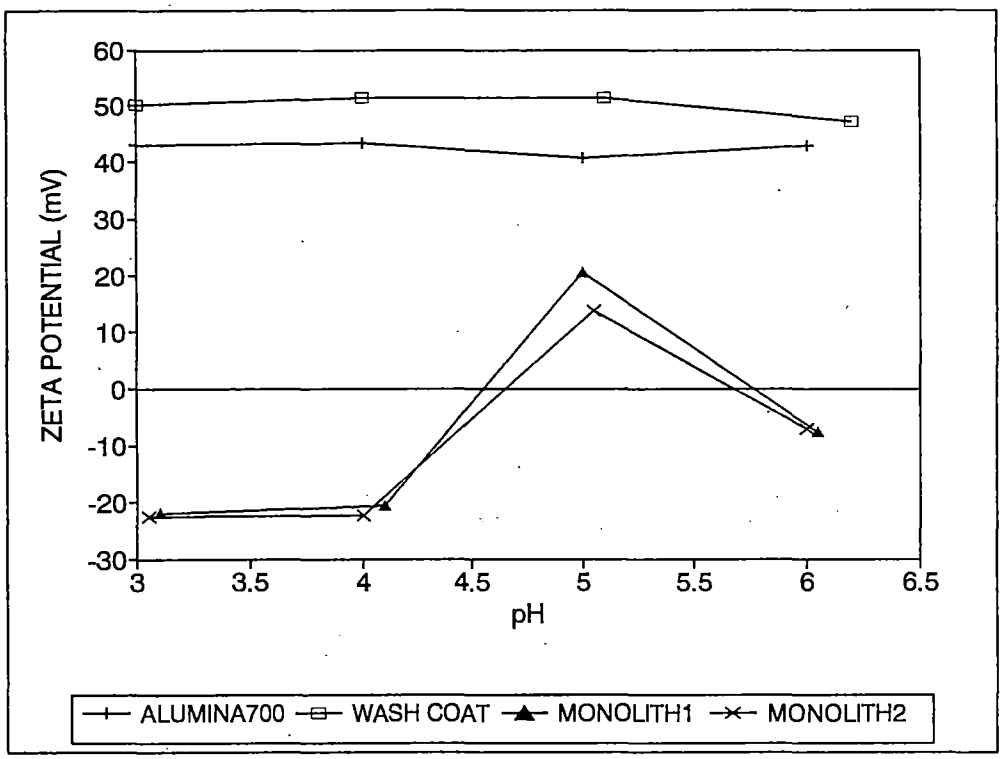

Figure 5.4 Zeta potentials as a function of pH for commercial alumina powder, wash coat slurry, and uncoated monolith.

at the interface between the monoliths and the alumina wash coat slurry. This is in accordance with the findings of Bockelmann (1994).

5.3.2.5 Factors affecting crack formation in wash coat layer

Migration of colloidal size particles during the drying of a swollen wash coat (in this case aqueous) system results in crack formation (Figure 6.5). These cracks can be avoided by collapsing the double layer. This, in turn, can involve one or more of the following: amount and valence of electrolyte, dielectric constant, modification of the adsorbed state (*e.g.*, acetate), changing the surface potential (pH), and bridging the particles with coagulants.

5.4 CONCLUSIONS

5.4.1 Factors affecting properties of spray-dried powders

1) *Ageing.* Ageing of aluminium hydroxide gels at 90 °C for 12 h enhanced pore volumes, pore diameter and surface area, but KED and KED (D^0) values, as well as bulk density, decreased.

2) *Flocculant.* When a polyacrylamide flocculant was employed after formation of *cis*-oleic acid-derived aluminium hydroxide gel, total and macropore volume as well as $\in$ and KED values increased, but pore diameter and TF values decreased. In the absence of *cis*-oleic acid, the flocculant caused all properties, except for the TF values, to increase.

3) *Combined effects.* The combined effects of *cis*-oleic acid, ageing of the gel, flocculation, and spray-drying enhanced BET surface area, $\in$, and KED values. However, mesopore volume, pore diameter, and TF values decreased. Uniform spherical particles were obtained with spray-dried COADA powders and well developed macropore structures were noted.

4) *Purity of cis-oleic acid.* Lower physical properties were obtained for γ-alumina derived from 62% and 88% *cis*-oleic acid than for pure (93%) COADA samples. Most notable were lower total and macropore volumes, smaller pore diameter, and lower KED values, but higher KED (D^0) values.

5) *Ceria.* All physical properties decreased when 3 wt% ceria was built into the γ-alumina structure and the most significant changes were found for the mesopore size and KED value.

6) *COADA vs. commercial powder.* Fresh and calcined (700 °C) commercial

alumina powders had lower total, meso- and macropore volumes, $\in$, and surface areas than the COADA samples, although no differences occurred between the former samples after calcination. Commercial alumina powder had a wider distribution of particle sizes and a greater fraction of particle sizes less than 1 μm than the COADA samples.

5.4.2 Factors affecting properties of wash coat composites

7) *Milling.* Milling of commercial alumina powder for 24 h resulted in a denser and harder calcined wash coat matrix compared to a milling period of 12 h.

8) *Peptisation and steam treatment.* Peptising with acetic acid and steam treating of commercial alumina powder wash coats resulted in a desirable wash coat layer which enhanced KED and KED (D^0) values.

9) *Ceria.* For equivalent amounts of ceria added, the sample containing ceria built into the crystallite had a larger fraction of mesoporosity and higher KED and KED (D^0) values, while macroporosity and pore diameter size increased when ceria was added prior to wash-coating. Increased amounts of ceria added to COADA samples, followed by wash-coating, increased mesoporosity, KED and KED (D^0) values and these were significantly higher than the commercial alumina samples, while macroporosity decreased.

10) *Packing of particles.* Higher KED and KED (D^0) values were obtained for the COADA wash coat composites compared to their respective spray-dried powders. This is linked to the packing of particles during preparation of the wash coat composites. Reverse results were obtained with the commercial alumina powder composites, which demonstrated the advantage of employing COADA material.

11) *Attrition resistance.* No differences in attrition resistance were noted whether 3 wt% ceria was added or built into the alumina crystallites, while addition of 11

wt% ceria and subsequent wash-coating, significantly improved attrition resistance of the wash coat layer. Higher attrition resistance was obtained for wash coats prepared with the commercial powder in the presence of acetic acid than with nitric acid. A high loss on peeling after sintering on COADA samples was a negative result.

12) *Mechanism*. Coating of monoliths was facilitated by charge neutralisation at the interface between monoliths (negatively charged) and the alumina wash coat slurry (positively charged) at pH value of approximately 3.

CHAPTER 6. CATALYTIC ACTIVITY OF WASH-COATED MONOLITHIC CATALYSTS

6.1 INTRODUCTION

This chapter deals with the catalytic activity of coated monoliths (Chapter 5), containing 1.1 wt% platinum, during the oxidation of carbon monoxide. The reaction conditions used simulated a typical automobile exhaust environment. The performances of these monoliths were evaluated by means of conversions, activation energies and surface and platinum properties. Platinum properties investigated were dispersion, surface area and crystallite sizes. The latter property allowed for the estimation of specific reaction rates. The effect of sintering of the monoliths and different wash coat thicknesses or weight loadings on activation energies and other surface properties were also investigated. Effectiveness factors, based on adsorption data (Carniglia's method) and on experimental kinetic data, were estimated to ensure that intrinsic kinetic measurements were obtained. Properties obtained with coated monoliths will be compared with a standard exhaust catalyst. This is not a study in diffusion phenomena, but an activity evaluation of catalysts.

Flow-chart 6.1 gives an outline of this chapter.

6.2 MATERIALS

6.2.1 Monoliths

The following wash-coated monoliths (5 and 60 mm lengths) were selected and impregnated with platinum to investigate their catalytic activity:

1) commercially coated monoliths denoted as standard (see Appendix O);
2) monoliths coated with commercial alumina powder containing 11 wt% ceria and with 19, 36 and 58 wt% wash coat loadings, respectively;

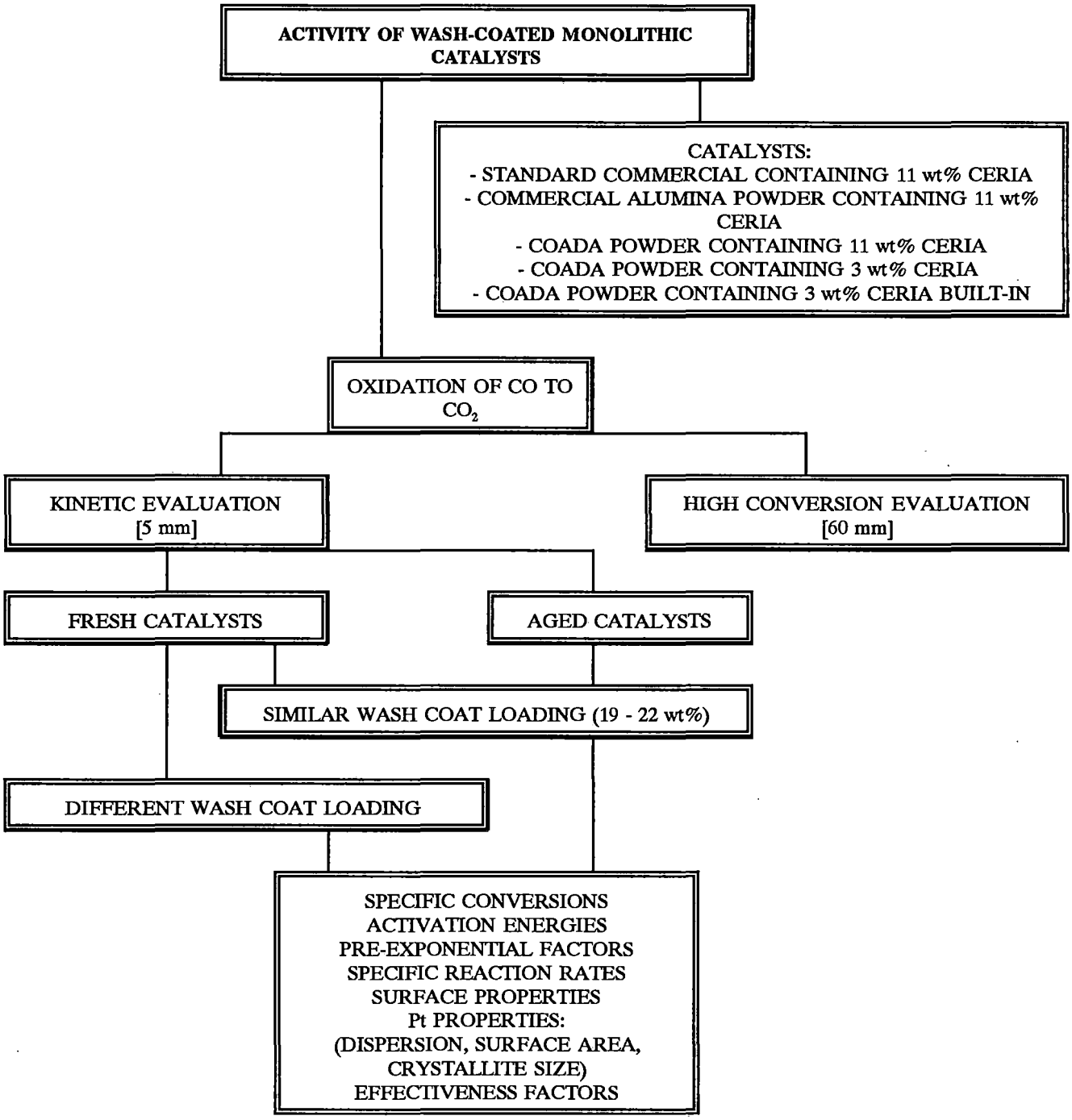

Flow-chart 6.1 Contents of chapter.

3) monoliths coated with pure *cis*-oleic acid-derived alumina (COADA) powder containing either 3 or 11 wt% ceria. Different wash coat loadings of 16, 22 and 38 wt% were investigated for layers containing 11 wt% ceria;

4) monoliths coated with COADA powder containing 3 wt% ceria built into the structure of the powder prior to wash-coating.

6.2.2 Hexachloroplatinic acid

A 20 mass/mass % solution of hexachloroplatinic acid was prepared (Metchem) from pure platinum metal (See Appendix H for specifications) as received from Impala Platinum Refineries. The solution was evaporated on a steam bath in order to obtain brown-red crystals of hexachloroplatinic acid. The crystals were chemically analysed and the platinum content was found to be 39.9%, while a theoretical calculation showed that this salt can contain 37.7% platinum if it contains 6 moles crystal water. Thermogravimetric analysis (TGA) (Du Pont 951 thermogravimetric analyzer and Du Pont 990 thermal analyzer) and typical TGA analysis found in the literature (Schweizer & Kerr, 1978) confirmed that the actual composition of the crystals was $H_2PtCl_6 \bullet 4H_2O$ and not hexachloroplatinic acid containing 6 moles of crystal water.

6.3 EXPERIMENTAL METHODS

6.3.1 Impregnation of wash-coated monoliths with hexachloroplatinic acid

The incipient wetness method was used to impregnate the wash-coated monoliths with hexachloroplatinic acid. Maximum water absorptive capacity of each dehydrated coated monolith was determined in order to ensure complete wetting of the wash-coated monoliths during impregnation. The 5 mm samples were dipped into the appropriate solutions, at pH 2.1, and the impregnant was allowed to be fully absorbed by the monolith. The concentration of platinum solution used was such that the final platinum content for each catalyst was 1.1 wt% based on the dry weight of applied wash coat

alumina layer. In the case of 60 mm samples, one side of the monolith was dipped into the hexachloroplatinic acid solution, at pH 1.7, until half of the solution was absorbed and then the monolith was inverted through 180° and the other end was inserted until all the solution was absorbed. The pH values used during impregnation approached the optimum pH impregnation conditions proposed by Blachou and Philippopoulos (1993). The impregnation step was followed by air drying at room temperature for 12 h, drying for 1 h at 40 °C and then at 150 °C for 1 h. The monoliths were calcined at 500 °C for 1 h. These catalysts were reduced in the reactor with pure hydrogen gas (99.9%) at 470 °C for 1 h at a flow rate of 100 cm^3/min for the 5 mm monoliths and 1000 cm^3/min for the 60 mm monoliths. These monoliths were then activated with CO/O_2/ balance N_2 feeding gas for 5 minutes at 470 °C.

6.3.2 Reactor set-up and conditions

Activity of the monolithic catalysts was evaluated in a reactor set-up illustrated in Figure 6.1. The plug flow reactor consisted of 25 mm inner diameter, 5 mm stainless steel cylinder wall thickness and length 750 mm. The outside of the reactor cylinder was alternatively covered with heat transfer clay and heating wire until the correct length of wire was obtained for an electrical resistance of 32 Ω, which was capable of heating the reactor to 1100 °C. This layer was insulated with thermal resistant fibre that could withstand temperatures of up to 1100 °C. The top 500 mm section was filled with silicon carbide chips, supported on a stainless steel wire mesh, which acted as preheater for the feed gases. Square monolithic samples were supported on hinges in another reactor tube, with 17 mm square internal sides, which fitted tightly into the major reactor tube. The top of this tube was placed 10 mm below the preheater section. J-type (Fe-Cu-Ni) thermocouples were spaced 2 mm above and below the monoliths and the temperature was monitored during the reaction. Temperatures indicated by the top thermocouple were assumed to reflect the surface temperature of the monoliths. The gas feed consisted of 2 volume per cent carbon monoxide, 1.1 to 1.3 volume per cent oxygen and balance nitrogen at 1 atmosphere pressure. Gas flow rate was controlled by a precalibrated rotameter. Unreacted carbon monoxide volume percentages were monitored with a Bosch

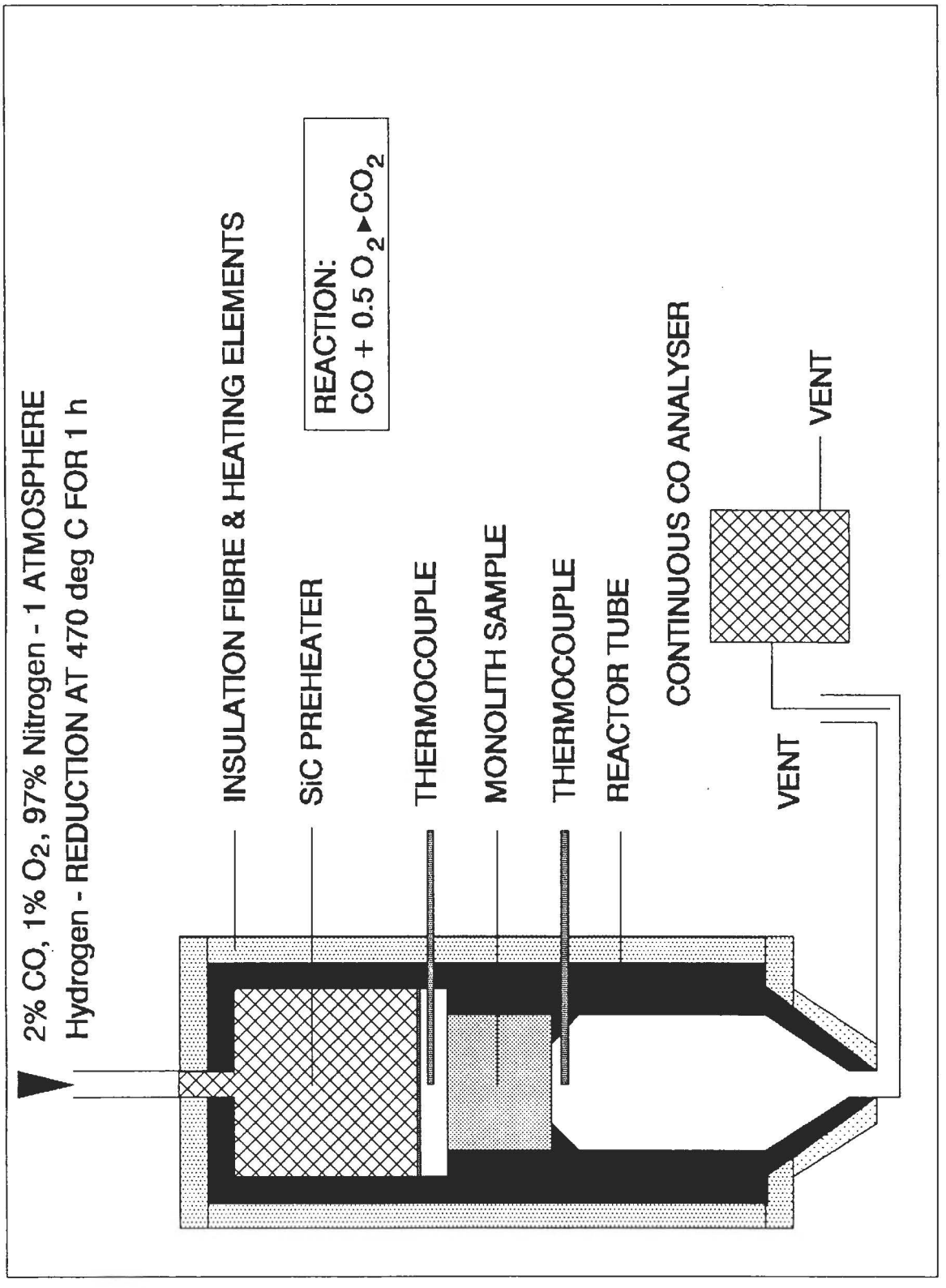

Figure 6.1 Reactor set-up.

ETT 008.14 continuous CO analyzer which was capable of analysing between 0 and 2 volume per cent CO at a tolerance of 0.02 volume per cent. This was equivalent to distinguishing between CO changes of 1 per cent conversion. The unreacted volume percentages were recorded with a video camera and the activation energies and conversions were calculated from these readings. Since conversion changes were rapid, especially for the 60 mm samples, the video tape readings allowed monitoring of changes that occurred every second during the oxidation reaction which is well within the response time of thermocouples.

Kinetic investigations with 5 mm samples were carried out at a gas flow rate of 2302 $\pm$ 10 cm^3/min which was equivalent to a gas hour space velocity (GHSV) of 112 500 h^{-1} and residence time of 0.025 seconds, depending on the catalyst surface temperature. Conversions were investigated starting at room temperature. Unreacted CO concentration was monitored after steady-state conditions were reached after approximately 5 minutes had elapsed. The temperature was then raised between 5 and 10 °C, depending on the activity of the specific catalyst, and the next unreacted CO concentration was monitored. This was repeated until conversions of about 20 % were obtained after which a temperature runaway occurred and control was no longer possible.

With 60 mm samples, only conversions were investigated because of temperature profiles which are known to exist in large pieces of monoliths (Cybulski & Moulijn, 1994). To study the kinetics of these monoliths, complex kinetic equations would be needed (Hlaváček *et al.*, 1976). Gas flow rates of 13 264 $\pm$ 85 cm^3/min were used which corresponded to a GHSV of 53 800 h^{-1} and a total residence time of 0.05 seconds. Gas residence time was equivalent to that found for a catalyst which is fitted to the exhaust of a motor vehicle with a displacement of 1.8 l that is under partial load (Koberstein, 1990). Reaction temperatures investigated, started from 100 °C and were increased at a heating rate of 5 °C/min until the maximum conversion was obtained.

6.3.3 Chemisorption analysis

Chemisorption analyses were carried out using a Micromeritics ASAP 2000 Chemisorption System (Micromeritics, 1991). The 5 mm monolithic catalyst samples were degassed at 250 °C until a pressure of 10^{-3} mm mercury was reached, followed by further evacuation for 30 minutes at 450 °C. This step was followed by further evacuation for 10 minutes at 100 °C until a pressure of 10^{-3} mm mercury was reached. Hydrogen gas (purity - 99.999%) was passed over the sample at this temperature for 10 minutes at a flow rate of 140 $\pm$ 5 cm^3/min. The temperature was raised to 450 °C under flowing hydrogen gas for another 2 h. The sample was then evacuated for 60 minutes at this temperature after a pressure of 10^{-4} mm mercury was reached. The temperature was decreased to 35 °C and the sample evacuated for 10 minutes after a pressure of 10^{-4} mm mercury was reached. Analysis was carried out at 35 °C with an equilibrium interval of 15 seconds and a manifold dose delay of 15 seconds. The analysis gas employed was pure carbon monoxide (99.97%). A stoichiometric factor of 1 CO molecule per 1 molecule of platinum was assumed to determine the platinum surface area as well as dispersion and average platinum particle size (Micromeritics, 1991). Only one analysis was carried out which gave the volume of gas adsorbed and corresponded to the weakly and strongly chemisorbed CO on platinum. Preliminary analysis had shown that a second analysis was unnecessary since the weakly chemisorbed CO volume was quite low and, therefore, negligible.

6.3.4 Surface properties

Surface areas of catalysts were obtained with the Micromeritics ASAP 2000 BET apparatus previously described, while the average pore size and total pore diameter were determined from the desorption branch of the N_2 isotherm of the BJH (Barrett *et al.*, 1951) method.

6.3.5 Sintering of catalysts

Catalysts were sintered at 980 °C for 4 h in static air after platinum impregnation and activation of the catalysts as described above. No attempt was made to control the water content during sintering.

6.4 PROCEDURES FOR KINETIC PARAMETER CALCULATIONS

A stoichiometric table for the concentrations of the variable-volume gas phase reaction

$$CO + 1/2O_2 \rightarrow CO_2, \qquad \text{..... (1)}$$

at constant pressure and temperature (steady state conditions), is given in Table 6.1.

Table 6.1 Stoichiometric table for CO oxidation reaction (After Fogler, 1986).

Species	Symbol	Initially	Change	Remaining
CO	A	C_{A_0}	$-C_{A_0}X$	$C_A=C_{A_0}[(1-X)/(1+\epsilon X)]$ ... (2)
O_2	B	$C_{B_0}=\theta_B C_{A_0}$	$-0.5C_{A_0}$	$C_B=C_{A_0}[(\theta_B-0.5X)/(1+\epsilon X)]$
CO_2	C	0	$+C_{A_0}$	$C_C=C_{A_0}[X/(1+\epsilon X)]$
N_2	I	$C_{I_0}=\theta_I C_{A_0}$	-	$C_I=C_{I_0}=\theta_I C_{A_0}$

where C = concentration in mol/l

X = conversion fraction

and $\epsilon = Y_{A_0}\delta$

with δ = 1 - 0.5 - 1 = -0.5 for this reaction and Y_{A_0} is the mole fraction of A initially present and

θ_B = ratio of Y_{B_0} to Y_{A_0}.

Thus, for this system with a feed of 2 volume per cent CO and 1.1 volume per cent O_2

θ_B = 0.011/0.02 = 0.55 and

ϵ = 0.02(-0.5) = -0.01.

For intrinsic kinetic investigations the conversion has to be kept below 10% (Cant *et al.* (1978), Chakrabarty *et al.* (1982), Akubuiro *et al.* (1985)). Therefore, for this reaction and gas feed the gas-phase volumetric flow rate

$$v = v_0 (1+\epsilon X), \quad \text{..... (3)}$$

became

$$v = v_0 (1\text{-}0.01(0.1))$$
$$= v_0 (0.999).$$

Thus, the volume change was negligible and the remaining concentrations were

$$C_A = C_{A_0}(1\text{-}X) \quad \text{..... (4)}$$

$$C_B = C_{A_0}(0.55\text{-}0.5X) \quad \text{..... (5)}$$

and

$$C_C = C_{A_0}X. \quad \text{..... (6)}$$

Only the disappearance of carbon monoxide and oxygen will be considered further. Since the system under consideration was a gas phase reaction, the concentration of each species was dependent on the surface temperature of the catalyst and the concentrations were calculated as follows:

$$C_A = Y_A P/RT, \quad \text{..... (7)}$$

and

$$C_B = Y_B P/RT, \quad \text{..... (8)}$$

with

P = pressure, 100 kPa or 1 atmosphere,
R = gas constant, 8.3144 J/K/mol
T = catalyst surface temperature in K.

The reaction rate, according to Voltz *et al.* (1973), for this reaction is given by

$$r_{CO} = kC_{CO}C_{O_2}/(1 + k_aC_{CO})^2, \quad \text{..... (9)}$$

where k is the rate constant and the denominator term provides for CO inhibition effects described in Section 2.6.4. The inhibition kinetic parameters used, described by Koberstein and Wannemacher (1987) as well as Voltz and co-workers (1973), are given in Section 2.6.4.

Because oxygen was slightly in excess, the rate equation changed to

$$r_{CO} = k_rC_{CO}/(1 + k_aC_{CO})^2, \quad \text{..... (10)}$$

where k_r was the rate parameter (1/s) = KC_{O_2}.

Integration of equation (10), with $C_A = C_{CO}$ yielded:

$$\ln (C_A/C_{A_0}) + 2k_a(C_A - C_{A_0}) + 0.5k_a^2(C_A^2 - C_{A_0}^2) = -k_r\Upsilon, \quad \text{..... (11)}$$

where Υ is the residence time of gas (seconds) in the catalyst and Υ can be determined from the relationship

$$\Upsilon = V/V_1, \quad \text{..... (12)}$$

where V = free volume of catalyst[1] available for reaction and

V_1 = volumetric gas flow rate through the reactor.

This gas flow rate depended on the temperature of the catalyst surface and the volume the gas occupied was calculated from the general gas law, *i.e.*,

[1] Free volume of catalysts was determined by multiplying the volume of the monoliths by the open porosity (76%) (Howitt, 1987), while the thickness of the wash coat layer was neglected.

$$V_2 = V_1T_2/T_1. \quad \text{..... (13)}$$

To account for the effect of the internal surface area (SA) of the support, equation (11) changed to

$$\ln (C_A/C_{A_0}) + 2k_a(C_A - C_{A_0}) + 0.5k_a^2(C_A^2 - C_{A_0}^2) = -k_s\Upsilon SA. \quad \text{..... (14)}$$

A general reaction rate equation, denoted as General, was also defined, namely

$$-r_{CO} = K'C_{CO}SA, \quad \text{..... (15)}$$

where the rate parameter, K', was defined as

$$K' = k_sC_{O_2}.$$

Integration of equation (15) yielded

$$\ln(C_{CO}/C_{CO_0}) = -K'\Upsilon SA, \quad \text{..... (16)}$$

where Υ was as described above and the conditions outlined above were still valid.

The intercept ($\ln A$) and the slope ($-E_a/R$) of an Arrhenius plot of $\ln k_s$ (equation 14) or $\ln K'$ (equation 16) against $1/T$ (with T the surface temperature in K) yielded the pre-exponential factor A (1/s) and the activation energy, E_a in kJ/mol, respectively.

6.5 RESULTS AND DISCUSSION

Two different types of investigations were performed,

1) kinetic investigations, where 5 mm monolithic samples were employed, and
2) high conversion investigations with 60 mm samples.

6.5.1 Catalytic activity of 5 mm monolithic catalysts

Three different types of 5 mm monolithic catalysts were investigated, namely

1) fresh catalysts containing similar amounts of wash coat loading,
2) fresh catalysts containing different amounts of wash coat loading, and
3) aged catalysts containing similar amounts of wash coat loading.

Reactor data obtained for each catalyst are summarised in Appendix I, while their respective Arrhenius plots are given in Appendix J.

6.5.1.1 Various fresh catalysts containing similar amounts of wash coat loading

The various fresh 5 mm monoliths contained similar amounts of wash coat loading, *i.e.*, 20 $\pm$ 2 wt%, with a platinum content of 1.1 wt%. The standard commercial sample, however, contained a wash coat loading of 31 wt%. No attempt was made to investigate high conversions for the 5 mm samples.

Specific conversions

Figure 6.2 shows specific conversion activity (conversion per unit surface area of support and wash coat - see Table 6.4) as a function of temperature. This is not necessarily proportional to the surface area of platinum. The commercial monolith showed the lowest activity. This catalyst showed acceptable activity reproducibility. All COADA catalysts had higher activities than the standard samples. The order of specific activity is: commercial powder containing 11 wt% ceria > COADA catalysts containing 11 wt% ceria > 3 wt% ceria built into the structure of COADA powder > COADA catalysts where 3 wt% ceria was added during the wash coat process. Increasing the ceria content did not deteriorate conversion activity as found by Summers and Ausen (1979) and Nunan *et al.* (1992).

Figure 6.2 also shows that inhibition of the CO oxidation reaction occurred in the

temperature range between 68 to 154 °C, which was also confirmed by Voltz *et al.* (1973) and Wei and Becker (1975). The COADA sample containing 11 wt% ceria and the commercial powder catalyst containing a similar amount of ceria did not show complete inhibition. This was due to the relatively high temperature increments used during activity measurements. No attempt was made to obtain complete inhibition for these two catalysts. Fresh materials had high conversion activity at low temperatures, *i.e.*, less than the inhibition temperature.

Kinetics

Typical Arrhenius plots are given in Figure 6.3 for each kinetic model under consideration for fresh commercial powder and COADA catalysts containing similar wash coat loadings. Other Arrhenius plots are given in Appendix J. The kinetic models investigated were denoted as General (Equation (17)), Kob&Wann (Koberstein & Wannemacher) (Equation (15) with the adsorption rate equation and constants described in Section 2.6.4 and Table 2.17, respectively) and Voltz *et al.* (Equation (14) with the adsorption rate equation and constants described in Section 2.6.4). Two distinctive activation energy regions were noted in Figure 6.3 (see also Appendix J), *i.e.*, a kinetic region where diffusion plays a negligible role (high K^{-1}) and a region where large diffusion resistance obscured kinetics (< 0.0028 K^{-1}), which agrees with findings of Smith (1981). No relationship was found between activation energies of these two distinctive regions. Activation energies reported in this study only will refer to the kinetic region.

Table 6.2 shows that similar linear fits were obtained for the different kinetic models investigated. This is an indication that the CO adsorption parameters defined by Voltz *et al.* (1973) and Koberstein and Wannemacher (1987) were in accordance with the kinetic data obtained in this study, but lower activation energy values were obtained with these kinetic models than the General equation. Only the results obtained with the General model will be discussed further.

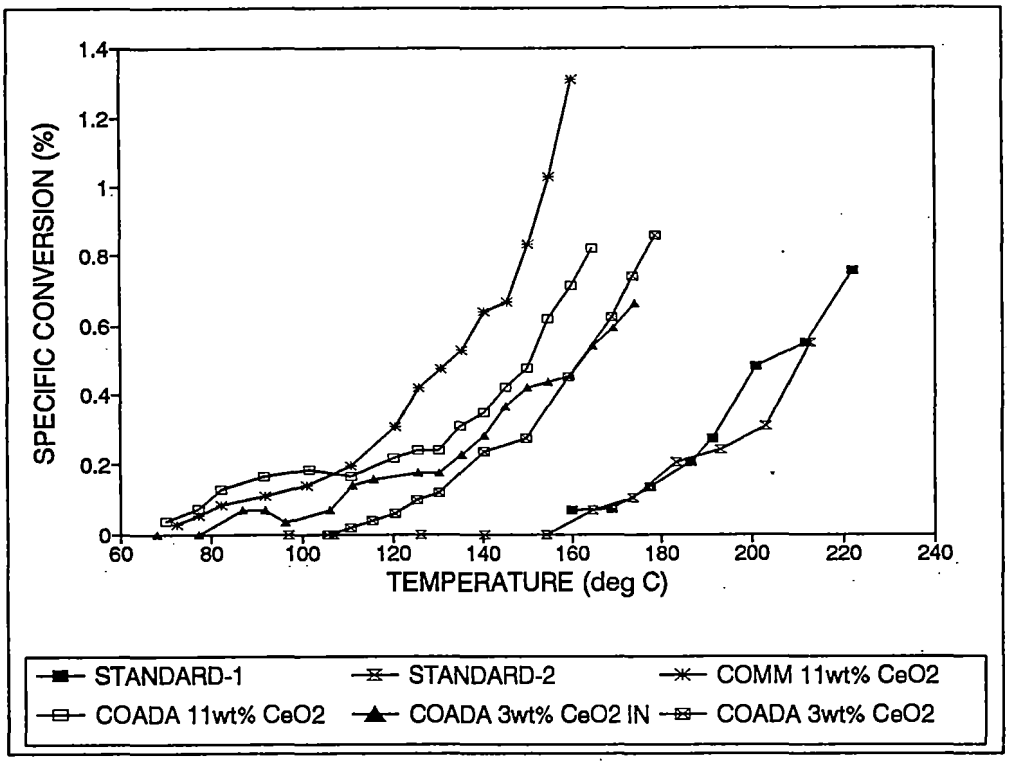

Figure 6.2 Specific conversion as a function of temperature for fresh 5 mm monolithic catalysts.

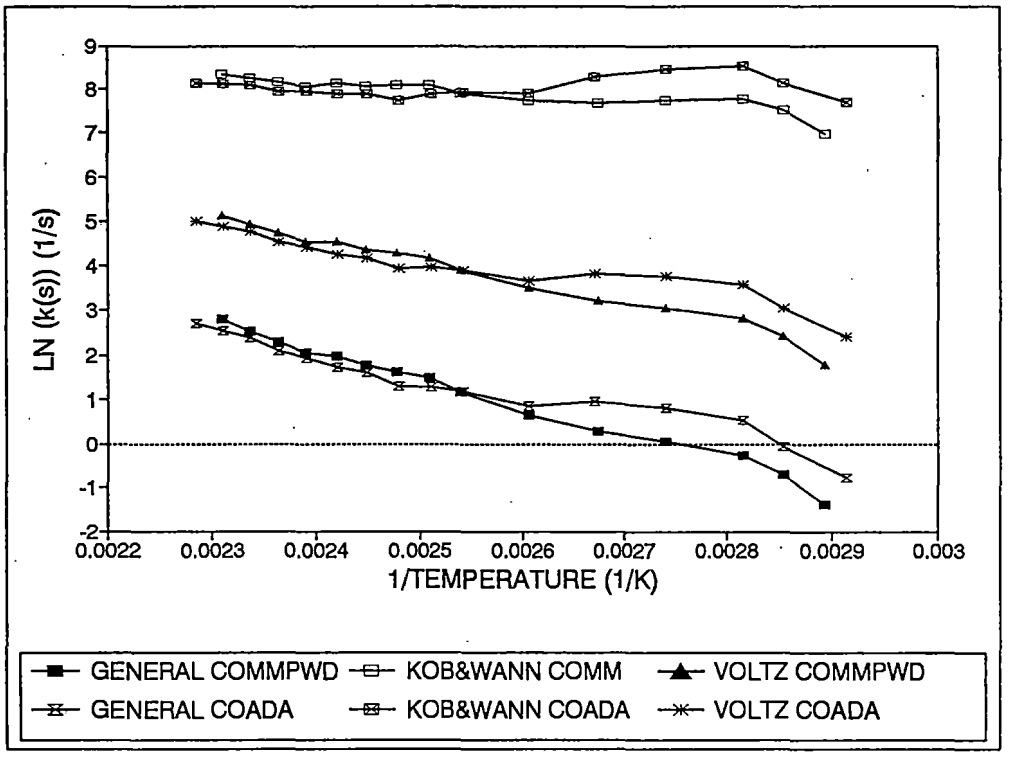

Figure 6.3 Arrhenius plots for commercial powder and COADA 5 mm monolithic catalysts containing 11 wt% ceria.

The standard commercial catalysts had significantly lower activation energies than the catalyst prepared from the commercial powder, *i.e.*, 86.2 to 100.5 kJ/mol and 120.4 kJ/mol, respectively. The former activation energies for fresh commercial monoliths were similar to those obtained by other workers as shown in Table 6.3. Activation energies obtained with COADA powder catalysts, which contained 11 wt% ceria and where 3 wt% ceria was built into the structure, 109.0 and 112.9 kJ/mol, respectively, were similar to the commercial powder catalyst (120.4 kJ/mol). In the case where 3 wt% ceria was added during the wash coat process, the activation energy increased significantly (140.8 kJ/mol).

Surface properties

Table 6.4 summarises the surface properties obtained for the different fresh catalysts. The standard and commercial powder catalysts, in general, have similar surface properties, but the average pore size was significantly lower for the latter sample (10.60 and 8.61 nm, respectively). The COADA catalysts had higher surface areas (26 to 29 m^2/g) than the standard and commercial alumina powder (15 and 18 m^2/g, respectively). However, average pore sizes were smaller for the COADA samples. Different ceria additions had no effect on the surface properties.

Platinum surface properties

Platinum dispersion (Micromeritics, 1991) was lower for the commercial powder sample than for the standard sample (30 and 45%, respectively), but it had no adverse effect on the platinum surface area and average platinum crystallite size (Table 6.4). There was a higher platinum dispersion for COADA catalysts (61 to 73%) as well as platinum surface area (140 to 230 m^2/g metal), while the platinum crystallite sizes decreased accordingly (1.2 to 2.0 nm). This can be related to the inherent high surface areas of the COADA powders (Tables 5.3 and 5.4). Addition of 3 wt% ceria to COADA catalysts

Table 6.2 Activation energies and pre-exponential factors obtained with three different kinetic models for fresh monolithic catalysts containing 19 to 22 wt% wash coat loadings.

Catalyst	Wash coat loading (wt %)	General (kJ/mol)	Koberstein & Wannemacher (kJ/mol)	Voltz *et al.* (kJ/mol)
Standard 1 (Commercial catalyst)	31	86.2 (0.99)[a] 8.17E8[b]	44.0 (0.95) 2.29E6	63.8 (0.97) 3.21E7
Standard 2 (Commercial catalyst)	31	100.5 (0.98) 3.83E10	62.1 (0.95) 2.82E8	81.7 (0.97) 3.80E9
Commercial powder + 11 wt% ceria added	19	120.4 (0.98) 2.26E16	82.2 (0.96) 1.65E14	100.9 (0.97) 1.59E15
COADA + 11 wt% ceria added	22	109.0 (1.00) 6.38E14	69.7 (0.99) 3.20E12	88.1 (0.99) 2.99E13
COADA + 3 wt% ceria built-in	21	112.9 (0.96) 1.55E14	73.4 (0.92) 7.67E11	92.8 (0.95) 9.02E12
COADA + 3 wt% ceria added	21	140.8 (0.99) 1.61E17	101.9 (0.98) 9.91E14	120.9 (0.99) 1.13E16

[a] R^2 linearity of line fit in Arrhenius plot.

[b] Pre-exponential factor in 1/s.

Table 6.3 Activation energies for platinum catalysts obtained by various workers.

Investigators	Activation energy (kJ/mol)	Type of catalyst
Shishu & Kowalczyk (1974)	67	Pt/alumina monolith
Voltz *et al.** (1973)	87	Pt/alumina pellets
Yao (1984)	126	Pt wire
Akubuiro *et al.* (1985)	92	Pt/γ-alumina small spheres < 0.4 mm diameter
Su *et al.* (1985)	93-114	Pt/γ-alumina monolith

* Calculated by Cant *et al.* (1978) from the data presented by Voltz and co-workers.

Table 6.4 Surface properties and chemisorption results of fresh monoliths containing similar wash coat loadings.

Catalyst	Wash coat loading (wt%)	N_2 surface area (m^2/g)	N_2 total pore volume (cm^3/g)	N_2 average pore size (nm)	Pt dispersion (%)	Pt surface area (m^2/g metal)	Average Pt crystallite diameter (nm)
Standard	31	14.55	0.06	10.6	45	45	6.2
Commercial powder + 11 wt% ceria added	19	17.97	0.05	8.61	30	44	6.4
COADA + 11 wt% ceria added	22	27.38	0.08	7.57	61	140	2.0
COADA + 3 wt% ceria added	21	25.59	0.08	7.83	61	162	1.7
COADA + 3 wt% ceria built in	21	28.70	0.08	7.4	73	234	1.2

resulted in slightly higher platinum surface areas and smaller platinum crystallites compared to the addition of 11 wt% ceria (162 and 140 m^2/g metal and 1.7 and 2.0 nm, respectively), which is in accordance with those obtained by Summers and Ausen (1979). Similar platinum dispersion (61%) was obtained for these ceria amounts. However, Summers and Ausen (1979) reported that platinum dispersion decreased with increasing ceria content. In the case where 3 wt% ceria was built into the COADA structure, a significant enhancement in platinum dispersion (73%) and platinum surface area (230 m^2/g metal) was obtained. The average platinum crystallite sizes also decreased from 1.7 to 1.2 nm.

No simple relationship was found between catalytic activity (conversion), activation energy and reaction rate with platinum dispersion, platinum surface area and platinum crystallite sizes. The only exception was the higher specific conversions and lower activation energies obtained for the COADA sample where 3 wt% ceria was built into the structure (dispersion - 73%, surface area- 230 m^2/g platinum, crystallite size - 1.2 nm) compared to the case where 3 wt% ceria was added during the wash coat process (dispersion - 61%, surface area - 162 m^2/g platinum, crystallite size - 1.7 nm).

It was expected that the smaller platinum crystallites would induce enhanced catalyst activity, but this was not found to be the case. This was due to a so-called size effect (Akubuiro *et al.* (1985), Anonymous (1993)). These workers found that when platinum crystallites become smaller than 10 nm, their catalytic behaviour varied, which is responsible for the inconsistent catalytic activity found with the size of the particle. Akubuiro and co-workers (1985) attributed the lower activity of small platinum crystallites to the fact that small particles chemisorb reactant molecules more strongly than larger molecules. Thus, strong adsorption of CO on small platinum particles may render it difficult for oxygen to adsorb or displace the adsorbed CO molecules. Small particles also have increased density of corner and edge sites and a larger number of centres of low surface coordination. Since oxygen preferentially adsorbs dissociatively on such centres, blocking of these sites by CO would inhibit oxygen adsorption and consequently catalytic activity (Akubuiro *et al.*, 1985).

Specific rates

Table 6.5 presents the specific rates (reaction rate divided by platinum surface area per gram of catalyst) as a function of platinum crystallite size calculated at 159.6 ± 0.4 °C for various fresh catalysts. The specific rate increased with increasing particle size, which correlates with the findings of Akubuiro and co-workers (1985). The only exception was the standard sample which had a low specific rate despite its relatively larger platinum crystallite size.

Specific rates associated with certain platinum crystallite sizes correlated with the trends found for the specific conversions and rates (Figures 6.2 and 6.4, respectively) of the fresh catalysts. This shows that the highest catalytic activity can be expected for the commercial powder sample, the only exception being the inversed specific rates obtained for the 3 wt% added and 3 wt% built-in ceria COADA samples (more pronounced at 110 °C). This phenomenon was probably due to the fact that the obtainable platinum crystallite sizes were average values and the sizes of these two samples were quite similar.

Effectiveness factors

Effectiveness factors were calculated for various fresh catalysts as described by Weisz and Prater (1954) and Satterfield and Sherwood (1963). The wash coat layer was considered to be analogous to a flat plate, while the oxidation reaction of carbon monoxide was assumed to be first order. The parameters used for these calculations and the results are shown in Table 6.6. It must be borne in mind that wash coat layers in practice consist of a distribution of various thicknesses (see Figure 6.5) and, therefore, not only a single value can be assigned to a specific catalyst. All wash coat layer thicknesses showed bimodal distributions in the regions 20 and 120 μm, as determined with SEM analysis. Average wash coat thicknesses as determined from SEM micrograph

Table 6.5 Specific rates as a function of platinum surface area for various fresh catalysts.

Catalyst	Rate [mol CO/(s m^3 catalyst)]	Pt surface area (m^2/g Pt)	Pt surface area (m^2 Pt/g catalyst)	Pt crystallite size (nm)	Specific rate [g mol CO/ (s m^2 Pt m^3 catalyst)]
COADA + 3 wt% ceria added	3.59	162	0.41	1.7	8.77
COADA + 3 wt% ceria built-in	4.06	230	0.49	1.2	8.35
COADA + 11 wt% ceria added	5.68	140	0.35	2.0	16.23
Commercial powder + 11 wt% ceria added	7.03	44	0.17	6.4	41.35
Standard	0.30	45	0.22	6.2	1.36

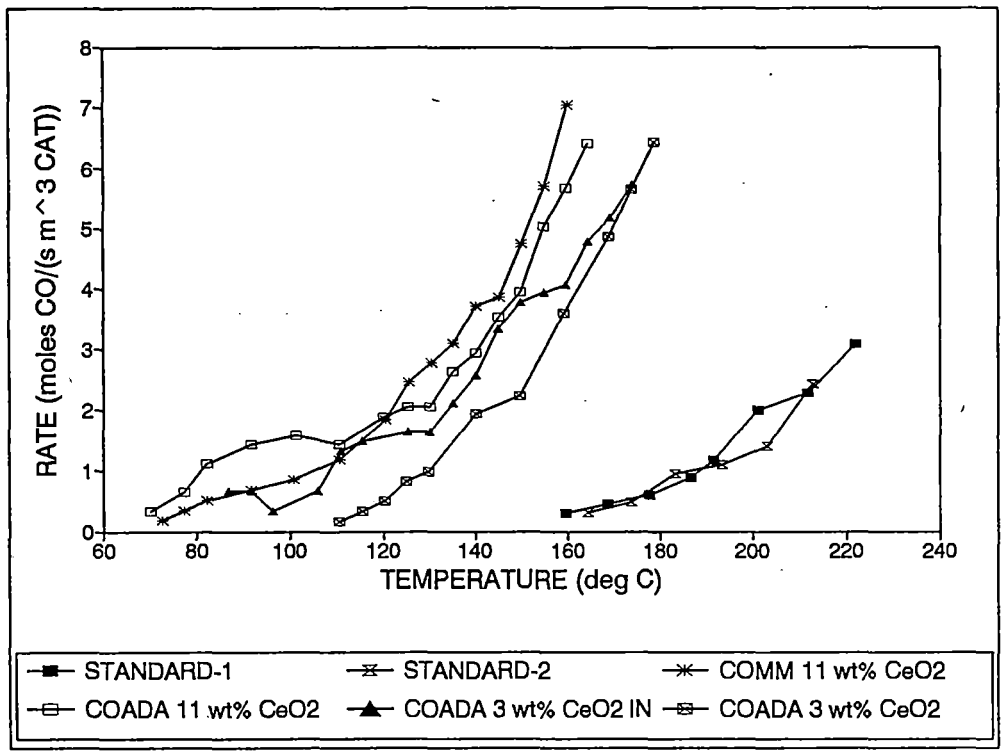

Figure 6.4 Reaction rates as a function of temperature for fresh 5 mm monolithic catalysts.

analysis were employed to compare effectiveness factors for various fresh catalysts. Average wash coat thicknesses calculated from density and mass loading data are also shown in Table 6.6.

Effectiveness factors of unity were obtained at 140 °C for all fresh catalysts under consideration. Therefore, pore diffusion based on adsorption data obtained with the average method of Knudsen and pore size distribution method (D^0) of Carniglia (see Chapter 4) was negligible for the fresh catalysts.

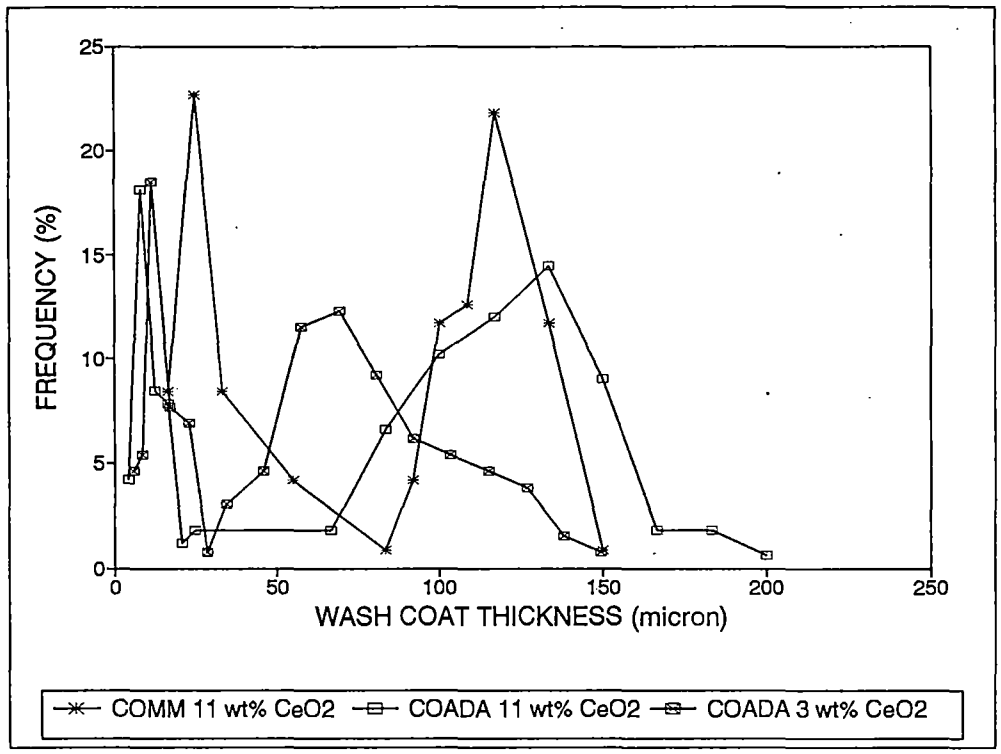

Figure 6.5 Typical wash coat thickness distributions obtained for 5 mm monolithic catalysts.

Table 6.6 Results and parameters used for effectiveness factor calculations for fresh catalysts containing similar wash coat loading.

Catalyst	Surface temperature (°C)	General[c] rate constant (k_g) (1/s)	SEM average wash coat thickness[d] (μm)	Calculated average wash coat thickness[e] (μm)	Adsorption data			
					$D_{K,eff,surface\ temp}$ (cm^2/s) (Average Knudsen)	$D_{K,eff,surface\ temp}$ D^0-based (cm^2/s) (Carniglia)	Effectiveness factor ($D_{K,eff}$ based)	Effectiveness factor ($D_{K,eff}$ D^0 based)
Commercial powder + 11 wt% ceria added	140.2	0.401	95.8	53.7	0.0078	0.1889	0.9984	0.9999
COADA + 11 wt% ceria added	140.1	0.204	83.3	124.2	0.0269	1.0379	0.9997	1.0000
COADA + 3 wt% ceria added	140.1	0.138	51.7	106.6	0.0272	0.4559	1.0000	1.0000
COADA + 3 wt% ceria built in	140.1	0.167	112.5	106.9	0.0237	0.6627	0.9998	1.0000

[c] From General kinetic equation.

[d] Determined by analysing wash coat distribution curve obtained from SEM micrographs.

[e] Calculated from the relationship: (Total wash coat volume)/(area of one monolith channel).

6.5.1.2 Fresh catalysts containing different amounts of wash coat loadings

The influence of different amounts of wash coat loading on catalytic activity and surface properties of the commercial alumina powder and COADA powder, where 11 wt% ceria was added during the wash coat process, was also investigated. The wash coat loadings prepared consisted of 19, 36 and 58 wt% for commercial powder and 16, 22 and 38 wt% for COADA powder.

Specific conversions

Figure 6.6 shows specific conversion as a function of temperature for various catalysts. Similar general trends considering CO inhibition also applied to these catalysts. For commercial alumina powder catalysts, the highest activity was obtained for catalysts containing a wash coat loading of 19 wt%, followed in decreasing order by wash coat loadings of 36 and 58 wt%. These results indicated that the activity of the commercial alumina powder catalysts depended on the thickness of the wash coat layer, but this trend was not observed for COADA catalysts, except for high loadings of 38 wt%. It seems, therefore, that high wash coat loading is detrimental to catalyst activity due to diffusion problems in the alumina wash coat layer.

Kinetics

Activation energies of the commercial powder, impregnated with different levels of platinum, did not show any consistent trend with increasing platinum content (Table 6.7). COADA samples, however, showed a reduced activation energy with increasing thickness, which is consistent with measured diffusional restriction.

Surface properties

Table 6.8 summarises the surface properties obtained for catalysts containing different amounts of wash coat loadings. Surface area and total pore volume of coated monoliths

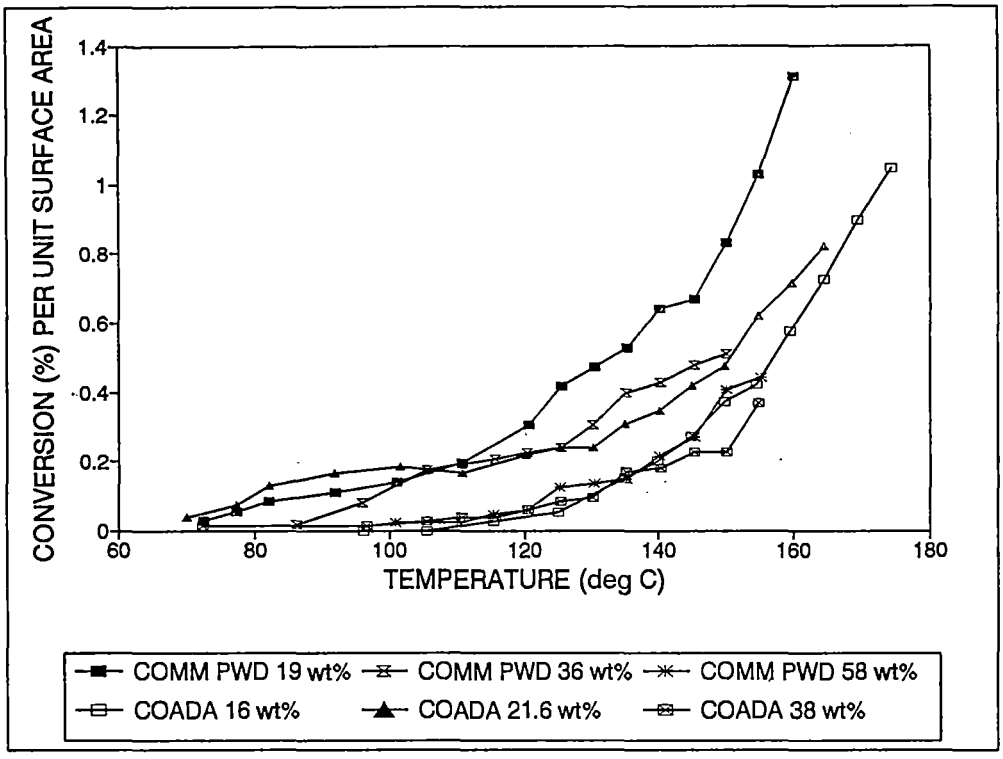

Figure 6.6 Specific conversion as a function of temperature for fresh 5 mm monolithic catalysts containing various wash coat loadings.

increased with wash coat loading for both commercial alumina powder and COADA powder. Higher wash coat thicknesses were obtained for the latter catalysts at similar wash coat loadings.

Platinum surface properties

Table 6.8 also shows that platinum dispersion, surface area and crystallite sizes were similarly independent of wash coat loading for both catalyst materials. The exception was the 58 wt% commercial powder loading, which resulted in lower platinum dispersion and surface area with a concomitantly larger crystallite size. It was again shown that the COADA catalysts resulted in higher platinum dispersion and platinum surface area, but smaller platinum crystallite sizes than the commercial powder catalysts. The high platinum dispersions and platinum surface areas of the COADA catalysts did not

Table 6.7 Activation energies and pre-exponential factors obtained with three different kinetic models for fresh monolithic catalysts containing various wash coat loadings.

Catalyst & wash coat loading	General (kJ/mol)	Koberstein & Wannemacher (kJ/mol)	Voltz *et al.* (kJ/mol)
Commercial powder + 11 wt% ceria added			
- 19 wt%	120.4 (0.98)[a] 2.26E16[b]	82.2 (0.96) 1.65E14	100.9 (0.97) 1.59E15
- 36 wt%	144.8 (0.97) 9.20E18	104.7 (0.94) 3.61E16	123.5 (0.96) 3.93E17
- 58 wt%	141.4 (0.96) 1.94E17	100.6 (0.93) 6.65E14	120.5 (0.95) 9.34E15
COADA + 11 wt% ceria added			
- 16 wt%	125.0 (0.98) 8.10E14	86.1 (0.96) 5.08E12	105.2 (0.97) 5.97E13
- 22 wt%	109.0 (1.00) 6.38E14	69.7 (0.99) 3.20E12	88.1 (0.99) 2.99E13
- 38 wt%	94.0 (1.00) 1.10E11	55.8 (1.00) 8.74E8	74.5 (1.00) 8.96E9

[a] R^2 linearity of line fit in Arrhenius plot.

[b] Pre-exponential factor 1/s.

correlate with their lower catalytic activity compared to the commercial powder catalysts shown in Figure 6.6. It is again noted that the performances of catalysts are inversely proportional to platinum crystallite sizes for crystallites smaller than 10 nm, as indicated previously.

Specific rates

Table 6.9 addresses the specific rates obtained at 150.0 $\pm$ 0.2 °C for the catalysts under consideration. These results, in general, confirmed the effect of platinum crystallite size as shown previously, *i.e.*, the larger platinum crystallite sizes resulted in the highest specific rates. This is especially true for similar wash coat loadings, *i.e.*, 19 to 22 wt% and 36 to 38 wt%, for the different catalysts. No attempt was made to determine the optimum

Table 6.8 Surface properties and chemisorption results of fresh monoliths containing different amounts of wash coat loadings.

Catalyst sample/wash coat loadings	N_2 surface area (m^2/g)	N_2 total pore volume (cm^3/g)	N_2 average pore size (nm)	Calculated average wash coat thickness (μm)	Pt dispersion (%)	Pt surface area (m^2/g metal)	Pt crystallite diameter (nm)
Commercial powder + 11 wt% ceria added - 19 wt%	17.97	0.05	8.61	53.7	30	44	6.4
- 36 wt%	31.36	0.09	8.54	123.5	37	44	6.4
- 58 wt%	44.06	0.13	8.58	247.8	11	16	17.2
COADA + 11 wt% ceria added - 16 wt%	20.03	0.06	7.67	81.4	59	140	2.0
- 22 wt%	27.38	0.08	7.57	124.2	61	140	2.0
- 38 wt%	41.77	0.12	7.83	241.2	60	122	2.3

Table 6.9 Specific rates as a function of platinum surface area for fresh catalysts containing various wash coat loadings.

Catalyst	Rate [mol CO/ (s m^3 cat)]	Pt surface area (m^2/g Pt)	Pt surface area (m^2 Pt/g cat)	Pt crystallite size (nm)	Specific rate [g mol CO/ (s m^2 Pt m^3 cat)]
Commercial powder + 11 wt% ceria added					
- 19 wt%	4.74	44	0.17	6.4	27.88
- 36 wt%	4.45	44	0.39	6.4	11.41
- 58 wt%	4.76	16	0.17	17.2	28.00
COADA + 11 wt% ceria added					
- 16 wt%	2.46	140	0.28	2.0	8.79
- 22 wt%	3.94	140	0.35	2.0	11.26
- 38 wt%	2.86	122	0.66	2.3	4.33

crystallite size. The specific conversions (Figure 6.6) obtained at 150 °C for the commercial powder catalyst did not follow the same trend as for the specific rates. In the case of the COADA catalysts, only the specific rate obtained for the 22 wt% wash coat loading correlated with its activity and rate (Figure 6.7). The higher specific rates obtained with the commercial alumina powder also indicated that this powder is more suitable for platinum CO oxidation than COADA catalysts.

Effectiveness factors and experimental Knudsen effective diffusivities

Effectiveness factors were calculated from observed rate constants (k_s) at various temperatures obtained with the Voltz method (see appropriate Appendixes) while those values of the lowest wash coat loading were assumed to reflect the intrinsic rate constants. Thiele moduli were obtained from effectiveness factor versus Thiele modulus curves reported by Wei & Becker (1975) for different $k_a C_{CO}$ (adsorption rate constant and CO concentration (reacted) at catalyst surfaces) values for first-order kinetics and flat plate configuration. These values and wash coat thicknesses were substituted in the

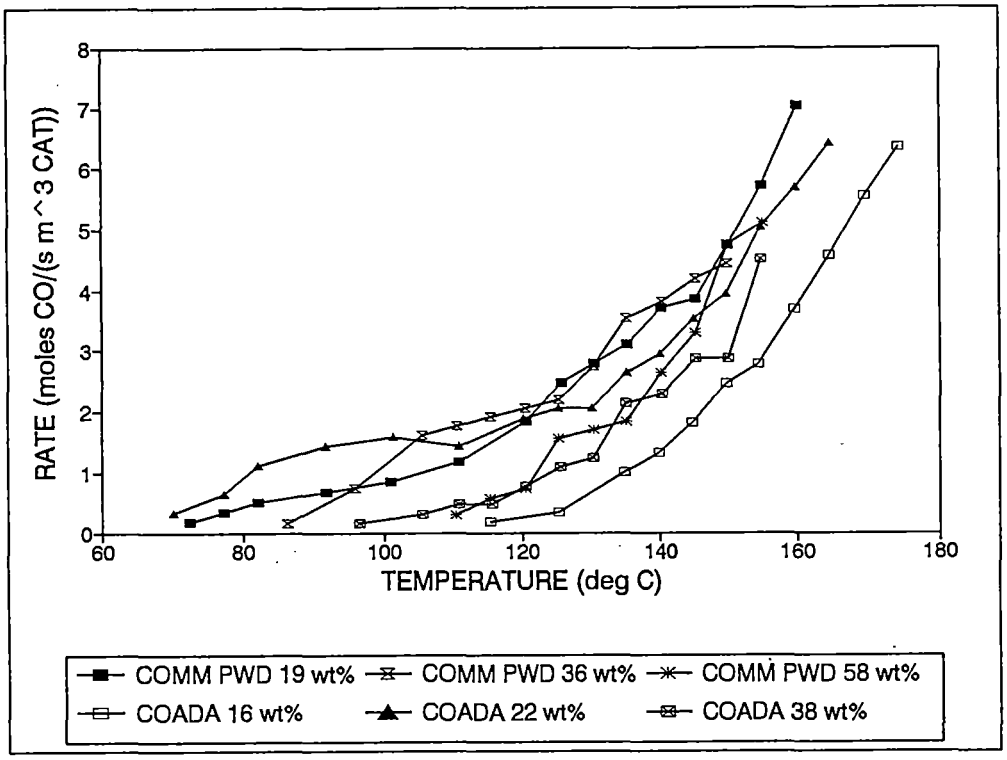

Figure 6.7 Reaction rates as a function of temperature for fresh 5 mm monolithic catalysts containing different amounts of wash coat loadings.

Thiele modulus expression for a flat plate to obtain the experimental Knudsen effective diffusivities (EKED).

Table 6.10 shows results obtained for calculated effectiveness factors and EKED values from rate constant data and wash coat thicknesses. According to Smith (1981) and Farkas (1986), effectiveness factors greater than unity, found especially for the 22 and 38 wt% COADA catalysts, are due to interaction of two opposing effects, *i.e.*, poor mass transfer lowers the efficiency of the catalyst, while insufficient heat transfer raises the catalyst surface temperature and reaction rate. However, no temperature runaway was observed at the experimental conditions under consideration. This effect could also have been due to experimental errors with data of the 16 wt% COADA catalyst. The lowest effectiveness factors (< 0.4) were obtained for the 58 wt% commercial alumina catalyst at all temperatures investigated. These low values implied that a very substantial portion of the active surface was not utilised (Smith, 1981). Similar tendencies were obtained for the 38 wt% COADA sample.

Table 6.10 Calculated effectiveness factors and experimental Knudsen effective diffusivities as a function of temperature obtained from different wash coat loadings.

Catalyst/ wash coat loading (weight (g), thickness (μm))	Temp. (°C)	Voltz k_a	C_{CO} on surface (reacted) 10(mol/m^3)	k_aC_{CO}	Voltz k_s (1/s)	Voltz k_s (1/s.g)	η	Thiele modulus	EKED (1000 cm^2/s)
Commercial powder + 11 wt% ceria - 19 wt% (0.1085, 53.65)	110.8	7.52	0.22	0.17	3.44	31.72	1.00	0.10	7.23
	120.6	7.07	0.34	0.24	4.78	44.07			8.95
	125.6	6.87	0.45	0.31	6.13	56.52			10.28
	135.3	6.79	0.56	0.39	6.97	64.26			10.38
	140.2	6.32	0.67	0.42	7.99	73.67			11.41
	145.3	6.15	0.69	0.42	7.92	73.02			11.31
	150.1	5.99	0.85	0.51	9.39	86.58			11.85
- 36 wt% (0.2158, 123.50)	110.6	8.01	0.38	0.30	3.30	15.29	0.48	2.31	0.06
	120.4	7.53	0.43	0.32	3.40	15.76	0.36	3.08	0.03
	125.4	7.30	0.46	0.34	3.44	15.94	0.28	3.83	0.02
	135.2	6.89	0.74	0.51	5.06	23.45	0.36	3.31	0.03
	140.3	6.69	0.61	0.41	4.06	18.82	0.26	4.89	0.01
	145.3	6.51	0.86	0.56	5.44	25.21	0.35	3.41	0.03
	150.0	6.35	0.90	0.57	5.53	25.63	0.30	3.73	0.02
- 58 wt% (0.3812, 247.78)	110.4	7.54	0.06	0.05	0.35	0.92	0.03	NO	NO
	120.4	7.08	0.15	0.11	0.77	2.02	0.05	NO	NO
	125.3	6.88	0.33	0.23	1.58	4.15	0.07	NO	NO
	135.2	6.50	0.38	0.25	1.68	4.41	0.07	NO	NO
	140.2	6.32	0.55	0.35	2.31	6.06	0.08	NO	NO
	145.3	6.15	0.69	0.42	2.76	7.24	0.10	16.00	0.00
	150.1	5.99	1.02	0.61	3.89	10.21	0.12	15.00	0.00
COADA + 11 wt% ceria - 16 wt% (0.0886, 81.40)	110.8	8.03	0.02	0.01	0.23	2.60	1.00	0.10	1.49
	120.2	7.54	0.04	0.03	0.64	7.23			4.00
	125.2	7.31	0.06	0.04	0.82	9.26			5.02
	134.9	6.90	0.18	0.12	2.21	24.96			11.67
	139.9	6.71	0.23	0.15	2.78	31.39			13.93
	144.8	6.53	0.32	0.21	3.63	40.99			16.43
	149.8	5.99	0.43	0.27	4.68	52.85			19.23
- 22 wt% (0.1235, 124.23)	110.8	8.00	0.29	0.23	2.96	23.98	9.23	NO	NO
	120.2	7.54	0.37	0.28	3.51	28.43	3.93	NO	NO
	125.3	7.31	0.40	0.29	3.58	29.00	3.13	NO	NO
	135.1	6.90	0.50	0.34	4.17	33.78	1.35	NO	NO
	140.1	6.70	0.55	0.37	4.41	35.72	1.14	NO	NO
	145.0	6.52	0.66	0.43	5.05	40.91	1.00	0.10	38.11
	149.8	6.35	0.74	0.47	5.42	43.90	0.83	0.93	0.45
- 38 wt% (0.2159, 241.23)	110.8	8.00	0.10	0.08	0.65	3.01	1.16	NO	NO
	120.5	7.53	0.15	0.11	0.97	4.49	0.62	1.39	0.24
	125.5	7.30	0.21	0.15	1.27	5.88	0.64	1.41	0.28
	135.2	6.89	0.41	0.28	2.26	10.47	0.42	2.50	0.13
	140.3	6.69	0.44	0.29	2.29	10.60	0.34	3.17	0.08
	145.3	6.51	0.55	0.36	2.74	12.69	0.31	3.25	0.08
	150.1	6.34	0.54	0.34	2.62	12.13	0.23	4.79	0.04

η = effectiveness factor k_a = adsorption rate constant (1/mol% CO)
NO = not obtainable

Catalysts having Thiele moduli below 0.4 can be considered to be free of pore diffusion effects (Levenspiel, 1979) and only those selected catalysts whose wash coat thicknesses were considered to represent intrinsic characteristics complied with this. Strong pore diffusion resistances (Thiele modulus > 4) were obtained for the commercial alumina powder containing 58 wt% wash coat loading, while the other catalysts showed intermediate pore diffusion resistances.

EKED values of the 19 wt% commercial powder catalyst and those of the 16 wt% COADA catalyst showed high linear relationships with temperature, *i.e.*, R^2 of 0.91 and 0.98, respectively (Figure 6.8). Adsorption KED values of both catalyst wash coat materials are also shown in Table 6.8. No correlation was, however, found between EKED and KED, as well as KED (D^0), values obtained from adsorption data. Average KED (D^0) values of 0.19 and 1.03 cm^2/s for the temperature range under consideration were obtained for the 19 wt% commercial alumina and 16 wt% COADA wash coat composites, respectively.

6.5.1.3 Aged catalysts containing similar amounts of wash coat loading

Reactor data obtained for aged catalysts is given in Appendix I. No attempt was made to determine effectiveness factors for aged catalysts.

Specific conversions

Figure 6.9 shows the specific conversions obtained, as a function of temperature, for various aged catalysts containing, in general, similar wash coat loadings (22 to 28 wt%). The effect of ageing was a large decrease in activity for the commercial powder after ageing at 980 °C. The standard commercial monolith, however, increased in activity. No significant activity differences are noted between COADA catalysts containing 3 wt% ceria. COADA catalysts containing 11 wt% ceria showed the highest activity after sintering.

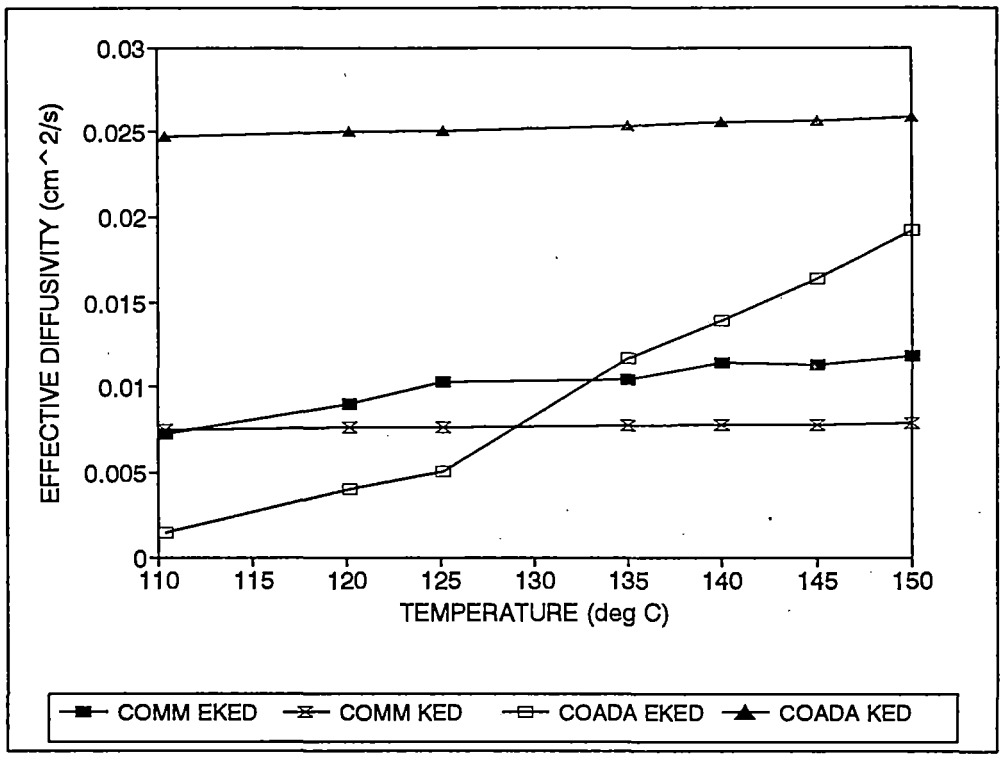

Figure 6.8 Knudsen effective diffusivities as a function of temperature for commercial alumina powder and COADA catalysts.

Kinetics

Arrhenius plots obtained from equations (15) and (17) for various aged catalysts are given in Appendix J. Table 6.11 contains activation energies and pre-exponential factors obtained for these catalysts. Activation energy of the aged standard catalyst (74.9 kJ/mol) did not change significantly during sintering compared to its fresh counterpart (see Table 6.2), which indicates the high stability of this catalyst. This stability was also evidenced for the commercial powder sample. The aged COADA powder catalyst, containing 11 wt% ceria, resulted in a similar activation energy to the standard sample, *i.e.*, 80.8 kJ/mol, but this activation energy was lower than that of its fresh counterpart.

The highest activation energy and change during sintering (216.1 kJ/mol and 140.8 kJ/mol, respectively) were obtained for the COADA catalyst where 3 wt% ceria was added during the wash coat process, although this catalyst showed the lowest ΔT_{10} value.

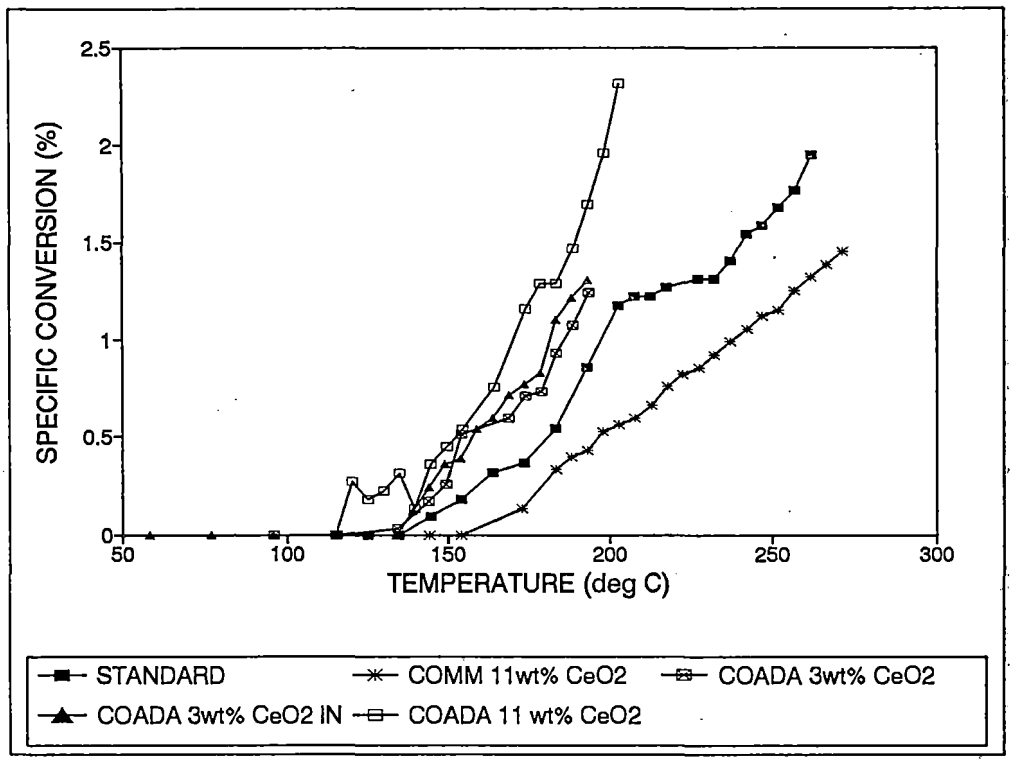

Figure 6.9 Specific conversion as a function of temperature for aged monolithic catalysts.

This implies that the high amount of ceria (11 wt%) enhanced the stability of the COADA catalysts to a higher degree than 3 wt% ceria addition. The high activation energy reflects a possible change in oxidation mechanism.

The reaction rate curves (Figure 6.10) did not follow similar trends to those obtained for the specific conversion curves for the catalysts under consideration. The two distinctive regions are presented by the two different materials under consideration, with the COADA catalysts showing higher conversion rates than the standard and commercial catalysts after sintering.

Table 6.11 Activation energies and pre-exponential factors obtained with three different kinetic models for aged monolithic catalysts.

Catalyst and wash coat loading	General (kJ/mol)	Koberstein & Wannemacher (kJ/mol)	Voltz *et al.* (kJ/mol)
Standard (31 wt%)[f]	74.9 (0.98)[a] 1.34E8[b]	35.0 (0.93) 6.45E5	55.4 (0.97) 1.03E7
Commercial powder + 11 wt% ceria added (27.6 wt%)	133.4 (0.98) 3.60E14	106.4 (1.00) 5.68E13	126.8 (1.00) 9.50E14
COADA + 11 wt% ceria added (22 wt%)	80.8 (0.99) 3.75E9	41.6 (0.96) 2.11E7	60.8 (0.98) 2.59E8
COADA + 3 wt% ceria built-in (22.7 wt%)	165.9 (0.98) 7.25E19	123.1 (0.97) 1.47E17	143.7 (0.98) 2.48E18
COADA + 3 wt% ceria added (21.7 wt%)	216.1 (0.98) 8.81E25	173.3 (0.97) 1.81E23	194.0 (0.98) 3.04E24

[a] R^2 linearity of line fit in Arrhenius plot.

[b] Pre-exponential factor 1/s.

[f] Wash coat loading

Surface properties

The results in Table 6.12 show the similarity between the surface properties obtained for all aged catalysts. When comparing these results with those obtained for fresh catalysts (Table 6.4 and 6.9), the following points were noted:

1) Surface areas of commercial powder and standard catalysts decreased slightly, while those for COADA catalysts decreased significantly from between 26 to 29 m^2/g to between 11 to 18 m^2/g after sintering of these samples.

2) No significant changes were observed for total pore volumes.

3) Average pore sizes increased notably for all catalysts during sintering and the standard catalyst showed the lowest degree of sintering or widening of pores. This indicated the high sintering resistance of the commercial standard catalyst, which

Table 6.12 Surface and platinum properties of aged monolithic catalysts.

Catalyst sample/wash coat loadings	N_2 surface area (m^2/g)	N_2 total pore volume (cm^3/g)	N_2 average pore size (nm)	Pt dispersion (%)	Pt surface area (m^2/g metal)	Pt crystallite diameter (nm)
Standard	11.05	0.05	12.2	NO	NO	NO
Commercial powder + 11 wt% ceria added (27.6 wt%)	15.16	0.07	11.0	NO	NO	NO
COADA + 11 wt% ceria added (22 wt%)	11.23	0.05	11.8	4.09	16.5	415.3
COADA + 3 wt% ceria added (22 wt%)	17.69	0.07	11.4	4.05	16.0	432.7
COADA + 3 wt% ceria built-in (23 wt%)	16.84	0.07	10.8	NO	NO	NO

NO = not obtainable.

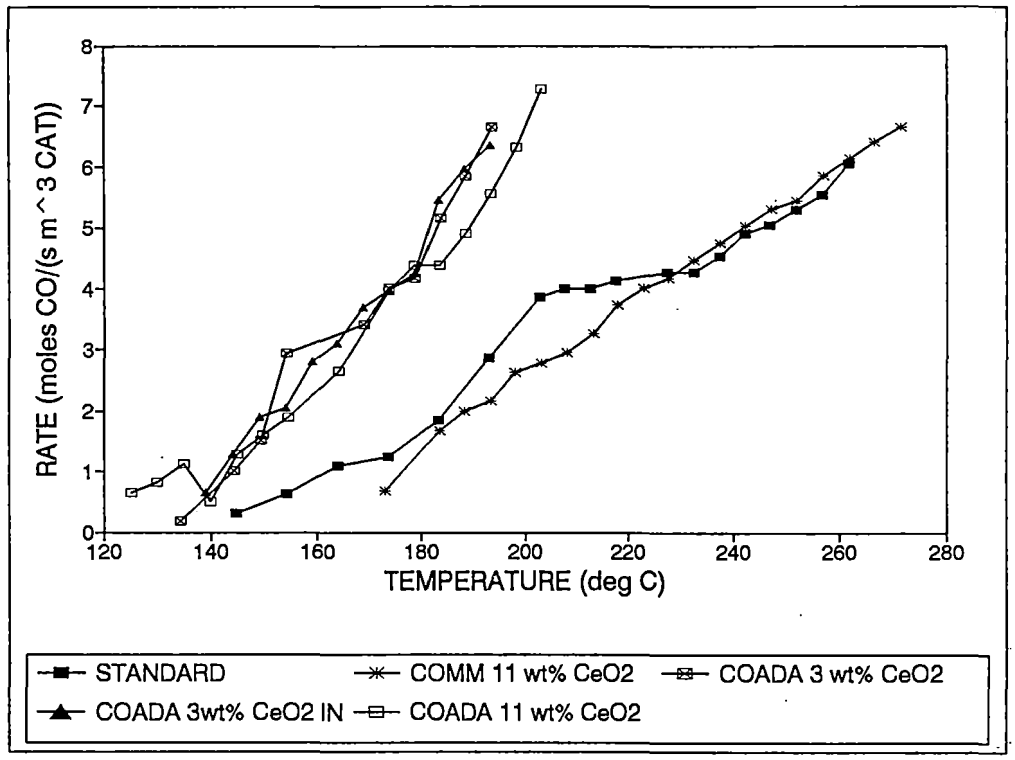

Figure 6.10 Reaction rates as a function of temperature for aged monolithic catalysts.

was probably due to additives built into this catalyst. Pore sizes increased by similar amounts for the COADA catalysts. This indicated that the sinter resistance of CO catalysts investigated depended to a large degree on the wash coat method employed, since no differences were noted between the different materials used.

Platinum properties

For some catalysts it was not possible to obtain chemisorption data. This was probably due to severe sintering of the platinum crystallites. In order to compare platinum properties of catalysts, similar chemisorption procedures have to be employed throughout. Sintering caused severe platinum crystallite growth when comparing platinum properties obtained for aged COADA catalysts with those of fresh catalysts. This, in turn, caused a drastic decrease in platinum surface area and subsequently dispersion. This is in accordance with results reported by Engler and co-workers (1989).

Addition of 3 wt% ceria resulted in a similar degree of platinum sintering to that of 11 wt% ceria (Table 6.4 and 6.12). Thus, platinum was not stabilised by addition of ceria.

6.5.2 Catalytic activity of 60 mm monolithic catalysts

Monoliths of 60 mm lengths are more representative of practical exhaust catalysts since high CO conversions are obtainable. Figures 6.11 and 6.12 present the conversion curves, as a function of temperature, obtained for fresh and aged 60 mm monolithic catalysts, respectively. The fact that 100% conversions were not achieved was mainly due to the insufficient length of the monoliths as shown by Bensalem and Ernst (1982) and Koberstein and Wannemacher (1987).

To compare activities of these catalysts, Table 6.13 was compiled for T_{50} values (light-off temperatures) for each catalyst. Fresh COADA catalysts (26.2 wt% wash coat loading), containing 11 wt% ceria, and the commercial powder catalyst ((23.8 wt% wash coat loading) showed similar activities. The fresh COADA catalyst containing 3 wt% ceria (18.3 wt% wash coat loading) showed a slightly higher activity than the COADA catalyst (18.0 wt% wash coat loading) containing 3 wt% ceria built into the structure of the γ-alumina powder. Due to different wash coat loadings, no comparison can be made between activities obtained for fresh 3 wt% and 11 wt% COADA samples.

The lowest T_{50} value was obtained for the standard sintered catalyst, which also had the lowest ΔT_{50} (difference between fresh and aged T_{50} values). This again indicated that the standard catalyst had the highest sinter resistance. T_{50} values for other sintered catalysts were similar irrespective of the material and ceria content, but the lowest ΔT_{50} values were obtained for COADA catalysts containing 3 wt% built-in ceria.

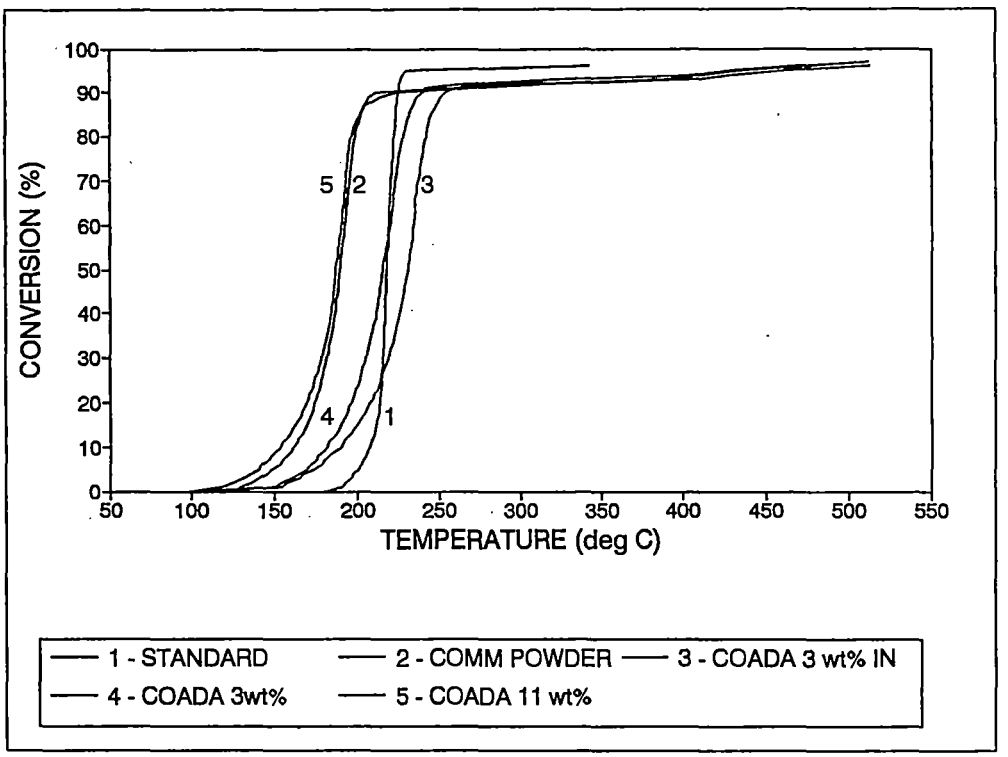

Figure 6.11 Conversion curves for fresh 60 mm monolithic catalysts.

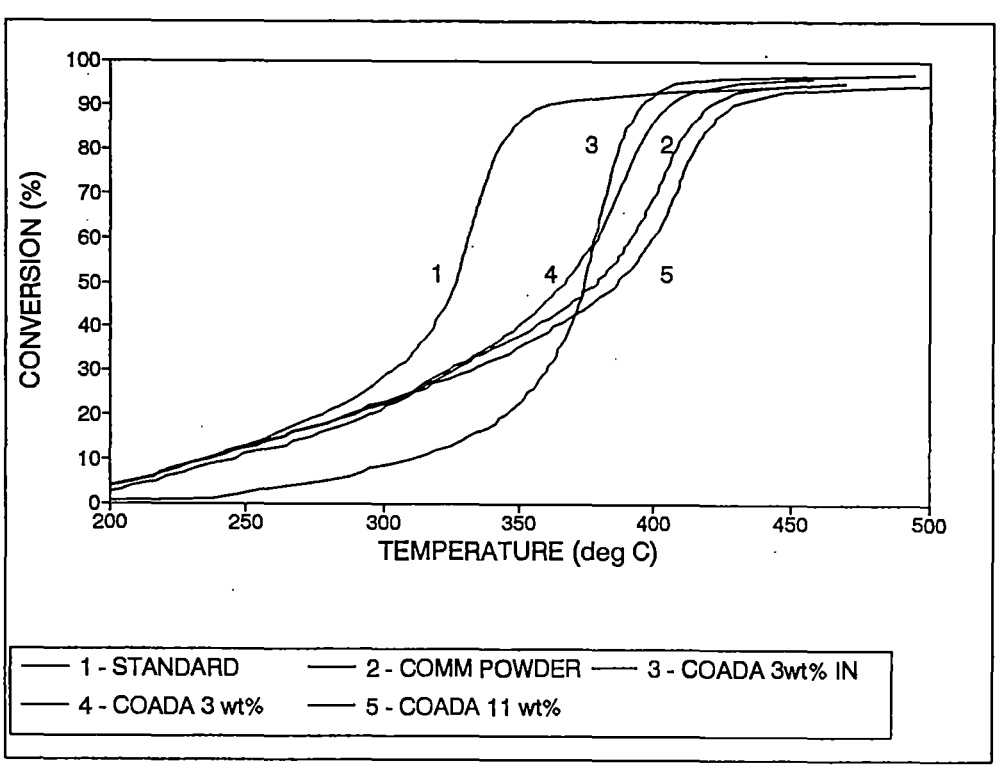

Figure 6.12 Conversion curves for aged 60 mm monolithic catalysts.

Table 6.13 Light-off temperatures for fresh and aged 60 mm monolithic catalysts.

Catalyst	T_{50} Fresh catalysts (°C)	Wash coat loading (wt%)	T_{50} Aged catalysts (°C)	Wash coat loading (wt%)	ΔT_{50} (°C)
Standard	217.6	31.0	326.6	31.0	109.0
Commercial powder + 11 wt% ceria added	189.6	23.8	378.8	30.4	-
COADA + 11 wt% ceria added	187.2	26.2	386.2	29.6	199.0
COADA + 3 wt% ceria added	215.2	18.3	367.2	29.6	-
COADA + 3 wt% ceria built-in	230.6	18.0	374.2	18.6	143.6

6.6 CONCLUSIONS

6.6.1 5 mm monolithic catalysts

6.6.1.1 Inhibition of CO reaction

Inhibition of the CO oxidation reaction was obtained in the temperature range between 68 to 150 °C depending on the catalyst.

6.6.1.2 Catalyst surface properties

COADA catalysts had higher surface areas, but smaller average pore sizes, than the standard and commercial alumina powder catalysts. Higher wash coat thicknesses were obtained for COADA catalysts than for the commercial alumina powder catalyst at similar wash coat loading.

Surface areas of commercial powder and standard catalysts decreased slightly, while those for COADA catalysts decreased significantly from about 28 m^2/g to 15 m^2/g after sintering of these samples. Average pore sizes increased notably for all catalysts during sintering and the standard catalyst showed the lowest degree of sintering or widening of pores. This indicated the high sintering resistance of the commercial standard catalyst.

Pore sizes increased with similar amounts for COADA catalysts.

6.6.1.3 Specific conversion

All fresh COADA catalysts had higher activities than the standard sample. The order of activity for fresh catalysts is: commercial alumina powder containing 11 wt% ceria > COADA catalysts containing 11 wt% ceria > 3 wt% ceria built into the structure of COADA powder > COADA catalysts where 3 wt% ceria was added during the wash coat process. Increasing ceria content did not have a detrimental effect on activity as has been found by other workers in this field.

Lower activities were obtained for fresh commercial alumina powder and COADA catalysts, in general, with increasing wash coat loading. Therefore, high wash coat loading is detrimental to catalyst activity.

The effect of ageing at 980 °C was a large decrease in activity for the commercial alumina powder. The commercial monolith, however, increased in activity. COADA catalysts containing 11 wt% ceria showed the highest activity after sintering. No significant activity differences are noted between sintered COADA catalysts containing 3 wt% ceria.

6.6.1.4 Activation energy

Lower activation energies were obtained for fresh commercial catalysts than catalysts prepared from the commercial alumina powder, *i.e.*, 86.2 to 100.5 kJ/mol and 120.4 kJ/mol, respectively. Similar activation energies (109 to 120 kJ/mol) were obtained with fresh COADA catalysts, containing 11 wt% ceria and where 3 wt% ceria was built into the structure, and the commercial powder catalyst. Activation energy increased (140.8 kJ/mol) in the case where 3 wt% ceria was added during the wash coat process.

Activation energies of the commercial powder, impregnated with different levels of

platinum, did not show any consistent trend with increasing platinum content. COADA samples, however, showed a reduced activation energy with increasing thickness, which is consistent with measured diffusional restriction.

Activation energy of the aged standard catalyst (74.9 kJ/mol) did not change significantly during sintering compared to its fresh counterpart, which indicates the high stability of this catalyst. This stability was also evidenced for the commercial powder sample. The aged COADA powder catalyst, containing 11 wt% ceria, resulted in a similar activation energy to that of the standard sample, *i.e.*, 80.8 kJ/mol, but this activation energy decreased compared to its fresh counterpart.

The highest activation energy and change during sintering (216.1 kJ/mol and 140.8 kJ/mol, respectively) were obtained for the COADA catalyst where 3 wt% ceria was added during the wash coat process, although this catalyst showed the lowest ΔT_{10} value. This implies that the high amount of ceria (11 wt%) enhanced the stability of the COADA catalysts to a higher degree than 3 wt% ceria addition.

6.6.1.5 Platinum properties

In the case of fresh catalysts, platinum dispersion was lower for the commercial powder sample than for the standard sample (30 and 45%, respectively), but it had no adverse effect on the platinum surface area and average platinum crystallite size. A higher Pt dispersion was obtained for fresh COADA catalysts (61 to 73%) than standard and commercial powder catalysts, as well as platinum surface area (140 to 230 m^2/g metal), while the platinum crystallite sizes decreased accordingly (1.2 to 2.0 nm). Addition of 3 wt% ceria for COADA catalysts resulted in slightly higher platinum surface areas and smaller platinum crystallites compared to the addition of 11 wt% ceria (162 and 140 m^2/g metal as well as 1.7 and 2.0 nm, respectively), but similar dispersions were obtained which differed from those reported by other workers. In the case where 3 wt% ceria was built into the COADA structure, a significant enhancement in platinum dispersion (73%) and platinum surface area (230 m^2/g metal) was obtained. The average platinum

crystallite sizes also decreased slightly from 1.7 to 1.2 nm. The absence of high CO activity with decreasing platinum particle size was due to strong adsorption of CO onto small platinum crystallites which retarded the oxidation of CO. Platinum dispersion, surface area and crystallite sizes were similar irrespective of wash coat loading.

Sintering caused severe platinum crystallite growth when comparing platinum properties obtained for aged COADA catalysts with those of fresh catalysts. Addition of 3 wt% ceria resulted in a similar degree of platinum sintering to 11 wt% for COADA catalysts. Thus, platinum was not stabilised by addition of ceria.

6.6.1.6 Specific rate

The specific rate, at 160 °C, increased with increasing platinum particle size for fresh catalysts, the only exception being for the standard sample which had a low specific rate despite its relatively larger platinum crystallite size. The activity of a catalyst is not related only to the high surface area of the support but to properties of active platinum on the support material.

Specific rates associated with certain platinum crystallite sizes correlated with the trends found for the specific conversions and rates. This shows that the highest catalytic activity can be expected for the commercial powder sample. Inverse specific rates were obtained for the 3 wt% ceria added and 3 wt% built-in ceria COADA samples.

Specific conversions obtained at 150 °C for the commercial powder catalyst did not follow the same trend as for the specific rates. In the case of the COADA catalysts, only the specific rate obtained for the 22 wt% wash coat loading correlated with its activity and reaction rate. The higher specific rates obtained with the commercial alumina powder also indicated that this powder is more suitable for platinum CO oxidation than COADA catalysts.

6.6.1.7 Effectiveness factor

Effectiveness factors of unity were obtained at 140 °C for all fresh catalysts under consideration. Therefore, pore diffusion, based on adsorption data obtained with the average method of Knudsen and pore size distribution method of Carniglia, was negligible for fresh catalysts.

An effectiveness factor greater than unity was obtained for 22 and 38 wt% COADA catalysts. Very low effectiveness factors (< 0.15) were obtained for the 58 wt% commercial alumina catalyst at all temperatures investigated. These low values implied that a very substantial portion of the active surface was not utilised.

Only those selected catalysts whose wash coat thicknesses were considered to represent intrinsic characteristics having Thiele moduli below 0.4, can be considered to be free of pore diffusion effects. Strong pore diffusion resistances (Thiele modulus > 4) were obtained for the commercial alumina powder containing 58 wt% wash coat loading, while other catalysts showed intermediate pore diffusion resistances.

Experimental Knudsen effective diffusivity (EKED) values of the 19 wt% commercial powder catalyst and those of the 16 wt% COADA catalyst showed high linear relationships with temperature, *i.e.*, R^2 of 0.91 and 0.98, respectively. No correlation was found between EKED, KED and KED (D^0) values obtained from adsorption data.

6.6.1.8 Conversion rates

The fresh commercial powder sample showed higher conversion rates than fresh COADA and standard catalysts, but sintered COADA catalysts resulted in higher conversion rates than the sintered standard and commercial catalysts.

6.6.2 Catalytic activity of 60 mm monolithic catalysts

Fresh COADA catalysts, containing 11 wt% ceria, and the commercial powder catalyst showed similar activities. The fresh COADA catalyst containing 3 wt% ceria showed a slightly higher activity than the COADA catalyst containing 3 wt% ceria built into the structure of the γ-alumina powder.

The lowest T_{50} was obtained for the standard sintered catalyst, which also showed the lowest ΔT_{50}. This again indicated that the standard catalyst had the highest sinter resistance. T_{50} values for other sintered catalysts were similar, irrespective of material and ceria content, but the lowest ΔT_{50} values were obtained for COADA catalysts containing 3 wt% built-in ceria.

CHAPTER 7. CONCLUSIONS AND RECOMMENDATIONS

7.1 CONCLUSIONS

This study demonstrated that pore size in alumina can be controlled with additives (porogens) during formation of aluminium hydroxide gel, starting from aluminium nitrate and ammonia. The porogens were largely effective in the mesopore volume range with sharply defined pore size distributions.

Those porogens that enhanced mesoporosity were: diethylene glycol, glycerine, benzoic acid, ammonium tartrate and fatty acids/alcohol, *i.e.* stearic, palmitic and *cis*-oleic acids, oleyl alcohol, castor, olive and sunflower oils. These additives caused the formation of aggregates by packing of particles at the iso-electric point (pH 9) of aluminium hydroxide. All additives produced cylindrical-shaped pores, except fatty acids which produced ink-bottle pores. Porogens that increased microporosity were tartaric, sebacic, lactic, citric and formic acids, 2-butanol, *n*-hexanol, propanol, 2-pentanol, ammonium formate and citrate. Pore sizes in the microporosity region were affected by alumina crystallite sizes, which, in turn, were determined by the inhibition effect of strong chelating agents on crystallite growth. No detectable microporosity was obtained with succinic, maleic, oxalic and adipic acids although they contain two functional groups. This confirmed that higher dicarboxylic acid concentrations than for hydroxycarboxylic acids are necessary to show similar effects. Macroporosities were introduced by filler or spacer effects of additives, such as adipic, tartaric and fatty acids/alcohol, as well as ammonium tartrate and carbonate.

Emulsified *cis*-oleic acid produced higher total pore volume, mesopore and macropore volumes as well as surface area and porosity, but smaller pore size than the commercial alumina powder which is being used in the automotive exhaust catalyst industry. Properties obtained for *cis*-oleic acid-derived γ-alumina increased linearly up to 60 wt% addition.

Of all fatty acids investigated, *cis*-oleic acid produced the highest surface area, largest pores and Knudsen effective diffusivity (KED) for sintered aluminas, while the highest KED (D^0) (Carniglia method) was obtained with castor oil. Sintering studies indicated that ceria (11 wt%) only stabilised the control samples to a certain degree, but it had no significant effect on fatty acid samples. Addition of 3 wt% ceria caused γ-alumina crystallite sizes to decrease for both control and *cis*-oleic acid-derived alumina samples after sintering at 1000°C for 2 hours, while this was not found with 11 wt% addition. Ceria crystallites sintered preferentially compared to γ-alumina crystallites. Ceria prevented the formation of θ-alumina during sintering at 1000 °C.

Materials having relatively high porosity are associated with high KED (D^0) values, such as fatty acids, although no linear relationship existed. KED (D^0) values obtained with ammonium carbonate- and 2-pentanol-derived γ-alumina approached those for molecular diffusion. The shorter members of porogens investigated, for example ethanol/acetic acid/ammonium acetate, resulted in the lowest KED (D^0) values. The development of non-cylindrical pores in γ-alumina is also evidenced at these low values. Two distinctive regions were observed when KED (D^0) and KED were plotted as a function of tortuosity factor (TF). These were assigned to cylindrical (TF < 2.00 and KED (D^0) > 0.200 cm^2/s) and non-cylindrical (TF > 2.00) pores.

Uniform spherical spray-dried alumina powders with well developed macropore structures were prepared from emulsified *cis*-oleic acid and aluminium hydroxide gel (COADA) after ageing of the hydroxide, flocculating with polyacrylamide and dispersion of the gel. These combined effects enhanced BET surface area, porosity and KED values. However, mesopore volume, pore diameter and tortuosity factor values decreased. Commercial alumina powder had a wider distribution of particle sizes and a greater fraction of particle sizes less than 1 μm than spray-dried COADA samples.

Factors such as purity of *cis*-oleic acid (lower macropore volume and KED values and smaller pore diameters were obtained with less pure acids), milling time, peptising with acetic acid (enhanced KED values and higher attrition resistance than with nitric acid),

steam treatment and ceria amount (3 wt% added or built into the structure of alumina prior to spray-drying and 11 wt% ceria addition) affected the properties of alumina spray-dried powders and wash coat layers. All physical properties of spray-dried powders decreased, but KED values increased, when 3 wt% ceria was built into the γ-alumina structure. Addition of 11 wt% ceria and subsequent wash-coating, significantly improved attrition resistance of the wash coat layer. A high loss on peeling after sintering at 980 °C in static air on COADA samples was a negative result. Coating of monoliths was facilitated during a charge neutralisation at the interface between monoliths (negatively charged) and the alumina wash coat slurry (positively charged) at about pH 3.

Activity evaluation of platinum-impregnated catalysts showed that inhibition of the CO oxidation reaction occurred in the temperature range between 68 to 150 °C, depending on the catalyst.

All fresh 5 mm COADA catalysts had higher activities than the standard sample, but the former activities were lower than that of the commercial alumina powder. Activities were higher for COADA catalysts containing 11 wt% ceria than those containing 3 wt% ceria. Lower activation energies were obtained for fresh commercial catalysts (45% Pt dispersion, Pt surface area 44 m^2/g, Pt size 6.2 nm) than for catalysts prepared from the commercial alumina powder (30% Pt dispersion, Pt surface area 45 m^2/g, Pt size 6.4 nm), *i.e.*, 86.2 to 100.5 kJ/mol and 120.4 kJ/mol, respectively. Similar activation energies (109 to 120 kJ/mol) were obtained with fresh COADA catalysts, containing 11 wt% ceria (61% Pt dispersion, Pt surface area 140 m^2/g, Pt size 2.0 nm) and where 3 wt% ceria was built into the structure (61% Pt dispersion, Pt surface area 162 m^2/g, Pt size 1.7 nm), and the commercial powder catalyst. Activation energy increased (140.8 kJ/mol) in the case where 3 wt% ceria was added during the wash coat process (73% Pt dispersion, Pt surface area 230 m^2/g, Pt size 1.7 nm).

The specific rate, at 160 °C, increased for fresh 5 mm catalysts with increasing platinum particle size, due to the so-called size effect. The only exception was for the standard sample which had a low specific rate despite its relatively larger platinum crystallite size.

Therefore, the activity of a catalyst is determined not only by the high surface area of the support but also by the properties of active platinum on the support material. Specific rates associated with certain platinum crystallite sizes correlated with the trends found for the specific conversions and rates. This shows that the highest catalytic activity can be expected for the commercial powder sample, followed by the COADA samples containing 11 wt% ceria and the 3 wt% ceria containing catalysts.

High wash coat loading was detrimental to catalyst activity. COADA catalysts showed a reduced apparent activation energy with increasing thickness, which was consistent with measured diffusional restriction.

The effect of ageing at 980 °C was a large decrease in activity for the commercial alumina powder catalyst. The commercial monolith, however, increased in activity. COADA catalysts containing 11 wt% ceria showed the highest activity after sintering compared to COADA catalysts containing 3 wt% ceria (no difference between added or built in). Activation energy of the aged standard catalyst (74.9 kJ/mol) did not change significantly during sintering compared to its fresh counterpart, which indicates the high stability of this catalyst. This stability was also evidenced for the commercial alumina powder sample. The aged COADA catalyst, containing 11 wt% ceria, resulted in a similar activation energy to that of the standard sample, *i.e.*, 80.8 kJ/mol, but this activation energy decreased compared to its fresh counterpart. Sintering caused severe platinum crystallite growth when comparing platinum properties obtained for aged COADA catalysts with those of fresh catalysts. Addition of 3 wt% ceria resulted in a similar degree of platinum sintering to 11 wt% for COADA catalysts. Thus, platinum was not stabilised by addition of ceria.

The highest activation energy and change during sintering (216.1 kJ/mol and 140.8 kJ/mol, respectively) were obtained for the COADA catalyst where 3 wt% ceria was added during the wash coat process. This implies that the high amount of ceria (11 wt%) enhanced the stability of the COADA catalysts to a greater degree than 3 wt% ceria addition.

COADA catalysts showed higher conversion rates than the standard and commercial catalysts after sintering.

Effectiveness factors of unity were obtained at 140 °C for all fresh 5 mm catalysts comprising of similar wash coat loadings. Therefore, pore diffusion, based on adsorption data, was negligible for these catalysts. An experimental effectiveness factor (based on intrinsic rate constants) higher than unity was obtained for 22 and 38 wt% COADA catalysts. Very low experimental effectiveness factors (< 0.15) and high Thiele moduli (> 4), *i.e.*, pore diffusion resistances, were obtained for the 58 wt% commercial alumina powder catalyst at all temperatures investigated. Thus, a very substantial portion of the active surface was not utilised. Other catalysts showed intermediate pore diffusion resistances. Only those selected catalysts whose wash coat thicknesses were considered to represent intrinsic characteristics having Thiele moduli below 0.4, can be considered to be free of pore diffusion effects. Experimental Knudsen effective diffusivity (EKED) values of the 19 wt% commercial powder catalyst and those of the 16 wt% COADA catalyst showed high linear relationships with temperature, *i.e.*, R^2 of 0.91 and 0.98, respectively.

Fresh 60 mm COADA catalysts, containing 11 wt% ceria, and the commercial powder catalyst, also containing 11 wt% ceria, showed similar activities. The fresh COADA catalyst containing 3 wt% ceria showed a slightly higher activity than the COADA catalyst containing 3 wt% ceria built into the structure of the γ-alumina powder. The lowest T_{50} was obtained for the standard sintered catalyst, which also showed the lowest ΔT_{50}. This again indicated that the standard catalyst had the highest sinter resistance. T_{50} values for other sintered catalysts were similar, irrespective of material and ceria content, but the lowest ΔT_{50} values were obtained for COADA catalysts containing 3 wt% ceria.

7.2 RECOMMENDATIONS

Emulsified *cis*-oleic acid-derived alumina (COADA), possessing unique characteristics such as high porosity and high surface area, proved to be a successful support material for fresh automotive exhaust catalysts despite some negative results after sintering of this material. Future investigations could be directed towards controlling globule sizes during emulsification of *cis*-oleic acid and improving the sinter resistance of COADA material. This material could also be utilised in other catalytic applications, especially where harsh sintering on the carrier material is not required. Other applications could be as adsorbent, as gas chromatographic carrier material and in thin-plate separation processes.

REFERENCES

AKUBUIRO, E. C., VERYKIOS, X. E., LESNICK, L. 1985. **Dispersion and support effects in carbon monoxide oxidation over platinum.** *Appl Catal*, 14, pp. 215-227.

AL-MAMUN, M. A. 1982. **Hydrophobic interaction in the fatty acids-nonionic-water systems.** *Dacca Univ Stud*, Part B, 30(1), pp. 1-6.

AL-MASHTA, F., AL-DERZI, N., AL-SAADI, A., AL-DAGHISTANI, P. 1988. **Preparation of aluminas: The effect of heat treatment on the properties of alumina.** *J Thermal Anal*, 34, pp. 269-277.

ANONYMOUS. 1988. **Autocatalyst coatings.** *Mater Edge*, July/August, pp. 22-24.

ANONYMOUS. 1993. **Tiny 'towers' may unravel chemical puzzle.** *Chem Eng Prog*, January, pp. 17-18.

BAILAR, J. C. 1956. **The chemistry of the coordination compounds.** *ACS Monograph* 131. Reinhold Publishers, New York. 834 pp.

BAKER, B. R., PEARSON, R. M. 1974. **Water content of pseudoboehmite: A new model and its structure.** *J Catal*, 33, pp. 265-278.

BARRETT, E. P., JOYNER, L. S., HALENDA, P. P. 1951. **Determination of pore volume and area distributions in porous substances. Part 1. Computations from nitrogen isotherms.** *J Am Chem Soc*, 73, pp. 373-380.

BELL, A. T. 1991. **Future directions of chemical reaction engineering.** ***In*: C. K. Colton, ed. Perspectives in chemical engineering. Research and education.** *Adv Chem Eng*, Vol 16, pp. 210-217.

BENSALEM, O., ERNST, W. R. 1982. **Mathematical modeling of homogeneous-heterogeneous reactions in monolithic catalysts.** *Combust Sci Technol*, 29, pp. 1-13.

BLACHOU, V., GOULA, D., PHILIPPOPOULOS, C. 1992. **Wet milling of alumina and preparation of slurries for monolithic structures impregnation.** *Ind Eng Chem Res*, 31(1), pp. 364-369.

BLACHOU, V. M., PHILIPPOPOULOS, C. J. 1993. **Adsorption of hexachloroplatinic acid on γ-alumina coatings for preparation of monolithic structure catalysts.** *Chem Eng Comm*, 119, pp. 41-53.

BOCKELMANN, D. 1994. **Method for attaching metal oxide catalyst particles to a support.** Ger DE 4237390. 21 April. 4 pp. *CA* 121:214150.

BROGAN, M. S., DINES, T. J., CAIRNS, J. A. 1994. **Raman spectroscopic study of the Pt-CeO_2 interaction in the Pt/Al_2O_3-CeO_2 catalyst.** *J Chem Soc Faraday Trans*, 90(10), pp. 1461-1466.

CAMERON, P., SCOTT, R. P., WATTS, P. 1986. **The oxidation of carbon monoxide on a platinum catalyst at atmospheric pressure.** *J Chem Soc, Faraday Trans*, 82, pp. 1389-1403.

CANT, N. W., HICKS, P. C., LENNON, B. S. 1978. **Steady-state oxidation of carbon monoxide over supported noble metals with particular reference to platinum.** *J Catal*, 54, pp. 372-383.

CARNIGLIA, S. C. 1986. **Construction on the tortuosity factor from porosimetry.** *J Catal*, 102, pp. 401-418.

CARNIGLIA, S. C. 1994. **Private communication.**

CHAKRABARTY, T., HUDGINS, R. R., SILVESTON, P. L. 1982. **Influence of diluent gases on CO oxidation over a platinum-alumina catalyst.** *J Catal*, 77, pp. 527-538.

CHANG, C., HUANG, T. 1995. **A solid-state electrochemical study of adsorbed oxygen species in the light-off phenomenon of CO oxidation over platinum catalysts.** *Ind Eng Chem Res*, 34, pp. 2364-2370.

CHEN, I., HWANG, S., CHEN, S. 1989. **Chemical kinetics and reaction mechanism of thermal decomposition of aluminum hydroxide and magnesium hydroxide at high temperatures (973-1123 K).** *Ind Eng Chem Res*, 28, pp. 738-742.

CHENG, S., ZOULALIAN, A., BRUNELLE, J. P. 1987. **Influence of the porous structure of alumina pellets and the internal convective flow on the effective diffusivity of exhaust gas catalyst.** *Stud Surf Sci Catal*, 30, pp. 323-332.

CHERTOV, V. M., OKOPNAYA, N. T. 1975. **Chromium (III) hydroxide.** *CA* 82:19078.

CHURCH, J. S., CANT, N. W., TRIMM, D. L. 1993. **Stabilisation of aluminas by rare earth and alkaline earth ions.** *Appl Catal*, 101, pp. 105-116.

CONNER, W. C., WEBB, S. W., BUCKLEY, P., CHRISTIANSEN, S. V., PARTHUN, G., HANSEN, J. A., TOPSØE, H. 1991. **Morphological influences on unsteady gas diffusivities in porous solids.** *Stud Surf Sci Catal*, 62, pp. 199-208.

COOPER, B. J. 1983. **Durability of platinum-containing automotive exhaust control catalysts. Improvements in resistance to thermal degradation.** *Platinum Met Rev*, 27(4), pp. 146-155.

CORMACK, B., FREEMAN, J. J., SING, K. S. W. 1980. **Porosity of alumina gels**

prepared from solutions of aluminium nitrate in various alcohols. *J Chem Technol Biotechnol*, 30, pp. 367-373.

CORNELL, R. M., SCHWERTMANN, U. 1979. **Influence of organic anions on the crystallization of ferrihydrite.** *Clay Clay M*, 27(6), pp. 402-410.

CYBULSKI, A., MOULIJN, J. A. 1994. **Monoliths in heterogeneous catalysis.** *Catal Rev Sci Eng*, 36(2), pp. 179-270.

DELUCA, J. P., CAMPBELL, L. E. 1977. **Monolithic catalyst supports.** *Adv Mater Catal*, pp. 293-324.

DEROUANE, E. G., DETREMMERIE, S., GABELICA, Z., BLOM, N. 1981. **Synthesis and characterization of ZSM-5 type zeolites. I. Physico-chemical properties of precursors and intermediates.** *Appl Catal*, 1, pp. 201-224.

DIRKSEN, F. 1983. **Aluminas & silica-aluminas as catalysts and/or catalyst support.** *CHEMSA*, July, pp. 122-124.

DIWELL, A. F., RAJARAM, R. R., SHAW, H. A., TRUEX, T. J. 1991. **The role of ceria in three-way catalysts.** *Stud Surf Sci Catal*, 71, pp. 139-152.

DOĞU, T., DOĞU, G. 1991. **A grain model for catalyst tortuosity.** *Chem Eng Comm*, 103, pp. 1-9.

DUDENEY, A. W. L., GHANI, M. A., KELSALL, G. H., ZHANG, L. 1991. **Alumina powders from aqueous precipitation, particle extraction and calcination.** *Br Ceram Proc*, 47, pp. 13-24.

EARL, K. D., SYERS, J. K., McLAUGHLIN, J. R. 1979. **Origin of the effects of citrate, tartrate and acetate on phosphate sorption by soils and synthetic gels.** *Soil Sci*

Soc Am J, 43, pp. 674-678.

ENGLER, B., KOBERSTEIN, E., SCHUBERT, P. 1989. **Automotive exhaust gas catalysts: Surface structure and activity.** *Appl Catal*, 48, pp. 71-92.

ERTL, G. 1983. **Kinetics of chemical processes on well-defined surfaces.** *Catal Sci Technol*, 4, pp. 209-282.

FARKAS, A. 1986. **Catalysis and catalysts.** *In*: Ullmans's encyclopedia of industrial chemistry. 5th ed. Vol A5. VCH, Weinheim. pp. 313-367.

FOGLER, H. S. 1986. **Elements of chemical reaction engineering.** Prentice-Hall, New Jersey, 769 pp.

FROMENT, G. F., BISCHOFF, K. B. 1979. **Chemical reactor analysis and design.** John Wiley & Sons, New York, 765 pp.

GANDHI, H. S., SHELEF, M. 1987. **The role of research in the development of new generation automotive catalysts.** *Stud Surf Sci Catal*, 30, pp. 199-214.

GANESAN, P., KUO, H. K., SAAVEDRA, A., DE ANGELIS, R. J. 1978. **Particle size distribution function of supported metal catalysts by x-ray diffraction.** *J Catal*, 52, pp. 310-320.

GASSER, R. P. H. 1985. **The catalytic oxidation of carbon monoxide on palladium and platinum.** *In*: An introduction to chemisorption and catalysis by metals. Claredon Press, Oxford. pp. 207-252.

GOLUNSKI, S. E., HATCHER, H. E., RAJARAM, R. R., TRUEX, T. J. 1995. **Origins of low-temperature three-way activity in Pt/CeO_2.** *Appl Catal*, 5, pp. 367-376.

HAROLD, M. P., LUSS, D. 1987. **Use of multiplicity features for kinetic modeling: CO oxidation on Pt/Al_2O_3.** *Ind Eng Chem Res*, 26, pp. 2099-2106.

HARRISON, B., DIWELL, A. F., HALLETT, C. 1988. **Promoting platinum metals by ceria. Metal-support interactions in autocatalysts.** *Platinum Metals Rev*, 32(2), pp. 73-83.

HEGEDUS, L. L. 1980. **Catalyst pore structures by constraint nonlinear optimization.** *Ind Eng Chem Prod Res Dev*, 19, pp. 533-537.

HEGEDUS, L. L., OH, S. H., BARON, K. 1977. **Multiple steady states in an isothermal, integral reactor: The catalytic oxidation of carbon monoxide over platinum-alumina.** *AIChE J*, 23(5), pp. 632-641.

HEISE, M. S., SCHWARZ, J. A. 1985. **Preparation of metal distributions within catalyst supports. I. Effect of pH on catalytic metal profiles.** *J Coll I Sc*, 107(1), pp. 237-243.

HINDIN, S. G., DETTLING, J. C. 1979. **Catalyst manufacture.** United States Patent 4134860. 16 January 1979. 9 pp.

HINES, A. L., MADDOX, R. N. 1985. **Mass transfer. Fundamentals and applications.** Prentice Hall, Inc, New Jersey. pp. 45-48.

HLAVÁČEK, V., NGUEN-KHUE, A., SINKULE, J., SKŘIVÁNEK, J., VOTRUBA, J. 1976. **Experimental study and mathematical modeling of monolithic converters.** *Chem React Proc Int Symp*, 4th. Dechema, Frankfurt. pp. VI-239 - VI-249.

HOUDRY, E. J. 1956. **Catalytic structure and composition.** United States Patent 2742437. 17 April 1956. 6 pp.

HOWITT, J. S. 1987. **Advances in automotive catalysts supports.** *Stud Surf Sci Catal,* 30, pp. 301-311.

HOYER, W. A., JOHNSON, L. W., SCHOENENBERGER, R. G. 1976. **Continuous system for providing a catalytic coating on support members.** United States Patent 3959520. 25 May 1976. 11 pp.

HUANG, Y., WHITE, A., WALPOLE, A., TRIMM, D. L. 1989. **Control of porosity and surface area in alumina. I. Effect of preparation conditions.** *Appl Catal,* 56, pp. 177-186.

HUDSON, L. K., MISRA, C., WEFERS, K. 1985. **Aluminum oxide.** *In*: Ullman's Encyclopedia of Industrial Chemistry. 5th ed. Vol A1. VCH, Weinheim. pp. 557-594.

IWAHASHI, M., YAMAGUCHI, Y., KATO, T., HORIUCHI, T., SAKURAI, I., SUZUKI, M. 1991. **Temperature dependence of molecular conformation and liquid structure of *cis*-9-octadecanoic acid.** *J Phys Chem,* 95, pp. 445-451.

KAGANOVA, E. M., SHAKHOVA, T. E. 1959. **Aluminium silicate catalysts and adsorbers.** *CA* 53:22618e.

KAINER, H., REH, H. 1991. **High performance ceramics. III The products: Catalysts (Part I).** *Interceram,* 40(1), pp. 21-24.

KATO, T., IKEMI, T., SAGAWA, T. 1980. **Method for forming activated alumina coating on refractory article and article whereby produced.** United States Patent 4231900. 4 November 1980. 12 pp.

KATZER, J. R., SAYERS, D. E. 1978. **Structural and electronic properties of supported metals.** Paper presented at the Materials Research Society Annual Meeting, November 28 - December 1, Boston, Mass. 10 pp.

KAUKONEN, H. P., NIEMINEN, R. M. 1989. **Computer simulations studies of the catalytic oxidation of carbon monoxide on platinum metals.** *J Chem Phys*, 91(7), pp. 4280-4386.

KOBERSTEIN, E. 1990. **Non-stationary catalysts - the basis of automotive emission control.** *In*: Matros, Y., ed. *Unsteady State Proc Catal Proc Int Conf.* VSP, Zeist pp. 643-650.

KOBERSTEIN, E., WANNEMACHER, G. 1987. **The A/F window with three-way catalysts. Kinetic and surface investigations.** *Stud Surf Sci Catal*, 30, pp. 155-172.

KOLB, W. B., PAPADIMITRIOU, A. A., CERRO, R. L., LEAVITT, D. D., SUMMERS, J. C. 1993. **The ins and outs of coating monolithic structures.** *CEP*, February, pp. 61-67.

KOLBRECKA, K., PRZYLUSKI, J., TUROWSKI, K. 1995. **Effect of CeO_2 addition on phase transitions in aluminum oxide.** *Szklo Ceram*, 46(3), pp. 19-23.

KOTANIGAWA, T., YAMAMOTO, M., UTIYAMA, M., HATTORI, H., TANABE, K. 1981. **The influence of preparation methods on the pore structure of alumina.** *Appl Catal*, 1, pp. 185-200.

KUMMER, J. T. 1980. **Catalysts for automotive emission control.** *Prog Energy Combust Sci*, 6, pp. 177-199.

KWONG, K .F. N., HUANG, P. M. 1975. **Influence of citric acid on the crystallization of aluminium hydroxides.** *Clay Clay M*, 23, pp. 164-165.

KWONG, K. F. N., HUANG, P. M. 1979. **Surface reactivity of aluminium hydroxides precipitated in the presence of low molecular weight organic acids.** *Soil Sci Soc Am J*, 43, pp. 1107-1113.

LACHMAN, I. M., BAGLEY, R. D., LEWIS, R. M. 1981. **Thermal expansion of extruded cordierite ceramics.** *Am Ceram S*, 60(2), pp. 202-205.

LACHMAN, I. M., McNALLY, R. N. 1985. **Monolithic honeycomb supports for catalysis.** *CEP*, January, pp. 29-31.

LANGFORD, J. I. 1979. **Accuracy of crystallite size and strain determined from the integral breadth of powder diffraction lines.** *In*: Proceedings of Symposium on Accuracy in Powder Diffraction, Gaithersburg, June 11-15. *NBS Spec Pub*, 567, pp. 255-269.

LARSSON, L. B., LÖWENDAHL, L. O., OTTERSTEDT, J. 1987. **The effect of the chemical nature of the washcoat on the catalytic performance of CO oxidation catalysts of monolith type.** *Stud Surf Sci Catal*, 30, pp. 333-344.

LEE, B. I., HENCH, L. L. 1987. **Electrophoretic behavior and surface reactions of sol-gel derived alumina.** *Colloids Surf*, 23(3), pp. 211-229.

LEVENSPIEL, O. 1979. **The chemical reactor omnibook.** OSU Book Stores, Corvallis. pp. 23-1.

LIM, J., BRADY, M., NOVAK, K. 1982. **Substrates with calibrated pore size and catalysts employing the same.** United States Patent 4356113, 26 October 1982. 8 pp.

LINDSAY, F. K., WILLEY, B. F. 1944. **Stable Na aluminate.** United States Patent 2345134. 28 March 1944. *CA* 38:4390[8].

LIPPENS, B. C., STEGGERADA, J. J. 1970. **Physical and chemical aspects of adsorbents and catalysts.** *In*: Linsen, B. G., ed. Active alumina. Academic Press, New York, pp. 171-211.

LÖÖF, P., KASEMO, B., ANDERSON, S., FRESTAD, A. 1991. **Influence of ceria on**

the interaction of CO and NO with highly dispersed Pt and Rh. *J Catal*, 130, pp. 181-191.

MACZURA, G., GOODBOY, K. P., KOENIG, J. J. 1978. **Aluminum oxide (Alumina).** *In*: Kirk-Othmer Encyclopedia of Chemical Technology. 3rd ed, Vol 2. John Wiley & Sons, New York. pp. 218-244.

MADEY, T. E., YATES, J. T. Jr, SANDSTROM, D. R., VOORHOEVE, R. J. H. 1976. **Catalysis by solid surfaces.** *In*: Hannay, N. B., ed. Treatise on solid state chemistry, Chapter 1, Vol 6B Surfaces II. Plenum Press, New York, pp. 1-124.

MANTON, M. R. S., DAVIDTZ, J. C. 1979. **Controlled pore sizes and active site spacings determining selectivity in amorphous silica-alumina catalysts.** *J Catal*, 60, pp. 156-166.

MARCANTONIO, P. J. 1987. **Process for producing a high surface area alumina.** Patent Cooperation Treaty WO 87/01365. 9 pp.

MEUNIER, Q., GARIN, F., SCHMITT, J., MAIRE, G., ROCHE, R. 1987. **Reactivity studies of automobile exhaust catalysts in presence of oxidizing or reducing conditions.** *Stud Surf Sci Catal*, 30, pp. 243-255.

MICROMERITICS. 1991. **ASAP 2000 Chemisystem Operator's manual.** V. 1.00, 18 January. 650 pp.

MIKI, T., OGAWA, T., HANEDA, M., KAKUTA, N., UENO, A., TATEISHI, S., MATSUURA, S., SATO, M. 1990. **Enhanced oxygen storage capacity of cerium oxides in $CeO_2/La_2O_3/Al_2O_3$ containing precious metals.** *J Phys Chem*, 94, pp. 6464-6467.

MISRA, C. 1986a. **Activated alumina.** *In*: Industrial alumina chemicals. *ACS Monograph* 184. American Chemical Society, Washington. pp. 73-95.

MISRA, C. 1986b. **Aluminum oxide and hydroxides.** *In*: Industrial Alumina Chemicals. *ACS Monograph* 184. American Chemical Society, Washington. pp. 7-30.

MORRISON, S. R. 1977. **The chemical physics of surfaces.** Plenum Press, New York. p. 415.

NAGAI, N., HOKAZONO, S., KATO, A. 1991. **Synthesis of aluminium hydroxide by a homogeneous precipitation method. I. Effect of additives on the morphology of aluminium hydroxide.** *Br Ceram Trans J*, 90, pp. 44-48.

NIESEN, H. 1940. **The chemistry of tall oil.** *CA* 35:3470[8].

NORTIER, P., SOUSTELLE, M. 1987. **Alumina carriers for automotive pollution control.** *Stud Surf Sci Catal*, 30, pp. 275-300.

NUNAN, J. G., ROBOTA, H. J., COHN, M. J., BRADLEY, S. A. 1992. **Physico-chemical properties of Ce-containing three-way catalysts and the effect of Ce on catalyst activity.** *J Catal*, 133(2), pp. 309-324.

OBERLANDER, R. K. 1984. **Aluminas for catalysts - their preparation and properties.** *Appl Ind Catal*, 3, pp. 63-112.

OZAWA, M., KIMURA, M. 1990. **Effect of cerium addition on the thermal stability of gamma alumina support.** *J Mater Sci Lett*, 9, pp. 291-293.

PARFITT, R. L. 1978. **Anion adsorption by soils and soil materials.** *Adv Agron*, 30, pp. 1-50.

PEREIRA, C. J., KUBSCH, J. E., HEGEDUS, L. L. 1988a. **Monolith washcoat having optimum pore structure and optimum method of designing the washcoat.** United States Patent 4771029. 13 September 1988. 10 pp.

PEREIRA, C. J., KUBSCH, J. E., HEGEDUS, L. L. 1988b. **Computer-aided design of catalytic monoliths for automobile emission control.** *Chem Eng Sci*, 43(8), pp. 2087-2094.

PHILIPPOPOULOS, C. 1992. **Effect of pore structure on the performance of catalytic monoliths used in automotive emission control.** *J Mater Sci Lett*, 11, pp. 592-594.

POTT, G. T., STORK, W. H. J. 1976. **Formation and inhibition of formation of compounds between deposited substance and acidic carriers.** *In*: Delmon, B., Jacobs, P. A., Poncelot, G., eds. Preparation of catalysts. Elsevier Scientific Publishing Company, Amsterdam, pp. 537-558.

RAZON, L. F., SCHMITZ, R. A. 1986. **Intrinsically unstable behavior during the oxidation of carbon monoxide on platinum.** *Catal Rev Sci Eng*, 28(1), pp. 89-164.

REED, J. R., WAY, T., LEAL, R. A. 1980. **Method for coating catalyst supports.** United States Patent 4208454. 17 June 1980. 9 pp.

RETALLICK, W. B. 1988. **Washcoat for a catalyst support.** United States Patent 4762567. 9 August 1988. 9 pp.

RHODES, J. F. 1978. **Catalyst support coating slurry and coatings.** United States Patent 4116883. 26 September 1978. 5 pp.

RUCKENSTEIN, E., KARPE, P. 1989. **Control of metal distribution in supported catalysts by pH, ionic strength, and coimpregnation.** *Langmuir*, 5(6), pp. 1393-1407.

SANFORD, R. A., ROGERS, E. S., MOOI, J. 1976. **Method of extruding catalyst.** Canadian Patent 988497. 4 May 1976. 14 pp.

SANTACESARIA, E., CARRÀ, S., ADAMI, I. 1977. **Adsorption of hexachloroplatinic**

acid on γ-alumina. *Ind Eng Chem Prod Res Dev*, 16(1), pp. 41-44.

SATTERFIELD, C. N. 1980. **Heterogeneous catalysis in practice.** ***In*: Catalyst preparation and manufacture.** Chapter 4. McGraw-Hill Book Company, New York. pp. 68-98.

SATTERFIELD, C. N., SHERWOOD, T. K. 1963. **The role of diffusion in catalysis.** Addison-Wesley, Massachusetts. 118 pp.

SCHUIT, G. C. A., GATES, B. C. 1973. **Chemistry and engineering of catalytic hydrodesulfurization.** *AIChE J*, 19(3), pp. 417-438.

SCHWEIZER, A. E., KERR, G. T. 1978. **Thermal decomposition of hexachloroplatinic acid.** *Inorg Chem*, 17(8), pp. 2326-2327.

SCHWERTMANN, U., CORNELL, R. M. 1991. **Iron oxides in the laboratory. Preparation and characterization.** VCH, Weinheim. p. 100.

SHIELDS, J. E., LOWELL, S. 1983. **A method for the estimation of micropore volume and micropore surface area.** *Powder Technol*, 36, pp. 1-4.

SHIMROCK, T., TAYLOR, R. D., COLLINS, J. M. Jr. 1985. **Method of impregnating ceramic monolithic structures with predetermined amounts of catalyst.** European Patent Application 0157651. 9 October 1985. 42 pp.

SHISHU, R. C., KOWALCZYK, L. S. 1974. **The oxidation of carbon monoxide on supported platinum. A study of honeycomb catalyst reaction kinetics.** *Platinum Met Rev*, 18(2), pp. 58-64.

SIVARAJ, B., REDDY, P., RAO, B. R., RAO, P. K. 1986. **Preparation of catalytically active γ-Al_2O_3 from a basic aluminum succinate precursor precipitated from**

homogeneous solution. *Appl Catal,* 24, pp. 25-35.

SLAUGH, L. H. 1985. **Process for producing wide pore catalyst supports.** United States Patent 4559321. 17 December 1985. 4 pp.

SMITH, J. M. 1981. **Chemical engineering kinetics.** 3rd ed. McGraw-Hill, New York. 496 pp.

SOLED, S. 1983. **γ-Al_2O_3 viewed as a defect oxyhydroxide.** *J Catal,* 81, pp. 252-257.

STILES, A. B. 1987. **Physical variations in support and their control.** *Catal Supports Supported Catal,* pp. 87-106.

SU, E. C., MONTREUIL, C. N., ROTHSCHILD, W. G. 1985. **Oxygen storage capacity of monolith three-way catalysts.** *Appl Catal,* 17, pp. 75-86.

SUMMERS, J. C., AUSEN, S. A. 1979. **Interaction of cerium oxide with noble metals.** *J Catal,* 58, pp. 131-143.

TAYAA, H., MOSSET, A., GALY, J. 1992. **Effect of chemical additives in the sol-gel processing of aluminas. II. Structural evolution during the thermal treatment. Specific areas of γ-aluminas.** *Eur J Solid State Inorg Chem,* 29, pp. 27-38.

TAYLOR, K. C. 1984. **Automobile catalytic converters.** *Catal Sci Technol,* 5, pp. 119-170.

TRIMM, D. L., STANISLAUS, A. 1986. **The control of pore size in alumina catalyst supports: A review.** *Appl Catal,* 21, pp. 215-238.

VIOLANTE, A., HUANG, P. M. 1985. **Influence of inorganic and organic ligands on the formation of aluminium hydroxides and oxyhydroxides.** *Clay Clay M,* 33(3), pp. 181-

192.

VIOLANTE, A., HUANG, P. M. 1992. **Effect of tartaric acid and pH on the nature and physicochemical properties of short-range ordered aluminium precipitation products.** *Clay Clay M*, 40(4), pp. 462-469.

VIOLANTE, A., VIOLANTE, P. 1978. **Influence of carboxylic acids on the stability of chlorite-like complexes and on the crystallization of $Al(OH)_3$ polymorphs.** *Agrochimica*, 22, pp. 335-343.

VIOLANTE, A., VIOLANTE, P. 1980. **Influence of pH, concentration, and chelating power of organic anions on the synthesis of aluminum hydroxides and oxyhydroxides.** *Clay Clay M*, 28(6), pp. 425-434.

VOGEL, R. F., MARCELIN, G., KEHL, W. L. 1984. **The preparation of controlled pore alumina.** *Appl Catal*, 12, pp. 237-248.

VOLTZ, S. E., MORGAN, C. R., LIEDERMAN, D., JACOB, S. M. 1973. **Kinetic study of carbon monoxide and propylene oxidation on platinum catalysts.** *Ind Eng Chem Prod Res Dev*, 12(4), pp. 294-301.

WAKAO, N., SMITH, J. M. 1962. **Diffusion in catalyst pellets.** *Chem Eng Sci*, 17, pp. 825-834.

WANKE, S. E., FLYNN, P. C. 1975. **The sintering of supported metal catalysts.** *Cat Rev Sci Eng*, 12, pp. 93-135.

WEI, J. 1975. **Catalysis for motor vehicle emissions.** *Adv Catal*, 24, pp. 57-129.

WEI, J., BECKER, E. R. 1975. **The optimum distribution of catalytic material on support layers in automotive catalysis.** *Adv Chem Ser*, 143, pp. 116-132.

WEISZ, P. B. 1973. **Zeolites - New horizons in catalysis.** *ChemTech*, August, pp. 498-505.

WEISZ, P. B., PRATER, C. D. 1954. **Interpretation of measurements in experimental catalysis.** *Adv Catal*, 6, pp. 143-196.

WHITE, A., WALPOLE, A., HUANG, Y., TRIMM, D. L. 1989. **Control of porosity and surface area in alumina. II. Alcohol and glycol derivatives.** *Appl Catal*, 56, pp. 187-196.

YAMADA, T., KAYANO, K., FUNABIKI, M. 1993. **Platinum metals-ceria synergism in autoexhaust catalyst.** *Stud Surf Sci Catal*, 77, pp. 329-332.

YAO, Y. Y. 1984. **The oxidation of CO and hydrocarbons over noble metal catalysts.** *J Catal*, 87, pp. 152-162.

YAO, Y. Y., KUMMER, J. T. 1987. **Low-concentration supported precious metal catalysts prepared by thermal transport.** *J Catal*, 106, pp. 307-312.

YOSHINOBU, J., KAWAI, M. 1995. **Thermal excitation of oxygen species as a trigger for the CO oxidation on Pt(111).** *J Chem Phys*, 103(8), pp. 3220-3229.

YOUNG, L. C., FINLAYSON, B. A. 1974. **Mathematical modeling of the monolith converter.** *Adv Chem Ser*, 133, pp. 629-643.

APPENDIXES

APPENDIX A. ANALYSIS OF FATTY ACIDS.

Fatty acids are well known to consist of mixtures of various fatty acids. Fatty acids analysed were: a highly pure *cis*-oleic acid sample obtained from Merck (Germany), commercial samples (Priolene 6952 and 6921) obtained from SCI (Durban - South Africa) and edible grade castor, sunflower and olive oil. These fatty acid mixtures were analysed, after derivatisation with trimethyl chlorosilane, on a SE30 fused silica column (25m x 0.32 mm) using a HP5890 Series II gas chromatograph with helium as carrier gas. Separation was accomplished by temperature programming analysis starting at 70°C and ramping the temperature at 5 °C/min up to 300 °C. Each fatty acid component was identified with a HP5890 Series II mass spectrometer.

The analysis results are represented in Table A1.

Table A.1 Analysis of fatty acids used in this investigation.

Acid\component	*cis*-Oleic acid (%)	Castor oil (%)	Sunflower oil (%)	Olive oil (%)	Priolene 6952 (%)	Priolene 6921 (%)
Lauric (dodecanoic)	0.20	-	-	0.28	0.28	0.50
trans+*cis*-Myristic (tetradecanoic)	1.17	-	-	7.94	7.27	2.37
cis-Palmitoleic (hexadecenoic)	1.68	-	-	14.77	14.76	2.98
Palmitic (hexadecanoic)	2.50	2.79	15.34	10.42	10.41	3.91
Margaric (heptadecanoic)	0.37	-	-	0.75	0.75	0.59
cis-Oleic (*cis*-octadecenoic)	93.0	1.92	17.85	64.20	62.42	84.46
Stearic (octadecanoic)	1.11	3.93	7.05	-	1.90	0.98
Linoleic (octadecadienoic)	-	1.81	28.69	-	-	-
Ricinoleic*	-	89.55	-	-	-	-
Azelaic (nonanedioic)	-	-	8.59	-	-	-
Unknown	-	-	22.49	-	-	-
Pentadecanoic	-	-	-	1.59	1.46	0.27
Elaidic (*trans*-octadecenoic)	-	-	-	-	-	3.92

* 12-Hydroxy-*cis*-9-octadecenoic acid

APPENDIX B. EXTRAPOLATION OF PORE SIZE DISTRIBUTION CURVES.

Various curve-fitting procedures were used to extrapolate the pore size distribution curves, such as Gaussian, Lorentzian and log-normal. The micropore region was calculated by applying the same procedures as used by the mercury porosimeter to calculate the different pore volumes and pore sizes.

Curve-fitting examples are shown for a blank/control, tartaric acid and 2-pentanol derived γ-alumina samples.

Example 1. Curve fitting for a typical Gaussian pore size distribution curve - blank/control.

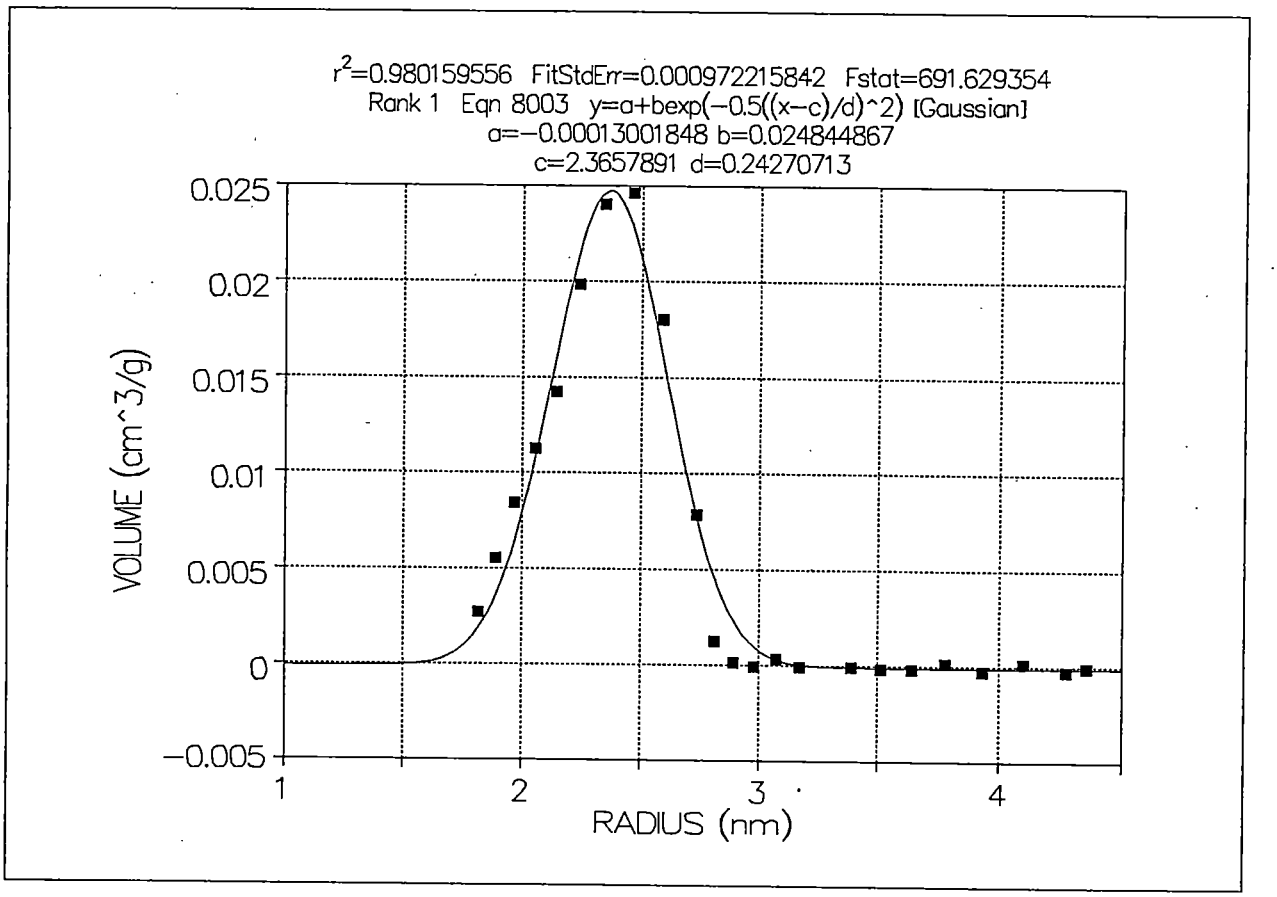

Example 2. Curve fitting for a typical Lorentzian pore size distribution curve - 2-pentanol.

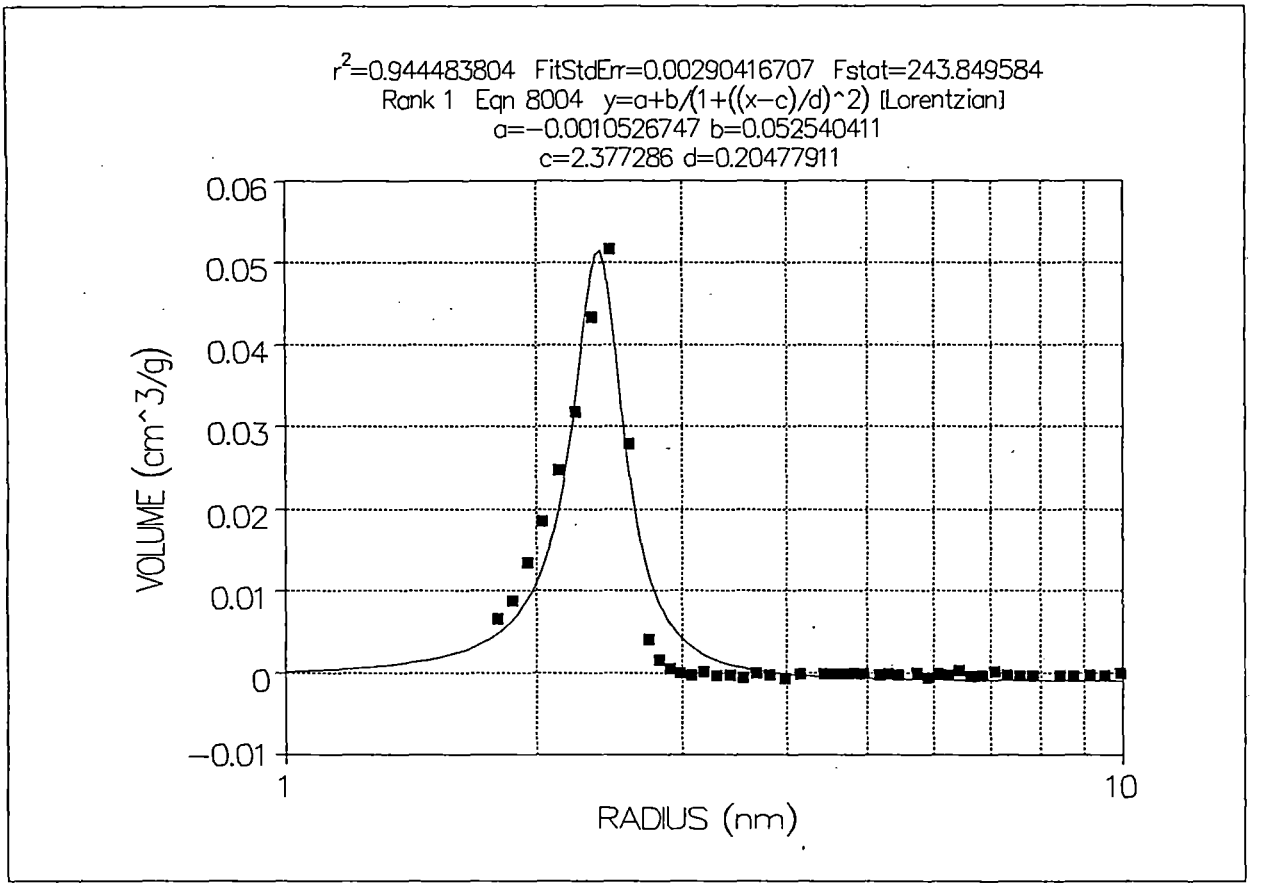

Example 3. Curve fitting for a typical log-normal pore size distribution curve - tartaric acid.

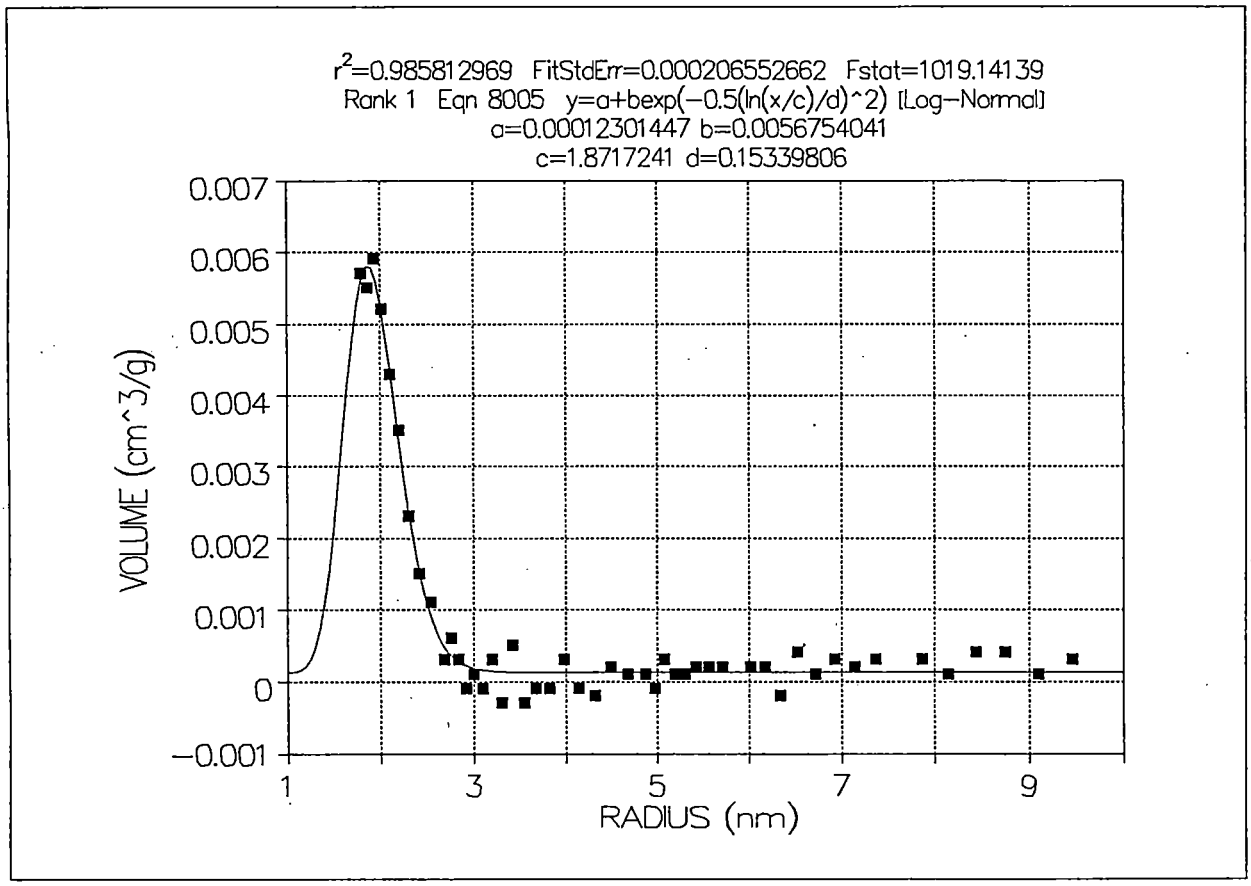

APPENDIX C. RESULTS OF ADDITIVES.

TABLE C.1 RESULTS OF ADDITIVES.

SAMPLE	SAMPLE NO.	CALCINATION TEMP (deg C)	ANALYSIS WEIGHT (g)	SOLID +PORE VOLUME/g (cm^3/g)	TRUE DENSITY (g/cm^3)	1/DENSITY TRUE SOLID VOLUME (cm^3/g)	NOMINAL BULK DENSITY 1/(Vs+1/DENS) (g/cm^3)	Vs TOTAL SPECIFIC PORE VOLUME (cm^3/g)	Vsd POROSITY	TAU(crit) Vs(based)	DV/RAD S(DVi/rti) (cm^3/cm)	PORE SHAPE y	TAU (FINAL) Vs	TAU (SMITH & WAKAO)	S(DViD(yrti)) (cm^2/s)	D(0) (383.95K) (cm^2/s)	D(K,eff,384K) (cm^2/s)	D(K,eff,384K) based on D(0) (cm^2/s)	Hg MACROPORE VOLUME (cm^3/g)	Hg MESOPORE VOLUME (cm^3/g)	Hg MICROPORE VOLUME (cm^3/g)	Hg SA (m^2/g)	N2 BET SA (m^2/g)	MEDIAN PORE RADIUS (AREA) (nm)	MEDIAN PORE DIAM (AREA) (nm)
AMM CARBONATE	131	550	0.7009	1.0178	3.0154	0.3316	0.9825	0.6862	0.6742	1.4682	842822.1	0.7150	1.4682	1.4833	1.3603	1.9824	0.0096	0.9103	0.3091	0.2834	0.0937	203.9787	235.7477	2.4298	4.8596
AMM ACETATE	132	550	0.6125	0.6242	3.0788	0.3248	1.6021	0.2994	0.4796	1.6880	1353046.2	1.2007	2.0597	2.0849	0.0135	0.0450	0.0022	0.0105	0.0044	0.2817	0.0133	210.4757	225.3815	2.6848	5.3696
AMM FORMATE	133	550	0.6589	0.6038	3.1876	0.3137	1.6562	0.2901	0.4804	1.6871	751295.3	0.6745	1.6871	2.0815	0.0013	0.0044	0.0027	0.0013	0.0011	0.2503	0.0387	206.4861	222.7769	2.4421	4.8842
AMM TARTRATE	135	550	0.6618	0.6310	3.1219	0.3203	1.2034	0.5107	0.6145	1.5356	948219.5	0.6716	1.5356	1.6272	0.3043	0.5959	0.0052	0.2385	0.0797	0.3623	0.0687	264.6340	282.3638	2.7880	5.5760
AMM CITRATE	136	550	0.8129	0.7334	3.1456	0.3179	1.3635	0.4155	0.5665	1.5898	1145180.0	0.8304	1.5898	1.7651	0.3697	0.8897	0.0039	0.3171	0.0547	0.2984	0.0624	227.3114	275.8172	2.6019	5.2038
ADIPIC ACID	137	550	0.7356	0.7238	3.1437	0.3181	1.3816	0.4057	0.5605	1.5966	907865.4	0.7492	1.5966	1.7841	0.2553	0.6292	0.0042	0.2209	0.0680	0.3008	0.0369	230.8057	242.3653	2.6107	5.2214
PALMITIC ACID	138	550	0.5412	1.0465	3.1268	0.3198	0.9556	0.7267	0.6944	1.4453	819969.8	0.5626	1.4453	1.4401	0.3278	0.4511	0.0098	0.2167	0.1666	0.5401	0.0199	291.4789	255.2500	3.5111	7.0222
SUCROSE	139	550	1.0359	0.6645	3.0972	0.3229	1.5049	0.3416	0.5141	1.6491	1203806.0	1.0591	1.6491	1.9451	0.0721	0.2111	0.0034	0.0658	0.0170	0.3048	0.0198	227.6252	227.3218	2.6677	5.3354
D-GLUCOSE	140	550	1.0661	0.6696	3.0981	0.3228	1.4934	0.3468	0.5180	1.6447	2359656.0	2.0844	6.0481	1.9306	0.2307	0.6652	0.0009	0.0570	0.0256	0.3162	0.0050	225.3191	226.4128	2.7572	5.5144
COADA	143	550	0.4532	1.2162	3.0591	0.3269	0.8222	0.8893	0.7312	1.4037	869949.4	0.4690	1.4037	1.3676	0.5801	0.6523	0.0105	0.3398	0.2307	0.6199	0.0387	371.0161	317.2546	3.2214	6.4428
GLYCERINE	144	550	0.7985	0.6871	3.1377	0.3187	1.4554	0.3684	0.5362	1.6241	1939331.0	1.5633	3.3597	1.8651	0.0869	0.2360	0.0017	0.0377	0.0151	0.3350	0.0183	243.2762	248.1010	2.7502	5.5004
OXALIC ACID	150	550	0.7403	0.6569	2.9247	0.3419	1.5223	0.3150	0.4795	1.6882	1012941.0	0.7555	1.6882	2.0855	0.0293	0.0931	0.0024	0.0264	0.0043	0.3042	0.0065	253.0945	268.1428	2.4298	4.8596
AMM OXALATE	152	550	0.7949	0.6811	3.1494	0.3175	1.4682	0.3636	0.5338	1.6268	1011483.0	0.8130	1.6268	1.8733	0.0797	0.2191	0.0035	0.0719	0.0048	0.3187	0.0401	248.8174	244.3668	2.5472	5.0944
TARTARIC ACID	153	550	0.4558	0.8616	3.1600	0.3165	1.1606	0.5451	0.6327	1.5150	511998.4	0.4599	1.5150	1.5805	0.5526	1.0136	0.0073	0.4233	0.2405	0.1031	0.2015	130.2227	222.6478	1.8807	3.7614
MALEIC ACID	154	550	0.8214	0.7450	3.0872	0.3239	1.3423	0.4211	0.5652	1.5913	1091784.0	0.8808	1.5913	1.7692	0.3085	0.7327	0.0044	0.2602	0.0625	0.2914	0.0672	247.8985	244.8708	2.4674	4.9348
SUCCINIC ACID	156	550	0.7718	0.7976	3.1504	0.3174	1.2538	0.4802	0.6020	1.5497	1041701.0	0.7851	1.5497	1.6611	0.3529	0.7350	0.0050	0.2855	0.1027	0.2949	0.0826	256.0194	265.3842	2.4924	4.9848
SEBACIC ACID	157	550	0.3660	0.8553	2.9324	0.3410	1.1692	0.5143	0.6013	1.5505	430709.6	0.3720	1.5505	1.6631	0.3328	0.6471	0.0062	0.2509	0.1789	0.1847	0.1506	181.2746	231.5842	2.1103	4.2206
OLEYL ALCOHOL	159	550	0.5116	0.8902	2.9562	0.3383	1.1233	0.5519	0.6200	1.5294	823736.3	0.5206	1.5294	1.6129	0.2927	0.5303	0.0055	0.2150	0.1232	0.4134	0.0154	316.4828	292.7682	2.8530	5.7060
DIETHYLENE GLYCOL	160	550	0.7056	0.7054	3.0817	0.3245	1.4176	0.3809	0.5400	1.6198	1796367.0	1.3801	2.6115	1.8519	0.1108	0.2908	0.0022	0.0601	0.0155	0.3380	0.0274	247.2516	260.3176	2.7858	5.5716
LACTIC ACID	161	550	0.5943	0.7468	3.0172	0.3314	1.3390	0.4154	0.5562	1.6015	907447.5	0.6063	1.6015	1.7979	0.1892	0.4554	0.0035	0.1582	0.0443	0.2503	0.1207	243.3024	299.3255	2.1644	4.3288
STEARIC ACID	162	550	0.4967	0.8947	3.1282	0.3197	1.1177	0.5750	0.6427	1.5037	821587.4	0.5074	1.5037	1.5559	0.5746	0.9992	0.0055	0.4271	0.1397	0.3920	0.0434	306.6986	323.8470	2.5423	5.0846
MANNITOL	163	550	0.7042	0.7486	3.1316	0.3193	1.3358	0.4293	0.5734	1.5820	882277.1	0.7185	1.5820	1.7439	0.2462	0.5735	0.0046	0.2079	0.0525	0.3167	0.0600	245.5923	241.0210	2.6569	5.3138
BENZOIC ACID	164	550	0.6172	0.7151	3.0501	0.3279	1.3984	0.3872	0.5415	1.6181	744162.6	0.6296	1.6181	1.8466	0.1452	0.3750	0.0040	0.1255	0.0378	0.3319	0.0175	236.3862	235.6391	2.8292	5.6584
ISO-BUTYRIC ACID	165	550	0.6349	0.7079	3.0931	0.3233	1.4126	0.3846	0.5433	1.6161	908708.6	0.6513	1.6161	1.8406	0.1060	0.2757	0.0033	0.0927	0.0345	0.3122	0.0379	250.8875	279.0414	2.5676	5.1352
PROPIONIC ACID	166	550	0.7949	0.6582	3.0641	0.3264	1.5193	0.3318	0.5042	1.6603	1906429.0	1.5561	3.4026	1.9835	0.0368	0.1109	0.0014	0.0164	0.0066	0.3100	0.0152	228.1486	245.0328	2.7623	5.5246
ACETIC ACID	167	550	1.0000	0.6463	3.1367	0.3188	1.5473	0.3275	0.5067	1.6574	2179195.0	1.8810	4.9632	1.9735	0.1711	0.5224	0.0010	0.0533	0.0085	0.2728	0.0462	224.1535	231.7100	2.5320	5.0640
TRIETHANOLAMINE	168	550	0.5225	0.8373	3.1258	0.3199	1.1943	0.5174	0.6179	1.5318	834398.5	0.6698	1.5318	1.6183	0.2596	0.5019	0.0060	0.2024	0.1119	0.3164	0.0890	236.6760	249.1309	2.7391	5.4782
BLANK	169	550	0.7250	0.5909	3.0489	0.3280	1.6923	0.2629	0.4449	1.7272	643511.9	0.6462	1.7272	2.2475	0.0973	0.3699	0.0024	0.0953	0.0258	0.1813	0.0558	173.6164	199.1639	2.3087	4.6174
ETHANOL	170	550	0.9335	0.6386	3.1464	0.3178	1.5659	0.3208	0.5023	1.6624	1000876.0	0.9553	1.6624	1.9908	0.1680	0.5238	0.0033	0.1583	0.0267	0.2486	0.0455	196.1909	209.5446	2.6605	5.3210
PROPANOL	171	550	0.7974	0.6333	3.0681	0.3259	1.5790	0.3074	0.4853	1.6816	1802018.0	1.5616	3.4707	2.0604	0.0700	0.2277	0.0013	0.0318	0.0118	0.2758	0.0198	210.2339	230.7932	2.6554	5.3108
BUTANOL	172	550	0.8105	0.6507	3.2242	0.3102	1.5368	0.3405	0.5234	1.6386	913365.7	0.8279	1.6386	1.9107	0.0378	0.1111	0.0035	0.0355	0.0000	0.2929	0.0476	220.8174	220.6337	2.6825	5.3650
ISO-BUTANOL	173	550	0.7402	0.6255	3.1406	0.3184	1.5987	0.3071	0.4910	1.6752	1586009.0	1.4435	2.9545	2.0369	0.0844	0.2748	0.0017	0.0457	0.0124	0.2592	0.0355	205.6384	219.7448	2.5926	5.1852
SEC/2-BUTANOL	174	550	0.7518	0.6294	3.2065	0.3119	1.5888	0.3175	0.5045	1.6599	824229.3	0.7966	1.6599	1.9821	0.1264	0.3980	0.0034	0.1210	0.0281	0.2178	0.0716	183.6324	206.9423	2.5825	5.1650
2-PENTANOL	175	550	0.8520	0.7720	3.0700	0.3257	1.2953	0.4463	0.5781	1.5768	1203584.6	0.8881	1.5768	1.7299	0.8940	2.0032	0.0043	0.7344	0.0983	0.2538	0.0941	245.0738	271.0486	2.3086	4.6172
HEXANOL	176	550	0.7589	0.6844	3.1419	0.3183	1.5051	0.3461	0.5210	1.6413	953894.3	0.7793	1.6413	1.9195	0.2593	0.7492	0.0032	0.2378	0.0740	0.2424	0.0297	216.1908	244.8143	2.3736	4.7472
FORMIC ACID	180	550	1.1670	0.6170	3.1487	0.3176	1.6207	0.2994	0.4853	1.6817	1524880.8	1.2078	2.0763	2.0608	0.1256	0.4194	0.0020	0.0980	0.0083	0.2452	0.0459	227.1494	252.5114	1.8922	3.7844
METHANOL	182	550	0.8111	0.6480	3.1837	0.3141	1.5432	0.3339	0.5153	1.6477	1023268.8	0.8296	1.6477	1.9407	0.0863	0.2585	0.0030	0.0808	0.0093	0.2478	0.0768	227.2605	246.6878	2.5525	5.1050
40 ml ETHANOL	183	550	1.4607	0.6453	2.7004	0.3703	1.5497	0.2750	0.4261	1.7485	1981096.0	1.4873	3.2736	2.3467	0.4956	1.8023	0.0010	0.2346	0.0422	0.2249	0.0079	207.8761	266.4051	2.4074	4.8148
BLANK	186	550	0.7081	0.6496	3.1916	0.3133	1.5394	0.3363	0.5177	1.6450	960402.3	0.8727	1.6450	1.9317	0.0816	0.2425	0.0035	0.0763	0.0160	0.2878	0.0325	220.0950	216.7717	2.6781	5.3562
BLANK	187	550	0.8469	0.6440	3.1535	0.3171	1.5528	0.3269	0.5076	1.6564	1071081.0	0.9187	1.6564	1.9701	0.1079	0.3301	0.0033	0.1012	0.0131	0.2747	0.0391	233.1740	218.4966	2.4101	4.8202
BLANK	188	550	0.9992	0.6387	3.1269	0.3198	1.5657	0.3189	0.4993	1.6658	1195601.0	1.0236	1.6658	2.0028	0.0891	0.2793	0.0029	0.0837	0.0148	0.2696	0.0345	221.4007	233.6165	2.4858	4.9716
CITRIC ACID	189	550	0.8313	0.7191	3.1698	0.3155	1.3906	0.4036	0.5613	1.5957	1172156.0	0.8517	1.5957	1.7816	0.3987	0.9877	0.0037	0.3474	0.0648	0.2318	0.1071	200.5582	275.2564	2.3819	4.7638
BLANK	193	700	0.9564	0.6537	3.2935	0.3036	1.5298	0.3501	0.5355	1.6249	945356.0	0.9736	2.6922	1.8673	0.0699	0.1996	0.0037	0.0397	0.0116	0.3281	0.0104	194.1888	134.6143	3.4575	6.9150
BLANK + 3 wt% CERIA	194	700	0.8397	0.6821	3.3472	0.2988	1.4661	0.3833	0.5620	1.5949	870806.6	0.8546	1.8075	1.7793	0.1226	0.3199	0.0058	0.0995	0.0209	0.3556	0.0068	203.7896	148.2306	3.5344	7.0688
BLANK + 11 wt% CERIA	195	700	1.0912	0.6120	3.4486	0.2900	1.6340	0.3220	0.5262	3.1200	1019218.0	1.1105	3.2564	1.9004	0.1499	0.4653	0.0027	0.0752	0.0110	0.2937	0.0173	183.5662	137.0000	3.2388	6.4776
CASTOR OIL	196	700	0.5632	1.2044	3.2025	0.3123	0.8303	0.8921	0.7407	1.3930	722099.2	0.5723	1.3930	1.3500	0.7810	0.8754	0.0162	0.4655	0.2536	0.5681	0.0704	252.3498	210.8960	4.3559	8.7118
PALMITIC ACID	197	700	0.6565	1.1700	3.2237	0.3102	0.8547	0.8598	0.7349	1.3996	876662.9	0.6658	1.3996	1.3608	0.6901	0.8026	0.0142	0.4214	0.1479	0.6321	0.0798	263.3301	228.7313	4.8250	9.6500
BLANK	199	800	1.1867	0.8004	3.3728	0.2965	1.6656	0.3039	0.5062	1.6580	983895.1	1.2077	2.0469	1.9756	0.1021	0.3360	0.0042	0.0831	0.0130	0.2890	0.0019	162.9360	128.1561	3.5858	7.1716
BLANK + 3 wt% CERIA	200	800	0.7597	0.6039	3.4299	0.2916	1.6559	0.3123	0.5172	1.6456	640324.1	0.7731	1.6456	1.9335	0.0443	0.1417	0.0057	0.0445	0.0081	0.3021	0.0021	165.6528	123.6045	3.7146	7.4292
BLANK + 11 wt% CERIA	201	800	1.0511	0.5958	3.5175	0.2843	1.6784	0.3115	0.5228	2.3100	838378.5	1.0693	1.6392	1.9126	0.1199	0.3851	0.0055	0.1228	0.0168	0.2985	0.0000	156.8150	129.0000	3.8441	7.6882
CASTOR OIL	202	800	0.6478	1.1353	3.2903	0.3039	0.8808	0.8314	0.7323	1.4025	795212.0	0.6580	1.4025	1.3656	0.8836	1.0628	0.0156	0.5549	0.1968	0.5641	0.0705	241.6913	199.6098	4.5898	9.1796
CASTOR OIL + 3 wt% CERIA	203	800	0.6122	1.1182	3.2732	0.3055	0.8943	0.8127	0.7268	1.4087	763232.7	0.6186	1.4087	1.3759	1.0580	1.3019	0.0151	0.6717	0.2307	0.5433	0.0387	246.7509	199.5334	4.5316	9.0632
CASTOR OIL + 11 wt% CERIA	204	880	0.6202	0.9025	3.3400	0.2994	1.1080	0.6031	0.6683	1.4749	602358.2	0.6307	1.4749	1.4964	0.5422	0.8990	0.0117	0.4073	0.1320	0.3735	0.0976	191.0258	167.3529	3.8378	7.6756
BLANK	205	900	0.9079	0.6007	3.4293	0.2916	1.6647	0.3091	0.5146	1.6486	677842.0	0.9241	1.6844	1.9434	0.0744	0.2407	0.0055	0.0735	0.0121	0.2938	0.0032	146.6537	122.3308	4.0876	8.1752
BLANK + 3 wt% CERIA	206	900	0.9068	0.6101	3.4422	0.2905	1.6391	0.3196	0.5238	1.6381	684006.4	0.9197	1.9471	1.9090	0.0721	0.2257	0.0054	0.0607	0.0105	0.3100	0.0000	148.7468	114.4647	4.2480	8.4960
BLANK + 11 wt% CERIA	207	900	0.9829	0.5803	3.5701	0.2801	1.7232	0.3002	0.5173	1.6454	736434.3	0.9992	2.1895	1.9330	0.0599	0.1995	0.0043	0.0471	0.0090	0.2847	0.0065	147.4048	117.2931	3.8826	7.7652
CASTOR OIL	208	900	0.7816	1.0743	3.3647	0.2972	0.9308	0.7771	0.7234	1.4126	748137.5	0.7938	1.4126	1.3825	0.9397	1.2092	0.0184	0.6192	0.2114	0.5150	0.0507	188.0028	154.9503	5.4085	10.8170
CASTOR OIL+ 3wt% CERIA	209	900	0.5992	0.8965	3.3524	0.2983	1.1154	0.5982	0.6673	1.4760	559503.8	0.6090	1.4760	1.4986	0.5602	0.9364	0.0123	0.4233	0.1741	0.3823	0.0418	183.7462	158.0710	3.9072	7.8144
CASTOR OIL + 11 wt% CERIA	210	900	0.6474	1.0433	3.4617	0.2889	0.9585	0.7544	0.7231	1.4129	588432.0	0.6567	1.4129	1.3829	0.9055	1.2003	0.0183	0.6143	0.2058	0.4788	0.0698	179.2130	151.3067	5.1418	10.2836
BLANK	211	550	0.9257	0.6431	3.2096	0.3116	1.5550	0.3315	0.5155	1.6475	1052960.0	0.8964	1.6475	1.9398	0.0503	0.1516	0.0032	0.0474	0.0091	0.3189	0.0035	223.6159	234.9306	2.8593	5.7186
COADA	214	550	0.5972	1.2309	3.1592	0.3165	0.8124	0.9144	0.7428	1.3906	941064.9	0.6081	1.3906	1.3462	1.1025	1.2057	0.0119	0.6441	0.3184	0.5976	0.0000	309.5256	295.8919	3.6884	7.3768
CASTOR OIL	215	550	0.5291	1.1985	3.0914	0.3235	0.8344	0.8750	0.7301	1.4050	850323.4	0.5387	1.4050	1.3697	0.9622	1.0996	0.0110	0.5714	0.3184	0.5425	0.0141	315.7062	295.9969	3.3003	6.6006
15 wt% COADA	216	550	0.8278	1.0092	3.0053	0.3327	0.9909	0.6765	0.6703	1.4726	1164834.0	0.8430	1.4726	1.4919	0.0191	0.0282	0.0080	0.0128	0.2264	0.3915	0.0585	261.5944	276.3508	2.9065	5.8130
60 wt% COADA	217	550	0.7659	1.3786	3.1067	0.3219	0.7254	1.0567	0.7665	1.3638	1555931.0	1.0168	1.3638	1.3046	1.6282	1.5409	0.0141	0.8660	0.3246	0.6631	0.0690	306.0309	303.1418	3.9323	7.8646
SUNFLOWER OIL	222	550	0.6737	0.9151	3.1986	0.3126	1.0928	0.6025	0.6584	1.4861	1129769.0	0.7649	1.4861	1.5189	0.5009	0.8314	0.0071	0.3683	0.1257	0.4792	0.0000	295.4070	271.3747	3.2248	6.4496
OLIVE OIL	223	550	0.6055	0.9576	3.2010	0.3124	1.0443	0.6452	0.6738	1.4686	894628.8	0.6160	1.4686	1.4842	0.7196	1.1154	0.0081	0.5117	0.1849	0.4589	0.0014	290.4527	263.5378	3.1301	6.2602
CASTOR OIL + 3 wt% CERIA	224	700	0.5924	1.1342	3.2535	0.3074	0.8817	0.8268	0.7290	1.4062	752772.7	0.6012	1.4062	1.3717	1.2753	1.5424	0.0142	0.7996	0.2518	0.5379	0.0372	250.4345	217.1500	4.3485	8.6970
CASTOR OIL + 11 wt% CERIA	225	700	0.5669	1.0940	3.3600	0.2976	0.9141	0.7964	0.7280	1.4074	727175.2	0.5758	1.4074	1.3737	1.1478	1.4412	0.0136	0.7454	0.2307	0.5167	0.0489	252.5759	218.2637	4.1518	8.3036
CASTOR OIL	226	700	0.5131	1.1644	3.2546	0.3073	0.8588	0.8571	0.7361	1.3982	668412.1	0.5215	1.3982	1.3585	0.6747	0.7871	0.0148	0.4144	0.1605	0.5397	0.1570	256.3411	219.3004	4.1458	8.2916
OLIVE OIL	227	700	0.8266	0.8751	3.2629	0.3065	1.1427	0.5686	0.6498	1.4957	868304.5	0.8415	1.4957	1.5390	0.9269	1.6301	0.0089	0.7081	0.2009	0.3659	0.0018	206.3589	200.3596	3.5321	7.0642
OLIVE OIL + 3 wt% CERIA	228	700	0.8065	0.8386	3.2848	0.3044	1.1925	0.5342	0.6370	1.5102	884899.9	0.8217	1.5102	1.5699	0.7148	1.3382	0.0077	0.5644	0.0923	0.4055	0.0364	215.3884	210.0521	3.7925	7.5850
OLIVE OIL + 11 wt% CERIA	229	700	0.7892	0.7114	3.3437	0.2991	1.4057	0.4123	0.5796	1.5751	816217.2	0.8014	1.5751	1.7253	0.4422	1.0724	0.0058	0.3946	0.0811	0.3207	0.0106	203.7012	187.0253	3.1794	6.3588

TABLE C.1 RESULTS OF ADDITIVES.

SAMPLE	SAMPLE NO.	CALCINATION TEMP (deg C)	ANALYSIS WEIGHT (g)	SOLID +PORE VOLUME/g (cm^3/g)	TRUE DENSITY (g/cm^3)	1/DENSITY TRUE SOLID VOLUME (cm^3/g)	NOMINAL BULK DENSITY 1/(Vs+1/DENS) (g/cm^3)	Vs TOTAL SPECIFIC PORE VOLUME (cm^3/g)	Vsd POROSITY	TAU(crit) Vs(based)	DV/RAD S(DVi/rti) (cm^3/cm)	PORE SHAPE y	TAU (FINAL) Vs	TAU (SMITH & WAKAO)	S(DViD(yrti)) (cm^2/s)	D(0) (383.95K) (cm^2/s)	D(K,eff,384K) (cm^2/s)	D(K,eff,384K) based on D(0) (cm^2/s)	Hg MACROPORE VOLUME (cm^3/g)	Hg MESOPORE VOLUME (cm^3/g)	Hg MICROPORE VOLUME (cm^3/g)	Hg SA (m^2/g)	N2 BET SA (m^2/g)	MEDIAN PORE RADIUS (AREA) (nm)	MEDIAN PORE DIAM (AREA) (nm)
SUNFLOWER OIL	230	700	0.8555	0.6614	3.2503	0.3077	1.5119	0.3537	0.5348	1.6256	767870.9	0.8722	1.6256	1.8698	0.3460	0.9781	0.0048	0.3218	0.0978	0.2435	0.0124	176.0803	175.4900	2.7293	5.4586
SUNFLOWER OIL + 3 wt% CERIA	231	700	0.8259	0.8093	3.3240	0.3008	1.2356	0.5085	0.6283	1.5201	1682983.0	1.6205	3.3786	1.5917	1.2773	2.5121	0.0033	0.4671	0.0802	0.3848	0.0435	206.7651	207.7121	3.7065	7.4130
SUNFLOWER OIL + 11 wt% CERIA	232	700	0.8378	0.6456	3.3098	0.3021	1.5489	0.3435	0.5320	1.6288	824588.6	0.8547	1.6288	1.8796	0.3225	0.9388	0.0042	0.3067	0.0633	0.2533	0.0269	192.9491	191.5557	2.5631	5.1262
COADA	233	800	0.5671	1.1605	3.3387	0.2995	0.8617	0.8610	0.7419	1.3916	667057.8	0.5751	1.3916	1.3479	0.7973	0.9260	0.0163	0.4937	0.1957	0.6518	0.0135	231.9687	202.1047	5.5588	11.1176
OLIVE OIL	234	800	0.8314	0.9693	3.2763	0.3052	1.0317	0.6641	0.6851	1.4558	830471.9	0.8421	1.4558	1.4596	0.8259	1.2436	0.0128	0.5852	0.1883	0.4834	0.0000	197.2300	174.8595	4.9476	9.8952
SUNFLOWER OIL	235	800	0.8253	0.9020	3.2732	0.3055	1.1086	0.5965	0.6613	1.4827	800582.5	0.8359	1.4827	1.5122	0.7092	1.1890	0.0111	0.5303	0.1362	0.4691	0.0000	191.5384	171.5309	4.9953	9.9906
COADA + 3 wt% CERIA	236	800	0.5189	1.2105	3.3100	0.3021	0.8261	0.9084	0.7504	1.3820	687279.6	0.5261	1.3820	1.3326	0.6337	0.6976	0.0173	0.3788	0.1703	0.7127	0.0254	261.2825	205.0781	5.5137	11.0274
COADA + 11 wt% CERIA	237	800	0.4674	1.2282	3.5236	0.2838	0.8142	0.9444	0.7689	1.3611	529571.1	0.4742	1.3611	1.3005	0.5828	0.6172	0.0215	0.3486	0.2237	0.7022	0.0185	223.3624	178.4173	6.1090	12.2180
OLIVE OIL + 3 wt% CERIA	238	800	0.9553	0.8823	3.2755	0.3053	1.1334	0.5770	0.6540	1.4910	898245.1	0.9679	1.4910	1.5291	0.6772	1.1736	0.0108	0.5147	0.1011	0.4405	0.0354	185.6085	168.7461	4.8258	9.6516
OLIVE OIL + 11 wt% CERIA	239	800	0.8204	0.8568	3.3399	0.2994	1.1671	0.5574	0.6505	1.4949	822730.6	0.8340	1.4949	1.5372	0.7244	1.2996	0.0096	0.5656	0.1492	0.3912	0.0170	197.2907	181.3618	3.8712	7.7424
SUNFLOWER OIL + 3 wt% CERIA	240	800	0.9017	0.5962	3.3400	0.2994	1.6773	0.2968	0.4978	1.6875	856876.8	0.9209	1.6875	2.0088	0.4554	1.5344	0.0036	0.4581	0.0857	0.1015	0.1096	186.0975	174.5051	1.7947	3.5894
SUNFLOWER OIL + 11 wt% CERIA	241	800	0.7820	0.8376	3.5051	0.2853	1.1939	0.5523	0.6594	1.4849	693993.0	0.7927	1.4849	1.5166	0.7043	1.2752	0.0108	0.5662	0.1153	0.3935	0.0435	175.1046	163.1626	4.5328	9.0656
PALMITIC ACID	242	800	0.4527	1.1266	3.2804	0.3048	0.8876	0.8218	0.7294	1.4058	471527.4	0.4590	1.4058	1.3710	0.4100	0.4990	0.0183	0.2589	0.2192	0.6112	0.0000	205.4558	167.6478	5.7335	11.4670
PALMITIC ACID + 3 wt% CERIA	243	800	0.3843	1.1708	3.2736	0.3055	0.8541	0.8653	0.7391	1.3948	440120.8	0.3897	1.3948	1.3530	0.3758	0.4342	0.0178	0.2301	0.1882	0.6859	0.0000	225.8716	184.9112	5.9306	11.8612
PALMITIC ACID + 11 wt% CERIA	244	800	0.4037	1.0975	3.4720	0.2880	0.9112	0.8095	0.7376	1.3965	426621.6	0.4097	1.3965	1.3558	0.3338	0.4124	0.0179	0.2178	0.1622	0.6176	0.0297	208.2737	171.8835	5.4514	10.9028
COADA	245	900	0.5573	1.1777	3.2655	0.3062	0.8491	0.8715	0.7400	1.3938	599200.0	0.5648	1.3938	1.3514	0.7106	0.8154	0.0176	0.4329	0.1778	0.6385	0.0551	212.1707	189.0336	5.9717	11.9434
COADA + 3 wt% CERIA	246	900	0.4849	1.1672	3.3500	0.2985	0.8568	0.8687	0.7443	1.3890	551383.5	0.4913	1.3890	1.3436	0.5597	0.6443	0.0184	0.3452	0.1509	0.6924	0.0254	224.4667	181.3993	6.0936	12.1872
COADA + 11 wt% CERIA	247	900	0.4998	1.1578	3.4988	0.2858	0.8637	0.8720	0.7531	1.3789	502408.9	0.5072	1.3789	1.3278	0.5343	0.6127	0.0216	0.3347	0.1880	0.6671	0.0169	198.1195	158.5130	6.5702	13.1404
SUNFLOWER OIL	248	900	0.8314	0.8590	3.3451	0.2989	1.1641	0.5601	0.6520	1.4933	640806.6	0.8421	1.4933	1.5338	0.7564	1.3506	0.0132	0.5897	0.1133	0.4219	0.0249	152.1882	133.4789	5.6166	11.2332
SUNFLOWER OIL + 3 wt% CERIA	249	900	0.7471	0.8028	3.3733	0.2964	1.2456	0.5064	0.6307	1.5173	609314.1	0.7566	1.5173	1.5855	0.4071	0.8039	0.0110	0.3342	0.0982	0.3953	0.0129	161.0743	137.0000	4.9844	9.9688
SUNFLOWER OIL + 11 wt% CERIA	250	900	0.8332	0.7871	3.5262	0.2836	1.2705	0.5035	0.6397	1.5071	648295.8	0.8445	1.5071	1.5632	0.4453	0.8843	0.0109	0.3754	0.0921	0.3652	0.0462	153.5289	140.5334	4.7686	9.5372
OLIVE OIL	251	900	0.7836	0.9250	3.3687	0.2968	1.0811	0.6282	0.6791	1.4626	696789.6	0.7938	1.4626	1.4726	0.7014	1.1167	0.0147	0.5185	0.1160	0.4963	0.0158	175.5496	142.5192	5.7043	11.4086
OLIVE OIL + 3 wt% CERIA	252	900	0.7892	0.8805	3.3673	0.2970	1.1357	0.5835	0.6627	1.4811	690363.8	0.7993	1.4811	1.5089	0.5188	0.8891	0.0127	0.3978	0.0811	0.4690	0.0335	172.7407	147.2214	5.5016	11.0032
OLIVE OIL + 11 wt% CERIA	253	900	0.7960	0.8032	3.5004	0.2857	1.2450	0.5175	0.6443	1.5019	593272.6	0.8062	1.5019	1.5520	0.6316	1.2204	0.0123	0.5236	0.0989	0.3951	0.0236	147.1787	130.0263	5.4660	10.9320
PALMITIC ACID	254	900	0.5570	0.9885	3.4368	0.2910	1.0116	0.6975	0.7056	1.4326	415820.1	0.5658	1.4326	1.4171	0.5240	0.7512	0.0195	0.3700	0.2464	0.4104	0.0408	146.9964	126.6168	4.9667	9.9334
PALMITIC ACID + 3 wt% CERIA	255	900	0.5739	1.0245	3.26	0.3067	0.9761	0.7178	0.7006	1.4383	474757.1	0.5825	1.4383	1.4274	0.8403	1.1708	0.0179	0.5703	0.2318	0.4862	0.0000	162.9968	140.2455	5.2942	10.5884
PALMITIC ACID + 11 wt% CERIA	256	900	0.5984	0.9838	3.4861	0.2869	1.0165	0.6969	0.7084	1.4295	555245.3	0.6074	1.4295	1.4116	0.2295	0.3292	0.0175	0.1632	0.0905	0.6136	0.0000	182.8147	141.9505	6.2645	12.5290
COADA	257	700	0.5221	1.2050	3.3379	0.2996	0.8299	0.9054	0.7514	1.3809	745261.6	0.5634	1.3809	1.3309	0.6473	0.7150	0.0157	0.3890	0.2149	0.6734	0.0171	264.5549	225.8635	5.1440	10.2880
COADA + 3 wt% CERIA	258	700	0.5352	1.2042	3.2600	0.3067	0.8304	0.8975	0.7453	1.3878	797005.7	0.5430	1.3878	1.3418	0.5433	0.6054	0.0140	0.3251	0.1659	0.7190	0.0125	293.5624	247.5948	4.8497	9.6994
COADA + 11 wt% CERIA	259	700	0.5285	1.1675	3.3155	0.3016	0.8565	0.8659	0.7417	1.3919	728763.4	0.5365	1.3919	1.3483	0.6010	0.6941	0.0146	0.3698	0.1588	0.6976	0.0095	271.6921	227.6258	4.9380	9.8760
PALMITIC ACID	260	700	0.6858	1.1217	3.2519	0.3075	0.8915	0.8142	0.7259	1.4098	881290.3	0.6953	1.4098	1.3777	0.6580	0.8082	0.0143	0.4161	0.1990	0.6247	0.0000	253.5078	211.0422	4.7800	9.5600
PALMITIC ACID + 3 wt% CERIA	261	700	0.4554	1.1156	3.2300	0.3096	0.8964	0.8060	0.7225	1.4136	603503.5	0.4616	1.4136	1.3841	0.3192	0.3960	0.0137	0.2024	0.1613	0.6442	0.0005	261.4697	216.1938	4.7884	9.5768
PALMITIC ACID + 11 wt% CERIA	262	700	0.5974	1.0486	3.3995	0.2942	0.9537	0.7544	0.7195	1.4170	769492.9	0.6068	1.4170	1.3899	0.3678	0.4875	0.0129	0.2475	0.1290	0.6205	0.0050	253.6074	213.6963	4.4059	8.8118
BLANK	266	800	0.9817	0.6115	3.2855	0.3044	1.6353	0.3071	0.5023	1.6624	828989.9	0.9994	1.6624	1.9910	0.0760	0.2474	0.0044	0.0748	0.0142	0.2991	0.0000	165.8894	152.1636	3.6707	7.3414
COADA	267	800	0.6488	1.1715	3.2513	0.3076	0.8536	0.8639	0.7375	1.3967	756407.6	0.6576	1.3967	1.3560	0.8494	0.9832	0.0168	0.5191	0.1792	0.6326	0.0521	230.0564	195.2170	5.4561	10.9122
COADA + 3 wt% CERIA	268	800	0.5121	1.2655	3.2771	0.3051	0.7902	0.9604	0.7589	1.3725	681042.2	0.5191	1.3725	1.3177	0.7766	0.8087	0.0188	0.4471	0.2552	0.7015	0.0037	262.3911	202.6944	5.2081	10.4162
BLANK	272	900	1.0156	0.6134	3.3654	0.2971	1.6303	0.3163	0.5156	1.6474	772625.8	1.0314	1.8172	1.9396	0.0874	0.2763	0.0048	0.0784	0.0158	0.3078	0.0000	149.8260	135.6598	4.2057	8.4114
COADA	273	900	0.4599	1.1733	3.2743	0.3054	0.8523	0.8679	0.7397	1.3941	471354.9	0.4661	1.3941	1.3519	0.6711	0.7732	0.0197	0.4103	0.1929	0.6360	0.0390	202.2428	168.1054	6.2222	12.4444
COADA + 3 wt% CERIA	274	900	0.5030	1.1483	3.3420	0.2992	0.8709	0.8491	0.7394	1.3945	595422.6	0.5096	1.3945	1.3524	0.3769	0.4439	0.0180	0.2354	0.1585	0.6980	0.0000	233.6597	180.0841	5.9119	11.8238
BLANK	279	550	0.7765	0.6103	3.1202	0.3205	1.6385	0.2898	0.4749	1.6934	920888.1	0.7935	1.6934	2.1059	0.0280	0.0967	0.0025	0.0271	0.0057	0.2770	0.0071	215.8380	232.1203	2.6874	5.3748
COADA	280	550	0.4759	1.2574	3.0629	0.3265	0.7953	0.9309	0.7403	1.3934	795460.6	0.4844	1.3934	1.3507	0.8323	0.8940	0.0122	0.4750	0.3022	0.6308	0.0000	328.4523	291.7162	3.7734	7.5468
BLANK	283	1000	0.8624	0.5685	3.5015	0.2856	1.7590	0.2829	0.4976	1.6677	500652.8	0.8724	1.6677	2.0095	0.0400	0.1413	0.0061	0.0422	0.0074	0.2783	0.0000	114.7788	99.0823	4.9434	9.8868
BLANK + 3 wt% CERIA	284	1000	0.9058	0.5696	3.5151	0.2845	1.7556	0.2851	0.5006	1.6644	532175.2	0.9171	1.6644	1.9978	0.0510	0.1789	0.0057	0.0538	0.0092	0.2766	0.0000	116.0589	108.9416	4.9229	9.8458
BLANK + 11 wt% CERIA	285	1000	0.8373	0.5479	3.6570	0.2734	1.8252	0.2745	0.5009	1.6640	418692.4	0.8479	1.6640	1.9963	0.0453	0.1650	0.0062	0.0497	0.0084	0.2677	0.0000	98.7614	95.2625	5.4330	10.8660
COADA	286	1000	0.8079	0.9396	3.5056	0.2853	1.0643	0.6543	0.6964	1.4431	581488.1	0.8203	1.4431	1.4360	0.5881	0.8988	0.0179	0.4338	0.1762	0.4835	0.0000	141.7693	126.3976	6.6829	13.3658
COADA + 3 wt% CERIA	287	1000	0.7826	0.9791	3.3725	0.2965	1.0213	0.6826	0.6972	1.4422	658367.4	0.7950	1.4422	1.4344	0.4799	0.7031	0.0178	0.3399	0.1241	0.5735	0.0000	165.6335	133.1970	6.8503	13.7006
COADA + 11 wt% CERIA	288	1000	0.8441	0.9383	3.6045	0.2774	1.0658	0.6609	0.7043	1.4341	604850.6	0.8589	1.4341	1.4198	0.4654	0.7043	0.0207	0.3459	0.1274	0.5435	0.0000	140.8498	112.8833	7.3926	14.7852
6.3 wt% COADA	289	550	0.5285	1.2076	3.0845	0.3242	0.8281	0.8834	0.7315	1.4034	1183680.0	0.8261	1.4034	1.3670	0.1020	0.1155	0.0115	0.0602	0.0254	0.3788	0.4792	283.7345	286.5634	2.6619	5.3238
1.6 wt% COADA	290	550	0.8917	0.6853	3.1649	0.3160	1.4592	0.3693	0.5389	1.6210	1206365.0	0.9107	1.6210	1.8555	0.1306	0.3535	0.0033	0.1175	0.0379	0.3040	0.0274	242.8751	264.9283	2.4807	4.9614
0.5/0.7 wt% COADA	291	550	0.8241	0.6601	3.1531	0.3171	1.5149	0.3430	0.5195	1.6429	1096910.0	0.8401	1.6429	1.9248	0.0252	0.0736	0.0030	0.0233	0.0114	0.3051	0.0265	238.4609	261.1238	2.3946	4.7892
1.06 wt% COADA	292	550	0.8431	0.6733	3.0857	0.3241	1.4852	0.3492	0.5187	1.6439	1146897.0	0.8601	1.6439	1.9280	0.0585	0.1676	0.0030	0.0529	0.0130	0.3272	0.0090	248.7357	266.6574	2.6322	5.2644
COADA	300	700	1.0218	1.0610	3.2167	0.3109	0.9425	0.7501	0.7070	1.4311	690154.6	0.5661	1.4311	1.4144	0.7308	0.9742	0.0116	0.4813	0.1522	0.5477	0.0502	243.8176	229.7467	4.3535	8.7070
BLANK	301	700	1.7921	0.5699	3.2310	0.3095	1.7547	0.2604	0.4569	1.7137	1424126.2	1.6348	3.8766	2.1886	0.1876	0.7205	0.0013	0.0849	0.0101	0.2312	0.0191	159.9520	174.2227	2.8852	5.7704
BLANK + 11 wt% CERIA	302	700	1.3874	0.5780	3.0305	0.3300	1.7301	0.2480	0.4291	1.7451	1017551.4	1.1484	1.9481	2.3304	0.1064	0.4291	0.0022	0.0945	0.0108	0.2448	0.0000	165.3120	177.2057	2.9743	5.9486
BLANK + 11 wt% CERIA	303	800	1.2824	0.5668	3.0318	0.3298	1.7643	0.2370	0.4181	1.7576	540096.9	0.6790	1.7576	2.3919	0.0615	0.2597	0.0025	0.0618	0.0008	0.2523	0.0000	155.5226	159.0835	3.2742	6.5484
COADA + 11 wt% CERIA	304	900	1.5457	0.5714	3.1037	0.3222	1.7501	0.2492	0.4361	1.7372	1096790.5	1.5344	3.4616	2.2929	0.2032	0.8154	0.0016	0.1027	0.0109	0.2560	0.0000	140.2143	142.9632	3.6767	7.3534
COADA + 11 wt% CERIA	305	700	0.9296	1.1484	3.0406	0.3289	0.8708	0.8195	0.7136	1.4236	813658.7	0.7146	1.4236	1.4013	0.1692	0.2065	0.0130	0.1035	0.0800	0.4220	0.3175	172.2313	227.7726	4.3494	8.6988
COADA + 11 wt% CERIA	306	800	1.0085	1.1005	2.9988	0.3335	0.9087	0.7670	0.6970	1.4424	1025680.9	1.0232	1.4424	1.4347	0.9331	1.2165	0.0142	0.5878	0.1771	0.5446	0.0454	200.4796	187.3287	5.0223	10.0446
COADA + 11 wt% CERIA	309	900	0.9123	0.9876	3.0791	0.3248	1.0126	0.6628	0.6712	1.4716	915041.4	0.9247	1.4716	1.4900	0.4845	0.7309	0.0140	0.3333	0.1265	0.5573	0.0000	197.9057	155.4926	5.3531	10.7062
SPRAY-DRIED COADA 2 h	321	700	0.1449	1.7507	3.1539	0.3171	0.5712	1.4336	0.8189	1.3047	397202.9	0.2869	1.3047	1.2212	0.9567	0.6673	0.0233	0.4189	0.8206	0.5424	0.0706	218.4198	276.8696	4.9601	9.9202
AS ABOVE + 3 wt% CERIA BUILT IN	327	700	0.1784	1.5499	3.0983	0.3228	0.6452	1.2271	0.7918	1.3353	274410.0	0.1814	1.3353	1.2630	0.6983	0.5690	0.0196	0.3374	0.6104	0.5208	0.0959	302.5800	266.4000	3.4570	6.9140
SPRAY-DRIED PRIOLENE 6921 2 h	332	700	0.2988	1.5147	3.1286	0.3196	0.6602	1.1951	0.7890	1.3385	631616.2	0.4772	1.3385	1.2675	1.2331	1.0318	0.0191	0.6082	0.7045	0.4468	0.0438	263.8300	264.7400	3.4260	6.8520
SPRAY- DRIED PRIOLENE 6952 2 h	333	700	0.2611	1.6251	3.0911	0.3235	0.6153	1.3016	0.8009	1.3249	351388.4	0.2685	1.3249	1.2485	1.1568	0.8887	0.0216	0.5372	0.7876	0.4982	0.0158	263.8800	261.7900	3.8363	7.6726
FRESH COMMERCIAL ALUMINA POWDER	STD15		0.3146	1.1886	3.3282	0.3005	0.8413	0.8881	0.7472	1.3856	259400.0	0.3246	1.3856	1.3383	1.4323	1.6128	0.0231	0.8697	0.4663	0.4205	0.0013	159.8100	148.8587	5.1011	10.2022
FRESH COMMERCIAL ALUMINA POWDER	ST40	900	3.3730	1.1669	3.2710	0.3057	0.8570	0.8612	0.7380	1.3960	219230.4	0.3038	1.3960	1.3550	0.2557	0.2970	0.0227	0.1570	0.3425	0.4147	0.1040	145.8300	144.3439	5.7654	11.5308
FRESH COMMERCIAL ALUMINA POWDER	ST41	550	3.3234	1.0659	3.2354	0.3091	0.9209	0.7768	0.7154	1.4216	268634.0	0.3436	1.4216	1.3979	0.2100	0.2703	0.0180	0.1360	0.4305	0.4260	0.0000	159.9621	156.3473	5.3972	10.7944
FRESH COMMERCIAL ALUMINA POWDER	ST42	700	0.2770	1.1819	3.2796	0.3049	0.8461	0.8770	0.7420	1.3915	219390.0	0.2842	1.3915	1.3477	0.9373	1.0687	0.0218	0.5699	0.4483	0.4149	0.0138	153.8910	154.4079	5.2344	10.4688
FRESH COMMERCIAL ALUMINA POWDER	ST43	800	3.2930	1.0494	3.2061	0.3119	0.9529	0.7375	0.7028	1.4359	231547.6	0.3078	1.4359	1.4229	0.2254	0.3056	0.0172	0.1496	0.3501	0.4249	0.0000	156.5909	150.4377	5.4837	10.9674
COMMERCIAL POWDER + ACETIC ACID	WASH32	700	0.9182	0.7006	3.3408	0.2993	1.4273	0.4013	0.5728	1.5828	570918.5	0.8203	1.5828	1.7460	0.2020	0.5033	0.0075	0.1821	0.1008	0.3593	0.0000	114.3400	139.2012	5.1941	10.3882
COADA + 11 wt% CERIA ADDED	WASH33	700	0.5452	1.3634	3.2672	0.3061	0.7335	1.0573	0.7755	1.3537	486275.1	0.5525	1.3537	1.2895	1.8468	1.7466	0.0259	1.0006	0.5499	0.4552	0.0522	176.0227	167.9359	5.2418	10.4836
COMMERCIAL POWDER + NITRIC ACID	WASH34	700	0.8647	0.7237	3.4108	0.2932	1.3818	0.4305	0.5949	1.5578	1349407.0	1.7077	3.8449	1.6810	0.3419	0.7942	0.0030	0.1229	0.0455	0.3307	0.0543	120.3706	158.0411	5.0293	10.0586
COADA + 3 wt% CERIA BUILT IN	WASH35	700	0.6514	1.3917	3.1346	0.3190	0.7185	1.0727	0.7708	1.3590	745306.3	0.6603	1.3590	1.2974	1.2083	1.1264	0.0228	0.6389	0.4891	0.5180	0.0656	225.7406	191.3291	4.5903	9.1806
COADA + 3 wt% CERIA ADDED	WASH39	700	0.4961	1.4864	3.1017	0.3224	0.6728	1.1640	0.7831	1.3451	686077.9	0.7382	1.3451	1.2770	0.8788	0.7550	0.0262	0.4395	0.4139	0.4317	0.3184	174.5840	185.8715	4.9579	9.9158
SPRAY-DRIED CONTROL + PN90B	185	550	0.5107	1.3404	3.0490	0.3280	0.7460	1.0124	0.7553	1.3765	592868.2	0.6792	1.3765	1.3240	1.5076	1.4891	0.0215	0.8171	0.4139	0.4317	0.1668	174.5840	185.8715	4.9579	9.9158
COADA - NON AGED	322	700	0.3372	1.5710	3.2618	0.3066	0.6365	1.2644	0.8049	1.3205	363460.4	0.3825	1.3205	1.2425	0.9022	0.7135	0.0292	0.4349	0.7880	0.3215	0.1549	190.0602	189.8884	3.1298	6.2596
SPRAY-DRIED COADA 2 h	321F	700	0.1766	1.7997	3.1539	0.3171	0.5556	1.4826	0.8238	1.2991	483600.4	0.3493	1.2991	1.2139	1.1167	0.7532	0.0244	0.4777	0.8206	0.5424	0.1196	218.4198	276.8696	4.9601	9.9202

APPENDIX D. PROPERTIES OF SINTERED SAMPLES.

Table D.1 Properties of γ-alumina samples (reference) as a function of ceria concentration and calcination temperature.

Sample	Total pore volume (cm^3/g)	Meso= pore volume (cm^3/g)	Micro= pore volume (cm^3/g)	Macro= pore volume (cm^3/g)	ϵ	Median pore diameter (nm)	Hg surface area (m^2/g)	N_2 surface area (m^2/g)	Bulk density (g/cm^3)	Skeletal density (g/cm^3)
550 °C	0.336	0.288	0.032	0.016	0.50	5.36	220	217	1.54	3.19
700 °C	0.350	0.328	0.010	0.012	0.54	6.92	194	135	1.53	3.29
800 °C	0.304	0.289	0.002	0.013	0.51	7.17	162	128	1.67	3.37
900 °C	0.309	0.294	0.003	0.012	0.51	8.18	147	122	1.66	3.43
1000 °C	0.283	0.278	-	0.005	0.50	9.89	115	99	1.76	3.50
700 °C + 3 wt% ceria	0.383	0.356	0.006	0.021	0.56	7.07	204	148	1.47	3.35
700 °C + 11 wt% ceria	0.322	0.294	0.017	0.011	0.53	6.48	184	137	1.63	3.45
800 °C + 3 wt% ceria	0.312	0.302	0.002	0.008	0.52	7.43	166	124	1.66	3.43
800 °C + 11 wt% ceria	0.312	0.299	-	0.013	0.52	4.69	157	129	1.68	3.52
900 °C + 3 wt% ceria	0.320	0.310	-	0.010	0.52	8.50	149	114	1.64	3.44
900 °C + 11 wt% ceria	0.300	0.285	0.006	0.009	0.52	7.77	147	117	1.72	3.57
1000 °C + 3 wt% ceria	0.285	0.277	-	0.008	0.50	9.85	116	109	1.76	3.52
1000 °C + 11 wt% ceria	0.275	0.268	-	0.007	0.50	10.87	99	95	1.83	3.66

Table D.2 Properties of γ-alumina prepared in the presence of palmitic acid as a function of ceria concentration and calcination temperature.

Sample	Total pore volume (cm^3/g)	Meso= pore volume (cm^3/g)	Micro= pore volume (cm^3/g)	Macro= pore volume (cm^3/g)	ϵ	Median pore diameter (nm)	Hg surface area (m^2/g)	N_2 surface area (m^2/g)	Bulk density (g/cm^3)	Skeletal density (g/cm^3)
550 °C	0.727	0.540	0.020	0.167	0.69	7.02	291	255	0.96	3.13
700 °C	0.860	0.632	0.054	0.174	0.73	9.65	263	229	0.85	3.22
800 °C	0.822	0.611	-	0.211	0.73	11.47	205	168	0.89	3.28
900 °C	0.698	0.410	0.001	0.287	0.71	9.93	147	127	1.01	3.44
700 °C + 3 wt% ceria	0.806	0.644	-	0.162	0.72	9.58	261	216	0.90	3.23
700 °C + 11 wt% ceria	0.754	0.621	-	0.133	0.72	8.81	254	214	0.95	3.40
800 °C + 3 wt% ceria	0.865	0.686	-	0.179	0.74	11.86	226	185	0.85	3.27
800 °C + 11 wt% ceria	0.810	0.618	-	0.192	0.74	10.90	208	172	0.91	3.47
900 °C + 3 wt% ceria	0.718	0.486	-	0.232	0.70	10.59	163	140	0.98	3.26
900 °C + 11 wt% ceria	0.697	0.614	-	0.083	0.71	12.53	183	142	1.02	3.49

Table D.3 Properties of γ-alumina prepared in the presence of castor oil as a function of ceria concentration and calcination temperature.

Sample	Total pore volume (cm^3/g)	Meso= pore volume (cm^3/g)	Micro= pore volume (cm^3/g)	Macro= pore volume (cm^3/g)	$\in$	Median pore diameter (nm)	Hg surface area (m^2/g)	N_2 surface area (m^2/g)	Bulk density (g/cm^3)	Skeletal density (g/cm^3)
550 °C	0.875	0.543	0.014	0.318	0.73	6.60	316	296	0.83	3.09
700 °C	0.857	0.540	-	0.317	0.74	8.29	256	211	0.86	3.25
800 °C	0.831	0.564	-	0.267	0.73	9.18	242	200	0.88	3.29
900 °C	0.777	0.515	-	0.262	0.78	10.82	188	155	0.93	3.36
700 °C + 3 wt% ceria	0.827	0.538	-	0.289	0.73	8.70	250	217	0.88	3.25
700 °C + 11 wt% ceria	0.797	0.517	-	0.280	0.73	8.30	253	218	0.91	3.36
800 °C + 3 wt% ceria	0.813	0.543	0.001	0.269	0.73	9.06	247	200	0.89	3.27
800 °C + 11 wt% ceria	0.604	0.374	-	0.230	0.67	7.68	191	167	1.11	3.34
900 °C + 3 wt% ceria	0.598	0.382	-	0.216	0.67	7.81	184	158	1.12	3.35
900 °C + 11 wt% ceria	0.754	0.479	-	0.275	0.72	10.28	179	151	0.96	3.46

Table D.4 Properties of γ-alumina prepared in the presence of sunflower oil as a function of ceria concentration and calcination temperature.

Sample	Total pore volume (cm^3/g)	Meso= pore volume (cm^3/g)	Micro= pore volume (cm^3/g)	Macro= pore volume (cm^3/g)	ϵ	Median pore diameter (nm)	Hg surface area (m^2/g)	N_2 surface area (m^2/g)	Bulk density (g/cm^3)	Skeletal density (g/cm^3)
550 °C	0.603	0.479	-	0.126	0.66	6.45	295	271	1.09	3.20
700 °C	0.354	0.244	-	0.110	0.53	5.46	176	175	1.51	3.25
800 °C	0.597	0.469	0.001	0.127	0.66	9.99	192	172	1.11	3.27
900 °C	0.560	0.422	-	0.138	0.65	11.23	152	133	1.16	3.35
700 °C + 3 wt% ceria	0.509	0.345	0.040	0.124	0.63	7.41	207	208	1.24	3.32
700 °C + 11 wt% ceria	0.344	0.253	0.001	0.090	0.53	5.13	193	192	1.55	3.31
800 °C + 3 wt% ceria	0.297	0.202	-	0.095	0.50	3.59	186	175	1.68	3.34
800 °C + 11 wt% ceria	0.552	0.394	-	0.158	0.66	9.07	175	163	1.19	3.51
900 °C + 3 wt% ceria	0.506	0.395	-	0.111	0.63	9.97	161	137	1.25	3.37
900 °C + 11 wt% ceria	0.504	0.365	0.001	0.138	0.64	9.54	154	141	1.27	3.53

Table D.5 Properties of γ-alumina prepared in the presence of olive oil as a function of ceria concentration and calcination temperature.

Sample	Total pore volume (cm^3/g)	Meso= pore volume (cm^3/g)	Micro= pore volume (cm^3/g)	Macro= pore volume (cm^3/g)	ϵ	Median pore diameter (nm)	Hg surface area (m^2/g)	N_2 surface area (m^2/g)	Bulk density (g/cm^3)	Skeletal density (g/cm^3)
550 °C	0.645	0.459	0.001	0.185	0.67	6.26	290	264	1.04	3.20
700 °C	0.569	0.366	-	0.201	0.65	7.06	206	207	1.14	3.26
800 °C	0.664	0.483	0.001	0.181	0.69	9.90	197	175	1.03	3.28
900 °C	0.628	0.496	-	0.132	0.68	11.41	176	143	1.08	3.37
700 °C + 3 wt% ceria	0.534	0.406	0.040	0.123	0.64	7.59	215	210	1.19	3.28
700 °C + 11 wt% ceria	0.412	0.321	0.001	0.092	0.58	6.36	204	187	1.41	3.34
800 °C + 3 wt% ceria	0.577	0.441	-	0.137	0.65	9.65	186	169	1.13	3.28
800 °C + 11 wt% ceria	0.557	0.391	-	0.166	0.65	7.74	197	181	1.17	3.34
900 °C + 3 wt% ceria	0.584	0.469	-	0.115	0.66	11.00	173	147	1.14	3.37
900 °C + 11 wt% ceria	0.518	0.395	0.001	0.122	0.64	10.93	147	130	1.25	3.50

Table D.6 Properties of γ-alumina prepared in the presence of *cis*-oleic acid as a function of ceria concentration and calcination temperature.

Sample	Total pore volume (cm^3/g)	Meso= pore volume (cm^3/g)	Micro= pore volume (cm^3/g)	Macro= pore volume (cm^3/g)	ϵ	Median pore diameter (nm)	Hg surface area (m^2/g)	N_2 surface area (m^2/g)	Bulk density (c/cm^3)	Skeletal density (g/cm^3)
550 °C	0.911	0.617	0.039	0.255	0.74	7.12	336	302	0.81	3.09
700 °C	0.905	0.673	-	0.232	0.75	10.29	265	228	0.83	3.34
800 °C	0.861	0.652	-	0.209	0.74	11.12	232	202	0.86	3.34
900 °C	0.872	0.639	-	0.233	0.74	11.94	212	189	0.85	3.27
1000 °C	0.654	0.484	-	0.170	0.70	13.37	142	126	1.06	3.51
700 °C + 3 wt% ceria	0.898	0.719	-	0.179	0.75	9.70	294	238	0.83	3.26
700 °C + 11 wt% ceria	0.866	0.698	-	0.168	0.74	9.88	272	228	0.86	3.32
800 °C + 3 wt% ceria	0.908	0.713	-	0.195	0.75	11.03	261	205	0.83	3.31
800 °C + 11 wt% ceria	0.944	0.702	-	0.242	0.77	12.22	223	182	0.81	3.52
900 °C + 3 wt% ceria	0.857	0.692	-	0.165	0.74	12.19	224	181	0.86	3.35
900 °C + 11 wt% ceria	0.872	0.667	-	0.205	0.75	13.14	198	157	0.87	3.50
1000 °C + 3 wt% ceria	0.683	0.574	-	0.109	0.70	13.70	166	133	1.02	3.37
1000 °C + 11 wt% ceria	0.661	0.544	-	0.117	0.70	14.79	141	113	1.07	3.60

APPENDIX E. X-RAY DIFFRACTION DATA.

Table E.1 X-ray diffraction data of additives.

Sample	Half-breadth (degrees)		2Theta		Corrected (radians/100)		Crystallite size (nm)	
	Alumina (400)	Ceria (311)	Alumina (400)	Ceria (311)	Alumina (400)	Ceria (311)	Alumina (400)	Ceria (311)
cis-Oleic acid	1.385	-	66.47	-	2.40	-	6.90	-
Citric acid	1.386	-	66.45	-	2.42	-	6.84	-
Tartaric acid	1.787	-	66.30	-	3.11	-	5.33	-
Control - 1000 °C	0.780	-	67.24	-	1.34	-	12.43	-
Control - 1000 °C + 3 wt% ceria	0.890	0.665	67.11	56.25	1.53	1.14	10.84	15.39
Control - 1000 °C + 11 wt% ceria	0.720	0.446	67.17	56.25	1.23	0.74	13.50	23.67
cis-Oleic acid - 1000 °C	0.720	-	67.24	-	1.23	-	13.50	-
cis-Oleic acid - 1000 °C + 3 wt% ceria	0.835	0.565	67.30	56.44	1.44	0.94	11.59	18.64
cis-Oleic acid - 1000 °C + 11 wt% ceria	0.720	0.390	67.17	56.31	1.23	0.64	13.50	27.47

APPENDIX F. COMPOSITION AND SURFACE PROPERTIES OF COMMERCIAL γ-ALUMINA POWDER.

Table F.1 Composition of commercial γ-alumina powder.

Component	Concentration
Alumina	91.3 wt%
Barium oxide	21 ppm
Ceria	< 1 ppm

Table F.2 Surface properties of commercial γ-alumina powder.

Total pore volume (cm^3/g)	0.888
Mesopore volume (cm^3/g)	0.421
Macropore volume (cm^3/g)	0.468
Porosity	0.74
Median pore diameter (nm)	10.20
Hg surface area (m^2/g)	160
BET N_2 surface area (m^2/g)	149
Bulk density (g/cm^3)	0.84
Skeletal density (g/cm^3)	3.33

APPENDIX G. SPECIFICATION OF ALUMINA SOL (BACOSOL 3C).

Table G.1 Specification of alumina sol (Bacosol 3C).

Dispersions	
Solids content (w/w)	34
Alumina content (w/w)	29
Silica content (w/w)	0.007
Medium	water
pH	3.5
Density (g/cm^3)	1.32
Viscosity (cP)	350
Particle charge	cationic
Solids	
Mineralogy	boehmite
Particle size (μm)	0.1 - 0.2
Surface area (m^2/g)	150 - 200
Sodium oxide (%)	0.15

APPENDIX H. SPECIFICATION OF PLATINUM METAL.

Table H.1 Specification of platinum metal.

Element	Concentration Parts per million	Element	Concentration Parts per million
Pt	99.99%	Cu	< 1
Pd	1	Fe	8
Rh	1	Pb	< 1
Au	15	Al	< 1
Ru	2	Ca	1
Ir	27	Si	14
Ag	< 1	Mg	10
Ni	< 1	Zn	< 1
Mn	< 1		

APPENDIX I. REACTOR DATA.

TABLE L1 REACTOR DATA FOR FRESH COMMERCIAL STANDARD CATALYST CONTAINING 11 wt% CERIA [SMCOM].
MONOLITH MASS:0.79329g DIM:5.60*15.7*15.6mm WASH COAT 31 wt% TOTAL SURFACE AREA SUPPORT + WASH COAT: 14.55 m^2/g
GENERAL METHOD

CO ANALYZER (VOL %)	CO CONVERTED (VOL %)	INITIAL C(C0) (mol/m^3)	REMAINING C(CO) (mol/m^3)	GAS FLOW RATE (m^3/min)	GAS VELOCITY (m/min)	GAS VELOCITY (m/s)	CONTACT TIME (s)	CO CONVERSION (%)	SURFACE TEMP (deg C)	OUTLET TEMP (deg C)	SURFACE TEMP (K)	1/TEMP (1/K)	RATE CONSTANT K(s) (1/s)	LN(K(s)) (1/s)	RATE (mol CO/s m^3 CAT)
1.98	0.02	0.553	0.548	3.358E-03	18.042	0.301	1.862E-02	1.0	161.6	159.7	434.75	2.300E-03	0.037	-3.294	0.296
1.97	0.03	0.544	0.536	3.414E-03	18.341	0.306	1.832E-02	1.5	168.8	161.5	441.95	2.263E-03	0.057	-2.870	0.442
1.96	0.04	0.534	0.523	3.482E-03	18.706	0.312	1.796E-02	2.0	177.6	167.7	450.75	2.219E-03	0.077	-2.560	0.588
1.94	0.06	0.523	0.508	3.551E-03	19.080	0.318	1.761E-02	3.0	186.6	175.0	459.75	2.175E-03	0.119	-2.130	0.878
1.92	0.08	0.518	0.497	3.590E-03	19.287	0.321	1.742E-02	4.0	191.6	179.6	464.75	2.152E-03	0.161	-1.826	1.164
1.86	0.14	0.507	0.472	3.663E-03	19.677	0.328	1.708E-02	7.0	201.0	188.5	474.15	2.109E-03	0.292	-1.231	2.005
1.84	0.16	0.496	0.456	3.746E-03	20.126	0.335	1.670E-02	8.0	211.8	198.1	484.95	2.062E-03	0.343	-1.069	2.279
1.78	0.22	0.486	0.432	3.825E-03	20.549	0.342	1.635E-02	11.0	222.0	207.9	495.15	2.020E-03	0.490	-0.714	3.082

METHOD OF KOBERSTEIN & WANNEMACHER

CO ANALYZER (VOL %)	CO CONVERTED (VOL %)	INITIAL C(C0) (mol/m^3)	REMAINING C(CO) (mol/m^3)	GAS FLOW RATE (m^3/min)	GAS VELOCITY (m/min)	GAS VELOCITY (m/s)	CONTACT TIME (s)	CO CONVERSION (%)	SURFACE TEMP (deg C)	OUTLET TEMP (deg C)	SURFACE TEMP (K)	1/TEMP (1/K)	ADSORPTION RATE CONSTANT (1/mol% CO)	RATE CONSTANT K(s) (1/s)	LN(K(s)) (1/s)	RATE (mol CO/s m^3 CAT)
1.98	0.02	0.556	0.550	3.344E-03	17.963	0.299	1.870E-02	1.0	159.7	159.7	432.85	2.310E-03	30.697	11.931	2.479	0.298
1.97	0.03	0.544	0.536	3.414E-03	18.341	0.306	1.832E-02	1.5	168.8	161.5	441.95	2.263E-03	28.012	14.757	2.692	0.449
1.96	0.04	0.534	0.523	3.482E-03	18.706	0.312	1.796E-02	2.0	177.6	167.7	450.75	2.219E-03	25.729	16.463	2.801	0.599
1.94	0.06	0.523	0.508	3.551E-03	19.080	0.318	1.761E-02	3.0	186.6	175.0	459.75	2.175E-03	23.666	20.702	3.030	0.903
1.92	0.08	0.518	0.497	3.590E-03	19.287	0.321	1.742E-02	4.0	191.6	179.6	464.75	2.152E-03	22.624	25.064	3.221	1.209
1.86	0.14	0.507	0.472	3.663E-03	19.677	0.328	1.708E-02	7.0	201.0	188.5	474.15	2.109E-03	20.841	36.647	3.601	2.144
1.84	0.16	0.496	0.456	3.746E-03	20.126	0.335	1.670E-02	8.0	211.8	198.1	484.95	2.062E-03	19.040	34.766	3.549	2.459
1.78	0.22	0.486	0.432	3.825E-03	20.549	0.342	1.635E-02	11.0	222.0	207.9	495.15	2.020E-03	17.545	40.119	3.692	3.423

METHOD OF VOLTZ et al.

CO ANALYZER (VOL %)	CO CONVERTED (VOL %)	INITIAL C(C0) (mol/m^3)	REMAINING C(CO) (mol/m^3)	GAS FLOW RATE (m^3/min)	GAS VELOCITY (m/min)	GAS VELOCITY (m/s)	CONTACT TIME (s)	CO CONVERSION (%)	SURFACE TEMP (deg C)	OUTLET TEMP (deg C)	SURFACE TEMP (K)	1/TEMP (1/K)	ADSORPTION RATE CONSTANT (1/mol% CO)	RATE CONSTANT K(s) (1/s)	LN(K(s)) (1/s)	RATE (mol CO/s m^3 CAT)
1.98	0.02	0.556	0.550	3.344E-03	17.963	0.299	1.870E-02	1.0	159.7	159.7	432.85	2.310E-03	6.032	0.694	-0.365	0.298
1.97	0.03	0.544	0.536	3.414E-03	18.341	0.306	1.832E-02	1.5	168.8	161.5	441.95	2.263E-03	5.763	0.959	-0.042	0.447
1.96	0.04	0.534	0.523	3.482E-03	18.706	0.312	1.796E-02	2.0	177.6	167.7	450.75	2.219E-03	5.523	1.187	0.171	0.597
1.94	0.06	0.523	0.508	3.551E-03	19.080	0.318	1.761E-02	3.0	186.6	175.0	459.75	2.175E-03	5.297	1.654	0.503	0.898
1.92	0.08	0.518	0.497	3.590E-03	19.287	0.321	1.742E-02	4.0	191.6	179.6	464.75	2.152E-03	5.179	2.119	0.751	1.199
1.86	0.14	0.507	0.472	3.663E-03	19.677	0.328	1.708E-02	7.0	201.0	188.5	474.15	2.109E-03	4.971	3.443	1.236	2.112
1.84	0.16	0.496	0.456	3.746E-03	20.126	0.335	1.670E-02	8.0	211.8	198.1	484.95	2.062E-03	4.752	3.653	1.295	2.416
1.78	0.22	0.486	0.432	3.825E-03	20.549	0.342	1.635E-02	11.0	222.0	207.9	495.15	2.020E-03	4.562	4.685	1.544	3.336

TABLE L2 REACTOR DATA FOR FRESH COMMERCIAL STANDARD CATALYST CONTAINING 11 wt% CERIA [SMCOMM2].
MONOLITH MASS:0.7143g DIM:5.25*15.65*15.6mm WASH COAT 31 wt% TOTAL SURFACE AREA SUPPORT + WASH COAT: 14.55 m^2/g
GENERAL METHOD

CO ANALYZER (VOL %)	CO CONVERTED (VOL %)	INITIAL C(CO) (mol/m^3)	REMAINING C(CO) (mol/m^3)	GAS FLOW RATE (m^3/min)	GAS VELOCITY (m/min)	GAS VELOCITY (m/s)	CONTACT TIME (s)	CO CONVERSION (%)	SURFACE TEMP (deg C)	OUTLET TEMP (deg C)	SURFACE TEMP (K)	1/TEMP (1/K)	RATE CONSTANT E(s) (1/s)	LN(E(s)) (1/s)	RATE (mol CO/s m^3 CAT)
1.94	0.06	0.794	0.770	2.340E-03	12.613	0.210	2.497E-02	3.0	29.8	32.1	302.95	3.301E-03	0.084	-2.479	0.939
1.92	0.08	0.766	0.735	2.427E-03	13.079	0.218	2.408E-02	4.0	41.0	41.0	314.15	3.183E-03	0.116	-2.150	1.246
1.92	0.08	0.743	0.713	2.502E-03	13.487	0.225	2.334E-02	4.0	50.8	49.9	323.95	3.087E-03	0.120	-2.119	1.246
1.90	0.10	0.723	0.686	2.572E-03	13.862	0.231	2.272E-02	5.0	59.8	56.9	332.95	3.003E-03	0.155	-1.863	1.549
1.95	0.05	0.703	0.686	2.642E-03	14.236	0.237	2.213E-02	2.5	68.8	64.1	341.95	2.924E-03	0.079	-2.543	0.785
1.94	0.06	0.685	0.665	2.713E-03	14.619	0.244	2.155E-02	3.0	78.0	72.2	351.15	2.848E-03	0.097	-2.331	0.939
1.93	0.07	0.666	0.660	2.788E-03	15.027	0.250	2.096E-02	1.0	87.8	80.3	360.95	2.770E-03	0.033	-3.413	0.316
2.00	0.00	0.650	0.650	2.859E-03	15.410	0.257	2.044E-02	0.0	97.0	88.8	370.15	2.702E-03	0.000	0.000	0.000
2.00	0.00	0.633	0.633	2.934E-03	15.810	0.264	1.992E-02	0.0	106.6	97.5	379.75	2.633E-03	0.000	0.000	0.000
2.00	0.00	0.603	0.603	3.083E-03	16.618	0.277	1.896E-02	0.0	126.0	114.4	399.15	2.505E-03	0.000	0.000	0.000
2.00	0.00	0.582	0.582	3.193E-03	17.209	0.287	1.830E-02	0.0	140.2	127.1	413.35	2.419E-03	0.000	0.000	0.000
2.00	0.00	0.563	0.563	3.301E-03	17.792	0.297	1.770E-02	0.0	154.2	139.1	427.35	2.340E-03	0.000	0.000	0.000
1.98	0.02	0.550	0.544	3.360E-03	18.216	0.304	1.729E-02	1.0	164.4	148.5	437.55	2.285E-03	0.057	0.712	0.319
1.97	0.03	0.538	0.530	3.453E-03	18.608	0.310	1.693E-02	1.5	173.8	156.9	446.95	2.237E-03	0.084	0.584	0.479
1.94	0.06	0.527	0.511	3.527E-03	19.007	0.317	1.657E-02	3.0	183.4	163.5	456.55	2.190E-03	0.179	1.814	0.961
1.93	0.07	0.516	0.498	3.604E-03	19.424	0.324	1.622E-02	3.5	193.4	175.4	466.55	2.143E-03	0.216	1.969	1.122
1.91	0.09	0.505	0.482	3.680E-03	19.832	0.331	1.588E-02	4.5	203.2	185.0	476.35	2.099E-03	0.283	2.345	1.445
1.84	0.16	0.495	0.455	3.754E-03	20.232	0.337	1.557E-02	8.0	212.8	194.0	485.95	2.058E-03	0.513	3.637	2.565

METHOD OF KOBERSTEIN & WANNEMACHER

CO ANALYZER (VOL %)	CO CONVERTED (VOL %)	INITIAL C(CO) (mol/m^3)	REMAINING C(CO) (mol/m^3)	GAS FLOW RATE (m^3/min)	GAS VELOCITY (m/min)	GAS VELOCITY (m/s)	CONTACT TIME (s)	CO CONVERSION (%)	SURFACE TEMP (deg C)	OUTLET TEMP (deg C)	SURFACE TEMP (K)	1/TEMP (1/K)	ADSORPTION RATE CONSTANT (1/mol% CO)	RATE CONSTANT E(s) (1/s)	LN(E(s)) (1/s)	RATE (mol CO/s m^3 CAT)
1.94	0.06	0.794	0.770	2.340E-03	12.613	0.210	2.497E-02	3.0	29.8	32.1	302.95	3.301E-03	284.531	2214.227	7.703	0.968
1.92	0.08	0.766	0.735	2.427E-03	13.079	0.218	2.408E-02	4.0	41.0	41.0	314.15	3.183E-03	164.677	1807.677	7.500	1.298
1.92	0.08	0.745	0.715	2.496E-03	13.450	0.224	2.342E-02	4.0	49.9	49.9	323.05	3.095E-03	139.105	1258.689	7.138	1.298
1.90	0.10	0.723	0.686	2.572E-03	13.862	0.231	2.272E-02	5.0	59.8	56.9	332.95	3.003E-03	114.525	1078.645	6.976	1.631
1.95	0.05	0.703	0.686	2.642E-03	14.236	0.237	2.213E-02	2.5	68.8	64.1	341.95	2.924E-03	104.681	391.136	5.969	0.805
1.94	0.06	0.685	0.665	2.713E-03	14.619	0.244	2.155E-02	3.0	78.0	72.2	351.15	2.848E-03	86.362	341.340	5.833	0.968
1.98	0.02	0.666	0.660	2.788E-03	15.027	0.250	2.096E-02	1.0	87.8	80.3	360.95	2.770E-03	74.422	83.542	4.425	0.319
2.00	0.00	0.650	0.650	2.859E-03	15.410	0.257	2.044E-02	0.0	97.0	88.8	370.15	2.702E-03	65.186	0.000	0.000	0.000
2.00	0.00	0.633	0.633	2.934E-03	15.810	0.264	1.992E-02	0.0	106.6	97.5	379.75	2.633E-03	57.158	0.000	0.000	0.000
2.00	0.00	0.603	0.603	3.083E-03	16.618	0.277	1.896E-02	0.0	126.0	114.4	399.15	2.505E-03	44.630	0.000	0.000	0.000
2.00	0.00	0.582	0.582	3.193E-03	17.209	0.287	1.830E-02	0.0	140.2	127.1	413.35	2.419E-03	37.868	0.000	0.000	0.000
2.00	0.00	0.563	0.563	3.301E-03	17.792	0.297	1.770E-02	0.0	154.2	139.1	427.35	2.340E-03	32.505	0.000	0.000	0.000
1.98	0.02	0.550	0.544	3.360E-03	18.216	0.304	1.729E-02	1.0	164.4	148.5	437.55	2.285E-03	29.265	11.537	2.447	0.319
1.97	0.03	0.538	0.530	3.453E-03	18.608	0.310	1.693E-02	1.5	173.8	156.9	446.95	2.237E-03	26.680	14.274	2.658	0.480
1.94	0.06	0.527	0.511	3.527E-03	19.007	0.317	1.657E-02	3.0	183.4	163.5	456.55	2.190E-03	24.371	23.529	3.158	0.966
1.93	0.07	0.516	0.498	3.604E-03	19.424	0.324	1.622E-02	3.5	193.4	175.4	466.55	2.143E-03	22.265	22.764	3.125	1.130
1.91	0.09	0.505	0.482	3.680E-03	19.832	0.331	1.588E-02	4.5	203.2	185.0	476.35	2.099E-03	20.454	24.529	3.200	1.458
1.84	0.16	0.495	0.455	3.754E-03	20.232	0.337	1.557E-02	8.0	212.8	194.0	485.95	2.058E-03	18.883	36.599	3.600	2.631

METHOD OF VOLTZ et al.

CO ANALYZER (VOL %)	CO CONVERTED (VOL %)	INITIAL C(CO) (mol/m^3)	REMAINING C(CO) (mol/m^3)	GAS FLOW RATE (m^3/min)	GAS VELOCITY (m/min)	GAS VELOCITY (m/s)	CONTACT TIME (s)	CO CONVERSION (%)	SURFACE TEMP (deg C)	OUTLET TEMP (deg C)	SURFACE TEMP (K)	1/TEMP (1/K)	ADSORPTION RATE CONSTANT (1/mol% CO)	RATE CONSTANT E(s) (1/s)	LN(E(s)) (1/s)	RATE (mol CO/s m^3 CAT)
1.94	0.06	0.794	0.770	2.340E-03	12.613	0.210	2.497E-02	3.0	29.8	32.1	302.95	3.301E-03	15.628	14.656	2.685	0.966
1.92	0.08	0.766	0.735	2.427E-03	13.079	0.218	2.408E-02	4.0	41.0	41.0	314.15	3.183E-03	13.957	15.334	2.730	1.294
1.92	0.08	0.745	0.715	2.496E-03	13.450	0.224	2.342E-02	4.0	49.9	49.9	323.05	3.095E-03	12.829	12.860	2.554	1.293
1.90	0.10	0.723	0.686	2.572E-03	13.862	0.231	2.272E-02	5.0	59.8	56.9	332.95	3.003E-03	11.743	13.334	2.590	1.622
1.95	0.05	0.703	0.686	2.642E-03	14.236	0.237	2.213E-02	2.5	68.8	64.1	341.95	2.924E-03	10.684	5.763	1.752	0.803
1.94	0.06	0.685	0.665	2.713E-03	14.619	0.244	2.155E-02	3.0	78.0	72.2	351.15	2.848E-03	10.111	5.945	1.783	0.965
1.98	0.02	0.666	0.660	2.788E-03	15.027	0.250	2.096E-02	1.0	87.8	80.3	360.95	2.770E-03	9.387	1.720	0.542	0.319
2.00	0.00	0.650	0.650	2.859E-03	15.410	0.257	2.044E-02	0.0	97.0	88.8	370.15	2.702E-03	8.786	0.000	0.000	0.000
2.00	0.00	0.633	0.633	2.934E-03	15.810	0.264	1.992E-02	0.0	106.6	97.5	379.75	2.633E-03	8.228	0.000	0.000	0.000
2.00	0.00	0.603	0.603	3.083E-03	16.618	0.277	1.896E-02	0.0	126.0	114.4	399.15	2.505E-03	7.276	0.000	0.000	0.000
2.00	0.00	0.582	0.582	3.193E-03	17.209	0.287	1.830E-02	0.0	140.2	127.1	413.35	2.419E-03	6.698	0.000	0.000	0.000
2.00	0.00	0.563	0.563	3.301E-03	17.792	0.297	1.770E-02	0.0	154.2	139.1	427.35	2.340E-03	6.207	0.000	0.000	0.000
1.98	0.02	0.550	0.544	3.360E-03	18.216	0.304	1.729E-02	1.0	164.4	148.5	437.55	2.285E-03	5.890	0.712	-0.340	0.319
1.97	0.03	0.538	0.530	3.453E-03	18.608	0.310	1.693E-02	1.5	173.8	156.9	446.95	2.237E-03	5.624	0.584	-0.016	0.479
1.94	0.06	0.527	0.511	3.527E-03	19.007	0.317	1.657E-02	3.0	183.4	163.5	456.55	2.190E-03	5.375	1.814	0.596	0.961
1.93	0.07	0.516	0.498	3.604E-03	19.424	0.324	1.622E-02	3.5	193.4	175.4	466.55	2.143E-03	5.138	1.969	0.678	1.122
1.91	0.09	0.505	0.482	3.680E-03	19.832	0.331	1.588E-02	4.5	203.2	185.0	476.35	2.099E-03	4.925	2.345	0.852	1.445
1.84	0.16	0.495	0.455	3.754E-03	20.232	0.337	1.557E-02	8.0	212.8	194.0	485.95	2.058E-03	4.733	3.683	1.357	2.585

TABLE I.3 REACTOR DATA FOR COMMERCIAL POWDER CATALYST CONTAINING A 19 wt% WASH COAT AND 11 wt% CERIA [SM54].
MONOLITH MASS:0.6643g DIM:4.45*15.45*15.45cm TOTAL SURFACE AREA SUPPORT + WASH COAT: 17.97 m^2/g
GENERAL METHOD

CO ANALYZER (VOL %)	CO CONVERTED (VOL %)	INITIAL C(CO) (mol/m^3)	REMAINING C(CO) (mol/m^3)	GAS FLOW RATE (m^3/min)	GAS VELOCITY (m/min)	GAS VELOCITY (m/s)	CONTACT TIME (s)	CO CONVERSION (%)	SURFACE TEMP (deg C)	OUTLET TEMP (deg C)	SURFACE TEMP (K)	1/TEMP (1/K)	RATE CONSTANT K(s) (1/s)	LN(K(s)) (1/s)	RATE (mol CO/s m^3 CAT)
1.63	0.37	0.806	0.657	2.306E-03	12.390	0.206	2.349E-02	18.5	25.4	25.0	298.55	3.350E-03	0.485	-0.724	5.720
1.88	0.12	0.757	0.711	2.456E-03	13.195	0.220	2.205E-02	6.0	44.8	42.1	317.95	3.145E-03	0.156	-1.857	1.995
1.91	0.09	0.736	0.702	2.526E-03	13.573	0.226	2.144E-02	4.5	53.9	50.7	327.05	3.058E-03	0.120	-2.124	1.509
1.95	0.05	0.716	0.698	2.594E-03	13.938	0.232	2.048E-02	2.5	62.7	59.1	335.85	2.978E-03	0.067	-2.696	0.847
1.99	0.01	0.696	0.692	2.670E-03	14.344	0.239	2.029E-02	0.5	72.5	67.3	345.65	2.893E-03	0.014	-4.287	0.171
1.98	0.02	0.686	0.680	2.707E-03	14.544	0.242	2.001E-02	1.0	77.3	72.0	350.45	2.853E-03	0.028	-3.577	0.341
1.97	0.03	0.677	0.657	2.744E-03	14.743	0.246	1.974E-02	1.5	82.1	75.6	355.25	2.815E-03	0.043	-3.156	0.511
1.96	0.04	0.659	0.646	2.819E-03	15.145	0.252	1.921E-02	2.0	91.8	84.5	364.95	2.740E-03	0.059	-2.839	0.679
1.95	0.05	0.643	0.627	2.890E-03	15.527	0.259	1.874E-02	2.5	101.0	92.8	374.15	2.673E-03	0.075	-2.588	0.847
1.93	0.07	0.627	0.605	2.966E-03	15.934	0.266	1.826E-02	3.5	110.8	101.5	383.95	2.605E-03	0.109	-2.220	1.179
1.89	0.11	0.611	0.577	3.042E-03	16.341	0.272	1.781E-02	5.5	120.6	110.4	393.75	2.540E-03	0.177	-1.733	1.834
1.85	0.15	0.603	0.538	3.088E-03	16.588	0.276	1.759E-02	7.5	125.6	114.8	398.75	2.508E-03	0.247	-1.400	2.474
1.83	0.17	0.596	0.545	3.118E-03	16.751	0.279	1.737E-02	8.5	130.5	119.6	403.65	2.477E-03	0.283	-1.257	2.788
1.81	0.19	0.589	0.533	3.155E-03	16.951	0.283	1.717E-02	9.5	135.3	124.3	408.45	2.448E-03	0.324	-1.128	3.099
1.77	0.23	0.582	0.515	3.193E-03	17.154	0.286	1.696E-02	11.5	140.2	129.1	413.35	2.419E-03	0.401	-0.914	3.709
1.76	0.24	0.575	0.506	3.232E-03	17.366	0.289	1.676E-02	12.0	145.3	134.3	418.45	2.390E-03	0.425	-0.857	3.859
1.70	0.30	0.568	0.483	3.270E-03	17.565	0.293	1.657E-02	15.0	150.1	138.8	423.25	2.363E-03	0.546	-0.605	4.739
1.63	0.37	0.562	0.458	3.307E-03	17.764	0.296	1.638E-02	18.5	154.9	143.6	428.05	2.336E-03	0.695	-0.364	5.720
1.53	0.47	0.555	0.425	3.346E-03	17.976	0.300	1.619E-02	23.5	160.0	149.1	433.15	2.309E-03	0.921	-0.082	7.030

METHOD OF KOBERSTEIN & WANNEMACHER

CO ANALYZER (VOL %)	CO CONVERTED (VOL %)	INITIAL C(CO) (mol/m^3)	REMAINING C(CO) (mol/m^3)	GAS FLOW RATE (m^3/min)	GAS VELOCITY (m/min)	GAS VELOCITY (m/s)	CONTACT TIME (s)	CO CONVERSION (%)	SURFACE TEMP (deg C)	OUTLET TEMP (deg C)	SURFACE TEMP (K)	1/TEMP (1/K)	ADSORPTION RATE CONSTANT (1/mol% CO)	RATE CONSTANT K(s) (1/s)	LN(K(s)) (1/s)	RATE (mol CO/s m^3 CAT)
1.63	0.37	0.806	0.657	2.306E-03	12.390	0.206	2.349E-02	18.5	25.4	25.0	298.55	3.350E-03	226.800	1.344E+04	9.506	7.057
1.88	0.12	0.757	0.711	2.456E-03	13.195	0.220	2.205E-02	6.0	44.8	42.1	317.95	3.145E-03	153.052	2.004E+03	7.603	2.123
1.91	0.09	0.736	0.702	2.526E-03	13.573	0.226	2.144E-02	4.5	53.9	50.7	327.05	3.058E-03	129.331	1.455E+03	6.962	1.579
1.95	0.05	0.716	0.698	2.594E-03	13.938	0.232	2.048E-02	2.5	62.7	59.1	335.85	2.978E-03	110.452	4.255E+02	6.053	0.868
1.99	0.01	0.696	0.692	2.670E-03	14.344	0.239	2.029E-02	0.5	72.5	67.3	345.65	2.893E-03	94.230	6.065E+01	4.105	0.172
1.98	0.02	0.686	0.680	2.707E-03	14.544	0.242	2.001E-02	1.0	77.3	72.0	350.45	2.853E-03	87.312	1.028E+02	4.632	0.345
1.97	0.03	0.677	0.667	2.744E-03	14.743	0.246	1.974E-02	1.5	82.1	75.6	355.25	2.815E-03	81.068	1.312E+02	4.876	0.518
1.96	0.04	0.659	0.646	2.819E-03	15.145	0.252	1.921E-02	2.0	91.8	84.5	364.95	2.740E-03	70.198	1.282E+02	4.854	0.693
1.95	0.05	0.643	0.627	2.890E-03	15.527	0.259	1.874E-02	2.5	101.0	92.8	374.15	2.673E-03	61.662	1.212E+02	4.797	0.868
1.93	0.07	0.627	0.605	2.966E-03	15.934	0.266	1.826E-02	3.5	110.8	101.5	383.95	2.605E-03	54.075	1.276E+02	4.849	1.221
1.89	0.11	0.611	0.577	3.042E-03	16.341	0.272	1.781E-02	5.5	120.6	110.4	393.75	2.540E-03	47.734	1.523E+02	5.026	1.938
1.85	0.15	0.603	0.538	3.088E-03	16.588	0.276	1.759E-02	7.5	125.6	114.8	398.75	2.508E-03	44.896	1.887E+02	5.197	2.669
1.83	0.17	0.596	0.545	3.118E-03	16.751	0.279	1.737E-02	8.5	130.5	119.6	403.65	2.477E-03	42.342	1.800E+02	5.193	3.040
1.81	0.19	0.589	0.533	3.155E-03	16.951	0.283	1.717E-02	9.5	135.3	124.3	408.45	2.448E-03	40.035	1.779E+02	5.181	3.415
1.77	0.23	0.582	0.515	3.193E-03	17.154	0.286	1.696E-02	11.5	140.2	129.1	413.35	2.419E-03	37.860	1.896E+02	5.245	4.177
1.76	0.24	0.575	0.506	3.232E-03	17.366	0.289	1.676E-02	12.0	145.3	134.3	418.45	2.390E-03	35.772	1.752E+02	5.166	4.368
1.70	0.30	0.568	0.483	3.270E-03	17.565	0.293	1.657E-02	15.0	150.1	138.8	423.25	2.363E-03	33.954	1.936E+02	5.266	5.548
1.63	0.37	0.562	0.458	3.307E-03	17.764	0.296	1.638E-02	18.5	154.9	143.6	428.05	2.336E-03	32.266	2.110E+02	5.352	6.976
1.53	0.47	0.555	0.425	3.346E-03	17.976	0.300	1.619E-02	23.5	160.0	149.1	433.15	2.309E-03	30.603	2.343E+02	5.457	9.124

METHOD OF VOLTZ et al.

CO ANALYZER (VOL %)	CO CONVERTED (VOL %)	INITIAL C(CO) (mol/m^3)	REMAINING C(CO) (mol/m^3)	GAS FLOW RATE (m^3/min)	GAS VELOCITY (m/min)	GAS VELOCITY (m/s)	CONTACT TIME (s)	CO CONVERSION (%)	SURFACE TEMP (deg C)	OUTLET TEMP (deg C)	SURFACE TEMP (K)	1/TEMP (1/K)	ADSORPTION RATE CONSTANT (1/mol% CO)	RATE CONSTANT K(s) (1/s)	LN(K(s)) (1/s)	RATE (mol CO/s m^3 CAT)
1.63	0.37	0.806	0.657	2.306E-03	12.390	0.206	2.349E-02	18.5	25.4	25.0	298.55	3.350E-03	15.108	7.011E+01	4.250	6.936
1.88	0.12	0.757	0.711	2.456E-03	13.195	0.220	2.205E-02	6.0	44.8	42.1	317.95	3.145E-03	12.475	1.610E+01	2.779	2.111
1.91	0.09	0.736	0.702	2.526E-03	13.573	0.226	2.144E-02	4.5	53.9	50.7	327.05	3.058E-03	11.493	1.025E+01	2.328	1.572
1.95	0.05	0.716	0.698	2.594E-03	13.938	0.232	2.048E-02	2.5	62.7	59.1	335.85	2.978E-03	10.662	4.923E+00	1.594	0.866
1.99	0.01	0.696	0.692	2.670E-03	14.344	0.239	2.029E-02	0.5	72.5	67.3	345.65	2.893E-03	9.851	8.449E-01	-0.169	0.172
1.98	0.02	0.686	0.680	2.707E-03	14.544	0.242	2.001E-02	1.0	77.3	72.0	350.45	2.853E-03	9.492	1.565E+00	0.448	0.344
1.97	0.03	0.677	0.667	2.744E-03	14.743	0.246	1.974E-02	1.5	82.1	75.6	355.25	2.815E-03	9.153	2.180E+00	0.779	0.517
1.96	0.04	0.659	0.646	2.819E-03	15.145	0.252	1.921E-02	2.0	91.8	84.5	364.95	2.740E-03	8.536	2.526E+00	0.926	0.691
1.95	0.05	0.643	0.627	2.890E-03	15.527	0.259	1.874E-02	2.5	101.0	92.8	374.15	2.673E-03	8.013	2.786E+00	1.025	0.865
1.93	0.07	0.627	0.605	2.966E-03	15.934	0.266	1.826E-02	3.5	110.8	101.5	383.95	2.605E-03	7.517	3.437E+00	1.235	1.215
1.89	0.11	0.611	0.577	3.042E-03	16.341	0.272	1.781E-02	5.5	120.6	110.4	393.75	2.540E-03	7.074	4.784E+00	1.565	1.920
1.85	0.15	0.603	0.538	3.088E-03	16.588	0.276	1.759E-02	7.5	125.6	114.8	398.75	2.508E-03	6.866	6.133E+00	1.814	2.634
1.83	0.17	0.596	0.545	3.118E-03	16.751	0.279	1.737E-02	8.5	130.5	119.6	403.65	2.477E-03	6.673	6.574E+00	1.883	2.993
1.81	0.19	0.589	0.533	3.155E-03	16.951	0.283	1.717E-02	9.5	135.3	124.3	408.45	2.448E-03	6.494	6.969E+00	1.941	3.354
1.77	0.23	0.582	0.515	3.193E-03	17.154	0.286	1.696E-02	11.5	140.2	129.1	413.35	2.419E-03	6.319	7.945E+00	2.074	4.082
1.76	0.24	0.575	0.506	3.232E-03	17.366	0.289	1.676E-02	12.0	145.3	134.3	418.45	2.390E-03	6.147	7.919E+00	2.069	4.262
1.70	0.30	0.568	0.483	3.270E-03	17.565	0.293	1.657E-02	15.0	150.1	138.8	423.25	2.363E-03	5.993	9.346E+00	2.239	5.570
1.63	0.37	0.562	0.458	3.307E-03	17.764	0.296	1.638E-02	18.5	154.9	143.6	428.05	2.336E-03	5.846	1.094E+01	2.396	6.682
1.53	0.47	0.555	0.425	3.346E-03	17.976	0.300	1.619E-02	23.5	160.0	149.1	433.15	2.309E-03	5.697	1.317E+01	2.578	8.594

TABLE I.4 REACTOR DATA FOR COMMERCIAL POWDER CATALYST CONTAINING A 36 wt% WASH COAT AND 11 wt% CERIA [SM7].
MONOLITH MASS:0.8333g DIM:5.55*15.55*15.55mm TOTAL SURFACE AREA SUPPORT + WASH COAT: 31.36 m^2/g

GENERAL METHOD

CO ANALYZER (VOL %)	CO CONVERTED (VOL %)	INITIAL C(CO) (mol/m^3)	REMAINING C(CO) (mol/m^3)	GAS FLOW RATE (m^3/min)	GAS VELOCITY (m/min)	GAS VELOCITY (m/s)	CONTACT TIME (s)	CO CONVERSION (%)	SURFACE TEMP (deg C)	OUTLET TEMP (deg C)	SURFACE TEMP (K)	1/TEMP (1/K)	RATE CONSTANT K(s) (1/s)	LN(K(s)) (1/K)	RATE (mol CO/s m^3 CAT)
1.68	0.32	0.810	0.680	2.294E-03	12.482	0.208	2.668E-02	16.0	23.8	23.3	296.95	3.368E-03	0.208	-1.568	4.447
1.86	0.14	0.769	0.716	2.415E-03	13.142	0.219	2.534E-02	7.0	39.5	37.2	312.65	3.198E-03	0.091	-2.393	2.049
1.92	0.08	0.726	0.697	2.560E-03	13.928	0.232	2.391E-02	4.0	58.2	53.7	331.35	3.018E-03	0.054	-2.911	1.190
1.96	0.04	0.687	0.673	2.706E-03	14.723	0.245	2.262E-02	2.0	77.1	70.5	350.25	2.855E-03	0.028	-3.558	0.601
1.99	0.01	0.669	0.666	2.776E-03	15.105	0.252	2.205E-02	0.5	86.2	79.7	359.35	2.783E-03	0.007	-4.927	0.151
1.95	0.05	0.652	0.636	2.851E-03	15.513	0.259	2.147E-02	2.5	95.9	87.5	369.05	2.710E-03	0.038	-3.280	0.750
1.89	0.11	0.635	0.600	2.926E-03	15.921	0.265	2.092E-02	5.5	105.6	96.3	378.75	2.640E-03	0.086	-2.451	1.623
1.88	0.12	0.627	0.589	2.964E-03	16.131	0.269	2.064E-02	6.0	110.6	100.8	383.75	2.606E-03	0.096	-2.348	1.766
1.87	0.13	0.619	0.579	3.002E-03	16.337	0.272	2.038E-02	6.5	115.5	105.7	388.65	2.573E-03	0.105	-2.252	1.908
1.86	0.14	0.611	0.568	3.040E-03	16.543	0.276	2.013E-02	7.0	120.4	110.5	393.55	2.541E-03	0.115	-2.163	2.049
1.85	0.15	0.604	0.558	3.079E-03	16.753	0.279	1.988E-02	7.5	125.4	115.5	398.55	2.509E-03	0.125	-2.079	2.190
1.81	0.19	0.596	0.540	3.117E-03	16.959	0.283	1.964E-02	9.5	130.3	120.9	403.45	2.479E-03	0.162	-1.819	2.743
1.75	0.25	0.589	0.515	3.154E-03	17.165	0.286	1.940E-02	12.5	135.2	125.4	408.35	2.449E-03	0.219	-1.516	3.548
1.73	0.27	0.582	0.503	3.194E-03	17.380	0.290	1.916E-02	13.5	140.3	131.3	413.45	2.419E-03	0.241	-1.421	3.809
1.70	0.30	0.575	0.489	3.232E-03	17.590	0.293	1.893E-02	15.0	145.3	136.8	418.45	2.390E-03	0.274	-1.296	4.195
1.68	0.32	0.568	0.478	3.269E-03	17.787	0.296	1.872E-02	16.0	150.0	143.1	423.15	2.363E-03	0.297	-1.214	4.447

METHOD OF KOBERSTEIN & WANNEMACHER

CO ANALYZER (VOL %)	CO CONVERTED (VOL %)	INITIAL C(CO) (mol/m^3)	REMAINING C(CO) (mol/m^3)	GAS FLOW RATE (m^3/min)	GAS VELOCITY (m/min)	GAS VELOCITY (m/s)	CONTACT TIME (s)	CO CONVERSION (%)	SURFACE TEMP (deg C)	OUTLET TEMP (deg C)	SURFACE TEMP (K)	1/TEMP (1/K)	ADSORPTION RATE CONSTANT (1/mol% CO)	RATE CONSTANT K(s) (1/s)	LN(K(s)) (1/K)	RATE (mol CO/s m^3 CAT)
1.68	0.32	0.810	0.680	2.294E-03	12.482	0.208	2.668E-02	16.0	23.8	23.3	296.95	3.368E-03	234.815	6.440E+03	8.770	5.316
1.86	0.14	0.769	0.716	2.415E-03	13.142	0.219	2.534E-02	7.0	39.5	37.2	312.65	3.198E-03	169.589	1.471E+03	7.293	2.204
1.92	0.08	0.726	0.697	2.560E-03	13.928	0.232	2.391E-02	4.0	58.2	53.7	331.35	3.018E-03	119.823	4.050E+02	6.004	1.239
1.96	0.04	0.687	0.673	2.706E-03	14.723	0.245	2.262E-02	2.0	77.1	70.5	350.25	2.855E-03	87.586	1.044E+02	4.649	0.613
1.99	0.01	0.669	0.666	2.776E-03	15.105	0.252	2.205E-02	0.5	86.2	79.7	359.35	2.783E-03	76.210	1.952E+01	2.972	0.152
1.95	0.05	0.652	0.636	2.851E-03	15.513	0.259	2.147E-02	2.5	95.9	87.5	369.05	2.710E-03	66.204	7.154E+01	4.270	0.768
1.89	0.11	0.635	0.600	2.926E-03	15.921	0.265	2.092E-02	5.5	105.6	96.3	378.75	2.640E-03	57.928	1.166E+02	4.759	1.716
1.88	0.12	0.627	0.589	2.964E-03	16.131	0.269	2.064E-02	6.0	110.6	100.8	383.75	2.606E-03	54.217	1.102E+02	4.703	1.877
1.87	0.13	0.619	0.579	3.002E-03	16.337	0.272	2.038E-02	6.5	115.5	105.7	388.65	2.573E-03	50.895	1.041E+02	4.646	2.038
1.86	0.14	0.611	0.568	3.040E-03	16.543	0.276	2.013E-02	7.0	120.4	110.5	393.55	2.541E-03	47.852	9.815E+01	4.587	2.200
1.85	0.15	0.604	0.558	3.079E-03	16.753	0.279	1.988E-02	7.5	125.4	115.5	398.55	2.509E-03	45.005	9.212E+01	4.523	2.363
1.81	0.19	0.596	0.540	3.117E-03	16.959	0.283	1.964E-02	9.5	130.3	120.9	403.45	2.479E-03	42.442	1.021E+02	4.626	3.024
1.75	0.25	0.589	0.515	3.154E-03	17.165	0.286	1.940E-02	12.5	135.2	125.4	408.35	2.449E-03	40.081	1.173E+02	4.765	4.042
1.79	0.21	0.582	0.521	3.194E-03	17.380	0.290	1.916E-02	10.5	140.3	131.3	413.45	2.419E-03	37.817	8.804E+01	4.478	3.357
1.70	0.30	0.575	0.489	3.232E-03	17.590	0.293	1.893E-02	15.0	145.3	136.8	418.45	2.390E-03	35.772	1.095E+02	4.696	4.913
1.68	0.32	0.568	0.478	3.269E-03	17.787	0.296	1.872E-02	16.0	150.0	143.1	423.15	2.363E-03	33.990	1.044E+02	4.649	5.268

METHOD OF VOLTZ et al.

CO ANALYZER (VOL %)	CO CONVERTED (VOL %)	INITIAL C(CO) (mol/m^3)	REMAINING C(CO) (mol/m^3)	GAS FLOW RATE (m^3/min)	GAS VELOCITY (m/min)	GAS VELOCITY (m/s)	CONTACT TIME (s)	CO CONVERSION (%)	SURFACE TEMP (deg C)	OUTLET TEMP (deg C)	SURFACE TEMP (K)	1/TEMP (1/K)	ADSORPTION RATE CONSTANT (1/mol% CO)	RATE CONSTANT K(s) (1/s)	LN(K(s)) (1/K)	RATE (mol CO/s m^3 CAT)
1.68	0.32	0.810	0.680	2.294E-03	12.482	0.208	2.668E-02	16.0	23.8	23.3	296.95	3.368E-03	16.663	3.743E+01	3.622	5.247
1.86	0.14	0.769	0.716	2.415E-03	13.142	0.219	2.534E-02	7.0	39.5	37.2	312.65	3.198E-03	14.163	1.211E+01	2.494	2.191
1.92	0.08	0.726	0.697	2.560E-03	13.928	0.232	2.391E-02	4.0	58.2	53.7	331.35	3.018E-03	11.908	4.884E+00	1.586	1.235
1.96	0.04	0.687	0.673	2.706E-03	14.723	0.245	2.262E-02	2.0	77.1	70.5	350.25	2.855E-03	10.183	1.788E+00	0.581	0.612
1.99	0.01	0.669	0.666	2.776E-03	15.105	0.252	2.205E-02	0.5	86.2	79.7	359.35	2.783E-03	9.499	3.910E-01	-0.939	0.152
1.95	0.05	0.652	0.636	2.851E-03	15.513	0.259	2.147E-02	2.5	95.9	87.5	369.05	2.710E-03	8.854	1.688E+00	0.524	0.766
1.89	0.11	0.635	0.600	2.926E-03	15.921	0.265	2.092E-02	5.5	105.6	96.3	378.75	2.640E-03	8.283	3.225E+00	1.171	1.703
1.88	0.12	0.627	0.589	2.964E-03	16.131	0.269	2.064E-02	6.0	110.6	100.8	383.75	2.606E-03	8.014	3.295E+00	1.193	1.860
1.87	0.13	0.619	0.579	3.002E-03	16.337	0.272	2.038E-02	6.5	115.5	105.7	388.65	2.573E-03	7.765	3.355E+00	1.210	2.018
1.86	0.14	0.611	0.568	3.040E-03	16.543	0.276	2.013E-02	7.0	120.4	110.5	393.55	2.541E-03	7.529	3.402E+00	1.224	2.175
1.85	0.15	0.604	0.558	3.079E-03	16.753	0.279	1.988E-02	7.5	125.4	115.5	398.55	2.509E-03	7.302	3.435E+00	1.234	2.334
1.81	0.19	0.596	0.540	3.117E-03	16.959	0.283	1.964E-02	9.5	130.3	120.9	403.45	2.479E-03	7.091	4.094E+00	1.410	2.974
1.75	0.25	0.589	0.515	3.154E-03	17.165	0.286	1.940E-02	12.5	135.2	125.4	408.35	2.449E-03	6.892	5.063E+00	1.622	3.949
1.79	0.21	0.582	0.521	3.194E-03	17.380	0.290	1.916E-02	10.5	140.3	131.3	413.45	2.419E-03	6.694	4.058E+00	1.401	3.293
1.70	0.30	0.575	0.489	3.232E-03	17.590	0.293	1.893E-02	15.0	145.3	136.8	418.45	2.390E-03	6.511	5.439E+00	1.694	4.767
1.68	0.32	0.568	0.478	3.269E-03	17.787	0.296	1.872E-02	16.0	150.0	143.1	423.15	2.363E-03	6.347	5.528E+00	1.710	5.095

TABLE L5 REACTOR DATA FOR COMMERCIAL POWDER CATALYST CONTAINING A 58 wt% WASH COAT AND 11 wt% CERIA [SM5].
MONOLITH MASS:1.0457g DIM:5.65*15.75*15.65mm TOTAL SURFACE AREA SUPPORT + WASH COAT: 44.06 m^2/g

GENERAL METHOD

CO ANALYZER (VOL %)	CO CONVERTED (VOL %)	INITIAL C(CO) (mol/m^3)	REMAINING C(CO) (mol/m^3)	GAS FLOW RATE (m^3/min)	GAS VELOCITY (m/min)	GAS VELOCITY (m/s)	CONTACT TIME (s)	CO CONVERSION (%)	SURFACE TEMP (deg C)	OUTLET TEMP (deg C)	SURFACE TEMP (K)	1/TEMP (1/K)	RATE CONSTANT K(s) (1/s)	LN(K(s)) (1/s)	RATE (mol CO/s m^3 CAT)
1.62	0.38	0.804	0.652	2.310E-03	12.332	0.206	2.749E-02	19.0	25.9	25.6	299.05	3.344E-03	0.174	-1.749	4.995
1.78	0.22	0.767	0.682	2.424E-03	12.938	0.216	2.620E-02	11.0	40.6	39.0	313.75	3.187E-03	0.101	-2.293	3.035
1.94	0.06	0.687	0.666	2.705E-03	14.439	0.241	2.348E-02	3.0	77.0	69.9	350.15	2.856E-03	0.029	-3.525	0.865
1.95	0.05	0.652	0.636	2.849E-03	15.210	0.254	2.229E-02	2.5	95.7	87.1	368.85	2.711E-03	0.026	-3.658	0.722
1.98	0.02	0.643	0.637	2.889E-03	15.420	0.257	2.198E-02	1.0	100.8	91.3	373.95	2.674E-03	0.010	-4.568	0.291
1.98	0.02	0.627	0.621	2.963E-03	15.816	0.264	2.143E-02	1.0	110.4	100.4	383.55	2.607E-03	0.011	-4.543	0.291
1.96	0.04	0.619	0.607	3.001E-03	16.022	0.267	2.116E-02	2.0	115.4	105.1	388.55	2.574E-03	0.022	-3.832	0.579
1.95	0.05	0.611	0.596	3.040E-03	16.229	0.270	2.089E-02	2.5	120.4	109.9	393.55	2.541E-03	0.028	-3.593	0.722
1.89	0.11	0.604	0.571	3.078E-03	16.431	0.274	2.063E-02	5.5	125.3	115.1	398.45	2.510E-03	0.062	-2.777	1.564
1.88	0.12	0.596	0.560	3.117E-03	16.641	0.277	2.037E-02	6.0	130.4	120.2	403.55	2.478E-03	0.069	-2.675	1.702
1.87	0.13	0.589	0.551	3.154E-03	16.839	0.281	2.013E-02	6.5	135.2	125.1	408.35	2.449E-03	0.076	-2.580	1.839
1.81	0.19	0.582	0.527	3.193E-03	17.045	0.284	1.989E-02	9.5	140.2	130.5	413.35	2.419E-03	0.114	-2.172	2.643
1.76	0.24	0.575	0.506	3.232E-03	17.255	0.288	1.965E-02	12.0	145.3	136.3	418.45	2.390E-03	0.148	-1.913	3.292
1.64	0.36	0.568	0.466	3.270E-03	17.453	0.291	1.942E-02	18.0	150.1	141.6	423.25	2.363E-03	0.232	-1.461	4.762
1.61	0.39	0.562	0.452	3.308E-03	17.659	0.294	1.920E-02	19.5	155.1	148.1	428.25	2.335E-03	0.256	-1.361	5.110

METHOD OF KOBERSTEIN & WANNEMACHER

CO ANALYZER (VOL %)	CO CONVERTED (VOL %)	INITIAL C(CO) (mol/m^3)	REMAINING C(CO) (mol/m^3)	GAS FLOW RATE (m^3/min)	GAS VELOCITY (m/min)	GAS VELOCITY (m/s)	CONTACT TIME (s)	CO CONVERSION (%)	SURFACE TEMP (deg C)	OUTLET TEMP (deg C)	SURFACE TEMP (K)	1/TEMP (1/K)	ADSORPTION RATE CONSTANT (1/mol% CO)	RATE CONSTANT K(s) (1/s)	LN(K(s)) (1/s)	RATE (mol CO/s m^3 CAT)
1.62	0.38	0.804	0.652	2.310E-03	12.332	0.206	2.749E-02	19.0	25.9	25.6	299.05	3.344E-03	224.369	4.681E+03	8.451	6.203
1.78	0.22	0.767	0.682	2.424E-03	12.938	0.216	2.620E-02	11.0	40.6	39.0	313.75	3.187E-03	165.969	1.482E+03	7.301	3.414
1.94	0.06	0.687	0.666	2.705E-03	14.439	0.241	2.348E-02	3.0	77.0	69.9	350.15	2.856E-03	87.724	1.073E+02	4.675	0.891
1.95	0.05	0.652	0.636	2.849E-03	15.210	0.254	2.229E-02	2.5	95.7	87.1	368.85	2.711E-03	66.391	4.936E+01	3.899	0.740
1.98	0.02	0.643	0.637	2.889E-03	15.420	0.257	2.198E-02	1.0	100.8	91.3	373.95	2.674E-03	61.831	1.708E+01	2.838	0.294
1.98	0.02	0.627	0.621	2.963E-03	15.816	0.264	2.143E-02	1.0	110.4	100.4	383.55	2.607E-03	54.359	1.298E+01	2.563	0.294
1.96	0.04	0.619	0.607	3.001E-03	16.022	0.267	2.116E-02	2.0	115.4	105.1	388.55	2.574E-03	50.960	2.252E+01	3.114	0.591
1.95	0.05	0.611	0.596	3.040E-03	16.229	0.270	2.089E-02	2.5	120.4	109.9	393.55	2.541E-03	47.852	2.457E+01	3.201	0.740
1.89	0.11	0.604	0.571	3.078E-03	16.431	0.274	2.063E-02	5.5	125.3	115.1	398.45	2.510E-03	45.060	4.690E+01	3.848	1.653
1.88	0.12	0.596	0.560	3.117E-03	16.641	0.277	2.037E-02	6.0	130.4	120.2	403.55	2.478E-03	42.392	4.485E+01	3.803	1.807
1.87	0.13	0.589	0.551	3.154E-03	16.839	0.281	2.013E-02	6.5	135.2	125.1	408.35	2.449E-03	40.081	4.306E+01	3.763	1.962
1.81	0.19	0.582	0.527	3.193E-03	17.045	0.284	1.989E-02	9.5	140.2	130.5	413.35	2.419E-03	37.860	5.502E+01	4.008	2.912
1.76	0.24	0.575	0.506	3.232E-03	17.255	0.288	1.965E-02	12.0	145.3	136.3	418.45	2.390E-03	35.772	6.096E+01	4.110	3.726
1.64	0.36	0.568	0.466	3.270E-03	17.453	0.291	1.942E-02	18.0	150.1	141.6	423.25	2.363E-03	33.954	7.963E+01	4.377	5.777
1.61	0.39	0.562	0.452	3.308E-03	17.659	0.294	1.920E-02	19.5	155.1	148.1	428.25	2.335E-03	32.198	7.666E+01	4.339	6.309

METHOD OF VOLTZ et al.

CO ANALYZER (VOL %)	CO CONVERTED (VOL %)	INITIAL C(CO) (mol/m^3)	REMAINING C(CO) (mol/m^3)	GAS FLOW RATE (m^3/min)	GAS VELOCITY (m/min)	GAS VELOCITY (m/s)	CONTACT TIME (s)	CO CONVERSION (%)	SURFACE TEMP (deg C)	OUTLET TEMP (deg C)	SURFACE TEMP (K)	1/TEMP (1/K)	ADSORPTION RATE CONSTANT (1/mol% CO)	RATE CONSTANT K(s) (1/s)	LN(K(s)) (1/s)	RATE (mol CO/s m^3 CAT)
1.62	0.38	0.804	0.652	2.310E-03	12.332	0.206	2.749E-02	19.0	25.9	25.6	299.05	3.344E-03	15.029	2.472E+01	3.207	6.092
1.78	0.22	0.767	0.682	2.424E-03	12.938	0.216	2.620E-02	11.0	40.6	39.0	313.75	3.187E-03	12.977	1.091E+01	2.390	3.377
1.94	0.06	0.687	0.666	2.705E-03	14.439	0.241	2.348E-02	3.0	77.0	69.9	350.15	2.856E-03	9.514	1.629E+00	0.488	0.888
1.95	0.05	0.652	0.636	2.849E-03	15.210	0.254	2.229E-02	2.5	95.7	87.1	368.85	2.711E-03	8.307	1.040E+00	0.039	0.738
1.98	0.02	0.643	0.637	2.889E-03	15.420	0.257	2.198E-02	1.0	100.8	91.3	373.95	2.674E-03	8.024	3.907E-01	-0.940	0.294
1.98	0.02	0.627	0.621	2.963E-03	15.816	0.264	2.143E-02	1.0	110.4	100.4	383.55	2.607E-03	7.536	3.461E-01	-1.061	0.294
1.96	0.04	0.619	0.607	3.001E-03	16.022	0.267	2.116E-02	2.0	115.4	105.1	388.55	2.574E-03	7.303	6.499E-01	-0.431	0.589
1.95	0.05	0.611	0.596	3.040E-03	16.229	0.270	2.089E-02	2.5	120.4	109.9	393.55	2.541E-03	7.083	7.655E-01	-0.267	0.737
1.89	0.11	0.604	0.571	3.078E-03	16.431	0.274	2.063E-02	5.5	125.3	115.1	398.45	2.510E-03	6.878	1.579E+00	0.457	1.637
1.88	0.12	0.596	0.560	3.117E-03	16.641	0.277	2.037E-02	6.0	130.4	120.2	403.55	2.478E-03	6.677	1.628E+00	0.488	1.788
1.87	0.13	0.589	0.551	3.154E-03	16.839	0.281	2.013E-02	6.5	135.2	125.1	408.35	2.449E-03	6.497	1.675E+00	0.516	1.939
1.81	0.19	0.582	0.527	3.193E-03	17.045	0.284	1.989E-02	9.5	140.2	130.5	413.35	2.419E-03	6.319	2.308E+00	0.836	2.859
1.76	0.24	0.575	0.506	3.232E-03	17.255	0.288	1.965E-02	12.0	145.3	136.3	418.45	2.390E-03	6.147	2.755E+00	1.013	3.635
1.64	0.36	0.568	0.466	3.270E-03	17.453	0.291	1.942E-02	18.0	150.1	141.6	423.25	2.363E-03	5.993	3.886E+00	1.357	5.545
1.61	0.39	0.562	0.452	3.308E-03	17.659	0.294	1.920E-02	19.5	155.1	148.1	428.25	2.335E-03	5.840	4.008E+00	1.388	6.025

TABLE 1.6 REACTOR DATA FOR COADA CATALYST CONTAINING A 16 wt% WASH COAT AND 11 wt% CERIA [SM28].
MOMOLITH MASS:0.6419g DIM:4.8*15.8*15.75mm TOTAL SURFACE AREA SUPPORT + WASH COAT: 20.03 m^2/g
GENERAL METHOD

CO ANALYZER (VOL %)	CO CONVERTED (VOL %)	INITIAL C(C0) (mol/m^3)	REMAINING C(CO) (mol/m^3)	GAS FLOW RATE (m^3/min)	GAS VELOCITY (m/min)	GAS VELOCITY (m/s)	CONTACT TIME (s)	CO CONVERSION (%)	SURFACE TEMP (deg C)	OUTLET TEMP (deg C)	SURFACE TEMP (K)	1/TEMP (1/K)	RATE CONSTANT K(s) (1/s)	LN(K(s)) (1/s)	RATE (mol CO/s m^3 CAT)
1.81	0.19	0.776	0.702	2.395E-03	12.664	0.211	2.274E-02	9.5	36.9	35.5	310.05	3.225E-03	0.219	-1.518	3.082
1.99	0.01	0.696	0.692	2.670E-03	14.118	0.235	2.040E-02	0.5	72.5	67.0	345.65	2.893E-03	0.012	-4.401	0.170
2.00	0.00	0.652	0.652	2.852E-03	15.078	0.251	1.910E-02	0.0	96.0	88.1	369.15	2.709E-03	0.000	0.000	0.000
2.00	0.00	0.635	0.635	2.926E-03	15.470	0.258	1.862E-02	0.0	105.6	96.2	378.75	2.640E-03	0.000	0.000	0.000
1.99	0.01	0.619	0.616	3.001E-03	15.870	0.265	1.815E-02	0.5	115.4	104.9	388.55	2.574E-03	0.014	-4.284	0.170
1.98	0.02	0.604	0.598	3.077E-03	16.271	0.271	1.770E-02	1.0	125.2	114.0	398.35	2.510E-03	0.028	-3.563	0.339
1.94	0.06	0.590	0.572	3.152E-03	16.667	0.278	1.728E-02	3.0	134.9	123.3	408.05	2.451E-03	0.088	-2.430	1.008
1.92	0.08	0.582	0.559	3.191E-03	16.871	0.281	1.707E-02	4.0	139.9	128.1	413.05	2.421E-03	0.119	-2.125	1.337
1.89	0.11	0.576	0.544	3.229E-03	17.071	0.285	1.687E-02	5.5	144.8	132.9	417.95	2.393E-03	0.167	-1.787	1.824
1.85	0.15	0.569	0.526	3.267E-03	17.275	0.288	1.667E-02	7.5	149.8	138.2	422.95	2.364E-03	0.233	-1.455	2.460
1.83	0.17	0.563	0.515	3.304E-03	17.467	0.291	1.649E-02	8.5	154.5	143.3	427.65	2.338E-03	0.269	-1.313	2.773
1.77	0.23	0.556	0.492	3.342E-03	17.672	0.295	1.630E-02	11.5	159.5	148.9	432.65	2.311E-03	0.374	-0.983	3.689
1.71	0.29	0.550	0.470	3.381E-03	17.876	0.298	1.611E-02	14.5	164.5	154.1	437.65	2.285E-03	0.485	-0.723	4.570
1.64	0.36	0.544	0.446	3.419E-03	18.076	0.301	1.593E-02	18.0	169.4	159.7	442.55	2.260E-03	0.622	-0.475	5.552
1.58	0.42	0.538	0.425	3.456E-03	18.276	0.305	1.576E-02	21.0	174.3	165.2	447.45	2.235E-03	0.747	-0.292	6.353

METHOD OF KOBERSTEIN & WANNEMACHER

CO ANALYZER (VOL %)	CO CONVERTED (VOL %)	INITIAL C(C0) (mol/m^3)	REMAINING C(CO) (mol/m^3)	GAS FLOW RATE (m^3/min)	GAS VELOCITY (m/min)	GAS VELOCITY (m/s)	CONTACT TIME (s)	CO CONVERSION (%)	SURFACE TEMP (deg C)	OUTLET TEMP (deg C)	SURFACE TEMP (K)	1/TEMP (1/K)	ADSORPTION RATE CONSTANT (1/mol% CO)	RATE CONSTANT K(s) (1/s)	LN(K(s)) (1/s)	RATE (mol CO/s m^3 CAT)
1.81	0.19	0.776	0.702	2.395E-03	12.664	0.211	2.274E-02	9.5	36.9	35.5	310.05	3.225E-03	178.572	3.871E+03	8.261	3.408
1.99	0.01	0.696	0.692	2.670E-03	14.118	0.235	2.040E-02	0.5	72.5	67.0	345.65	2.893E-03	94.230	5.411E+01	3.991	0.171
2.00	0.00	0.652	0.652	2.852E-03	15.078	0.251	1.910E-02	0.0	96.0	88.1	369.15	2.709E-03	66.110	0.000E+00	0.000	0.000
2.00	0.00	0.635	0.635	2.926E-03	15.470	0.258	1.862E-02	0.0	105.6	96.2	378.75	2.640E-03	57.928	0.000E+00	0.000	0.000
1.99	0.01	0.619	0.616	3.001E-03	15.870	0.265	1.815E-02	0.5	115.4	104.9	388.55	2.574E-03	50.960	1.454E+01	2.677	0.171
1.98	0.02	0.604	0.598	3.077E-03	16.271	0.271	1.770E-02	1.0	125.2	114.0	398.35	2.510E-03	45.114	2.240E+01	3.109	0.343
1.94	0.06	0.590	0.572	3.152E-03	16.667	0.278	1.728E-02	3.0	134.9	123.3	408.05	2.451E-03	40.220	5.220E+01	3.955	1.038
1.92	0.08	0.582	0.559	3.191E-03	16.871	0.281	1.707E-02	4.0	139.9	128.1	413.05	2.421E-03	37.988	6.141E+01	4.118	1.391
1.89	0.11	0.576	0.544	3.229E-03	17.071	0.285	1.687E-02	5.5	144.8	132.9	417.95	2.393E-03	35.969	7.475E+01	4.314	1.926
1.85	0.15	0.569	0.526	3.267E-03	17.275	0.288	1.667E-02	7.5	149.8	138.2	422.95	2.364E-03	34.063	9.008E+01	4.501	2.652
1.83	0.17	0.563	0.515	3.304E-03	17.467	0.291	1.649E-02	8.5	154.5	143.3	427.65	2.338E-03	32.402	9.152E+01	4.517	3.019
1.77	0.23	0.556	0.492	3.342E-03	17.672	0.295	1.630E-02	11.5	159.5	148.9	432.65	2.311E-03	30.760	1.095E+02	4.696	4.147
1.71	0.29	0.550	0.470	3.381E-03	17.876	0.298	1.611E-02	14.5	164.5	154.1	437.65	2.285E-03	29.236	1.225E+02	4.808	5.310
1.64	0.36	0.544	0.446	3.419E-03	18.076	0.301	1.593E-02	18.0	169.4	159.7	442.55	2.260E-03	27.847	1.353E+02	4.907	6.715
1.58	0.42	0.538	0.425	3.456E-03	18.276	0.305	1.576E-02	21.0	174.3	165.2	447.45	2.235E-03	26.552	1.411E+02	4.949	7.963

METHOD OF VOLTZ et al.

CO ANALYZER (VOL %)	CO CONVERTED (VOL %)	INITIAL C(C0) (mol/m^3)	REMAINING C(CO) (mol/m^3)	GAS FLOW RATE (m^3/min)	GAS VELOCITY (m/min)	GAS VELOCITY (m/s)	CONTACT TIME (s)	CO CONVERSION (%)	SURFACE TEMP (deg C)	OUTLET TEMP (deg C)	SURFACE TEMP (K)	1/TEMP (1/K)	ADSORPTION RATE CONSTANT (1/mol% CO)	RATE CONSTANT K(s) (1/s)	LN(K(s)) (1/s)	RATE (mol CO/s m^3 CAT)
1.81	0.19	0.776	0.702	2.395E-03	12.664	0.211	2.274E-02	9.5	36.9	35.5	310.05	3.225E-03	14.533	3.018E+01	3.407	3.381
1.99	0.01	0.696	0.692	2.670E-03	14.118	0.235	2.040E-02	0.5	72.5	67.0	345.65	2.893E-03	10.561	8.516E-01	-0.161	0.171
2.00	0.00	0.652	0.652	2.852E-03	15.078	0.251	1.910E-02	0.0	96.0	88.1	369.15	2.709E-03	8.848	0.000E+00	0.000	0.000
2.00	0.00	0.635	0.635	2.926E-03	15.470	0.258	1.862E-02	0.0	105.6	96.2	378.75	2.640E-03	8.283	0.000E+00	0.000	0.000
1.99	0.01	0.619	0.616	3.001E-03	15.870	0.265	1.815E-02	0.5	115.4	104.9	388.55	2.574E-03	7.770	4.636E-01	-0.769	0.171
1.98	0.02	0.604	0.598	3.077E-03	16.271	0.271	1.770E-02	1.0	125.2	114.0	398.35	2.510E-03	7.311	8.244E-01	-0.193	0.342
1.94	0.06	0.590	0.572	3.152E-03	16.667	0.278	1.728E-02	3.0	134.9	123.3	408.05	2.451E-03	6.903	2.208E+00	0.792	1.033
1.92	0.08	0.582	0.559	3.191E-03	16.871	0.281	1.707E-02	4.0	139.9	128.1	413.05	2.421E-03	6.709	2.784E+00	1.024	1.381
1.89	0.11	0.576	0.544	3.229E-03	17.071	0.285	1.687E-02	5.5	144.8	132.9	417.95	2.393E-03	6.529	3.626E+00	1.288	1.907
1.85	0.15	0.569	0.526	3.267E-03	17.275	0.288	1.667E-02	7.5	149.8	138.2	422.95	2.364E-03	6.354	4.680E+00	1.543	2.615
1.83	0.17	0.563	0.515	3.304E-03	17.467	0.291	1.649E-02	8.5	154.5	143.3	427.65	2.338E-03	6.197	5.058E+00	1.621	2.971
1.77	0.23	0.556	0.492	3.342E-03	17.672	0.295	1.630E-02	11.5	159.5	148.9	432.65	2.311E-03	6.038	6.482E+00	1.869	4.051
1.71	0.29	0.550	0.470	3.381E-03	17.876	0.298	1.611E-02	14.5	164.5	154.1	437.65	2.285E-03	5.887	7.757E+00	2.049	5.147
1.64	0.36	0.544	0.446	3.419E-03	18.076	0.301	1.593E-02	18.0	169.4	159.7	442.55	2.260E-03	5.746	9.151E+00	2.214	6.443
1.58	0.42	0.538	0.425	3.456E-03	18.276	0.305	1.576E-02	21.0	174.3	165.2	447.45	2.235E-03	5.611	1.018E+01	2.320	7.566

TABLE L7 REACTOR DATA FOR COADA CATALYST CONTAINING A 22 wt% WASH COAT AND 11 wt% CERIA [SM19].
MONOLITH MASS: 0.7122 g DIM: 5.15*15.6*15.6mm TOTAL SURFACE AREA OF SUPPORT + WASH COAT: 27.38 m^2/g
GENERAL METHOD

CO ANALYZER (VOL %)	CO CONVERTED (VOL %)	INITIAL C(CO) (mol/m^3)	REMAINING C(CO) (mol/m^3)	GAS FLOW RATE (m^3/min)	GAS VELOCITY (m/min)	GAS VELOCITY (m/s)	CONTACT TIME (s)	CO CONVERSION (%)	SURFACE TEMP (deg C)	OUTLET TEMP (deg C)	SURFACE TEMP (K)	1/TEMP (1/K)	RATE CONSTANT K(s) (1/s)	LN(K(s)) (1/s)	RATE (mol CO/s m^3 CAT)
1.64	0.36	0.807	0.662	2.303E-03	12.453	0.208	2.481E-02	18.0	25.0	24.7	298.15	3.354E-03	0.292	-1.231	5.291
1.89	0.11	0.757	0.715	2.455E-03	13.275	0.221	2.328E-02	5.5	44.7	41.9	317.85	3.146E-03	0.089	-2.422	1.738
1.91	0.09	0.735	0.702	2.529E-03	13.672	0.228	2.260E-02	4.5	54.2	50.7	327.35	3.055E-03	0.074	-2.598	1.430
1.93	0.07	0.716	0.691	2.594E-03	14.027	0.234	2.203E-02	3.5	62.7	58.1	335.85	2.978E-03	0.059	-2.829	1.118
1.98	0.02	0.701	0.694	2.632E-03	14.336	0.239	2.155E-02	1.0	70.1	65.2	343.25	2.913E-03	0.017	-4.073	0.324
1.96	0.04	0.686	0.673	2.707E-03	14.637	0.244	2.111E-02	2.0	77.3	71.4	350.45	2.853E-03	0.035	-3.354	0.644
1.93	0.07	0.677	0.653	2.744E-03	14.837	0.247	2.083E-02	3.5	82.1	75.3	355.25	2.815E-03	0.062	-2.773	1.118
1.91	0.09	0.659	0.630	2.818E-03	15.238	0.254	2.028E-02	4.5	91.7	83.6	364.85	2.741E-03	0.083	-2.490	1.430
1.90	0.10	0.642	0.610	2.893E-03	15.644	0.261	1.975E-02	5.0	101.4	92.9	374.55	2.670E-03	0.095	-2.356	1.584
1.91	0.09	0.677	0.598	2.966E-03	16.036	0.267	1.927E-02	4.5	110.8	101.4	383.95	2.605E-03	0.087	-2.439	1.430
1.88	0.12	0.612	0.575	3.039E-03	16.429	0.274	1.881E-02	6.0	120.2	109.5	393.35	2.542E-03	0.120	-2.119	1.891
1.87	0.13	0.604	0.564	3.078E-03	16.642	0.277	1.857E-02	6.5	125.3	113.9	398.45	2.510E-03	0.132	-2.023	2.043
1.87	0.13	0.596	0.558	3.116E-03	16.846	0.281	1.834E-02	6.5	130.2	118.7	403.35	2.479E-03	0.134	-2.011	2.043
1.83	0.17	0.589	0.539	3.154E-03	17.051	0.284	1.812E-02	8.5	135.1	123.5	408.25	2.449E-03	0.179	-1.720	2.643
1.81	0.19	0.582	0.527	3.192E-03	17.260	0.288	1.790E-02	9.5	140.1	128.4	413.25	2.420E-03	0.204	-1.591	2.937
1.77	0.23	0.575	0.509	3.230E-03	17.465	0.291	1.769E-02	11.5	145.0	133.3	418.15	2.391E-03	0.252	-1.378	3.516
1.74	0.26	0.569	0.495	3.267E-03	17.665	0.294	1.749E-02	13.0	149.8	138.2	422.95	2.364E-03	0.291	-1.235	3.939
1.66	0.34	0.562	0.467	3.305E-03	17.870	0.298	1.729E-02	17.0	154.7	143.4	427.85	2.337E-03	0.394	-0.933	5.029
1.61	0.39	0.556	0.447	3.344E-03	18.079	0.301	1.709E-02	19.5	159.7	149.0	432.85	2.310E-03	0.464	-0.769	5.678
1.55	0.45	0.550	0.426	3.381E-03	18.279	0.305	1.690E-02	22.5	164.5	154.1	437.65	2.285E-03	0.551	-0.597	6.423

METHOD OF KOBERSTEIN & WANNEMACHER

CO ANALYZER (VOL %)	CO CONVERTED (VOL %)	INITIAL C(CO) (mol/m^3)	REMAINING C(CO) (mol/m^3)	GAS FLOW RATE (m^3/min)	GAS VELOCITY (m/min)	GAS VELOCITY (m/s)	CONTACT TIME (s)	CO CONVERSION (%)	SURFACE TEMP (deg C)	OUTLET TEMP (deg C)	SURFACE TEMP (K)	1/TEMP (1/K)	ADSORPTION RATE CONSTANT (1/mol% CO)	RATE CONSTANT K(s) (1/s)	LN(K(s)) (1/s)	RATE (mol CO/s m^3 CAT)
1.64	0.36	0.807	0.662	2.303E-03	12.139	0.202	2.545E-02	18.0	25.0	24.7	298.15	3.354E-03	228.779	8.103E+03	9.000	6.324
1.89	0.11	0.757	0.715	2.455E-03	12.941	0.216	2.348E-02	5.5	44.7	41.9	317.85	3.146E-03	153.344	1.122E+03	7.023	1.793
1.91	0.09	0.735	0.702	2.529E-03	13.328	0.222	2.316E-02	4.5	54.2	50.7	327.35	3.055E-03	128.635	6.327E+02	6.450	1.459
1.93	0.07	0.716	0.691	2.594E-03	13.674	0.228	2.260E-02	3.5	62.7	58.1	335.85	2.978E-03	110.852	3.594E+02	5.885	1.129
1.98	0.02	0.701	0.694	2.632E-03	13.976	0.233	2.211E-02	1.0	70.1	65.2	343.25	2.913E-03	97.971	7.977E+01	4.379	0.319
1.96	0.04	0.686	0.673	2.707E-03	14.269	0.238	2.166E-02	2.0	77.5	71.4	350.45	2.853E-03	87.312	1.240E+02	4.820	0.640
1.93	0.07	0.677	0.653	2.744E-03	14.464	0.241	2.136E-02	3.5	82.1	75.3	355.25	2.815E-03	81.968	1.834E+02	5.214	1.129
1.91	0.09	0.659	0.630	2.818E-03	14.855	0.248	2.080E-02	4.5	91.7	83.6	364.85	2.741E-03	70.299	1.733E+02	5.155	1.439
1.90	0.10	0.642	0.610	2.893E-03	15.250	0.254	2.026E-02	5.0	101.4	92.9	374.55	2.670E-03	61.524	1.435E+02	4.966	1.624
1.91	0.09	0.677	0.598	2.966E-03	15.633	0.261	1.977E-02	4.5	110.8	101.4	383.95	2.605E-03	54.876	8.902E+01	4.595	1.458
1.88	0.12	0.612	0.575	3.039E-03	16.015	0.267	1.929E-02	6.0	120.2	109.5	393.35	2.542E-03	47.972	1.016E+02	4.621	1.958
1.87	0.13	0.604	0.564	3.078E-03	16.223	0.270	1.905E-02	6.5	125.3	113.9	398.45	2.510E-03	43.050	9.615E+01	4.566	2.127
1.87	0.13	0.596	0.558	3.116E-03	16.423	0.274	1.882E-02	6.5	130.2	118.7	403.35	2.479E-03	42.492	8.492E+01	4.442	2.126
1.83	0.17	0.589	0.539	3.154E-03	16.622	0.277	1.859E-02	8.5	135.1	123.5	408.25	2.449E-03	40.127	9.747E+01	4.580	2.688
1.81	0.19	0.582	0.527	3.192E-03	16.826	0.280	1.836E-02	9.5	140.1	128.4	413.25	2.420E-03	37.903	9.614E+01	4.566	3.154
1.77	0.23	0.575	0.509	3.230E-03	17.023	0.284	1.815E-02	11.5	145.0	133.3	418.15	2.391E-03	35.890	1.028E+02	4.633	3.858
1.74	0.26	0.569	0.495	3.267E-03	17.221	0.287	1.794E-02	13.0	149.8	138.2	422.95	2.364E-03	34.043	1.034E+02	4.639	4.394
1.66	0.34	0.562	0.467	3.305E-03	17.420	0.290	1.774E-02	17.0	154.7	143.4	427.85	2.337E-03	32.334	1.190E+02	4.779	5.872
1.61	0.39	0.556	0.447	3.344E-03	17.624	0.294	1.753E-02	19.5	159.7	149.0	432.85	2.310E-03	30.697	1.210E+02	4.796	6.828
1.55	0.45	0.550	0.426	3.381E-03	17.819	0.297	1.734E-02	22.5	164.5	154.1	437.65	2.285E-03	29.236	1.244E+02	4.823	8.014

METHOD OF VOLTZ et al.

CO ANALYZER (VOL %)	CO CONVERTED (VOL %)	INITIAL C(CO) (mol/m^3)	REMAINING C(CO) (mol/m^3)	GAS FLOW RATE (m^3/min)	GAS VELOCITY (m/min)	GAS VELOCITY (m/s)	CONTACT TIME (s)	CO CONVERSION (%)	SURFACE TEMP (deg C)	OUTLET TEMP (deg C)	SURFACE TEMP (K)	1/TEMP (1/K)	ADSORPTION RATE CONSTANT (1/mol% CO)	RATE CONSTANT K(s) (1/s)	LN(K(s)) (1/s)	RATE (mol CO/s m^3 CAT)
1.64	0.36	0.807	0.662	2.303E-03	12.139	0.202	2.545E-02	18.0	25.0	24.7	298.15	3.354E-03	16.447	4.853E+01	3.882	6.227
1.89	0.11	0.757	0.715	2.455E-03	12.941	0.216	2.348E-02	5.5	44.7	41.9	317.85	3.146E-03	13.469	1.030E+01	2.332	1.785
1.91	0.09	0.735	0.702	2.529E-03	13.328	0.222	2.316E-02	4.5	54.2	50.7	327.35	3.055E-03	12.337	7.054E+00	1.954	1.453
1.93	0.07	0.716	0.691	2.594E-03	13.674	0.228	2.260E-02	3.5	62.7	58.1	335.85	2.978E-03	11.454	4.727E+00	1.553	1.125
1.98	0.02	0.701	0.694	2.632E-03	13.976	0.233	2.211E-02	1.0	70.1	65.2	343.25	2.913E-03	10.769	1.202E+00	0.184	0.318
1.96	0.04	0.686	0.673	2.707E-03	14.269	0.238	2.166E-02	2.0	77.3	71.4	350.45	2.853E-03	10.167	2.131E+00	0.757	0.639
1.93	0.07	0.677	0.653	2.744E-03	14.464	0.241	2.136E-02	3.5	82.1	75.3	355.25	2.815E-03	9.797	3.442E+00	1.236	1.124
1.91	0.09	0.659	0.630	2.818E-03	14.855	0.248	2.080E-02	4.5	91.7	83.6	364.85	2.741E-03	9.124	3.826E+00	1.342	1.450
1.90	0.10	0.642	0.610	2.893E-03	15.250	0.254	2.026E-02	5.0	101.4	92.9	374.55	2.670E-03	8.522	3.712E+00	1.311	1.613
1.91	0.09	0.677	0.598	2.966E-03	15.633	0.261	1.977E-02	4.5	110.8	101.4	383.95	2.605E-03	8.003	2.963E+00	1.086	1.448
1.88	0.12	0.612	0.575	3.039E-03	16.015	0.267	1.929E-02	6.0	120.2	109.5	393.35	2.542E-03	7.539	3.506E+00	1.255	1.948
1.87	0.13	0.604	0.564	3.078E-03	16.223	0.270	1.905E-02	6.5	125.3	113.9	398.45	2.510E-03	7.307	3.575E+00	1.274	2.104
1.87	0.13	0.596	0.558	3.116E-03	16.423	0.274	1.882E-02	6.5	130.2	118.7	403.35	2.479E-03	7.096	3.384E+00	1.219	2.103
1.83	0.17	0.589	0.539	3.154E-03	16.622	0.277	1.859E-02	8.5	135.1	123.5	408.25	2.449E-03	6.896	4.171E+00	1.428	2.767
1.81	0.19	0.582	0.527	3.192E-03	16.826	0.280	1.836E-02	9.5	140.1	128.4	413.25	2.420E-03	6.702	4.412E+00	1.484	3.100
1.77	0.23	0.575	0.509	3.230E-03	17.025	0.284	1.815E-02	11.5	145.0	133.3	418.15	2.391E-03	6.522	5.053E+00	1.620	3.773
1.74	0.26	0.569	0.495	3.267E-03	17.221	0.287	1.794E-02	13.0	149.8	138.2	422.95	2.364E-03	6.354	5.427E+00	1.691	4.282
1.66	0.34	0.562	0.467	3.305E-03	17.420	0.290	1.774E-02	17.0	154.7	143.4	427.85	2.337E-03	6.191	6.701E+00	1.902	5.661
1.61	0.39	0.556	0.447	3.344E-03	17.624	0.294	1.753E-02	19.5	159.7	149.0	432.85	2.310E-03	6.032	7.295E+00	1.987	6.532
1.55	0.45	0.550	0.426	3.381E-03	17.819	0.297	1.734E-02	22.5	164.5	154.1	437.65	2.285E-03	5.887	8.007E+00	2.080	7.590

TABLE L8 REACTOR DATA FOR COADA CATALYST CONTAINING A 38 wt% WASH COAT AND 11 wt% CERIA [SM21].
MONOLITH MASS:0.7882g DIM:5.25*15.65*15.65mm TOTAL SURFACE AREA SUPPORT + WASH COAT: 41.77 m^2/g
GENERAL METHOD

CO ANALYZER (VOL %)	CO CONVERTED (VOL %)	INITIAL C(CO) (mol/m^3)	REMAINING C(CO) (mol/m^3)	GAS FLOW RATE (m^3/min)	GAS VELOCITY (m/min)	GAS VELOCITY (m/s)	CONTACT TIME (s)	CO CONVERSION (%)	SURFACE TEMP (deg C)	OUTLET TEMP (deg C)	SURFACE TEMP (K)	1/TEMP (1/K)	RATE CONSTANT K(s) (1/s)	LN(K(s)) (1/s)	RATE (mol CO/s m^3 CAT)
1.68	0.32	0.805	0.676	2.309E-03	12.406	0.207	2.539E-02	16.0	25.8	25.5	298.95	3.345E-03	0.164	-1.805	4.642
1.89	0.11	0.747	0.706	2.488E-03	13.365	0.223	2.357E-02	5.5	48.9	46.2	322.05	3.105E-03	0.057	-2.857	1.694
1.99	0.01	0.696	0.693	2.669E-03	14.340	0.239	2.197E-02	0.5	72.4	66.5	345.55	2.894E-03	0.005	-5.210	0.158
1.99	0.01	0.651	0.648	2.855E-03	15.340	0.256	2.053E-02	0.5	96.5	87.8	369.65	2.705E-03	0.006	-5.142	0.158
1.98	0.02	0.635	0.629	2.926E-03	15.718	0.262	2.004E-02	1.0	105.6	96.8	378.75	2.640E-03	0.012	-4.422	0.315
1.97	0.03	0.627	0.617	2.966E-03	15.934	0.266	1.977E-02	1.5	110.8	101.8	383.95	2.605E-03	0.018	-4.001	0.472
1.97	0.03	0.619	0.609	3.004E-03	16.137	0.269	1.952E-02	1.5	115.7	106.6	388.85	2.572E-03	0.019	-3.988	0.472
1.95	0.05	0.611	0.596	3.041E-03	16.336	0.272	1.928E-02	2.5	120.5	111.3	393.65	2.540E-03	0.031	-3.460	0.782
1.93	0.07	0.603	0.582	3.080E-03	16.544	0.276	1.904E-02	3.5	125.5	116.0	398.65	2.508E-03	0.045	-3.106	1.090
1.92	0.08	0.596	0.572	3.117E-03	16.743	0.279	1.881E-02	4.0	130.3	121.0	403.45	2.479E-03	0.052	-2.958	1.242
1.86	0.14	0.589	0.548	3.154E-03	16.946	0.282	1.859E-02	7.0	135.2	126.3	408.35	2.449E-03	0.093	-2.370	2.139
1.85	0.15	0.582	0.538	3.194E-03	17.158	0.286	1.836E-02	7.5	140.3	131.5	413.45	2.419E-03	0.102	-2.286	2.285
1.81	0.19	0.575	0.520	3.232E-03	17.366	0.289	1.814E-02	9.5	145.3	136.8	418.45	2.390E-03	0.132	-2.027	2.863
1.81	0.19	0.568	0.514	3.270E-03	17.565	0.293	1.793E-02	9.5	150.1	140.6	423.25	2.363E-03	0.133	-2.015	2.863
1.69	0.31	0.562	0.475	3.307E-03	17.764	0.296	1.773E-02	15.5	154.9	147.9	428.05	2.336E-03	0.227	-1.481	4.510

METHOD OF KOBERSTEIN & WANNEMACHER

CO ANALYZER (VOL %)	CO CONVERTED (VOL %)	INITIAL C(CO) (mol/m^3)	REMAINING C(CO) (mol/m^3)	GAS FLOW RATE (m^3/min)	GAS VELOCITY (m/min)	GAS VELOCITY (m/s)	CONTACT TIME (s)	CO CONVERSION (%)	SURFACE TEMP (deg C)	OUTLET TEMP (deg C)	SURFACE TEMP (K)	1/TEMP (1/K)	ADSORPTION RATE CONSTANT (1/mol% CO)	RATE CONSTANT K(s) (1/s)	LN(K(s)) (1/s)	RATE (mol CO/s m^3 CAT)
1.68	0.32	0.805	0.676	2.309E-03	12.406	0.207	2.539E-02	16.0	25.8	25.5	298.95	3.345E-03	224.853	4.599E+03	8.433	5.547
1.89	0.11	0.747	0.706	2.488E-03	13.365	0.223	2.357E-02	5.5	48.9	46.2	322.05	3.105E-03	141.702	6.206E+02	6.431	1.793
1.99	0.01	0.696	0.693	2.669E-03	14.340	0.239	2.197E-02	0.5	72.4	66.5	345.55	2.894E-03	94.382	2.419E+01	3.186	0.159
1.99	0.01	0.651	0.648	2.855E-03	15.340	0.256	2.053E-02	0.5	96.5	87.8	369.65	2.705E-03	65.646	1.112E+01	2.408	0.159
1.98	0.02	0.635	0.629	2.926E-03	15.718	0.262	2.004E-02	1.0	105.6	96.8	378.75	2.640E-03	57.928	1.698E+01	2.832	0.318
1.97	0.03	0.627	0.617	2.966E-03	15.934	0.266	1.977E-02	1.5	110.8	101.8	383.95	2.605E-03	54.075	2.194E+01	3.088	0.479
1.97	0.03	0.619	0.609	3.004E-03	16.137	0.269	1.952E-02	1.5	115.7	106.6	388.85	2.572E-03	50.766	1.918E+01	2.954	0.479
1.95	0.05	0.611	0.596	3.041E-03	16.336	0.272	1.928E-02	2.5	120.5	111.3	393.65	2.540E-03	47.793	2.799E+01	3.332	0.802
1.93	0.07	0.603	0.582	3.080E-03	16.544	0.276	1.904E-02	3.5	125.5	116.0	398.65	2.508E-03	44.951	3.424E+01	3.534	1.128
1.92	0.08	0.596	0.572	3.117E-03	16.743	0.279	1.881E-02	4.0	130.3	121.0	403.45	2.479E-03	42.442	3.457E+01	3.543	1.292
1.86	0.14	0.589	0.548	3.154E-03	16.946	0.282	1.859E-02	7.0	135.2	126.3	408.35	2.449E-03	40.081	5.286E+01	3.968	2.295
1.85	0.15	0.582	0.538	3.194E-03	17.158	0.286	1.836E-02	7.5	140.3	131.5	413.45	2.419E-03	37.817	4.998E+01	3.912	2.464
1.81	0.19	0.575	0.520	3.232E-03	17.366	0.289	1.814E-02	9.5	145.3	136.8	418.45	2.390E-03	35.772	5.579E+01	4.022	3.153
1.81	0.19	0.568	0.514	3.270E-03	17.565	0.293	1.793E-02	9.5	150.1	140.6	423.25	2.363E-03	33.954	5.001E+01	3.912	3.152
1.69	0.31	0.562	0.475	3.307E-03	17.764	0.296	1.773E-02	15.5	154.9	147.9	428.05	2.336E-03	32.266	7.129E+01	4.267	5.308

METHOD OF VOLTZ et al.

CO ANALYZER (VOL %)	CO CONVERTED (VOL %)	INITIAL C(CO) (mol/m^3)	REMAINING C(CO) (mol/m^3)	GAS FLOW RATE (m^3/min)	GAS VELOCITY (m/min)	GAS VELOCITY (m/s)	CONTACT TIME (s)	CO CONVERSION (%)	SURFACE TEMP (deg C)	OUTLET TEMP (deg C)	SURFACE TEMP (K)	1/TEMP (1/K)	ADSORPTION RATE CONSTANT (1/mol% CO)	RATE CONSTANT K(s) (1/s)	LN(K(s)) (1/s)	RATE (mol CO/s m^3 CAT)
1.68	0.32	0.805	0.676	2.309E-03	12.406	0.207	2.539E-02	16.0	25.8	25.5	298.95	3.345E-03	16.306	2.802E+01	3.333	5.474
1.89	0.11	0.747	0.706	2.488E-03	13.365	0.223	2.357E-02	5.5	48.9	46.2	322.05	3.105E-03	12.948	6.220E+00	1.828	1.784
1.99	0.01	0.696	0.693	2.669E-03	14.340	0.239	2.197E-02	0.5	72.4	66.5	345.55	2.894E-03	10.570	3.800E-01	-0.968	0.159
1.99	0.01	0.651	0.648	2.855E-03	15.340	0.256	2.053E-02	0.5	96.5	87.8	369.65	2.705E-03	8.817	2.642E-01	-1.331	0.159
1.98	0.02	0.635	0.629	2.926E-03	15.718	0.262	2.004E-02	1.0	105.6	96.8	378.75	2.640E-03	8.283	4.667E-01	-0.762	0.318
1.97	0.03	0.627	0.617	2.966E-03	15.934	0.266	1.977E-02	1.5	110.8	101.8	383.95	2.605E-03	8.003	6.538E-01	-0.425	0.478
1.97	0.03	0.619	0.609	3.004E-03	16.137	0.269	1.952E-02	1.5	115.7	106.6	388.85	2.572E-03	7.755	6.153E-01	-0.486	0.478
1.95	0.05	0.611	0.596	3.041E-03	16.336	0.272	1.928E-02	2.5	120.5	111.3	393.65	2.540E-03	7.525	9.650E-01	-0.036	0.799
1.93	0.07	0.603	0.582	3.080E-03	16.544	0.276	1.904E-02	3.5	125.5	116.0	398.65	2.508E-03	7.298	1.271E+00	0.240	1.122
1.92	0.08	0.596	0.572	3.117E-03	16.743	0.279	1.881E-02	4.0	130.3	121.0	403.45	2.479E-03	7.091	1.374E+00	0.318	1.284
1.86	0.14	0.589	0.548	3.154E-03	16.946	0.282	1.859E-02	7.0	135.2	126.3	408.35	2.449E-03	6.892	2.259E+00	0.815	2.267
1.85	0.15	0.582	0.538	3.194E-03	17.158	0.286	1.836E-02	7.5	140.3	131.5	413.45	2.419E-03	6.694	2.292E+00	0.829	2.432
1.81	0.19	0.575	0.520	3.232E-03	17.366	0.289	1.814E-02	9.5	145.3	136.8	418.45	2.390E-03	6.511	2.744E+00	1.009	3.097
1.81	0.19	0.568	0.514	3.270E-03	17.565	0.293	1.793E-02	9.5	150.1	140.6	423.25	2.363E-03	6.344	2.618E+00	0.962	3.095
1.69	0.31	0.562	0.475	3.307E-03	17.764	0.296	1.773E-02	15.5	154.9	147.9	428.05	2.336E-03	6.184	4.014E+00	1.390	5.137

TABLE 19 REACTOR DATA FOR COADA CATALYST CONTAINING A 21 wt% WASH COAT AND 3 wt% CERIA [SM64].
MONOLITH MASS:0.64992g DIM:4.985*15.65*15.75mm TOTAL SURFACE AREA SUPPORT + WASH COAT: 25.59 m^2/g
GENERAL METHOD

CO ANALYZER (VOL %)	CO CONVERTED (VOL %)	INITIAL C(CO) (mol/m^3)	REMAINING C(CO) (mol/m^3)	GAS FLOW RATE (m^3/min)	GAS VELOCITY (m/min)	GAS VELOCITY (m/s)	CONTACT TIME (s)	CO CONVERSION (%)	SURFACE TEMP (deg C)	OUTLET TEMP (deg C)	SURFACE TEMP (K)	1/TEMP (1/K)	RATE CONSTANT K(s) (1/s)	LN(K(s)) (1/s)	RATE (mol CO/s m^3 CAT)
1.69	0.31	0.770	0.651	2.414E-03	12.884	0.215	2.321E-02	15.5	39.3	37.6	312.45	3.201E-03	0.284	-1.261	4.720
1.88	0.12	0.726	0.682	2.561E-03	13.672	0.228	2.188E-02	6.0	58.4	54.5	331.55	3.016E-03	0.111	-2.203	1.929
1.98	0.02	0.687	0.680	2.706E-03	14.447	0.241	2.070E-02	1.0	77.2	71.1	350.35	2.854E-03	0.019	-3.965	0.330
2.00	0.00	0.669	0.669	2.778E-03	14.831	0.247	2.017E-02	0.0	86.5	79.3	359.65	2.780E-03	0.000	0.000	0.000
1.98	0.02	0.651	0.645	2.852E-03	15.227	0.254	1.964E-02	1.0	96.1	88.0	369.25	2.708E-03	0.020	-3.912	0.330
2.00	0.00	0.635	0.635	2.925E-03	15.614	0.260	1.916E-02	0.0	105.5	96.5	378.65	2.641E-03	0.000	0.000	0.000
1.99	0.01	0.627	0.624	2.964E-03	15.824	0.264	1.890E-02	0.5	110.6	100.9	383.75	2.606E-03	0.010	-4.569	0.165
1.98	0.02	0.619	0.613	3.002E-03	16.027	0.267	1.866E-02	1.0	115.5	105.2	388.65	2.573E-03	0.021	-3.861	0.330
1.97	0.03	0.611	0.602	3.040E-03	16.229	0.270	1.843E-02	1.5	120.4	109.7	393.55	2.541E-03	0.032	-3.441	0.494
1.95	0.05	0.604	0.589	3.077E-03	16.427	0.274	1.821E-02	2.5	125.2	114.2	398.35	2.510E-03	0.054	-2.913	0.819
1.94	0.06	0.597	0.579	3.114E-03	16.624	0.277	1.799E-02	3.0	130.0	118.7	403.15	2.480E-03	0.066	-2.716	0.980
1.88	0.12	0.582	0.547	3.192E-03	17.041	0.284	1.755E-02	6.0	140.1	123.6	413.25	2.420E-03	0.138	-1.982	1.929
1.86	0.14	0.569	0.529	3.266E-03	17.433	0.291	1.716E-02	7.0	149.6	137.3	422.75	2.365E-03	0.165	-1.800	2.238
1.77	0.23	0.556	0.492	3.340E-03	17.829	0.297	1.678E-02	11.5	159.2	146.3	432.35	2.313E-03	0.285	-1.257	3.586
1.68	0.32	0.544	0.457	3.416E-03	18.233	0.304	1.640E-02	16.0	169.0	154.9	442.15	2.262E-03	0.415	-0.879	4.857
1.62	0.38	0.538	0.436	3.453E-03	18.431	0.307	1.623E-02	19.0	173.8	159.0	446.95	2.237E-03	0.507	-0.678	5.661
1.56	0.44	0.532	0.415	3.490E-03	18.633	0.311	1.605E-02	22.0	178.7	163.6	451.85	2.213E-03	0.605	-0.503	6.427

METHOD OF KOBERSTEIN & WANNEMACHER

CO ANALYZER (VOL %)	CO CONVERTED (VOL %)	INITIAL C(CO) (mol/m^3)	REMAINING C(CO) (mol/m^3)	GAS FLOW RATE (m^3/min)	GAS VELOCITY (m/min)	GAS VELOCITY (m/s)	CONTACT TIME (s)	CO CONVERSION (%)	SURFACE TEMP (deg C)	OUTLET TEMP (deg C)	SURFACE TEMP (K)	1/TEMP (1/K)	ADSORPTION RATE CONSTANT (1/mol% CO)	RATE CONSTANT K(s) (1/s)	LN(K(s)) (1/s)	RATE (mol CO/s m^3 CAT)
1.69	0.31	0.770	0.651	2.414E-03	12.884	0.215	2.321E-02	15.5	39.3	37.6	312.45	3.201E-03	170.258	4.205E+03	8.344	5.604
1.88	0.12	0.726	0.682	2.561E-03	13.672	0.228	2.188E-02	6.0	58.4	54.5	331.55	3.016E-03	119.404	7.989E+02	6.683	2.052
1.98	0.02	0.687	0.680	2.706E-03	14.447	0.241	2.070E-02	1.0	77.2	71.1	350.35	2.854E-03	87.449	7.000E+01	4.248	0.333
2.00	0.00	0.669	0.669	2.778E-03	14.831	0.247	2.017E-02	0.0	86.5	79.3	359.65	2.780E-03	75.870	0.000E+00	0.000	0.000
1.98	0.02	0.651	0.645	2.852E-03	15.227	0.254	1.964E-02	1.0	96.1	88.0	369.25	2.708E-03	66.017	3.835E+01	3.647	0.333
2.00	0.00	0.635	0.635	2.925E-03	15.614	0.260	1.916E-02	0.0	105.5	96.5	378.65	2.641E-03	58.005	0.000E+00	0.000	0.000
1.99	0.01	0.627	0.624	2.964E-03	15.824	0.264	1.890E-02	0.5	110.6	100.9	383.75	2.606E-03	54.217	1.262E+01	2.536	0.166
1.98	0.02	0.619	0.613	3.002E-03	16.027	0.267	1.866E-02	1.0	115.5	105.2	388.65	2.573E-03	50.895	2.202E+01	3.092	0.333
1.97	0.03	0.611	0.602	3.040E-03	16.229	0.270	1.843E-02	1.5	120.4	109.7	393.55	2.541E-03	47.852	2.890E+01	3.364	0.501
1.95	0.05	0.604	0.589	3.077E-03	16.427	0.274	1.821E-02	2.5	125.2	114.2	398.35	2.510E-03	45.114	4.230E+01	3.745	0.839
1.94	0.06	0.597	0.579	3.114E-03	16.624	0.277	1.799E-02	3.0	130.0	118.7	403.15	2.480E-03	42.593	4.484E+01	3.803	1.009
1.88	0.12	0.582	0.547	3.192E-03	17.041	0.284	1.755E-02	6.0	140.1	123.6	413.25	2.420E-03	37.903	6.911E+01	4.236	2.048
1.86	0.14	0.569	0.529	3.266E-03	17.433	0.291	1.716E-02	7.0	149.6	137.3	422.75	2.365E-03	34.137	6.441E+01	4.165	2.400
1.77	0.23	0.556	0.492	3.340E-03	17.829	0.297	1.678E-02	11.5	159.2	146.3	432.35	2.313E-03	30.855	8.389E+01	4.430	4.031
1.68	0.32	0.544	0.457	3.416E-03	18.233	0.304	1.640E-02	16.0	169.0	154.9	442.15	2.262E-03	27.956	9.313E+01	4.534	5.739
1.62	0.38	0.538	0.436	3.453E-03	18.431	0.307	1.623E-02	19.0	173.8	159.0	446.95	2.237E-03	26.680	9.902E+01	4.595	6.924
1.56	0.44	0.532	0.415	3.490E-03	18.633	0.311	1.605E-02	22.0	178.7	163.6	451.85	2.213E-03	25.463	1.027E+02	4.632	8.149

METHOD OF VOLTZ et al.

CO ANALYZER (VOL %)	CO CONVERTED (VOL %)	INITIAL C(CO) (mol/m^3)	REMAINING C(CO) (mol/m^3)	GAS FLOW RATE (m^3/min)	GAS VELOCITY (m/min)	GAS VELOCITY (m/s)	CONTACT TIME (s)	CO CONVERSION (%)	SURFACE TEMP (deg C)	OUTLET TEMP (deg C)	SURFACE TEMP (K)	1/TEMP (1/K)	ADSORPTION RATE CONSTANT (1/mol% CO)	RATE CONSTANT K(s) (1/s)	LN(K(s)) (1/s)	RATE (mol CO/s m^3 CAT)
1.69	0.31	0.770	0.651	2.414E-03	12.884	0.215	2.321E-02	15.5	39.3	37.6	312.45	3.201E-03	14.191	3.472E+01	3.547	5.520
1.88	0.12	0.726	0.682	2.561E-03	13.672	0.228	2.188E-02	6.0	58.4	54.5	331.55	3.016E-03	11.887	9.692E+00	2.271	2.040
1.98	0.02	0.687	0.680	2.706E-03	14.447	0.241	2.070E-02	1.0	77.2	71.1	350.35	2.854E-03	10.175	1.199E+00	0.182	0.333
2.00	0.00	0.669	0.669	2.778E-03	14.831	0.247	2.017E-02	0.0	86.5	79.3	359.65	2.780E-03	9.478	0.000E+00	0.000	0.000
1.98	0.02	0.651	0.645	2.852E-03	15.227	0.254	1.964E-02	1.0	96.1	88.0	369.25	2.708E-03	8.842	9.060E-01	-0.099	0.333
2.00	0.00	0.635	0.635	2.925E-03	15.614	0.260	1.916E-02	0.0	105.5	96.5	378.65	2.641E-03	8.289	0.000E+00	0.000	0.000
1.99	0.01	0.627	0.624	2.964E-03	15.824	0.264	1.890E-02	0.5	110.6	100.9	383.75	2.606E-03	8.014	3.744E-01	-0.982	0.166
1.98	0.02	0.619	0.613	3.002E-03	16.027	0.267	1.866E-02	1.0	115.5	105.2	388.65	2.573E-03	7.765	7.035E-01	-0.352	0.333
1.97	0.03	0.611	0.602	3.040E-03	16.229	0.270	1.843E-02	1.5	120.4	109.7	393.55	2.541E-03	7.529	9.934E-01	-0.007	0.500
1.95	0.05	0.604	0.589	3.077E-03	16.427	0.274	1.821E-02	2.5	125.2	114.2	398.35	2.510E-03	7.311	1.561E+00	0.445	0.836
1.94	0.06	0.597	0.579	3.114E-03	16.624	0.277	1.799E-02	3.0	130.0	118.7	403.15	2.480E-03	7.104	1.772E+00	0.572	1.004
1.88	0.12	0.582	0.547	3.192E-03	17.041	0.284	1.755E-02	6.0	140.1	123.6	413.25	2.420E-03	6.702	3.152E+00	1.148	2.026
1.86	0.14	0.569	0.529	3.266E-03	17.433	0.291	1.716E-02	7.0	149.6	137.3	422.75	2.365E-03	6.361	3.335E+00	1.204	2.369
1.77	0.23	0.556	0.492	3.340E-03	17.829	0.297	1.678E-02	11.5	159.2	146.3	432.35	2.313E-03	6.048	4.946E+00	1.599	3.938
1.68	0.32	0.544	0.457	3.416E-03	18.233	0.304	1.640E-02	16.0	169.0	154.9	442.15	2.262E-03	5.757	6.243E+00	1.831	5.538
1.62	0.38	0.538	0.436	3.453E-03	18.431	0.307	1.623E-02	19.0	173.8	159.0	446.95	2.237E-03	5.624	7.071E+00	1.956	6.621
1.56	0.44	0.532	0.415	3.490E-03	18.633	0.311	1.605E-02	22.0	178.7	163.6	451.85	2.213E-03	5.494	7.816E+00	2.056	7.713

TABLE L10 REACTOR DATA FOR COADA CATALYST CONTAINING A 21 wt% WASH COAT AND 3 wt% CERIA BUILT INTO THE STRUCTURE [SM37].
MONOLITH MASS: 0.6292g DIM: 4.96" 15.65" 13.65cm³ TOTAL SURFACE AREA SUPPORT + WASH COAT: 28.70 m^2/g

GENERAL METHOD

CO ANALYZER (VOL %)	CO CONVERTED (VOL %)	INITIAL C(CO) (mol/m^3)	REMAINING C(CO) (mol/m^3)	GAS FLOW RATE (m^3/min)	GAS VELOCITY (m/min)	GAS VELOCITY (m/s)	CONTACT TIME (s)	CO CONVERSION (%)	SURFACE TEMP (deg C)	OUTLET TEMP (deg C)	SURFACE TEMP (K)	1/TEMP (1/K)	RATE CONSTANT K(s) (1/s)	LN(K(s)) (1/K)	RATE (mol CO/s m^3 CAT)
1.66	0.34	0.808	0.671	2.299E-03	12.348	0.206	2.419E-02	17.0	24.4	24.1	297.55	3.361E-03	0.269	-1.312	5.188
1.84	0.16	0.769	0.707	2.417E-03	12.983	0.216	2.292E-02	8.0	39.7	37.7	312.85	3.196E-03	0.127	-2.056	2.573
1.92	0.08	0.726	0.697	2.560E-03	13.751	0.229	2.164E-02	4.0	58.2	54.2	331.35	3.018E-03	0.066	-2.722	1.315
2.00	0.00	0.705	0.705	2.635E-03	14.154	0.236	2.103E-02	0.0	67.9	62.3	341.05	2.932E-03	0.000	0.000	0.000
2.00	0.00	0.686	0.686	2.707E-03	14.544	0.242	2.046E-02	0.0	77.3	71.3	350.45	2.853E-03	0.000	0.000	0.000
1.96	0.04	0.668	0.655	2.781E-03	14.938	0.249	1.992E-02	2.0	86.8	79.7	359.95	2.778E-03	0.035	-3.343	0.664
1.96	0.04	0.659	0.646	2.819E-03	15.145	0.252	1.965E-02	2.0	91.8	84.1	364.95	2.740E-03	0.036	-3.329	0.664
1.98	0.02	0.651	0.644	2.835E-03	15.336	0.256	1.940E-02	1.0	96.4	88.6	369.53	2.706E-03	0.018	-4.015	0.334
1.96	0.04	0.634	0.622	2.929E-03	15.735	0.262	1.891E-02	2.0	106.0	97.3	379.15	2.637E-03	0.037	-3.291	0.664
1.92	0.08	0.626	0.601	2.967E-03	15.938	0.266	1.867E-02	4.0	110.9	101.6	384.05	2.604E-03	0.076	-2.575	1.315
1.91	0.09	0.619	0.591	3.003E-03	16.133	0.269	1.845E-02	4.5	115.6	105.8	388.75	2.572E-03	0.087	-2.442	1.475
1.90	0.10	0.604	0.573	3.079E-03	16.540	0.276	1.799E-02	5.0	125.4	114.7	398.53	2.509E-03	0.099	-2.309	1.635
1.90	0.10	0.596	0.567	3.116E-03	16.739	0.279	1.778E-02	5.0	130.2	119.1	403.33	2.479E-03	0.101	-2.297	1.635
1.87	0.13	0.589	0.551	3.154E-03	16.946	0.282	1.756E-02	6.5	135.2	123.7	408.35	2.449E-03	0.133	-2.015	2.108
1.84	0.16	0.582	0.536	3.192E-03	17.150	0.286	1.735E-02	8.0	140.1	128.1	413.25	2.420E-03	0.167	-1.787	2.573
1.79	0.21	0.575	0.515	3.230E-03	17.353	0.289	1.715E-02	10.5	145.0	132.5	418.15	2.391E-03	0.225	-1.490	3.331
1.76	0.24	0.569	0.501	3.267E-03	17.552	0.293	1.695E-02	12.0	149.8	136.9	422.95	2.364E-03	0.263	-1.337	3.774
1.75	0.25	0.562	0.492	3.305E-03	17.756	0.296	1.676E-02	12.5	154.7	141.4	427.85	2.337E-03	0.278	-1.282	3.919
1.74	0.26	0.556	0.484	3.342E-03	17.953	0.299	1.657E-02	13.0	159.5	145.7	432.65	2.311E-03	0.293	-1.228	4.064
1.69	0.31	0.550	0.465	3.380E-03	18.158	0.303	1.639E-02	15.5	164.4	150.1	437.55	2.285E-03	0.358	-1.027	4.774
1.66	0.34	0.544	0.451	3.417E-03	18.357	0.306	1.621E-02	17.0	169.2	154.6	442.35	2.261E-03	0.400	-0.915	5.188
1.62	0.38	0.538	0.436	3.455E-03	18.561	0.309	1.603E-02	19.0	174.1	159.1	447.25	2.236E-03	0.458	-0.781	5.726

METHOD OF KOBERSTEIN & WANNEMACHER

CO ANALYZER (VOL %)	CO CONVERTED (VOL %)	INITIAL C(CO) (mol/m^3)	REMAINING C(CO) (mol/m^3)	GAS FLOW RATE (m^3/min)	GAS VELOCITY (m/min)	GAS VELOCITY (m/s)	CONTACT TIME (s)	CO CONVERSION (%)	SURFACE TEMP (deg C)	OUTLET TEMP (deg C)	SURFACE TEMP (K)	1/TEMP (1/K)	ADSORPTION RATE CONSTANT (1/mol% CO)	RATE CONSTANT K(s) (1/s)	LN(K(s)) (1/K)	RATE (mol CO/s m^3 CAT)
1.66	0.34	0.808	0.671	2.299E-03	12.348	0.206	2.410E-02	17.0	24.4	24.1	297.55	3.361E-03	231.767	7.988E+03	8.986	6.279
1.84	0.16	0.769	0.707	2.417E-03	12.983	0.216	2.292E-02	8.0	39.7	37.7	312.85	3.196E-03	168.923	2.001E+03	7.602	2.798
1.92	0.08	0.726	0.697	2.560E-03	13.751	0.229	2.164E-02	4.0	58.2	54.2	331.35	3.018E-03	119.823	4.889E+02	6.192	1.369
2.00	0.00	0.705	0.705	2.635E-03	14.154	0.236	2.103E-02	0.0	67.9	62.3	341.05	2.932E-03	101.579	0.000E+00	0.000	0.000
2.00	0.00	0.686	0.686	2.707E-03	14.544	0.242	2.046E-02	0.0	77.3	71.3	350.45	2.853E-03	87.312	0.000E+00	0.000	0.000
1.96	0.04	0.668	0.655	2.781E-03	14.938	0.249	1.992E-02	2.0	86.8	79.7	359.95	2.778E-03	75.333	9.181E+01	4.520	0.677
1.96	0.04	0.659	0.646	2.819E-03	15.145	0.252	1.965E-02	2.0	91.8	84.1	364.95	2.740E-03	70.198	7.849E+01	4.363	0.677
1.98	0.02	0.651	0.644	2.835E-03	15.336	0.256	1.940E-02	1.0	96.4	88.6	369.53	2.706E-03	65.758	3.427E+01	3.534	0.337
1.96	0.04	0.634	0.622	2.929E-03	15.735	0.262	1.891E-02	2.0	106.0	97.3	379.15	2.637E-03	57.618	5.144E+01	3.941	0.677
1.92	0.08	0.626	0.601	2.967E-03	15.938	0.266	1.867E-02	4.0	110.9	101.6	384.05	2.604E-03	54.005	8.883E+01	4.487	1.368
1.91	0.09	0.619	0.591	3.003E-03	16.133	0.269	1.845E-02	4.5	115.6	105.8	388.75	2.572E-03	50.830	8.764E+01	4.473	1.543
1.90	0.10	0.604	0.573	3.079E-03	16.540	0.276	1.799E-02	5.0	125.4	114.7	398.53	2.509E-03	45.005	7.502E+01	4.318	1.718
1.90	0.10	0.596	0.567	3.116E-03	16.739	0.279	1.778E-02	5.0	130.2	119.1	403.33	2.479E-03	42.492	6.643E+01	4.196	1.718
1.87	0.13	0.589	0.551	3.154E-03	16.946	0.282	1.756E-02	6.5	135.2	123.7	408.35	2.449E-03	40.881	7.579E+01	4.328	2.250
1.84	0.16	0.582	0.536	3.192E-03	17.150	0.286	1.735E-02	8.0	140.1	128.1	413.25	2.420E-03	37.903	8.232E+01	4.411	2.789
1.79	0.21	0.575	0.515	3.230E-03	17.353	0.289	1.715E-02	10.5	145.0	132.5	418.15	2.391E-03	35.890	9.529E+01	4.556	3.708
1.76	0.24	0.569	0.501	3.267E-03	17.552	0.293	1.695E-02	12.0	149.8	136.9	422.95	2.364E-03	34.063	9.643E+01	4.573	4.270
1.72	0.28	0.562	0.484	3.305E-03	17.754	0.296	1.676E-02	14.0	154.7	141.4	427.85	2.337E-03	32.334	1.004E+02	4.609	5.033
1.74	0.26	0.556	0.484	3.342E-03	17.953	0.299	1.657E-02	13.0	159.5	145.7	432.65	2.311E-03	30.760	8.434E+01	4.433	4.646
1.69	0.31	0.550	0.465	3.380E-03	18.158	0.303	1.639E-02	15.5	164.4	150.1	437.55	2.285E-03	29.285	8.964E+01	4.496	5.611
1.66	0.34	0.544	0.451	3.417E-03	18.357	0.306	1.621E-02	17.0	169.2	154.6	442.35	2.261E-03	27.902	8.846E+01	4.483	6.201
1.62	0.38	0.538	0.436	3.455E-03	18.561	0.309	1.603E-02	19.0	174.1	159.1	447.25	2.236E-03	26.603	8.878E+01	4.486	7.003

METHOD OF VOLTZ et al.

CO ANALYZER (VOL %)	CO CONVERTED (VOL %)	INITIAL C(CO) (mol/m^3)	REMAINING C(CO) (mol/m^3)	GAS FLOW RATE (m^3/min)	GAS VELOCITY (m/min)	GAS VELOCITY (m/s)	CONTACT TIME (s)	CO CONVERSION (%)	SURFACE TEMP (deg C)	OUTLET TEMP (deg C)	SURFACE TEMP (K)	1/TEMP (1/K)	ADSORPTION RATE CONSTANT (1/mol% CO)	RATE CONSTANT K(s) (1/s)	LN(K(s)) (1/K)	RATE (mol CO/s m^3 CAT)
1.66	0.34	0.808	0.671	2.299E-03	12.348	0.206	2.410E-02	17.0	24.4	24.1	297.55	3.361E-03	15.269	4.060E+01	3.704	6.183
1.84	0.16	0.769	0.707	2.417E-03	12.983	0.216	2.292E-02	8.0	39.7	37.7	312.85	3.196E-03	13.089	1.440E+01	2.667	2.778
1.92	0.08	0.726	0.697	2.560E-03	13.751	0.229	2.164E-02	4.0	58.2	54.2	331.35	3.018E-03	11.074	5.180E+00	1.645	1.363
2.00	0.00	0.705	0.705	2.635E-03	14.154	0.256	2.103E-02	0.0	67.9	62.3	341.05	2.932E-03	10.218	0.000E+00	0.000	0.000
2.00	0.00	0.686	0.686	2.707E-03	14.544	0.242	2.046E-02	0.0	77.3	71.3	350.45	2.853E-03	9.492	0.000E+00	0.000	0.000
1.96	0.04	0.668	0.655	2.781E-03	14.938	0.249	1.992E-02	2.0	86.8	79.7	359.95	2.778E-03	8.846	1.459E+00	0.506	0.676
1.96	0.04	0.659	0.646	2.819E-03	15.145	0.252	1.965E-02	2.0	91.8	84.1	364.95	2.740E-03	8.536	1.346E+00	0.436	0.676
1.98	0.02	0.651	0.644	2.835E-03	15.336	0.256	1.940E-02	1.0	96.4	88.6	369.53	2.706E-03	8.267	7.287E-01	-0.316	0.337
1.96	0.04	0.634	0.622	2.929E-03	15.735	0.262	1.891E-02	2.0	106.0	97.3	379.15	2.637E-03	7.753	1.282E+00	0.249	0.675
1.92	0.08	0.626	0.601	2.967E-03	15.938	0.266	1.867E-02	4.0	110.9	101.6	384.05	2.604E-03	7.512	2.398E+00	0.875	1.360
1.91	0.09	0.619	0.591	3.003E-03	16.133	0.269	1.845E-02	4.5	115.6	105.8	388.75	2.572E-03	7.294	2.347E+00	0.935	1.532
1.90	0.10	0.604	0.573	3.079E-03	16.540	0.276	1.799E-02	5.0	125.4	114.7	398.53	2.509E-03	6.874	2.528E+00	0.927	1.704
1.90	0.10	0.596	0.567	3.116E-03	16.739	0.279	1.778E-02	5.0	130.2	119.1	403.33	2.479E-03	6.685	2.600E+00	0.876	1.703
1.87	0.13	0.589	0.551	3.154E-03	16.946	0.282	1.756E-02	6.5	135.2	123.7	408.35	2.449E-03	6.497	2.945E+00	1.081	2.223
1.84	0.16	0.582	0.536	3.192E-03	17.150	0.286	1.735E-02	8.0	140.1	128.1	413.25	2.420E-03	6.323	3.439E+00	1.235	2.747
1.79	0.21	0.575	0.515	3.230E-03	17.353	0.289	1.715E-02	10.5	145.0	132.5	418.15	2.391E-03	6.157	4.273E+00	1.452	3.631
1.76	0.24	0.569	0.501	3.267E-03	17.552	0.293	1.695E-02	12.0	149.8	136.9	422.95	2.364E-03	6.003	4.648E+00	1.537	4.164
1.72	0.28	0.562	0.484	3.305E-03	17.756	0.296	1.676E-02	14.0	154.7	141.4	427.85	2.337E-03	5.852	5.159E+00	1.641	4.882
1.74	0.26	0.556	0.484	3.342E-03	17.953	0.299	1.657E-02	13.0	159.5	145.7	432.65	2.311E-03	5.712	4.606E+00	1.527	4.516
1.69	0.31	0.550	0.465	3.380E-03	18.158	0.303	1.639E-02	15.5	164.4	150.1	437.55	2.285E-03	5.575	5.294E+00	1.655	5.415
1.66	0.34	0.544	0.451	3.417E-03	18.357	0.306	1.621E-02	17.0	169.2	154.6	442.35	2.261E-03	5.447	5.498E+00	1.704	5.955
1.62	0.38	0.538	0.436	3.455E-03	18.561	0.309	1.603E-02	19.0	174.1	159.1	447.25	2.236E-03	5.322	5.883E+00	1.772	6.680

TABLE L11 REACTOR DATA FOR AGED COMMERCIAL STANDARD CATALYST CONTAINING A 31 wt% WASH COAT AND 11 wt% CERIA [SMCOMMAG].
MONOLITH MASS:0.79199g DIM:5.25*15.65*15.6mm TOTAL SURFACE AREA SUPPORT + WASH COAT: 11.05 m^2/g

GENERAL METHOD

CO ANALYZER (VOL %)	CO CONVERTED (VOL %)	INITIAL C(CO) (mol/m^3)	REMAINING C(CO) (mol/m^3)	GAS FLOW RATE (m^3/min)	GAS VELOCITY (m/min)	GAS VELOCITY (m/s)	CONTACT TIME (s)	CO CONVERSION (%)	SURFACE TEMP (deg C)	OUTLET TEMP (deg C)	SURFACE TEMP (K)	1/TEMP (1/K)	RATE CONSTANT K(s) (1/s)	LN(K(s)) (1/s)	RATE (mol CO/s m^3 CAT)
1.74	0.26	0.806	0.701	2.306E-03	12.429	0.207	2.534E-02	13.0	25.4	25.2	298.55	3.350E-03	0.497	-0.699	3.852
1.88	0.12	0.769	0.723	2.417E-03	13.025	0.217	2.418E-02	6.0	39.7	37.8	312.85	3.196E-03	0.232	-1.463	1.849
1.90	0.10	0.726	0.689	2.560E-03	13.799	0.230	2.283E-02	5.0	58.3	53.9	331.45	3.017E-03	0.203	-1.593	1.549
1.90	0.10	0.687	0.652	2.706E-03	14.582	0.243	2.160E-02	5.0	77.1	70.5	350.25	2.855E-03	0.215	-1.538	1.549
1.89	0.11	0.652	0.616	2.850E-03	15.360	0.256	2.051E-02	5.5	95.8	87.2	368.95	2.710E-03	0.250	-1.388	1.700
1.89	0.11	0.635	0.600	2.927E-03	15.773	0.263	1.997E-02	5.5	105.7	95.7	378.85	2.640E-03	0.256	-1.361	1.700
2.00	0.00	0.619	0.619	3.002E-03	16.181	0.270	1.947E-02	0.0	115.5	104.8	388.65	2.573E-03	0.000	0.000	0.000
2.00	0.00	0.604	0.604	3.076E-03	16.580	0.276	1.900E-02	0.0	125.1	113.2	398.25	2.511E-03	0.000	0.000	0.000
2.00	0.00	0.590	0.590	3.152E-03	16.988	0.283	1.854E-02	0.0	134.9	122.3	408.05	2.451E-03	0.000	0.000	0.000
1.98	0.02	0.576	0.570	3.228E-03	17.396	0.290	1.811E-02	1.0	144.7	126.9	417.85	2.393E-03	0.050	-2.991	0.316
1.96	0.04	0.563	0.552	3.302E-03	17.796	0.297	1.770E-02	2.0	154.3	139.2	427.45	2.339E-03	0.103	-2.270	0.629
1.93	0.07	0.550	0.531	3.377E-03	18.200	0.303	1.731E-02	3.5	164.0	148.5	437.15	2.288E-03	0.186	-1.680	1.093
1.92	0.08	0.538	0.517	3.451E-03	18.599	0.310	1.694E-02	4.0	173.6	156.9	446.75	2.238E-03	0.218	-1.523	1.246
1.88	0.12	0.527	0.495	3.526E-03	19.003	0.317	1.658E-02	6.0	183.3	165.8	456.45	2.191E-03	0.338	-1.085	1.849
1.81	0.19	0.516	0.467	3.601E-03	19.407	0.323	1.623E-02	9.5	193.0	173.4	466.15	2.145E-03	0.557	-0.586	2.872
1.74	0.26	0.505	0.440	3.677E-03	19.815	0.330	1.590E-02	13.0	202.8	182.4	475.95	2.101E-03	0.793	-0.232	3.852
1.73	0.27	0.500	0.433	3.714E-03	20.015	0.334	1.574E-02	13.5	207.6	186.5	480.75	2.080E-03	0.834	-0.182	3.988
1.73	0.27	0.495	0.428	3.753E-03	20.227	0.337	1.557E-02	13.5	212.7	190.9	485.85	2.058E-03	0.843	-0.171	3.988
1.72	0.28	0.490	0.422	3.790E-03	20.427	0.340	1.542E-02	14.0	217.5	195.7	490.65	2.038E-03	0.885	-0.122	4.124
1.71	0.29	0.481	0.411	3.866E-03	20.835	0.347	1.512E-02	14.5	227.3	204.7	500.45	1.998E-03	0.938	-0.064	4.258
1.71	0.29	0.476	0.407	3.905E-03	21.043	0.351	1.497E-02	14.5	232.3	209.6	505.45	1.978E-03	0.947	-0.054	4.258
1.69	0.31	0.471	0.398	3.942E-03	21.247	0.354	1.483E-02	15.5	237.2	214.0	510.35	1.959E-03	1.028	0.028	4.525
1.66	0.34	0.467	0.388	3.980E-03	21.451	0.358	1.468E-02	17.0	242.1	218.6	515.25	1.941E-03	1.148	0.138	4.917
1.65	0.35	0.463	0.382	4.017E-03	21.647	0.361	1.455E-02	17.5	246.8	223.0	519.95	1.923E-03	1.196	0.179	5.046
1.63	0.37	0.458	0.373	4.055E-03	21.855	0.364	1.441E-02	18.5	251.8	227.3	524.95	1.905E-03	1.284	0.250	5.301
1.61	0.39	0.454	0.365	4.093E-03	22.059	0.368	1.428E-02	19.5	256.7	231.4	529.85	1.887E-03	1.375	0.318	5.552
1.57	0.43	0.450	0.353	4.131E-03	22.263	0.371	1.415E-02	21.5	261.6	236.1	534.75	1.870E-03	1.548	0.437	6.042

METHOD OF KOBERSTEIN & WANNEMACHER

CO ANALYZER (VOL %)	CO CONVERTED (VOL %)	INITIAL C(CO) (mol/m^3)	REMAINING C(CO) (mol/m^3)	GAS FLOW RATE (m^3/min)	GAS VELOCITY (m/min)	GAS VELOCITY (m/s)	CONTACT TIME (s)	CO CONVERSION (%)	SURFACE TEMP (deg C)	OUTLET TEMP (deg C)	SURFACE TEMP (K)	1/TEMP (1/K)	ADSORPTION RATE CONSTANT (1/mol% CO)	RATE CONSTANT K(s) (1/s)	LN(K(s)) (1/s)	RATE (mol CO/s m^3 CAT)
1.74	0.26	0.806	0.701	2.306E-03	12.429	0.207	2.534E-02	13.0	25.4	25.2	298.55	3.350E-03	226.800	1.467E+04	9.593	4.438
1.88	0.12	0.769	0.723	2.417E-03	13.025	0.217	2.418E-02	6.0	39.7	37.8	312.85	3.196E-03	168.923	3.733E+03	8.225	1.968
1.90	0.10	0.726	0.689	2.560E-03	13.799	0.230	2.283E-02	5.0	58.3	53.9	331.45	3.017E-03	119.613	1.491E+03	7.307	1.631
1.90	0.10	0.687	0.652	2.706E-03	14.582	0.243	2.160E-02	5.0	77.1	70.5	350.25	2.855E-03	87.586	7.645E+02	6.639	1.630
1.89	0.11	0.652	0.616	2.850E-03	15.360	0.256	2.051E-02	5.5	95.8	87.2	368.95	2.710E-03	66.297	4.623E+02	6.136	1.797
1.89	0.11	0.635	0.600	2.927E-03	15.773	0.263	1.997E-02	5.5	105.7	95.7	378.85	2.640E-03	57.850	3.456E+02	5.845	1.797
2.00	0.00	0.619	0.619	3.002E-03	16.181	0.270	1.947E-02	0.0	115.5	104.8	388.65	2.573E-03	50.895	0.000E+00	0.000	0.000
2.00	0.00	0.604	0.604	3.076E-03	16.580	0.276	1.900E-02	0.0	125.1	113.2	398.25	2.511E-03	45.169	0.000E+00	0.000	0.000
2.00	0.00	0.590	0.590	3.152E-03	16.988	0.283	1.854E-02	0.0	134.9	122.3	408.05	2.451E-03	40.220	0.000E+00	0.000	0.000
1.98	0.02	0.576	0.570	3.228E-03	17.396	0.290	1.811E-02	1.0	144.7	126.9	417.85	2.393E-03	36.009	2.349E+01	3.157	0.319
1.96	0.04	0.563	0.552	3.302E-03	17.796	0.297	1.770E-02	2.0	154.3	139.2	427.45	2.339E-03	32.470	3.764E+01	3.628	0.642
1.93	0.07	0.550	0.531	3.377E-03	18.200	0.303	1.731E-02	3.5	164.0	148.5	437.15	2.288E-03	29.383	5.311E+01	3.972	1.131
1.92	0.08	0.538	0.517	3.451E-03	18.599	0.310	1.694E-02	4.0	173.6	156.9	446.75	2.238E-03	26.731	4.977E+01	3.907	1.295
1.88	0.12	0.527	0.495	3.526E-03	19.003	0.317	1.658E-02	6.0	183.3	165.8	456.45	2.191E-03	24.393	6.127E+01	4.115	1.959
1.81	0.19	0.516	0.467	3.601E-03	19.407	0.323	1.623E-02	9.5	193.0	173.4	466.15	2.145E-03	22.344	7.985E+01	4.380	3.151
1.74	0.26	0.505	0.440	3.677E-03	19.815	0.330	1.590E-02	13.0	202.8	182.4	475.95	2.101E-03	20.523	9.060E+01	4.506	4.381
1.72	0.28	0.500	0.430	3.714E-03	20.015	0.334	1.574E-02	14.0	207.6	186.5	480.75	2.080E-03	19.711	8.958E+01	4.495	4.737
1.76	0.24	0.495	0.436	3.753E-03	20.227	0.337	1.557E-02	12.0	212.7	190.9	485.85	2.058E-03	18.900	7.120E+01	4.265	4.019
1.72	0.28	0.490	0.422	3.790E-03	20.427	0.340	1.542E-02	14.0	217.5	195.7	490.65	2.038E-03	18.182	7.625E+01	4.334	4.730
1.69	0.31	0.481	0.406	3.866E-03	20.835	0.347	1.512E-02	15.5	227.3	204.7	500.45	1.998E-03	16.838	7.209E+01	4.278	5.266
1.72	0.28	0.476	0.409	3.905E-03	21.043	0.351	1.497E-02	14.0	232.3	209.6	505.45	1.978E-03	16.209	6.082E+01	4.108	4.719
1.69	0.31	0.471	0.398	3.942E-03	21.247	0.354	1.483E-02	15.5	237.2	214.0	510.35	1.959E-03	15.628	6.233E+01	4.132	5.256
1.66	0.34	0.467	0.388	3.980E-03	21.451	0.358	1.468E-02	17.0	242.1	218.6	515.25	1.941E-03	15.077	6.340E+01	4.149	5.798
1.66	0.34	0.463	0.384	4.017E-03	21.647	0.361	1.455E-02	17.0	246.8	223.0	519.95	1.923E-03	14.577	5.942E+01	4.085	5.792
1.63	0.37	0.458	0.373	4.055E-03	21.855	0.364	1.441E-02	18.5	251.8	227.3	524.95	1.905E-03	14.072	6.010E+01	4.096	6.338
1.61	0.39	0.454	0.365	4.093E-03	22.059	0.368	1.428E-02	19.5	256.7	231.4	529.85	1.887E-03	13.603	5.918E+01	4.081	6.702
1.57	0.43	0.450	0.353	4.131E-03	22.263	0.371	1.415E-02	21.5	261.6	236.1	534.75	1.870E-03	13.157	6.082E+01	4.108	7.445

TABLE I.11 cont.

METHOD OF VOLTZ et al.

CO ANALYZER (VOL %)	CO CONVERTED (VOL %)	INITIAL C(C0) (mol/m^3)	REMAINING C(CO) (mol/m^3)	GAS FLOW RATE (m^3/min)	GAS VELOCITY (m/min)	GAS VELOCITY (m/s)	CONTACT TIME (s)	CO CONVERSION (%)	SURFACE TEMP (deg C)	OUTLET TEMP (deg C)	SURFACE TEMP (K)	1/TEMP (1/K)	ADSORPTION RATE CONSTANT (1/mol% CO)	RATE CONSTANT K(s) (1/s)	LN(K(s)) (1/s)	RATE (mol CO/s m^3 CAT)
1.74	0.26	0.806	0.701	2.306E-03	12.429	0.207	2.534E-02	13.0	25.4	25.2	298.55	3.350E-03	15.108	7.613E+01	4.332	4.389
1.88	0.12	0.769	0.723	2.417E-03	13.025	0.217	2.418E-02	6.0	39.7	37.8	312.85	3.196E-03	13.089	2.681E+01	3.289	1.957
1.90	0.10	0.726	0.689	2.560E-03	13.799	0.230	2.283E-02	5.0	58.3	53.9	331.45	3.017E-03	11.064	1.585E+01	2.763	1.622
1.90	0.10	0.687	0.652	2.706E-03	14.582	0.243	2.160E-02	5.0	77.1	70.5	350.25	2.855E-03	9.507	1.166E+01	2.456	1.620
1.89	0.11	0.652	0.616	2.850E-03	15.360	0.256	2.051E-02	5.5	95.8	87.2	368.95	2.710E-03	8.301	9.792E+00	2.282	1.783
1.89	0.11	0.635	0.600	2.927E-03	15.773	0.263	1.997E-02	5.5	105.7	95.7	378.85	2.640E-03	7.768	8.612E+00	2.153	1.782
2.00	0.00	0.619	0.619	3.002E-03	16.181	0.270	1.947E-02	0.0	115.5	104.8	388.65	2.573E-03	7.299	0.000E+00	0.000	0.000
2.00	0.00	0.604	0.604	3.076E-03	16.580	0.276	1.900E-02	0.0	125.1	113.2	398.25	2.511E-03	6.887	0.000E+00	0.000	0.000
2.00	0.00	0.590	0.590	3.152E-03	16.988	0.283	1.854E-02	0.0	134.9	122.3	408.05	2.451E-03	6.508	0.000E+00	0.000	0.000
1.98	0.02	0.576	0.570	3.228E-03	17.396	0.290	1.811E-02	1.0	144.7	126.9	417.85	2.393E-03	6.167	1.032E+00	0.031	0.319
1.96	0.04	0.563	0.552	3.302E-03	17.796	0.297	1.770E-02	2.0	154.3	139.2	427.45	2.339E-03	5.864	1.881E+00	0.632	0.639
1.93	0.07	0.550	0.531	3.377E-03	18.200	0.303	1.731E-02	3.5	164.0	148.5	437.15	2.288E-03	5.586	3.010E+00	1.102	1.123
1.92	0.08	0.538	0.517	3.451E-03	18.599	0.310	1.694E-02	4.0	173.6	156.9	446.75	2.238E-03	5.334	3.174E+00	1.155	1.284
1.88	0.12	0.527	0.495	3.526E-03	19.003	0.317	1.658E-02	6.0	183.3	165.8	456.45	2.191E-03	5.102	4.396E+00	1.481	1.934
1.81	0.19	0.516	0.467	3.601E-03	19.407	0.323	1.623E-02	9.5	193.0	173.4	466.15	2.145E-03	4.888	6.440E+00	1.863	3.083
1.74	0.26	0.505	0.440	3.677E-03	19.815	0.330	1.590E-02	13.0	202.8	182.4	475.95	2.101E-03	4.690	8.190E+00	2.103	4.243
1.72	0.28	0.500	0.430	3.714E-03	20.015	0.334	1.574E-02	14.0	207.6	186.5	480.75	2.080E-03	4.599	8.537E+00	2.144	4.574
1.76	0.24	0.495	0.436	3.753E-03	20.227	0.337	1.557E-02	12.0	212.7	190.9	485.85	2.058E-03	4.506	7.117E+00	1.962	3.902
1.72	0.28	0.490	0.422	3.790E-03	20.427	0.340	1.542E-02	14.0	217.5	195.7	490.65	2.038E-03	4.422	8.038E+00	2.084	4.565
1.69	0.31	0.481	0.406	3.866E-03	20.835	0.347	1.512E-02	15.5	227.3	204.7	500.45	1.998E-03	4.259	8.395E+00	2.128	5.055
1.72	0.28	0.476	0.409	3.905E-03	21.043	0.351	1.497E-02	14.0	232.3	209.6	505.45	1.978E-03	4.181	7.397E+00	2.001	4.551
1.69	0.31	0.471	0.398	3.942E-03	21.247	0.354	1.483E-02	15.5	237.2	214.0	510.35	1.959E-03	4.107	7.963E+00	2.075	5.044
1.66	0.34	0.467	0.388	3.980E-03	21.451	0.358	1.468E-02	17.0	242.1	218.6	515.25	1.941E-03	4.036	8.501E+00	2.140	5.537
1.66	0.34	0.463	0.384	4.017E-03	21.647	0.361	1.455E-02	17.0	246.8	223.0	519.95	1.923E-03	3.971	8.308E+00	2.117	5.530
1.63	0.37	0.458	0.373	4.055E-03	21.855	0.364	1.441E-02	18.5	251.8	227.3	524.95	1.905E-03	3.903	8.812E+00	2.176	6.021
1.61	0.39	0.454	0.365	4.093E-03	22.059	0.368	1.428E-02	19.5	256.7	231.4	529.85	1.887E-03	3.839	9.071E+00	2.205	6.344
1.57	0.43	0.450	0.353	4.131E-03	22.263	0.371	1.415E-02	21.5	261.6	236.1	534.75	1.870E-03	3.777	9.766E+00	2.279	6.996

TABLE I.12 REACTOR DATA FOR AGED COMMERCIAL POWDER CATALYST CONTAINING A 28 wt% WASH COAT AND 11 wt% CERIA [SM38].
MONOLITH MASS:0.70035g DIM:4.75*15.8*15.8mm TOTAL SURFACE AREA SUPPORT + WASH COAT: 15.16 m^2/g
GENERAL METHOD

CO ANALYZER (VOL %)	CO CONVERTED (VOL %)	INITIAL C(CO) (mol/m^3)	REMAINING C(CO) (mol/m^3)	GAS FLOW RATE (m^3/min)	GAS VELOCITY (m/min)	GAS VELOCITY (m/s)	CONTACT TIME (s)	CO CONVERSION (%)	SURFACE TEMP (deg C)	OUTLET TEMP (deg C)	SURFACE TEMP (K)	1/TEMP (1/K)	RATE CONSTANT K(s) (1/s)	LN(K(s)) (1/s)	RATE (mol CO/s m^3 CAT)
1.85	0.15	0.809	0.748	2.297E-03	12.107	0.202	2.354E-02	7.5	24.2	23.8	297.35	3.363E-03	0.218	-1.521	2.478
2.00	0.00	0.725	0.725	2.562E-03	13.503	0.225	2.111E-02	0.0	58.5	54.1	331.65	3.015E-03	0.000	0.000	0.000
1.98	0.02	0.687	0.680	2.706E-03	14.265	0.238	1.998E-02	1.0	77.2	70.6	350.35	2.854E-03	0.033	-3.406	0.342
2.00	0.00	0.652	0.652	2.852E-03	15.030	0.251	1.896E-02	0.0	96.0	87.7	369.15	2.709E-03	0.000	0.000	0.000
2.00	0.00	0.619	0.619	3.000E-03	15.812	0.264	1.802E-02	0.0	115.2	104.6	388.35	2.575E-03	0.000	0.000	0.000
2.00	0.00	0.590	0.590	3.150E-03	16.602	0.277	1.717E-02	0.0	134.6	122.2	407.75	2.452E-03	0.000	0.000	0.000
2.00	0.00	0.576	0.576	3.227E-03	17.009	0.283	1.676E-02	0.0	144.6	131.1	417.75	2.394E-03	0.000	0.000	0.000
2.00	0.00	0.563	0.563	3.302E-03	17.404	0.290	1.638E-02	0.0	154.3	139.8	427.45	2.339E-03	0.000	0.000	0.000
1.96	0.04	0.539	0.528	3.447E-03	18.169	0.303	1.569E-02	2.0	173.1	156.7	446.25	2.241E-03	0.085	-2.466	0.680
1.90	0.10	0.527	0.500	3.528E-03	18.593	0.310	1.533E-02	5.0	183.5	165.6	456.65	2.190E-03	0.221	-1.511	1.675
1.88	0.12	0.521	0.490	3.565E-03	18.792	0.313	1.517E-02	6.0	188.4	170.7	461.55	2.167E-03	0.269	-1.313	1.999
1.87	0.13	0.516	0.482	3.604E-03	18.996	0.317	1.500E-02	6.5	193.4	175.5	466.55	2.143E-03	0.295	-1.219	2.160
1.84	0.16	0.510	0.470	3.640E-03	19.187	0.320	1.485E-02	8.0	198.1	180.0	471.25	2.122E-03	0.370	-0.993	2.636
1.83	0.17	0.505	0.462	3.679E-03	19.391	0.323	1.470E-02	8.5	203.1	184.7	476.25	2.100E-03	0.399	-0.920	2.793
1.82	0.18	0.500	0.455	3.717E-03	19.590	0.327	1.455E-02	9.0	208.0	189.3	481.15	2.078E-03	0.428	-0.850	2.949
1.80	0.20	0.495	0.445	3.756E-03	19.798	0.330	1.440E-02	10.0	213.1	193.8	486.25	2.057E-03	0.483	-0.728	3.259
1.77	0.23	0.490	0.434	3.793E-03	19.993	0.333	1.425E-02	11.5	217.9	198.4	491.05	2.036E-03	0.565	-0.570	3.716
1.75	0.25	0.485	0.424	3.831E-03	20.193	0.337	1.411E-02	12.5	222.8	202.7	495.95	2.016E-03	0.624	-0.471	4.015
1.74	0.26	0.480	0.418	3.868E-03	20.388	0.340	1.398E-02	13.0	227.6	207.1	500.75	1.997E-03	0.657	-0.420	4.164
1.72	0.28	0.476	0.409	3.905E-03	20.584	0.343	1.385E-02	14.0	232.4	211.8	505.55	1.978E-03	0.719	-0.331	4.458
1.70	0.30	0.471	0.400	3.944E-03	20.787	0.346	1.371E-02	15.0	237.4	216.4	510.55	1.959E-03	0.782	-0.246	4.747
1.68	0.32	0.467	0.392	3.981E-03	20.983	0.350	1.358E-02	16.0	242.2	220.8	515.35	1.940E-03	0.847	-0.166	5.033
1.66	0.34	0.462	0.384	4.019E-03	21.182	0.353	1.345E-02	17.0	247.1	225.1	520.25	1.922E-03	0.914	-0.090	5.315
1.65	0.35	0.458	0.378	4.057E-03	21.382	0.356	1.333E-02	17.5	252.0	229.6	525.15	1.904E-03	0.952	-0.049	5.454
1.62	0.38	0.454	0.368	4.094E-03	21.577	0.360	1.321E-02	19.0	256.8	233.7	529.95	1.887E-03	1.052	0.051	5.866
1.60	0.40	0.450	0.360	4.132E-03	21.781	0.363	1.308E-02	20.0	261.8	238.0	534.95	1.869E-03	1.125	0.118	6.135
1.58	0.42	0.446	0.352	4.169E-03	21.972	0.366	1.297E-02	21.0	266.5	242.3	539.65	1.853E-03	1.199	0.181	6.400
1.56	0.44	0.442	0.345	4.207E-03	22.176	0.370	1.285E-02	22.0	271.5	246.6	544.65	1.836E-03	1.275	0.243	6.660

METHOD OF KOBBERSTEIN & WANNEMACHER

CO ANALYZER (VOL %)	CO CONVERTED (VOL %)	INITIAL C(CO) (mol/m^3)	REMAINING C(CO) (mol/m^3)	GAS FLOW RATE (m^3/min)	GAS VELOCITY (m/min)	GAS VELOCITY (m/s)	CONTACT TIME (s)	CO CONVERSION (%)	SURFACE TEMP (deg C)	OUTLET TEMP (deg C)	SURFACE TEMP (K)	1/TEMP (1/K)	ADSORPTION RATE CONSTANT (1/mol% CO)	RATE CONSTANT K(s) (1/s)	LN(K(s)) (1/s)	RATE (mol CO/s m^3 CAT)
1.85	0.15	0.809	0.748	2.297E-03	12.107	0.202	2.354E-02	7.5	24.2	23.8	297.35	3.363E-03	232.777	7.253E+03	8.889	2.681
2.00	0.00	0.725	0.725	2.562E-03	13.503	0.225	2.111E-02	0.0	58.5	54.1	331.65	3.015E-03	119.195	0.000E+00	0.000	0.000
1.98	0.02	0.687	0.680	2.706E-03	14.265	0.238	1.998E-02	1.0	77.2	70.6	350.35	2.854E-03	87.449	1.224E+02	4.808	0.345
2.00	0.00	0.652	0.652	2.852E-03	15.030	0.251	1.896E-02	0.0	96.0	87.7	369.15	2.709E-03	66.110	0.000E+00	0.000	0.000
2.00	0.00	0.619	0.619	3.000E-03	15.812	0.264	1.802E-02	0.0	115.2	104.6	388.35	2.575E-03	51.090	0.000E+00	0.000	0.000
2.00	0.00	0.590	0.590	3.150E-03	16.602	0.277	1.717E-02	0.0	134.6	122.2	407.75	2.452E-03	40.360	0.000E+00	0.000	0.000
2.00	0.00	0.576	0.576	3.227E-03	17.009	0.283	1.676E-02	0.0	144.6	131.1	417.75	2.394E-03	36.048	0.000E+00	0.000	0.000
2.00	0.00	0.563	0.563	3.302E-03	17.404	0.290	1.638E-02	0.0	154.3	139.8	427.45	2.339E-03	32.470	0.000E+00	0.000	0.000
1.96	0.04	0.539	0.528	3.447E-03	18.169	0.303	1.569E-02	2.0	173.1	156.7	446.25	2.241E-03	26.861	1.998E+01	2.995	0.693
1.90	0.10	0.527	0.500	3.528E-03	18.593	0.310	1.533E-02	5.0	183.5	165.6	456.65	2.190E-03	24.348	4.025E+01	3.695	1.757
1.86	0.14	0.521	0.485	3.565E-03	18.792	0.313	1.517E-02	7.0	188.4	170.7	461.55	2.167E-03	23.283	5.097E+01	3.931	2.481
1.87	0.13	0.516	0.482	3.604E-03	18.996	0.317	1.500E-02	6.5	193.4	175.5	466.55	2.143E-03	22.265	4.330E+01	3.768	2.298
1.84	0.16	0.510	0.470	3.640E-03	19.187	0.320	1.485E-02	8.0	198.1	180.0	471.25	2.122E-03	21.368	4.870E+01	3.886	2.847
1.83	0.17	0.505	0.462	3.679E-03	19.391	0.323	1.470E-02	8.5	203.1	184.7	476.25	2.100E-03	20.471	4.734E+01	3.857	3.031
1.82	0.18	0.500	0.455	3.717E-03	19.590	0.327	1.455E-02	9.0	208.0	189.3	481.15	2.078E-03	19.646	4.604E+01	3.830	3.215
1.80	0.20	0.495	0.445	3.756E-03	19.798	0.330	1.440E-02	10.0	213.1	193.8	486.25	2.057E-03	18.839	4.684E+01	3.847	3.587
1.77	0.23	0.490	0.434	3.793E-03	19.993	0.333	1.425E-02	11.5	217.9	198.4	491.05	2.036E-03	18.124	4.955E+01	3.903	4.151
1.75	0.25	0.485	0.424	3.831E-03	20.193	0.337	1.411E-02	12.5	222.8	202.7	495.95	2.016E-03	17.436	4.968E+01	3.906	4.530
1.74	0.26	0.480	0.418	3.868E-03	20.388	0.340	1.398E-02	13.0	227.6	207.1	500.75	1.997E-03	16.799	4.791E+01	3.869	4.719
1.72	0.28	0.476	0.409	3.905E-03	20.584	0.343	1.385E-02	14.0	232.4	211.8	505.55	1.978E-03	16.197	4.784E+01	3.868	5.101
1.70	0.30	0.471	0.400	3.944E-03	20.787	0.346	1.371E-02	15.0	237.4	216.4	510.55	1.959E-03	15.604	4.748E+01	3.860	5.485
1.68	0.32	0.467	0.392	3.981E-03	20.983	0.350	1.358E-02	16.0	242.2	220.8	515.35	1.940E-03	15.066	4.713E+01	3.853	5.872
1.66	0.34	0.462	0.384	4.019E-03	21.182	0.353	1.345E-02	17.0	247.1	225.1	520.25	1.922E-03	14.546	4.662E+01	3.842	6.260
1.65	0.35	0.458	0.378	4.057E-03	21.382	0.356	1.333E-02	17.5	252.0	229.6	525.15	1.904E-03	14.052	4.484E+01	3.803	6.452
1.62	0.38	0.454	0.368	4.094E-03	21.577	0.360	1.321E-02	19.0	256.8	233.7	529.95	1.887E-03	13.593	4.546E+01	3.817	7.043
1.60	0.40	0.450	0.360	4.132E-03	21.781	0.363	1.308E-02	20.0	261.8	238.0	534.95	1.869E-03	13.140	4.472E+01	3.800	7.436
1.58	0.42	0.446	0.352	4.169E-03	21.972	0.366	1.297E-02	21.0	266.5	242.3	539.65	1.853E-03	12.734	4.412E+01	3.787	7.831
1.56	0.44	0.442	0.345	4.207E-03	22.176	0.370	1.285E-02	22.0	271.5	246.6	544.65	1.836E-03	12.324	4.334E+01	3.769	8.226

TABLE I.12 cont.
METHOD OF VOLTZ et al.

CO ANALYZER (VOL %)	CO CONVERTED (VOL %)	INITIAL C(C0) (mol/m^3)	REMAINING C(CO) (mol/m^3)	GAS FLOW RATE (m^3/min)	GAS VELOCITY (m/min)	GAS VELOCITY (m/s)	CONTACT TIME (s)	CO CONVERSION (%)	SURFACE TEMP (deg C)	OUTLET TEMP (deg C)	SURFACE TEMP (K)	1/TEMP (1/K)	ADSORPTION RATE CONSTANT (1/mol% CO)	RATE CONSTANT K(s) (1/s)	LN(K(s)) (1/s)	RATE (mol CO/s m^3 CAT)
1.85	0.15	0.809	0.748	2.297E-03	12.107	0.202	2.354E-02	7.5	24.2	23.8	297.35	3.363E-03	16.590	4.230E+01	3.745	2.666
2.00	0.00	0.725	0.725	2.562E-03	13.503	0.225	2.111E-02	0.0	58.5	54.1	331.65	3.015E-03	11.877	0.000E+00	0.000	0.000
1.98	0.02	0.687	0.680	2.706E-03	14.265	0.238	1.998E-02	1.0	77.2	70.6	350.35	2.854E-03	10.175	2.098E+00	0.741	0.345
2.00	0.00	0.652	0.652	2.852E-03	15.030	0.251	1.896E-02	0.0	96.0	87.7	369.15	2.709E-03	8.848	0.000E+00	0.000	0.000
2.00	0.00	0.619	0.619	3.000E-03	15.812	0.264	1.802E-02	0.0	115.2	104.6	388.35	2.575E-03	7.780	0.000E+00	0.000	0.000
2.00	0.00	0.590	0.590	3.150E-03	16.602	0.277	1.717E-02	0.0	134.6	122.2	407.75	2.452E-03	6.915	0.000E+00	0.000	0.000
2.00	0.00	0.576	0.576	3.227E-03	17.009	0.283	1.676E-02	0.0	144.6	131.1	417.75	2.394E-03	6.536	0.000E+00	0.000	0.000
2.00	0.00	0.563	0.563	3.302E-03	17.404	0.290	1.638E-02	0.0	154.3	139.8	427.45	2.339E-03	6.204	0.000E+00	0.000	0.000
1.96	0.04	0.539	0.528	3.447E-03	18.169	0.303	1.569E-02	2.0	173.1	156.7	446.25	2.241E-03	5.643	1.367E+00	0.313	0.691
1.90	0.10	0.527	0.500	3.528E-03	18.593	0.310	1.533E-02	5.0	183.5	165.6	456.65	2.190E-03	5.373	3.119E+00	1.138	1.739
1.86	0.14	0.521	0.485	3.565E-03	18.792	0.313	1.517E-02	7.0	188.4	170.7	461.55	2.167E-03	5.254	4.187E+00	1.432	2.445
1.87	0.13	0.516	0.482	3.604E-03	18.996	0.317	1.500E-02	6.5	193.4	175.5	466.55	2.143E-03	5.138	3.750E+00	1.322	2.267
1.84	0.16	0.510	0.470	3.640E-03	19.187	0.320	1.485E-02	8.0	198.1	180.0	471.25	2.122E-03	5.034	4.448E+00	1.492	2.798
1.83	0.17	0.505	0.462	3.679E-03	19.391	0.323	1.470E-02	8.5	203.1	184.7	476.25	2.100E-03	4.927	4.560E+00	1.517	2.975
1.82	0.18	0.500	0.455	3.717E-03	19.590	0.327	1.455E-02	9.0	208.0	189.3	481.15	2.078E-03	4.827	4.667E+00	1.541	3.151
1.80	0.20	0.495	0.445	3.756E-03	19.798	0.330	1.440E-02	10.0	213.1	193.8	486.25	2.057E-03	4.727	5.006E+00	1.611	3.506
1.77	0.23	0.490	0.434	3.793E-03	19.993	0.333	1.425E-02	11.5	217.9	198.4	491.05	2.036E-03	4.636	5.570E+00	1.717	4.041
1.75	0.25	0.485	0.424	3.831E-03	20.193	0.337	1.411E-02	12.5	222.8	202.7	495.95	2.016E-03	4.548	5.866E+00	1.769	4.396
1.74	0.26	0.480	0.418	3.868E-03	20.388	0.340	1.398E-02	13.0	227.6	207.1	500.75	1.997E-03	4.464	5.926E+00	1.779	4.572
1.72	0.28	0.476	0.409	3.905E-03	20.584	0.343	1.385E-02	14.0	232.4	211.8	505.55	1.978E-03	4.383	6.199E+00	1.824	4.927
1.70	0.30	0.471	0.400	3.944E-03	20.787	0.346	1.371E-02	15.0	237.4	216.4	510.55	1.959E-03	4.302	6.451E+00	1.864	5.282
1.68	0.32	0.467	0.392	3.981E-03	20.983	0.350	1.358E-02	16.0	242.2	220.8	515.35	1.940E-03	4.228	6.698E+00	1.902	5.636
1.66	0.34	0.462	0.384	4.019E-03	21.182	0.353	1.345E-02	17.0	247.1	225.1	520.25	1.922E-03	4.154	6.929E+00	1.936	5.990
1.65	0.35	0.458	0.378	4.057E-03	21.382	0.356	1.333E-02	17.5	252.0	229.6	525.15	1.904E-03	4.083	6.956E+00	1.940	6.162
1.62	0.38	0.454	0.368	4.094E-03	21.577	0.360	1.321E-02	19.0	256.8	233.7	529.95	1.887E-03	4.016	7.366E+00	1.997	6.694
1.60	0.40	0.450	0.360	4.132E-03	21.781	0.363	1.308E-02	20.0	261.8	238.0	534.95	1.869E-03	3.949	7.566E+00	2.024	7.043
1.58	0.42	0.446	0.352	4.169E-03	21.972	0.366	1.297E-02	21.0	266.5	242.3	539.65	1.853E-03	3.887	7.770E+00	2.050	7.392
1.56	0.44	0.442	0.345	4.207E-03	22.176	0.370	1.285E-02	22.0	271.5	246.6	544.65	1.836E-03	3.824	7.957E+00	2.074	7.738

TABLE L13 REACTOR DATA FOR AGED COADA CATALYST CONTAINING A 22 wt% WASH COAT AND 11 wt% CERIA [SM13].
MONOLITH MASS:0.79276g DIM:5.05*15.75*15.7mm TOTAL SURFACE AREA OF SUPPORT + WASH COAT: 11.23 m^2/g

GENERAL METHOD

CO ANALYZER (VOL %)	CO CONVERTED (VOL %)	INITIAL C(CO) (mol/m^3)	REMAINING C(CO) (mol/m^3)	GAS FLOW RATE (m^3/min)	GAS VELOCITY (m/min)	GAS VELOCITY (m/s)	CONTACT TIME (s)	CO CONVERSION (%)	SURFACE TEMP (deg C)	OUTLET TEMP (deg C)	SURFACE TEMP (K)	1/TEMP (1/K)	RATE CONSTANT K(s) (1/s)	LN(K(s)) (1/s)	RATE (mol CO/s m^3 CAT)
1.58	0.42	0.793	0.626	2.343E-03	12.469	0.208	2.430E-02	21.0	30.2	29.4	303.35	3.297E-03	0.864	-0.146	6.877
1.88	0.12	0.726	0.682	2.560E-03	13.624	0.227	2.224E-02	6.0	58.3	54.3	331.45	3.017E-03	0.248	-1.395	1.898
1.97	0.03	0.669	0.659	2.778E-03	14.783	0.246	2.050E-02	1.5	86.5	79.3	359.65	2.780E-03	0.066	-2.723	0.486
1.96	0.04	0.635	0.623	2.925E-03	15.564	0.259	1.947E-02	2.0	105.5	95.9	378.65	2.641E-03	0.092	-2.382	0.646
1.94	0.06	0.627	0.609	2.962E-03	15.762	0.263	1.922E-02	3.0	110.3	99.9	383.45	2.608E-03	0.141	-1.958	0.964
2.00	0.00	0.619	0.619	3.000E-03	15.963	0.266	1.898E-02	0.0	115.2	104.4	388.35	2.575E-03	0.000	0.000	0.000
1.94	0.06	0.612	0.593	3.034E-03	16.165	0.269	1.874E-02	3.0	120.1	108.8	393.25	2.543E-03	0.145	-1.933	0.964
1.96	0.04	0.604	0.592	3.076E-03	16.370	0.273	1.851E-02	2.0	125.1	113.3	398.25	2.511E-03	0.097	-2.331	0.646
1.95	0.05	0.597	0.582	3.114E-03	16.572	0.276	1.828E-02	2.5	130.0	118.1	403.15	2.480E-03	0.123	-2.093	0.806
1.93	0.07	0.589	0.569	3.153E-03	16.777	0.280	1.806E-02	3.5	135.0	123.0	408.15	2.450E-03	0.176	-1.739	1.122
1.92	0.08	0.575	0.532	3.229E-03	17.184	0.286	1.763E-02	4.0	144.9	132.2	418.05	2.392E-03	0.206	-1.579	1.279
1.90	0.10	0.569	0.540	3.267E-03	17.385	0.290	1.743E-02	5.0	149.8	136.8	422.95	2.364E-03	0.262	-1.339	1.590
1.88	0.12	0.562	0.529	3.304E-03	17.583	0.293	1.723E-02	6.0	154.6	141.1	427.75	2.336E-03	0.320	-1.140	1.898
1.83	0.17	0.550	0.503	3.378E-03	17.977	0.300	1.685E-02	8.5	164.2	150.2	437.35	2.286E-03	0.469	-0.756	2.633
1.74	0.26	0.538	0.468	3.453E-03	18.372	0.306	1.649E-02	13.0	173.8	158.6	446.95	2.237E-03	0.752	-0.285	3.954
1.71	0.29	0.532	0.455	3.490E-03	18.573	0.310	1.631E-02	14.5	178.7	162.7	451.85	2.213E-03	0.855	-0.157	4.371
1.71	0.29	0.527	0.450	3.528E-03	18.775	0.313	1.614E-02	14.5	183.6	167.0	456.75	2.189E-03	0.864	-0.146	4.371
1.67	0.33	0.521	0.435	3.566E-03	18.976	0.316	1.597E-02	16.5	188.5	171.3	461.65	2.166E-03	1.006	0.006	4.914
1.62	0.38	0.516	0.418	3.604E-03	19.178	0.320	1.580E-02	19.0	193.4	176.0	466.55	2.143E-03	1.188	0.172	5.570
1.56	0.44	0.510	0.398	3.641E-03	19.375	0.323	1.564E-02	22.0	198.2	180.3	471.35	2.122E-03	1.415	0.347	6.324
1.48	0.52	0.505	0.374	3.679E-03	19.576	0.326	1.548E-02	26.0	203.1	184.6	476.25	2.100E-03	1.732	0.549	7.271

METHOD OF KOBERSTEIN AND WANNEMACHER

CO ANALYZER (VOL %)	CO CONVERTED (VOL %)	INITIAL C(CO) (mol/m^3)	REMAINING C(CO) (mol/m^3)	GAS FLOW RATE (m^3/min)	GAS VELOCITY (m/min)	GAS VELOCITY (m/s)	CONTACT TIME (s)	CO CONVERSION (%)	SURFACE TEMP (deg C)	OUTLET TEMP (deg C)	SURFACE TEMP (K)	1/TEMP (1/K)	ADSORPTION RATE CONSTANT (1/mol% CO)	RATE CONSTANT K(s) (1/s)	LN(K(s)) (1/s)	RATE (mol CO/s m^3 CAT)
1.58	0.42	0.793	0.626	2.343E-03	12.469	0.208	2.430E-02	21.0	30.2	29.4	303.35	3.297E-03	204.609	1.842E+04	9.821	7.750
1.88	0.12	0.726	0.682	2.560E-03	13.624	0.227	2.224E-02	6.0	58.3	54.3	331.45	3.017E-03	119.613	1.795E+03	7.495	2.019
1.97	0.03	0.669	0.659	2.778E-03	14.783	0.246	2.050E-02	1.5	86.5	79.3	359.65	2.780E-03	75.870	1.732E+02	5.153	0.493
1.96	0.04	0.635	0.623	2.925E-03	15.564	0.259	1.947E-02	2.0	105.5	95.9	378.65	2.641E-03	58.005	1.298E+02	4.866	0.659
1.94	0.06	0.627	0.609	2.962E-03	15.762	0.263	1.922E-02	3.0	110.3	99.9	383.45	2.608E-03	54.430	1.692E+02	5.131	0.993
2.00	0.00	0.619	0.619	3.000E-03	15.963	0.266	1.898E-02	0.0	115.2	104.4	388.35	2.575E-03	51.090	0.000E+00	0.000	0.000
1.94	0.06	0.612	0.593	3.034E-03	16.165	0.269	1.874E-02	3.0	120.1	108.8	393.25	2.543E-03	48.031	1.297E+02	4.865	0.993
1.96	0.04	0.604	0.592	3.076E-03	16.370	0.273	1.851E-02	2.0	125.1	113.3	398.25	2.511E-03	45.169	7.626E+01	4.334	0.659
1.95	0.05	0.597	0.582	3.114E-03	16.572	0.276	1.828E-02	2.5	130.0	118.1	403.15	2.480E-03	42.593	8.397E+01	4.430	0.828
1.93	0.07	0.589	0.569	3.153E-03	16.777	0.280	1.806E-02	3.5	135.0	123.0	408.15	2.450E-03	40.174	1.034E+02	4.639	1.161
1.92	0.08	0.575	0.532	3.229E-03	17.184	0.286	1.763E-02	4.0	144.9	132.2	418.05	2.392E-03	35.929	9.314E+01	4.535	1.330
1.90	0.10	0.569	0.540	3.267E-03	17.385	0.290	1.743E-02	5.0	149.8	136.8	422.95	2.364E-03	34.063	1.037E+02	4.641	1.670
1.88	0.12	0.562	0.529	3.304E-03	17.583	0.293	1.723E-02	6.0	154.6	141.1	427.75	2.336E-03	32.368	1.113E+02	4.712	2.014
1.83	0.17	0.550	0.503	3.378E-03	17.977	0.300	1.685E-02	8.5	164.2	150.2	437.35	2.286E-03	29.324	1.268E+02	4.843	2.686
1.74	0.26	0.538	0.468	3.453E-03	18.372	0.306	1.649E-02	13.0	173.8	158.6	446.95	2.237E-03	26.680	1.562E+02	5.051	4.513
1.71	0.29	0.532	0.455	3.490E-03	18.573	0.310	1.631E-02	14.5	178.7	162.7	451.85	2.213E-03	25.443	1.572E+02	5.058	5.070
1.71	0.29	0.527	0.450	3.528E-03	18.775	0.313	1.614E-02	14.5	183.6	167.0	456.75	2.189E-03	24.326	1.432E+02	4.964	5.066
1.67	0.33	0.521	0.435	3.566E-03	18.976	0.316	1.597E-02	16.5	188.5	171.3	461.65	2.166E-03	23.262	1.474E+02	4.993	5.821
1.62	0.38	0.516	0.418	3.604E-03	19.178	0.320	1.580E-02	19.0	193.4	176.0	466.55	2.143E-03	22.263	1.535E+02	5.034	6.787
1.56	0.44	0.510	0.398	3.641E-03	19.375	0.323	1.564E-02	22.0	198.2	180.3	471.35	2.122E-03	21.349	1.611E+02	5.082	7.981
1.48	0.52	0.505	0.374	3.679E-03	19.576	0.326	1.548E-02	26.0	203.1	184.6	476.25	2.100E-03	20.471	1.718E+02	5.146	9.635

METHOD OF VOLTZ et al.

CO ANALYZER (VOL %)	CO CONVERTED (VOL %)	INITIAL C(CO) (mol/m^3)	REMAINING C(CO) (mol/m^3)	GAS FLOW RATE (m^3/min)	GAS VELOCITY (m/min)	GAS VELOCITY (m/s)	CONTACT TIME (s)	CO CONVERSION (%)	SURFACE TEMP (deg C)	OUTLET TEMP (deg C)	SURFACE TEMP (K)	1/TEMP (1/K)	ADSORPTION RATE CONSTANT (1/mol% CO)	RATE CONSTANT K(s) (1/s)	LN(K(s)) (1/s)	RATE (mol CO/s m^3 CAT)
1.58	0.42	0.793	0.626	2.343E-03	12.469	0.208	2.430E-02	21.0	30.2	29.4	303.35	3.297E-03	15.563	1.244E+02	4.826	7.596
1.88	0.12	0.726	0.682	2.560E-03	13.624	0.227	2.224E-02	6.0	58.3	54.3	331.45	3.017E-03	11.897	2.177E+01	3.081	2.007
1.97	0.03	0.669	0.659	2.778E-03	14.783	0.246	2.050E-02	1.5	86.5	79.3	359.65	2.780E-03	9.478	3.491E+00	1.250	0.492
1.96	0.04	0.635	0.623	2.925E-03	15.564	0.259	1.947E-02	2.0	105.5	95.9	378.65	2.641E-03	8.289	3.567E+00	1.272	0.657
1.94	0.06	0.627	0.609	2.962E-03	15.762	0.263	1.922E-02	3.0	110.3	99.9	383.45	2.608E-03	8.029	5.014E+00	1.612	0.989
2.00	0.00	0.619	0.619	3.000E-03	15.963	0.266	1.898E-02	0.0	115.2	104.4	388.35	2.575E-03	7.780	0.000E+00	0.000	0.000
1.94	0.06	0.612	0.593	3.034E-03	16.165	0.269	1.874E-02	3.0	120.1	108.8	393.25	2.543E-03	7.543	4.449E+00	1.493	0.989
1.96	0.04	0.604	0.592	3.076E-03	16.370	0.273	1.851E-02	2.0	125.1	113.3	398.25	2.511E-03	7.315	2.807E+00	1.032	0.657
1.95	0.05	0.597	0.582	3.114E-03	16.572	0.276	1.828E-02	2.5	130.0	118.1	403.15	2.480E-03	7.104	3.316E+00	1.199	0.822
1.93	0.07	0.589	0.569	3.153E-03	16.777	0.280	1.806E-02	3.5	135.0	123.0	408.15	2.450E-03	6.899	4.383E+00	1.478	1.155
1.92	0.08	0.575	0.532	3.229E-03	17.184	0.286	1.763E-02	4.0	144.9	132.2	418.05	2.392E-03	6.525	4.514E+00	1.507	1.321
1.90	0.10	0.569	0.540	3.267E-03	17.385	0.290	1.743E-02	5.0	149.8	136.8	422.95	2.364E-03	6.354	5.361E+00	1.679	1.655
1.88	0.12	0.562	0.529	3.304E-03	17.583	0.293	1.723E-02	6.0	154.6	141.1	427.75	2.336E-03	6.194	6.129E+00	1.813	1.991
1.83	0.17	0.550	0.503	3.378E-03	17.977	0.300	1.685E-02	8.5	164.2	150.2	437.35	2.286E-03	5.896	7.904E+00	2.067	2.834
1.74	0.26	0.538	0.468	3.453E-03	18.372	0.306	1.649E-02	13.0	173.8	158.6	446.95	2.237E-03	5.624	1.101E+01	2.399	4.387
1.71	0.29	0.532	0.455	3.490E-03	18.573	0.310	1.631E-02	14.5	178.7	162.7	451.85	2.213E-03	5.494	1.177E+01	2.465	4.907
1.71	0.29	0.527	0.450	3.528E-03	18.775	0.313	1.614E-02	14.5	183.6	167.0	456.75	2.189E-03	5.370	1.133E+01	2.427	4.902
1.67	0.33	0.521	0.435	3.566E-03	18.976	0.316	1.597E-02	16.5	188.5	171.3	461.65	2.166E-03	5.252	1.236E+01	2.515	5.568
1.62	0.38	0.516	0.418	3.604E-03	19.178	0.320	1.580E-02	19.0	193.4	176.0	466.55	2.143E-03	5.138	1.366E+01	2.615	6.475
1.56	0.44	0.510	0.398	3.641E-03	19.375	0.323	1.564E-02	22.0	198.2	180.3	471.35	2.122E-03	5.032	1.520E+01	2.721	7.535
1.48	0.52	0.505	0.374	3.679E-03	19.576	0.326	1.548E-02	26.0	203.1	184.6	476.25	2.100E-03	4.927	1.724E+01	2.847	8.961

TABLE L14 REACTOR DATA FOR AGED COADA CATALYST CONTAINING A 22 wt% WASH COAT AND 3 wt% CERIA [SM65].
MONOLITH MASS:0.66776g DIM:4.85*15.6*15.7mm TOTAL SURFACE AREA SUPPORT + WASH COAT: 17.69 m^2/g
GENERAL METHOD

CO ANALYZER (VOL %)	CO CONVERTED (VOL %)	INITIAL C(CO) (mol/m^3)	REMAINING C(CO) (mol/m^3)	GAS FLOW RATE (m^3/min)	GAS VELOCITY (m/min)	GAS VELOCITY (m/s)	CONTACT TIME (s)	CO CONVERSION (%)	SURFACE TEMP (deg C)	OUTLET TEMP (deg C)	SURFACE TEMP (K)	1/TEMP (1/K)	RATE CONSTANT K(s) (1/s)	LN(K(s)) (1/s)	RATE (mol CO/s m^3 CAT)
1.73	0.27	0.782	0.677	2.376E-03	12.763	0.213	2.280E-02	13.5	34.4	32.9	307.55	3.252E-03	0.360	-1.023	4.304
1.88	0.12	0.726	0.682	2.561E-03	13.759	0.229	2.115E-02	6.0	58.4	54.4	331.55	3.016E-03	0.165	-1.799	1.995
1.98	0.02	0.687	0.680	2.705E-03	14.531	0.242	2.003E-02	1.0	77.0	71.1	350.15	2.856E-03	0.028	-3.562	0.341
2.00	0.00	0.652	0.652	2.852E-03	15.320	0.255	1.899E-02	0.0	96.0	88.3	369.15	2.709E-03	0.000	0.000	0.000
2.00	0.00	0.620	0.620	2.999E-03	16.112	0.269	1.806E-02	0.0	115.1	105.0	388.25	2.576E-03	0.000	0.000	0.000
1.99	0.01	0.590	0.587	3.149E-03	16.918	0.282	1.720E-02	0.5	134.5	121.6	407.65	2.453E-03	0.016	-4.106	0.171
1.94	0.06	0.576	0.559	3.225E-03	17.324	0.289	1.680E-02	3.0	144.3	130.5	417.45	2.395E-03	0.103	-2.278	1.014
1.91	0.09	0.569	0.544	3.264E-03	17.536	0.292	1.659E-02	4.5	149.4	134.9	422.55	2.367E-03	0.157	-1.852	1.509
1.82	0.18	0.563	0.512	3.301E-03	17.735	0.296	1.641E-02	9.0	154.2	139.6	427.35	2.340E-03	0.325	-1.124	2.944
1.81	0.19	0.550	0.498	3.378E-03	18.146	0.302	1.604E-02	9.5	164.1	149.3	437.25	2.287E-03	0.352	-1.045	3.099
1.79	0.21	0.544	0.487	3.416E-03	18.349	0.306	1.586E-02	10.5	169.0	153.6	442.15	2.262E-03	0.395	-0.928	3.406
1.75	0.25	0.538	0.471	3.453E-03	18.553	0.309	1.569E-02	12.5	173.9	158.3	447.05	2.237E-03	0.481	-0.731	4.008
1.74	0.26	0.532	0.463	3.492E-03	18.760	0.313	1.551E-02	13.0	178.9	162.9	452.05	2.212E-03	0.508	-0.678	4.157
1.67	0.33	0.527	0.440	3.529E-03	18.959	0.316	1.535E-02	16.5	183.7	167.4	456.85	2.189E-03	0.664	-0.409	5.166
1.62	0.38	0.521	0.422	3.567E-03	19.163	0.319	1.519E-02	19.0	188.6	171.7	461.75	2.166E-03	0.784	-0.243	5.856
1.56	0.44	0.515	0.402	3.606E-03	19.370	0.323	1.502E-02	22.0	193.6	176.3	466.75	2.142E-03	0.935	-0.067	6.649

METHOD OF KOBERSTEIN & WANNEMACHER

CO ANALYZER (VOL %)	CO CONVERTED (VOL %)	INITIAL C(CO) (mol/m^3)	REMAINING C(CO) (mol/m^3)	GAS FLOW RATE (m^3/min)	GAS VELOCITY (m/min)	GAS VELOCITY (m/s)	CONTACT TIME (s)	CO CONVERSION (%)	SURFACE TEMP (deg C)	OUTLET TEMP (deg C)	SURFACE TEMP (K)	1/TEMP (1/K)	ADSORPTION RATE CONSTANT (1/mol% CO)	RATE CONSTANT K(s) (1/s)	LN(K(s)) (1/s)	RATE (mol CO/s m^3 CAT)
1.73	0.27	0.782	0.677	2.376E-03	12.763	0.213	2.280E-02	13.5	34.4	32.9	307.55	3.252E-03	187.813	6.834E+03	8.830	4.987
1.88	0.12	0.726	0.682	2.561E-03	13.759	0.229	2.115E-02	6.0	58.4	54.4	331.55	3.016E-03	119.404	1.196E+03	7.086	2.122
1.98	0.02	0.687	0.680	2.705E-03	14.531	0.242	2.003E-02	1.0	77.0	71.1	350.15	2.856E-03	87.724	1.054E+02	4.658	0.345
2.00	0.00	0.652	0.652	2.852E-03	15.320	0.255	1.899E-02	0.0	96.0	88.3	369.15	2.709E-03	66.110	0.000E+00	0.000	0.000
2.00	0.00	0.620	0.620	2.999E-03	16.112	0.269	1.806E-02	0.0	115.1	105.0	388.25	2.576E-03	51.156	0.000E+00	0.000	0.000
1.99	0.01	0.590	0.587	3.149E-03	16.918	0.282	1.720E-02	0.5	134.5	121.6	407.65	2.453E-03	40.407	1.012E+01	2.314	0.172
1.94	0.06	0.576	0.559	3.225E-03	17.324	0.289	1.680E-02	3.0	144.3	130.5	417.45	2.395E-03	36.168	4.751E+01	3.861	1.044
1.91	0.09	0.569	0.544	3.264E-03	17.536	0.292	1.659E-02	4.5	149.4	134.9	422.55	2.367E-03	34.210	6.297E+01	4.143	1.576
1.82	0.18	0.563	0.512	3.301E-03	17.735	0.296	1.641E-02	9.0	154.2	139.6	427.35	2.340E-03	32.505	1.108E+02	4.708	3.223
1.81	0.19	0.550	0.498	3.378E-03	18.146	0.302	1.604E-02	9.5	164.1	149.3	437.25	2.287E-03	29.354	9.436E+01	4.547	3.408
1.79	0.21	0.544	0.487	3.416E-03	18.349	0.306	1.586E-02	10.5	169.0	153.6	442.15	2.262E-03	27.956	9.382E+01	4.541	3.785
1.73	0.27	0.538	0.465	3.453E-03	18.553	0.309	1.569E-02	13.5	173.9	158.3	447.05	2.237E-03	26.654	1.078E+02	4.680	4.939
1.74	0.26	0.532	0.463	3.492E-03	18.760	0.313	1.551E-02	13.0	178.9	162.9	452.05	2.212E-03	25.415	9.435E+01	4.547	4.741
1.67	0.33	0.527	0.440	3.529E-03	18.959	0.316	1.535E-02	16.5	183.7	167.4	456.85	2.189E-03	24.303	1.075E+02	4.678	6.125
1.62	0.38	0.521	0.422	3.567E-03	19.163	0.319	1.519E-02	19.0	188.6	171.7	461.75	2.166E-03	23.241	1.117E+02	4.716	7.142
1.56	0.44	0.515	0.402	3.606E-03	19.370	0.323	1.502E-02	22.0	193.6	176.3	466.75	2.142E-03	22.226	1.166E+02	4.759	8.399

METHOD OF VOLTZ et al.

CO ANALYZER (VOL %)	CO CONVERTED (VOL %)	INITIAL C(CO) (mol/m^3)	REMAINING C(CO) (mol/m^3)	GAS FLOW RATE (m^3/min)	GAS VELOCITY (m/min)	GAS VELOCITY (m/s)	CONTACT TIME (s)	CO CONVERSION (%)	SURFACE TEMP (deg C)	OUTLET TEMP (deg C)	SURFACE TEMP (K)	1/TEMP (1/K)	ADSORPTION RATE CONSTANT (1/mol% CO)	RATE CONSTANT K(s) (1/s)	LN(K(s)) (1/s)	RATE (mol CO/s m^3 CAT)
1.73	0.27	0.782	0.677	2.376E-03	12.763	0.213	2.280E-02	13.5	34.4	32.9	307.55	3.252E-03	13.783	4.385E+01	3.781	4.923
1.88	0.12	0.726	0.682	2.561E-03	13.759	0.229	2.115E-02	6.0	58.4	54.4	331.55	3.016E-03	11.055	1.275E+01	2.545	2.109
1.98	0.02	0.687	0.680	2.705E-03	14.531	0.242	2.003E-02	1.0	77.0	71.1	350.15	2.856E-03	9.514	1.597E+00	0.468	0.344
2.00	0.00	0.652	0.652	2.852E-03	15.320	0.255	1.899E-02	0.0	96.0	88.3	369.15	2.709E-03	8.290	0.000E+00	0.000	0.000
2.00	0.00	0.620	0.620	2.999E-03	16.112	0.269	1.806E-02	0.0	115.1	105.0	388.25	2.576E-03	7.317	0.000E+00	0.000	0.000
1.99	0.01	0.590	0.587	3.149E-03	16.918	0.282	1.720E-02	0.5	134.5	121.6	407.65	2.453E-03	6.523	3.858E-01	-0.952	0.172
1.94	0.06	0.576	0.559	3.225E-03	17.324	0.289	1.680E-02	3.0	144.3	130.5	417.45	2.395E-03	6.180	2.083E+00	0.734	1.038
1.91	0.09	0.569	0.544	3.264E-03	17.536	0.292	1.659E-02	4.5	149.4	134.9	422.55	2.367E-03	6.015	2.964E+00	1.087	1.563
1.82	0.18	0.563	0.512	3.301E-03	17.735	0.296	1.641E-02	9.0	154.2	139.6	427.35	2.340E-03	5.867	5.603E+00	1.723	3.165
1.81	0.19	0.550	0.498	3.378E-03	18.146	0.302	1.604E-02	9.5	164.1	149.3	437.25	2.287E-03	5.583	5.418E+00	1.690	3.340
1.79	0.21	0.544	0.487	3.416E-03	18.349	0.306	1.586E-02	10.5	169.0	153.6	442.15	2.262E-03	5.452	5.736E+00	1.747	3.699
1.73	0.27	0.538	0.465	3.453E-03	18.553	0.309	1.569E-02	13.5	173.9	158.3	447.05	2.237E-03	5.327	7.040E+00	1.952	4.788
1.74	0.26	0.532	0.463	3.492E-03	18.760	0.313	1.551E-02	13.0	178.9	162.9	452.05	2.212E-03	5.205	6.530E+00	1.876	4.600
1.67	0.33	0.527	0.440	3.529E-03	18.959	0.316	1.535E-02	16.5	183.7	167.4	456.85	2.189E-03	5.093	7.933E+00	2.071	5.881
1.62	0.38	0.521	0.422	3.567E-03	19.163	0.319	1.519E-02	19.0	188.6	171.7	461.75	2.166E-03	4.983	8.770E+00	2.171	6.801
1.56	0.44	0.515	0.402	3.606E-03	19.370	0.323	1.502E-02	22.0	193.6	176.3	466.75	2.142E-03	4.876	9.748E+00	2.277	7.912

TABLE I.15 REACTOR DATA FOR AGED COADA CATALYST CONTAINING A 23 wt% WASH COAT AND 3 wt% CERIA BUILT INTO THE STRUCTURE [SM45].
MONOLITH MASS:0.72175g DIM:5.05*15.7*15.7mm TOTAL SURFACE AREA SUPPORT + WASH COAT: 16.84 m^2/g
GENERAL METHOD

CO ANALYZER (VOL %)	CO CONVERTED (VOL %)	INITIAL C(CO) (mol/m^3)	REMAINING C(CO) (mol/m^3)	GAS FLOW RATE (m^3/min)	GAS VELOCITY (m/min)	GAS VELOCITY (m/s)	CONTACT TIME (s)	CO CONVERSION (%)	SURFACE TEMP (deg C)	OUTLET TEMP (deg C)	SURFACE TEMP (K)	1/TEMP (1/K)	RATE CONSTANT K(s) (1/s)	LN(K(s)) (1/s)	RATE (mol CO/s m^3 CAT)
1.73	0.27	0.804	0.695	2.312E-03	12.340	0.206	2.455E-02	13.5	26.1	25.5	299.25	3.342E-03	0.351	-1.048	4.107
2.00	0.00	0.726	0.726	2.560E-03	13.668	0.228	2.217E-02	0.0	58.3	53.8	331.45	3.017E-03	0.000	0.000	0.000
2.00	0.00	0.687	0.687	2.706E-03	14.443	0.241	2.098E-02	0.0	77.1	70.5	350.25	2.855E-03	0.000	0.000	0.000
2.00	0.00	0.652	0.652	2.851E-03	15.218	0.254	1.991E-02	0.0	95.9	87.3	369.05	2.710E-03	0.000	0.000	0.000
2.00	0.00	0.620	0.620	2.998E-03	16.006	0.267	1.893E-02	0.0	115.0	104.4	388.15	2.576E-03	0.000	0.000	0.000
2.00	0.00	0.590	0.590	3.147E-03	16.802	0.280	1.803E-02	0.0	134.3	121.4	407.45	2.454E-03	0.000	0.000	0.000
1.96	0.04	0.584	0.572	3.185E-03	17.000	0.283	1.782E-02	2.0	139.1	125.6	412.25	2.426E-03	0.067	-2.698	0.648
1.92	0.08	0.576	0.553	3.224E-03	17.210	0.287	1.761E-02	4.0	144.2	130.2	417.35	2.396E-03	0.138	-1.983	1.283
1.88	0.12	0.570	0.536	3.262E-03	17.412	0.290	1.740E-02	6.0	149.1	134.3	422.25	2.368E-03	0.211	-1.555	1.904
1.87	0.13	0.563	0.527	3.300E-03	17.614	0.294	1.720E-02	6.5	154.0	139.0	427.15	2.341E-03	0.232	-1.461	2.057
1.82	0.18	0.557	0.507	3.338E-03	17.820	0.297	1.700E-02	9.0	159.0	143.8	432.15	2.314E-03	0.329	-1.111	2.810
1.80	0.20	0.551	0.495	3.375E-03	18.018	0.300	1.682E-02	10.0	163.8	148.5	436.95	2.289E-03	0.372	-0.989	3.104
1.76	0.24	0.544	0.479	3.414E-03	18.224	0.304	1.663E-02	12.0	168.8	153.1	441.95	2.263E-03	0.457	-0.784	3.683
1.74	0.26	0.538	0.468	3.452E-03	18.426	0.307	1.644E-02	13.0	173.7	157.5	446.85	2.238E-03	0.503	-0.687	3.966
1.72	0.28	0.532	0.458	3.490E-03	18.632	0.311	1.626E-02	14.0	178.7	162.3	451.85	2.213E-03	0.551	-0.596	4.246
1.63	0.37	0.527	0.429	3.527E-03	18.826	0.314	1.609E-02	18.5	183.4	166.7	456.55	2.190E-03	0.755	-0.281	5.458
1.59	0.41	0.521	0.414	3.565E-03	19.028	0.317	1.592E-02	20.5	188.3	170.0	461.45	2.167E-03	0.856	-0.156	5.971
1.56	0.44	0.516	0.402	3.603E-03	19.235	0.321	1.575E-02	22.0	193.3	175.4	466.45	2.144E-03	0.937	-0.065	6.345

METHOD OF KOBERSTEIN & WANNEMACHER

CO ANALYZER (VOL %)	CO CONVERTED (VOL %)	INITIAL C(CO) (mol/m^3)	REMAINING C(CO) (mol/m^3)	GAS FLOW RATE (m^3/min)	GAS VELOCITY (m/min)	GAS VELOCITY (m/s)	CONTACT TIME (s)	CO CONVERSION (%)	SURFACE TEMP (deg C)	OUTLET TEMP (deg C)	SURFACE TEMP (K)	1/TEMP (1/K)	ADSORPTIO RATE CONSTANT (1/mol% CO)	RATE CONSTANT K(s) (1/s)	LN(K(s)) (1/s)	RATE (mol CO/s m^3 CAT)
1.73	0.27	0.804	0.695	2.312E-03	12.340	0.206	2.455E-02	13.5	26.1	25.5	299.25	3.342E-03	223.406	9.937E+03	9.204	4.760
2.00	0.00	0.726	0.726	2.560E-03	13.668	0.228	2.217E-02	0.0	58.3	53.8	331.45	3.017E-03	119.613	0.000E+00	0.000	0.000
2.00	0.00	0.687	0.687	2.706E-03	14.443	0.241	2.098E-02	0.0	77.1	70.5	350.25	2.855E-03	87.586	0.000E+00	0.000	0.000
2.00	0.00	0.652	0.652	2.851E-03	15.218	0.254	1.991E-02	0.0	95.9	87.3	369.05	2.710E-03	66.204	0.000E+00	0.000	0.000
2.00	0.00	0.620	0.620	2.998E-03	16.006	0.267	1.893E-02	0.0	115.0	104.4	388.15	2.576E-03	51.221	0.000E+00	0.000	0.000
2.00	0.00	0.590	0.590	3.147E-03	16.802	0.280	1.803E-02	0.0	134.3	121.4	407.45	2.454E-03	40.500	0.000E+00	0.000	0.000
1.96	0.04	0.584	0.572	3.185E-03	17.000	0.283	1.782E-02	2.0	139.1	125.6	412.25	2.426E-03	38.333	3.605E+01	3.585	0.661
1.92	0.08	0.576	0.553	3.224E-03	17.210	0.287	1.761E-02	4.0	144.2	130.2	417.35	2.396E-03	36.208	6.336E+01	4.149	1.334
1.88	0.12	0.570	0.536	3.262E-03	17.412	0.290	1.740E-02	6.0	149.1	134.3	422.25	2.368E-03	34.321	8.415E+01	4.433	2.021
1.87	0.13	0.563	0.527	3.300E-03	17.614	0.294	1.720E-02	6.5	154.0	139.0	427.15	2.341E-03	32.573	8.152E+01	4.401	2.194
1.82	0.18	0.557	0.507	3.338E-03	17.820	0.297	1.700E-02	9.0	159.0	143.8	432.15	2.314E-03	30.919	1.001E+02	4.606	3.075
1.80	0.20	0.551	0.495	3.375E-03	18.018	0.300	1.682E-02	10.0	163.8	148.5	436.95	2.289E-03	29.443	9.996E+01	4.605	3.432
1.76	0.24	0.544	0.479	3.414E-03	18.224	0.304	1.663E-02	12.0	168.8	153.1	441.95	2.263E-03	28.012	1.072E+02	4.675	4.159
1.71	0.29	0.538	0.460	3.452E-03	18.426	0.307	1.644E-02	14.5	173.7	157.5	446.85	2.238E-03	26.706	1.160E+02	4.754	5.089
1.72	0.28	0.532	0.458	3.490E-03	18.632	0.311	1.626E-02	14.0	178.7	162.3	451.85	2.213E-03	25.463	1.018E+02	4.623	4.898
1.63	0.37	0.527	0.429	3.527E-03	18.826	0.314	1.609E-02	18.5	183.4	166.7	456.55	2.190E-03	24.371	1.204E+02	4.791	6.625
1.59	0.41	0.521	0.414	3.565E-03	19.028	0.317	1.592E-02	20.5	188.3	170.0	461.45	2.167E-03	23.304	1.207E+02	4.793	7.415
1.56	0.44	0.516	0.402	3.603E-03	19.235	0.321	1.575E-02	22.0	193.3	175.4	466.45	2.144E-03	22.285	1.175E+02	4.766	8.016

METHOD OF VOLTZ et al.

CO ANALYZER (VOL %)	CO CONVERTED (VOL %)	INITIAL C(CO) (mol/m^3)	REMAINING C(CO) (mol/m^3)	GAS FLOW RATE (m^3/min)	GAS VELOCITY (m/min)	GAS VELOCITY (m/s)	CONTACT TIME (s)	CO CONVERSION (%)	SURFACE TEMP (deg C)	OUTLET TEMP (deg C)	SURFACE TEMP (K)	1/TEMP (1/K)	ADSORPTIO RATE CONSTANT (1/mol% CO)	RATE CONSTANT K(s) (1/s)	LN(K(s)) (1/s)	RATE (mol CO/s m^3 CAT)
1.73	0.27	0.804	0.695	2.312E-03	12.340	0.206	2.455E-02	13.5	26.1	25.5	299.25	3.342E-03	14.998	5.248E+01	3.960	4.704
2.00	0.00	0.726	0.726	2.560E-03	13.668	0.228	2.217E-02	0.0	58.3	53.8	331.45	3.017E-03	11.064	0.000E+00	0.000	0.000
2.00	0.00	0.687	0.687	2.706E-03	14.443	0.241	2.098E-02	0.0	77.1	70.5	350.25	2.855E-03	9.507	0.000E+00	0.000	0.000
2.00	0.00	0.652	0.652	2.851E-03	15.218	0.254	1.991E-02	0.0	95.9	87.3	369.05	2.710E-03	8.296	0.000E+00	0.000	0.000
2.00	0.00	0.620	0.620	2.998E-03	16.006	0.267	1.893E-02	0.0	115.0	104.4	388.15	2.576E-03	7.321	0.000E+00	0.000	0.000
2.00	0.00	0.590	0.590	3.147E-03	16.802	0.280	1.803E-02	0.0	134.3	121.4	407.45	2.454E-03	6.530	0.000E+00	0.000	0.000
1.96	0.04	0.584	0.572	3.185E-03	17.000	0.283	1.782E-02	2.0	139.1	125.6	412.25	2.426E-03	6.358	1.470E+00	0.385	0.659
1.92	0.08	0.576	0.553	3.224E-03	17.210	0.287	1.761E-02	4.0	144.2	130.2	417.35	2.396E-03	6.184	2.779E+00	1.022	1.325
1.88	0.12	0.570	0.536	3.262E-03	17.412	0.290	1.740E-02	6.0	149.1	134.3	422.25	2.368E-03	6.025	3.956E+00	1.375	1.997
1.87	0.13	0.563	0.527	3.300E-03	17.614	0.294	1.720E-02	6.5	154.0	139.0	427.15	2.341E-03	5.873	4.091E+00	1.409	2.166
1.82	0.18	0.557	0.507	3.338E-03	17.820	0.297	1.700E-02	9.0	159.0	143.8	432.15	2.314E-03	5.726	5.383E+00	1.683	3.018
1.80	0.20	0.551	0.495	3.375E-03	18.018	0.300	1.682E-02	10.0	163.8	148.5	436.95	2.289E-03	5.591	5.725E+00	1.745	3.360
1.76	0.24	0.544	0.479	3.414E-03	18.224	0.304	1.663E-02	12.0	168.8	153.1	441.95	2.263E-03	5.457	6.558E+00	1.881	4.050
1.71	0.29	0.538	0.460	3.452E-03	18.426	0.307	1.644E-02	14.5	173.7	157.5	446.85	2.238E-03	5.332	7.573E+00	2.025	4.920
1.72	0.28	0.532	0.458	3.490E-03	18.632	0.311	1.626E-02	14.0	178.7	162.3	451.85	2.213E-03	5.210	7.044E+00	1.952	4.739
1.63	0.37	0.527	0.429	3.527E-03	18.826	0.314	1.609E-02	18.5	183.4	166.7	456.55	2.190E-03	5.100	8.895E+00	2.185	6.322
1.59	0.41	0.521	0.414	3.565E-03	19.028	0.317	1.592E-02	20.5	188.3	170.0	461.45	2.167E-03	4.990	9.475E+00	2.249	7.026
1.56	0.44	0.516	0.402	3.603E-03	19.235	0.321	1.575E-02	22.0	193.3	175.4	466.45	2.144E-03	4.882	9.792E+00	2.282	7.551

APPENDIX J. ARRHENIUS PLOTS.

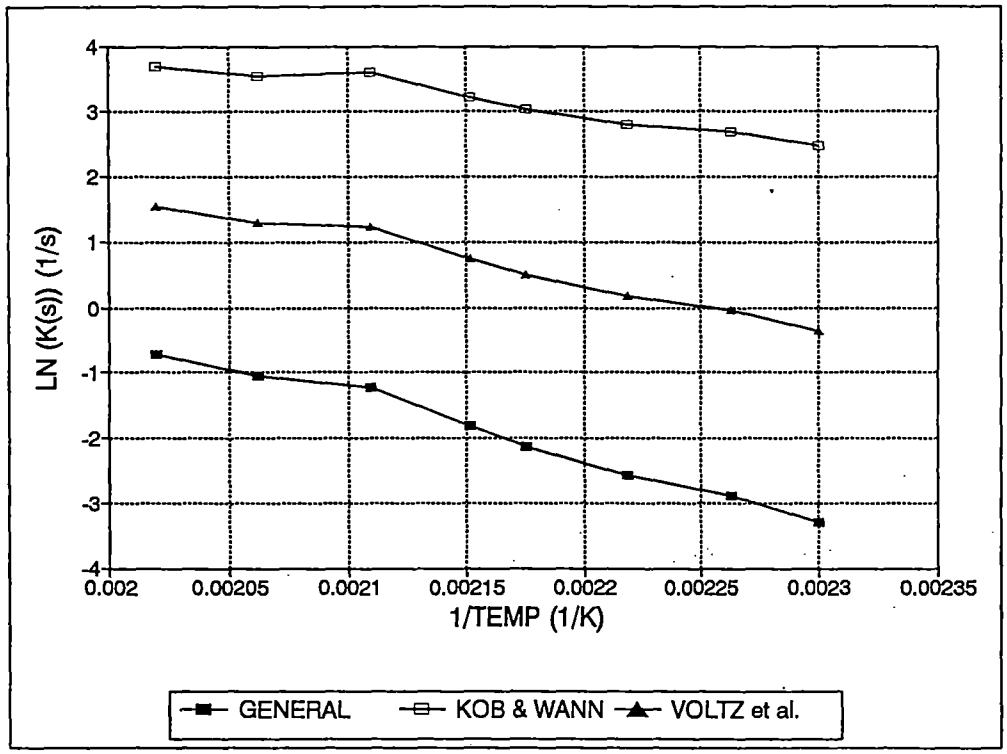

Figure J.1 Arrhenius plots for fresh commercial standard catalyst containing 11 wt% ceria.

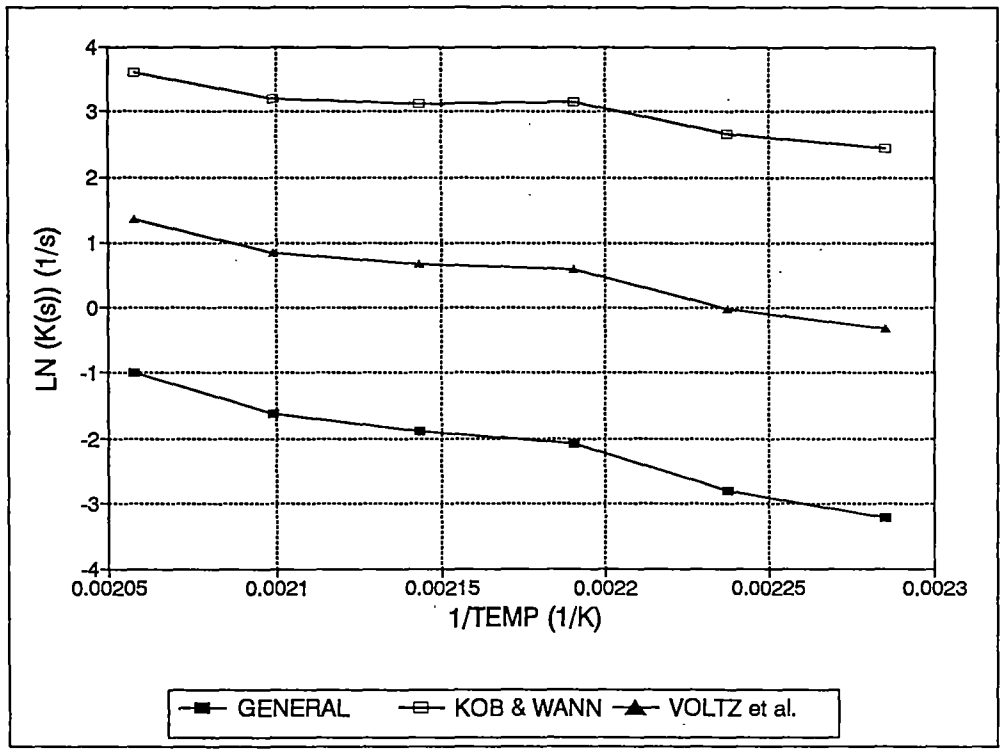

Figure J.2 Arrhenius plots for second fresh commercial standard catalyst containing 11 wt% ceria.

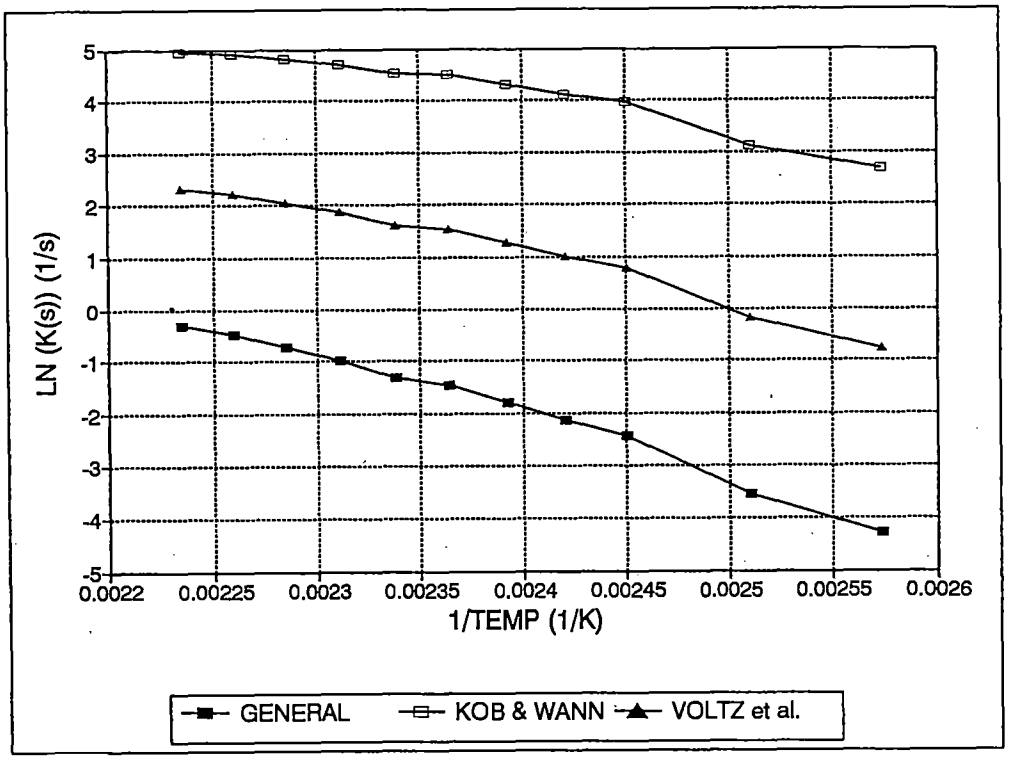

Figure J.3 Arrhenius plots for fresh 16 wt% COADA catalyst containing 11 wt% ceria.

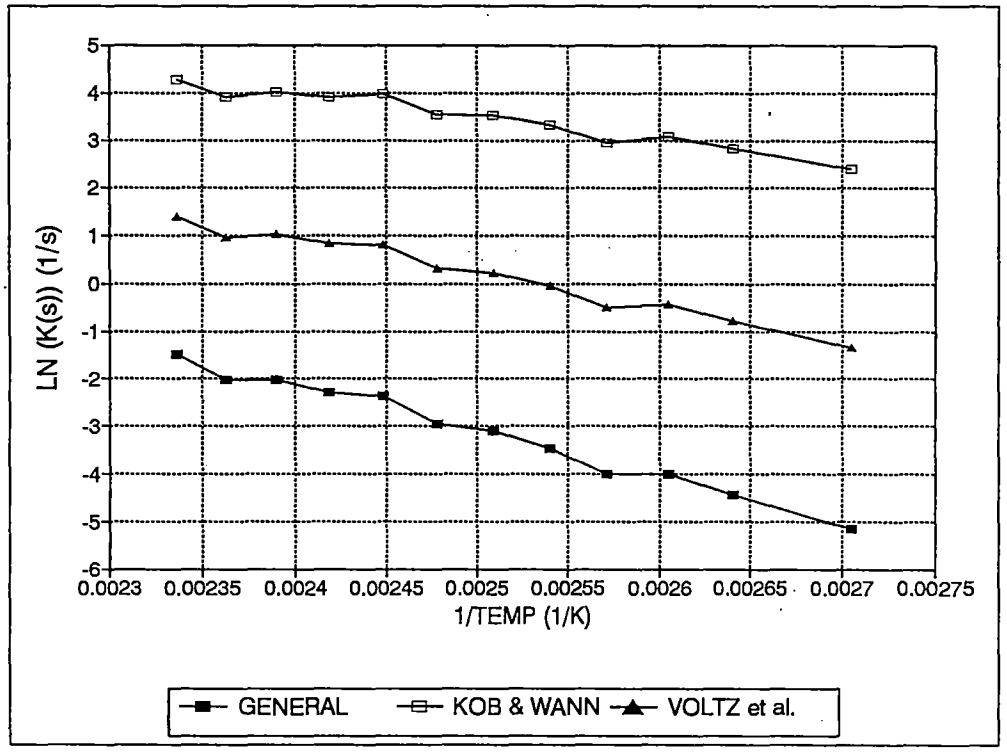

Figure J.4 Arrhenius plots for fresh 38 wt% COADA catalyst containing 11 wt% ceria.

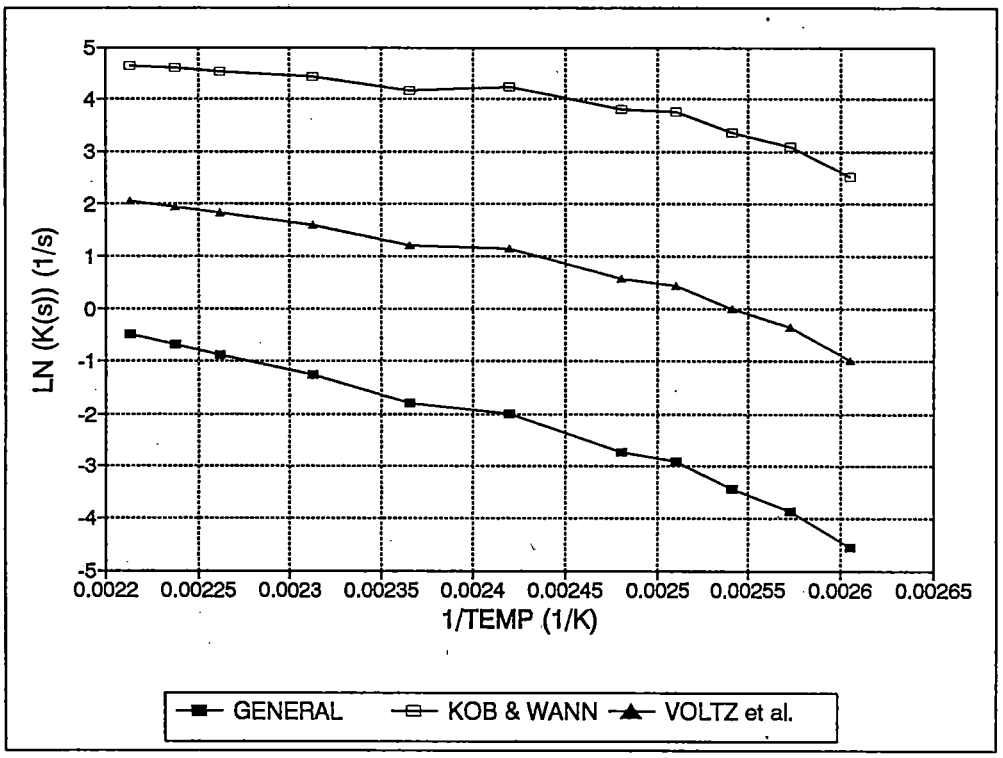

Figure J.5 Arrhenius plots for fresh 20.5 wt% COADA catalyst containing 3 wt% ceria.

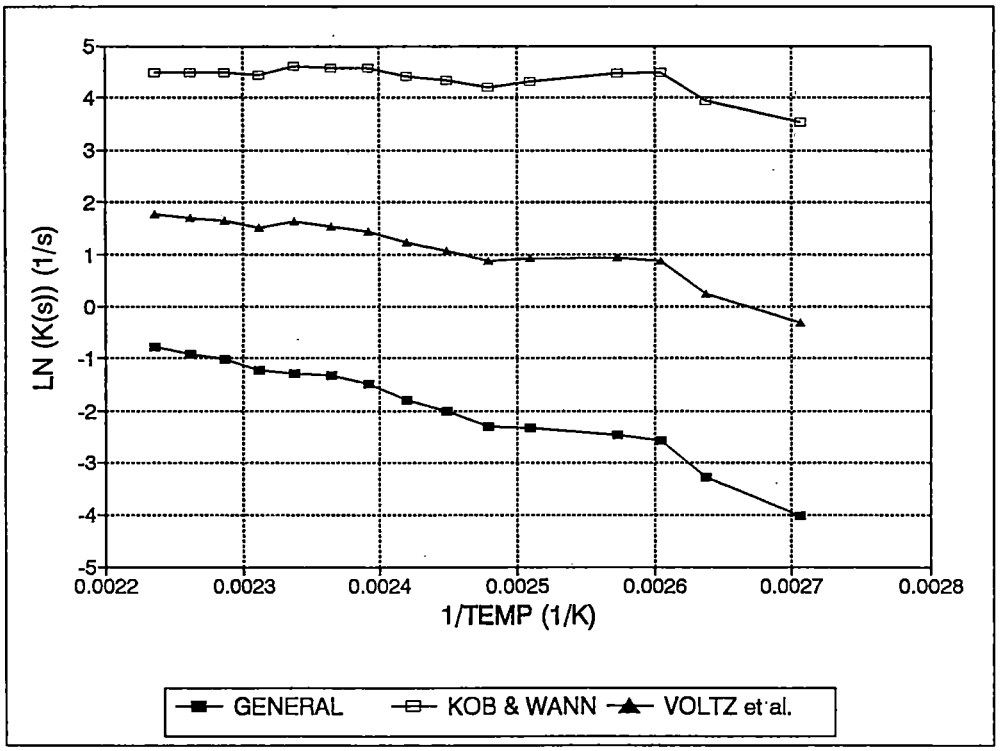

Figure J.6 Arrhenius plots for fresh 20.8 wt% COADA catalyst containing 3 wt% built in ceria.

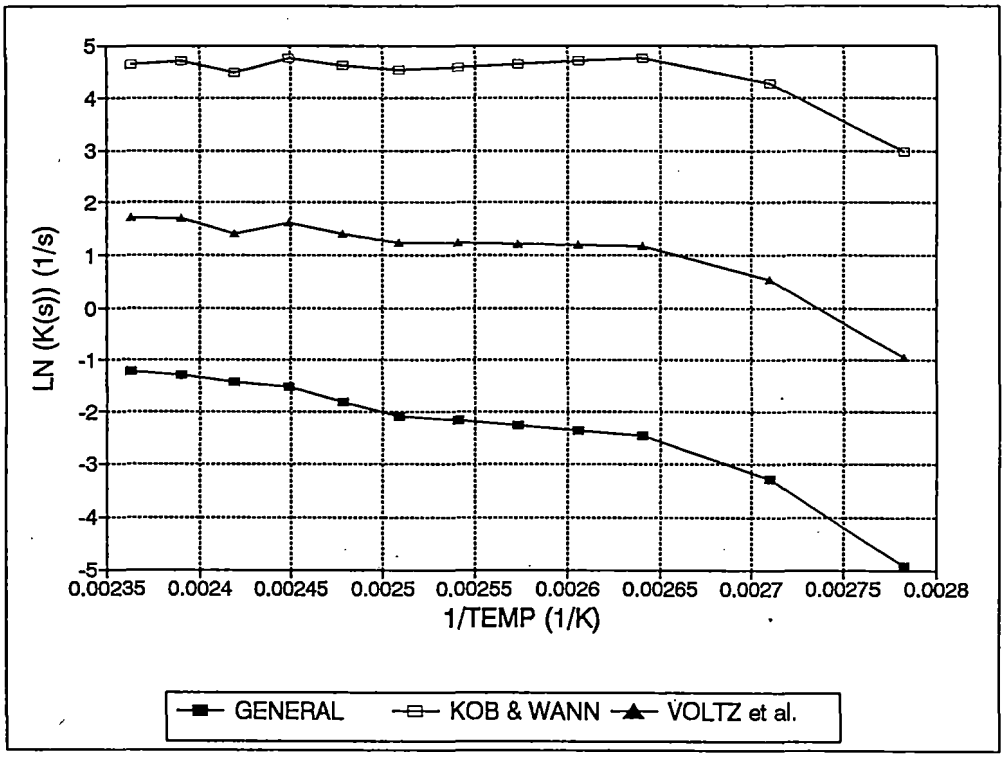

Figure **J.7** Arrhenius plots for fresh 36 wt% commercial powder catalyst containing 11 wt% ceria.

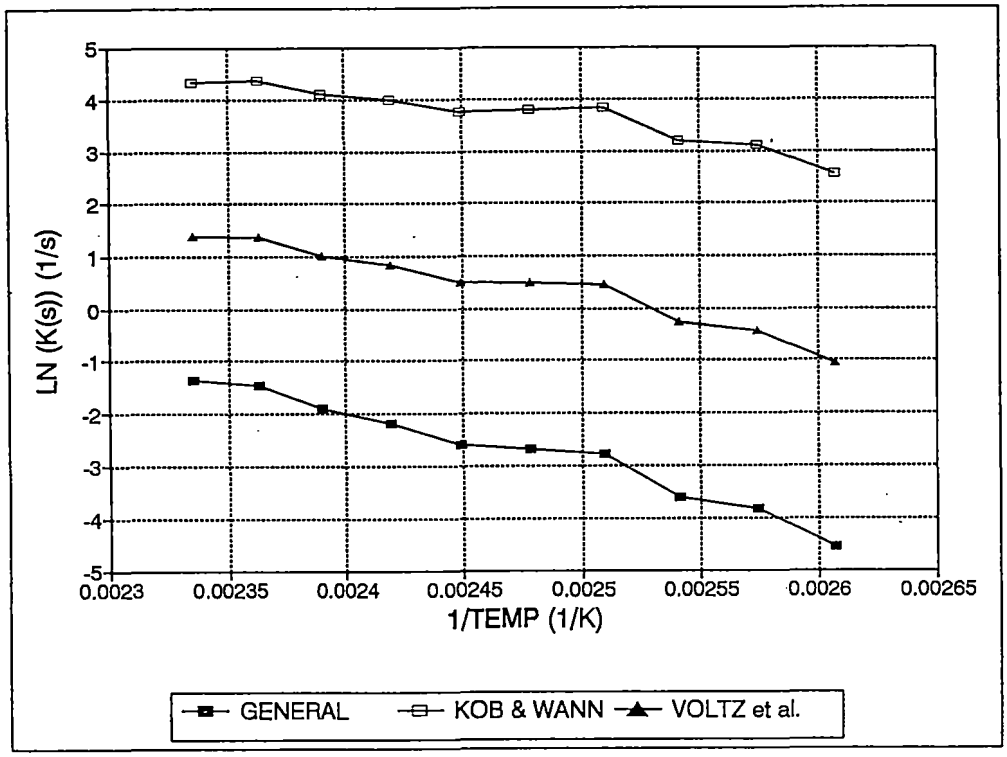

Figure **J.8** Arrhenius plots for fresh 58 wt% commercial powder catalyst containing 11 wt% ceria.

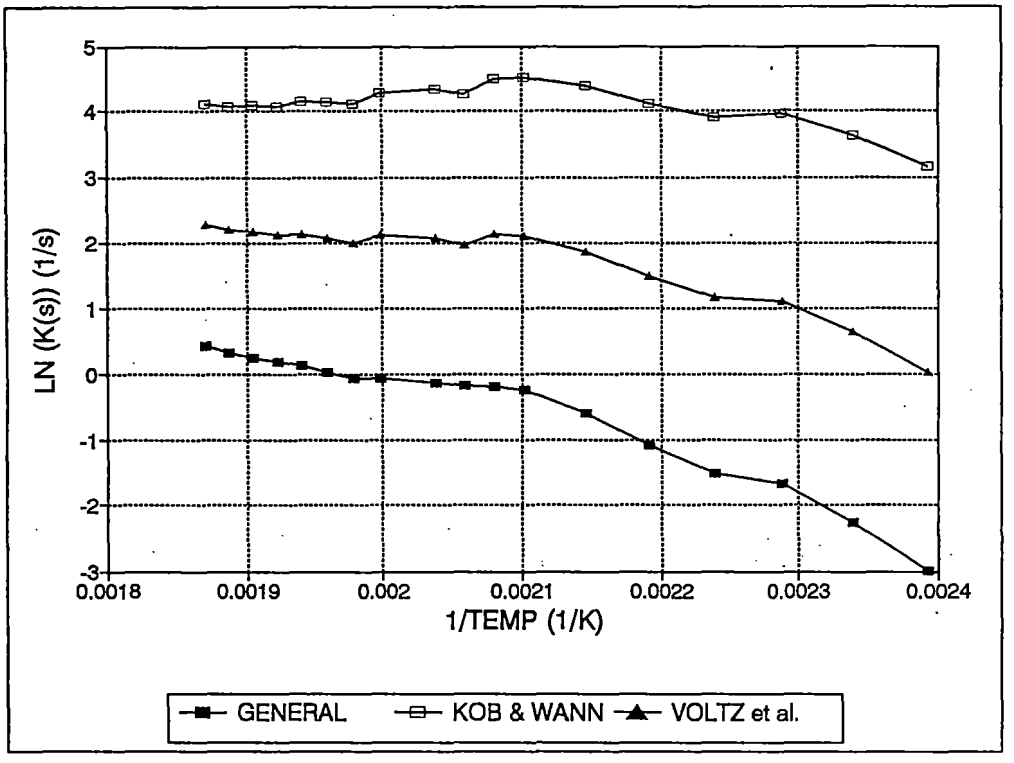

Figure **J.9** Arrhenius plots for aged 31 wt% commercial standard catalyst containing 11 wt% ceria.

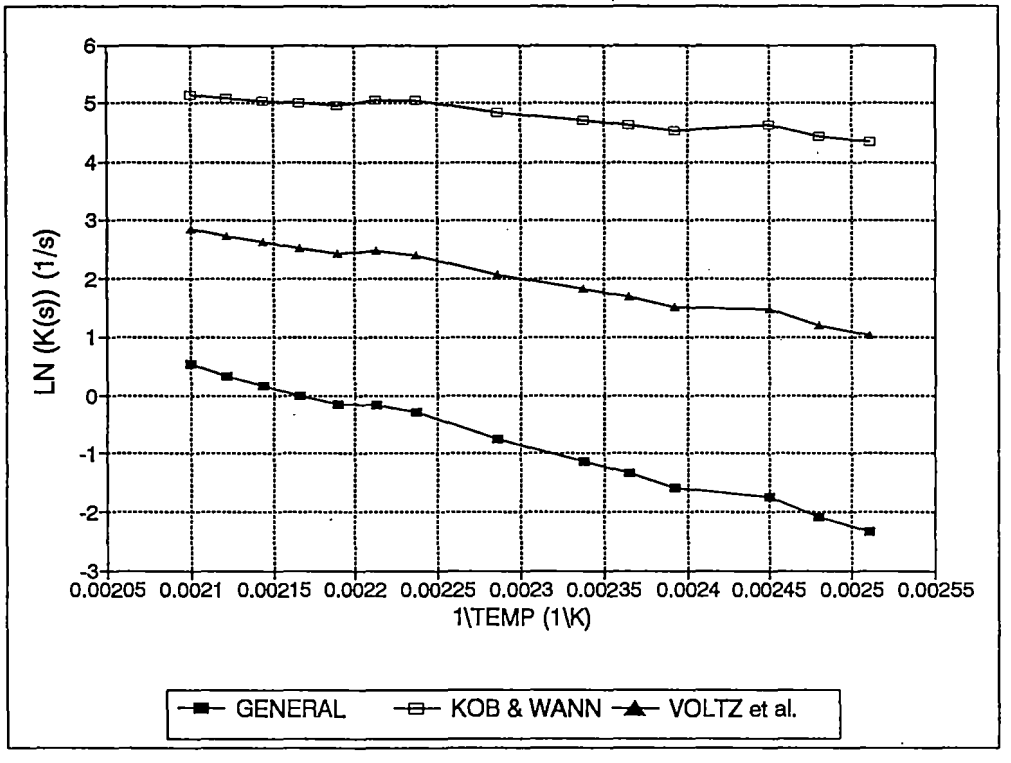

Figure **J.10** Arrhenius plots for aged 22 wt% COADA catalyst containing 11 wt% ceria.

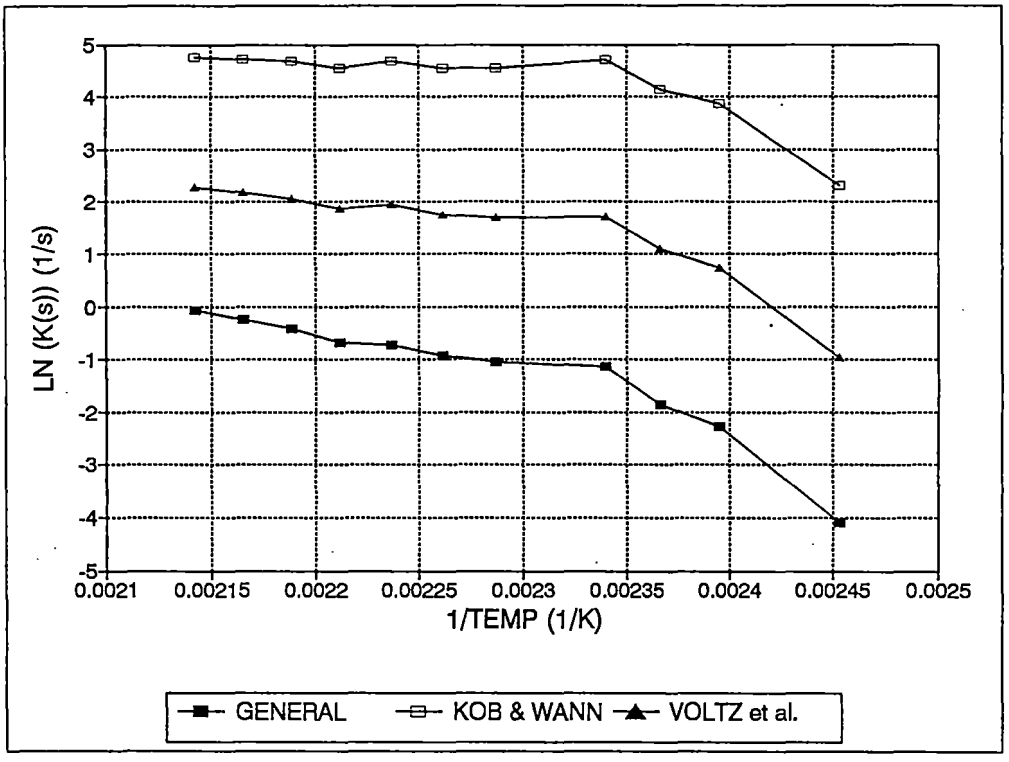

Figure **J.11** Arrhenius plots for aged 22 wt% COADA catalyst containing 3 wt% ceria.

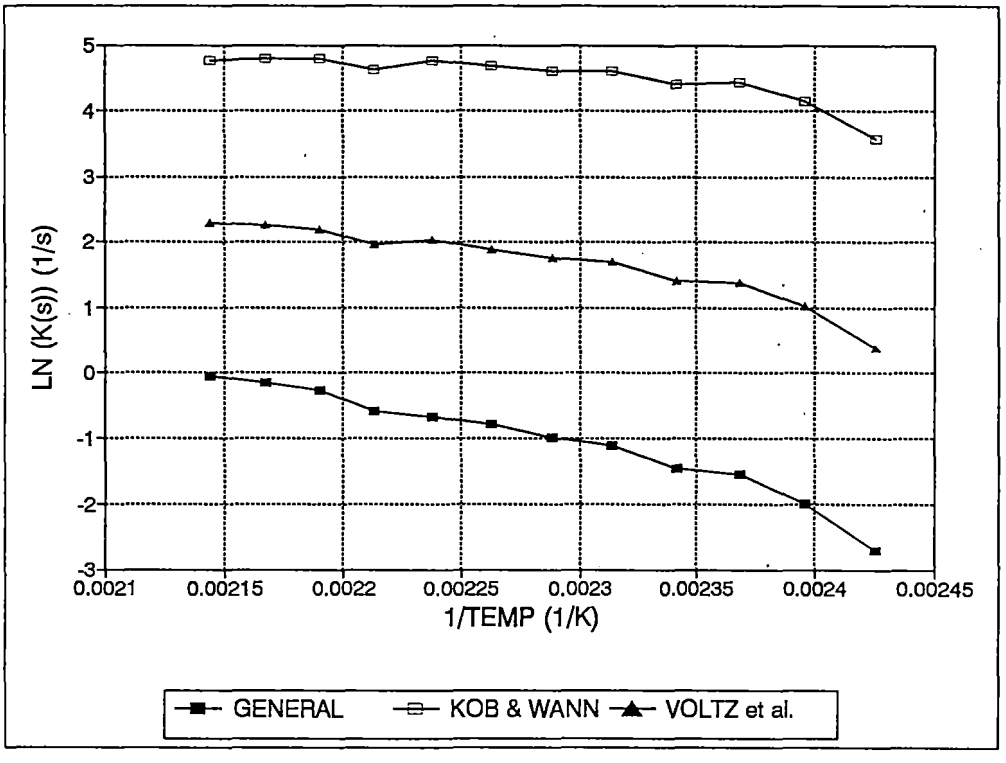

Figure **J.12** Arrhenius plots for aged 23 wt% COADA catalyst containing 3 wt% built in ceria.

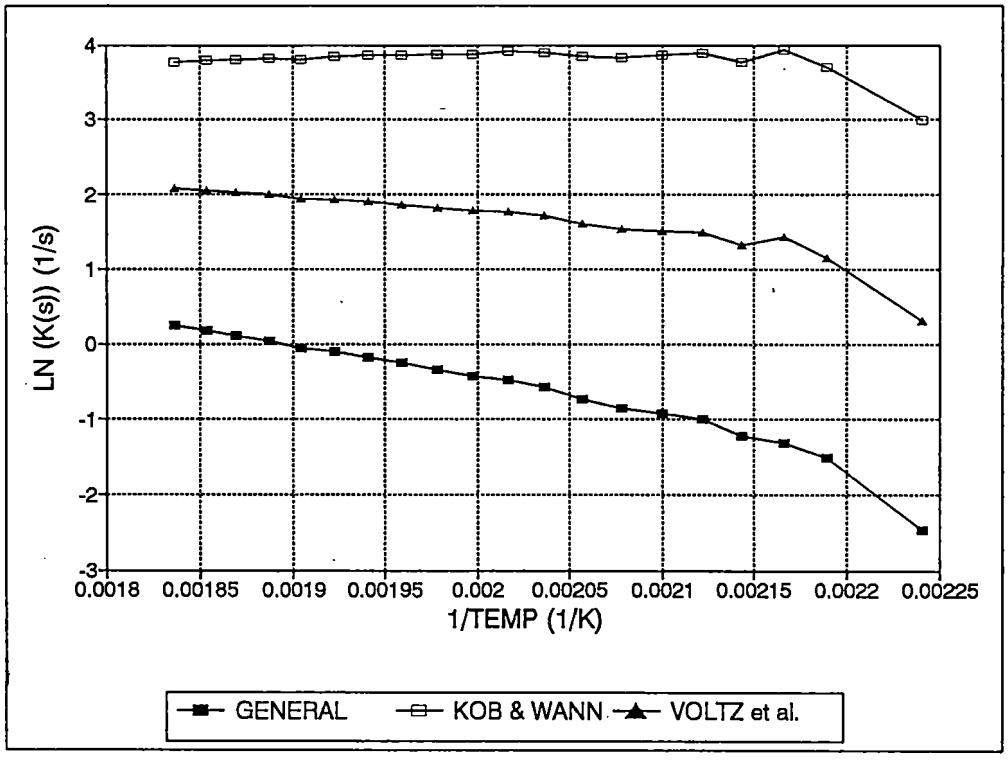

Figure J.13 Arrhenius plots for aged 28 wt% commercial powder catalyst containing 11 wt% ceria.

APPENDIX K. COMPOSITION OF COMMERCIALLY COATED MONOLITH.

The alumina layer was removed from a commercially coated monolith by means of a mechanical method and chemically analysed and its composition is shown in Table K.1.

Table K.1 Composition of commercially coated monolith.

Component	Concentration (weight percent)
Al_2O_3	73.5
Fe_2O_3	1.78
CeO_2	10.7
ZrO_2	5.2
Pt	1.1
Rh	0.162
La_2O_3	0.035
BaO	0.128
Total	92.61

Note: Phosphorus and bromine were also detected by x-ray fluorescence, but the sample was insufficient to determine the amounts present.

APPENDIX L. TYPICAL RESULTS OBTAINED DURING MERCURY POROSIMETER ANALYSIS.

CAT 214 14/10/91
VOLUME MAX = .5 ML.
PRESSURE MAX= 70000 PSI.

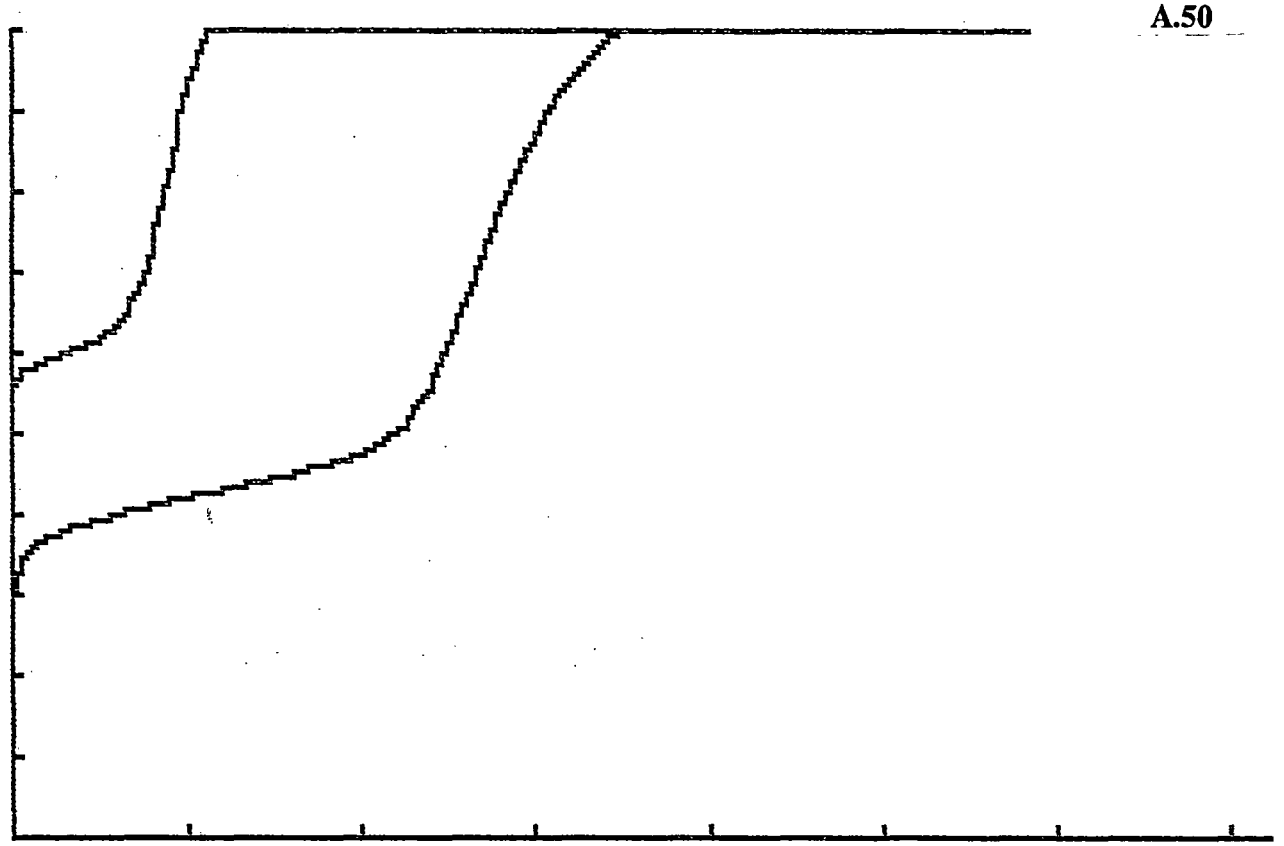

RUN- CAT 214 14/10/91 WEIGHT- .5972 G.

PRESS (PSI)	VOL (ML)	RAD (NM)	DV/DP (ML/PSI)	DV(R) (ML/NM)	DS(R) (SQM/NM)	AREA (SQM)
20	1E-10	5333	0	0	0	0
30	.0484	3555.333	4.8399E-03	2.7226E-05	1.2252E-05	.0226
50	.0753	2133.2	1.345E-03	1.8915E-05	1.3300E-05	.0428
70	.0936	1523.714	9.15E-04	3.0025E-05	3.2842E-05	.0634
100	.1085	1066.6	4.9666E-04	3.2595E-05	5.0334E-05	.0871
130	.1218	820.461	4.4333E-04	5.4034E-05	1.1453E-04	.1158
160	.1307	666.625	2.9666E-04	5.7853E-05	1.5561E-04	.1400
190	.136	561.368	1.7666E-04	5.0353E-05	1.6401E-04	.1574
230	.1425	463.739	1.6249E-04	6.6578E-05	2.5979E-04	.1830
260	.1465	410.23	1.3333E-04	7.4754E-05	3.4213E-04	.2014
300	.1507	355.533	1.05E-04	7.6786E-05	4.0109E-04	.2234
340	.1542	313.705	8.7499E-05	8.3677E-05	5.0013E-04	.2444
390	.1574	273.487	6.4000E-05	7.9564E-05	5.4200E-04	.2663
420	.1599	253.952	8.3333E-05	1.2797E-04	9.7055E-04	.2853
500	.1631	213.32	4.0000E-05	7.8754E-05	6.7416E-04	.3129
580	.1662	183.896	3.8749E-05	1.0535E-04	1.0609E-03	.3443
660	.1683	161.606	2.6249E-05	9.4210E-05	1.0907E-03	.3687
740	.1705	144.135	2.7499E-05	1.2592E-04	1.6474E-03	.3976
820	.1723	130.073	2.2500E-05	1.2800E-04	1.8672E-03	.4239
910	.1739	117.208	1.7777E-05	1.2437E-04	2.0118E-03	.4499
1010	.1751	105.604	1.2000E-05	1.0340E-04	1.8563E-03	.4715
1100	.1764	96.963	1.4444E-05	1.5045E-04	2.9710E-03	.4972
1200	.1778	88.883	1.4E-05	1.7326E-04	3.7291E-03	.5274
1330	.1788	80.195	7.6923E-06	1.1510E-04	2.7230E-03	.5511

1460	.1802	73.054	1.0769E-05	1.9605E-04	5.1173E-03	.5877
1590	.1812	67.081	7.6923E-06	1.6741E-04	4.7787E-03	.6163
1730	.1821	61.653	6.4285E-06	1.6578E-04	5.1513E-03	.6443
1860	.1829	57.344	6.1538E-06	1.8565E-04	6.2406E-03	.6712
1960	.1837	54.418	7.9999E-06	2.7343E-04	9.7863E-03	.6999
2080	.1842	51.278	4.1666E-06	1.5925E-04	6.0270E-03	.7188
2190	.1846	48.703	3.6363E-06	1.5530E-04	6.2131E-03	.7348
2290	.185	46.576	4.0000E-06	1.8807E-04	7.8958E-03	.7516
2410	.1854	44.257	3.3333E-06	1.7247E-04	7.5952E-03	.7693
2640	.1866	40.401	5.2173E-06	3.1122E-04	.0147	.8261
2880	.1876	37.034	4.1666E-06	2.9701E-04	.0153	.8778
3110	.1886	34.295	4.3478E-06	3.6510E-04	.0204	.9340
3360	.1894	31.744	3.1999E-06	3.1350E-04	.0189	.9825
3600	.1903	29.627	3.7500E-06	4.2527E-04	.0277	1.0412
3840	.1916	27.776	5.4166E-06	7.0204E-04	.0489	1.1319
4090	.1921	26.078	1.9999E-06	2.9449E-04	.0218	1.1691
4340	.1929	24.576	3.2000E-06	5.3255E-04	.0420	1.2323
4600	.1936	23.187	2.6923E-06	5.0393E-04	.0422	1.2910
4850	.1946	21.991	3.9999E-06	8.3667E-04	.0740	1.3796
5280	.196	20.2	3.2558E-06	7.8168E-04	.0741	1.5125
5700	.1971	18.712	2.6190E-06	7.3901E-04	.0759	1.6258
6150	.1986	17.343	3.3333E-06	1.0955E-03	.1215	1.7924
6590	.2	16.185	3.1818E-06	1.2090E-03	.1442	1.9596
7040	.2013	15.15	2.8888E-06	1.2565E-03	.1604	2.1257
7500	.2026	14.221	2.8260E-06	1.3990E-03	.1905	2.3029
7960	.2037	13.399	2.3913E-06	1.3384E-03	.1938	2.4624
8440	.2054	12.637	3.5416E-06	2.2308E-03	.3427	2.7237
8920	.2068	11.957	2.9166E-06	2.0586E-03	.3348	2.9516
9410	.2079	11.334	2.2448E-06	1.7666E-03	.3033	3.1406
9850	.2088	10.828	2.0454E-06	1.7775E-03	.3208	3.3031
10310	.2102	10.345	3.0434E-06	2.8977E-03	.5474	3.5677
10770	.2112	9.903	2.1739E-06	2.2631E-03	.4470	3.7653
11220	.2122	9.506	2.2222E-06	2.5176E-03	.5188	3.9715
11660	.2133	9.147	2.4999E-06	3.0664E-03	.6575	4.2074
12100	.2145	8.814	2.7272E-06	3.6075E-03	.8033	4.4748
12550	.2156	8.498	2.4444E-06	3.4802E-03	.8040	4.7290
13000	.2162	8.204	1.3333E-06	2.0395E-03	.4884	4.8727
13450	.2178	7.93	3.5555E-06	5.8286E-03	1.4450	5.2694
13900	.2188	7.673	2.2222E-06	3.8951E-03	.9985	5.5258
14380	.2198	7.417	2.0833E-06	3.9041E-03	1.0348	5.7910
14830	.2213	7.192	3.3333E-06	6.6646E-03	1.8247	6.2017
15300	.2222	6.971	1.9148E-06	4.0735E-03	1.1504	6.4559
15770	.2231	6.763	1.9148E-06	4.3317E-03	1.2615	6.7181
16240	.2243	6.567	2.5531E-06	6.1305E-03	1.8394	7.0782
16710	.2257	6.383	2.9787E-06	7.5786E-03	2.3407	7.5107
17190	.227	6.204	2.7083E-06	7.2937E-03	2.3177	7.9238
17680	.2284	6.032	2.8571E-06	8.1412E-03	2.6610	8.3815
18160	.2297	5.873	2.7083E-06	8.1526E-03	2.7389	8.8183
18610	.2312	5.731	3.3333E-06	.0105	3.6405	9.3354
19070	.2326	5.593	3.0434E-06	.0101	3.5769	9.8299
19530	.2344	5.461	3.9130E-06	.0136	4.9441	10.4813
19980	.2361	5.338	3.7777E-06	.0138	5.1189	11.1110
20450	.2381	5.215	4.2553E-06	.0163	6.1782	11.8691
20930	.2406	5.096	5.2083E-06	.0209	8.1075	12.8389
21410	.2435	4.981	6.0416E-06	.0253	10.0747	13.9900
21900	.247	4.87	7.1428E-06	.0314	12.7485	15.4111
22370	.2512	4.768	8.9361E-06	.0410	17.0340	17.1543
22810	.2563	4.676	1.1590E-05	.0554	23.4860	19.3144
23300	.2627	4.577	1.3061E-05	.0650	28.1324	22.0810
23770	.2707	4.487	1.7021E-05	.0883	39.0009	25.6113
24250	.2793	4.398	1.7916E-05	.0968	43.5886	29.4829
24720	.2892	4.314	2.1063E-05	.1183	54.3481	34.0279
25800	.3152	4.134	2.4074E-05	.1439	68.1521	46.3422
26870	.3454	3.969	2.8224E-05	.1834	90.5506	61.2544
27930	.3771	3.818	2.9905E-05	.2104	108.0704	77.5402
28990	.4069	3.679	2.8113E-05	.2134	113.8519	93.4423

30150	.4325	3.537	2.2068E-05	.1808	100.2371	107.6359
31360	.456	3.401	1.9421E-05	.1721	99.2476	121.1873
32500	.473	3.281	1.4912E-05	.1424	85.2885	131.3650
33690	.487	3.166	1.1764E-05	.1207	74.9228	140.0524
34900	.4975	3.056	8.6776E-06	.0956	61.4968	146.8042
36140	.5065	2.951	7.2580E-06	.0858	57.1481	152.7982
37290	.5135	2.86	6.0869E-06	.0769	52.9351	157.6171
38460	.519	2.773	4.7008E-06	.0632	44.8801	161.5229
39650	.524	2.69	4.2016E-06	.0600	43.9823	165.1843
41700	.53	2.557	2.9268E-06	.0453	34.5824	169.7603
43800	.5345	2.435	2.1428E-06	.0366	29.3970	173.3673
45850	.538	2.326	1.7073E-06	.0321	27.0052	176.3090
48000	.541	2.222	1.3953E-06	.0287	25.3201	178.9485
50050	.5425	2.131	7.3170E-07	.0164	15.1438	180.3273
52100	.544	2.047	7.3170E-07	.0178	17.1253	181.7638
54150	.545	1.969	4.8780E-07	.0129	12.8483	182.7599
56200	.5465	1.897	7.3170E-07	.0208	21.5919	184.3117
58350	.547	1.828	2.3255E-07	7.1500E-03	7.6762	184.8486

VOL(DISTR.CURVE)= .547 AREA(DISTR.CURVE)= 184.789735

SURFACE AREA= 309.525609 SQ.M/ G
MEAN PORE RADIUS(VOLUME)= 28.8463046
MEAN PORE RADIUS(AREA)= 3.75215878
MEDIAN PORE RADIUS(VOLUME)= 4.45825115
MEDIAN PORE RADIUS(AREA)= 3.68839701
MACROPORE VOL = .318388651 ML./G (30-5333NM)
MESOPORE VOL = .597552407 ML/G (1.8-30NM)

CAT 214 14/10/91
VOL/LOGR DISTRIBUTION
MAX= 2 MIN= 0 PRESS.MIN= 20 PSI

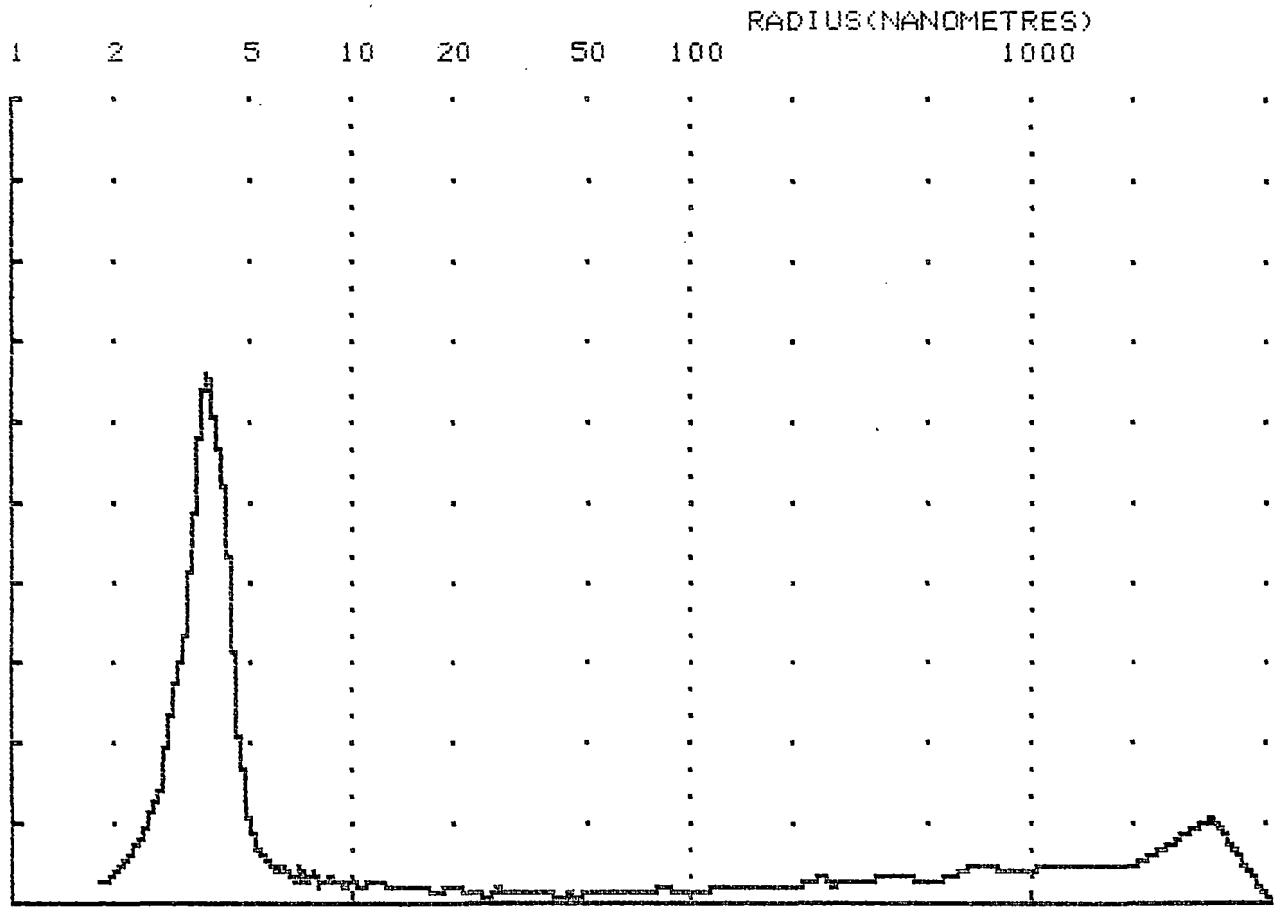

APPENDIX M. TYPICAL RESULTS OBTAINED DURING NITROGEN BJH ADSORPTION/DESORPTION ANALYSIS.

ASAP 2000 V2.01

SAMPLE DIRECTORY/NUMBER: DATA2 /230
SAMPLE ID: SM19
SUBMITTER: GC
OPERATOR: GC
UNIT NUMBER: 1
ANALYSIS GAS: Nitrogen

START 21:05:45 04/07/93
COMPL 01:24:34 04/08/93
REPRT 12:14:58 09/02/93
SAMPLE WT: 0.6448 g
FREE SPACE: 53.8666 cc
EQUIL INTRVL: 5 sec

ANALYSIS LOG

RELATIVE PRESSURE	PRESSURE (mmHg)	VOL ADSORBED (cc/g STP)	ELAPSED TIME (HR:MN)	SATURATION PRESS. (mmHg)
			0:29	647.265
0.0097	6.309	4.4858	0:37	
0.0328	21.203	5.3143	0:40	
0.0640	41.424	5.8910	0:42	
0.0886	57.352	6.2431	0:44	
0.1118	72.349	6.5443	0:45	
0.1350	87.398	6.8322	0:47	
0.1581	102.344	7.0947	0:49	
0.1802	116.669	7.3500	0:50	
0.2188	141.596	7.7742	0:52	
0.2678	173.349	8.3225	0:54	
0.3626	234.683	9.4308	0:58	
0.4603	297.930	10.7437	1:01	
0.5563	360.092	12.4280	1:05	
0.6490	420.133	14.8507	1:10	
0.7490	484.880	19.4104	1:20	
0.8045	520.770	24.4769	1:33	
0.8381	542.542	30.2749	1:48	
0.8718	564.417	39.4303	2:08	
0.9040	585.259	45.0992	2:22	
0.9320	603.411	46.6726	2:26	
0.9546	617.994	47.4487	2:30	
			2:31	647.420
0.9763	632.061	48.5038	2:35	
0.9888	640.180	49.6197	2:39	
0.9974	645.714	51.3367	2:45	
0.9743	630.768	50.3194	2:48	
0.9660	625.389	49.5298	2:52	
0.9575	619.908	48.8975	2:55	
0.9480	613.754	48.4074	2:58	
0.9363	606.203	47.9551	3:01	
0.9227	597.360	47.5378	3:03	
0.9034	584.897	47.1080	3:06	
0.8747	566.279	46.5921	3:08	
0.8395	543.525	45.9947	3:11	
0.8044	520.770	44.7875	3:16	
0.7424	480.639	23.2585	3:54	
0.5933	384.087	14.1152	4:03	
0.4740	306.877	11.2506	4:07	
0.4019	260.230	10.0322	4:11	
0.3257	210.842	9.0317	4:14	
0.2439	157.938	8.0660	4:17	
0.1425	92.260	6.8974	4:19	

ISOTHERM PLOT
+ ads, * des

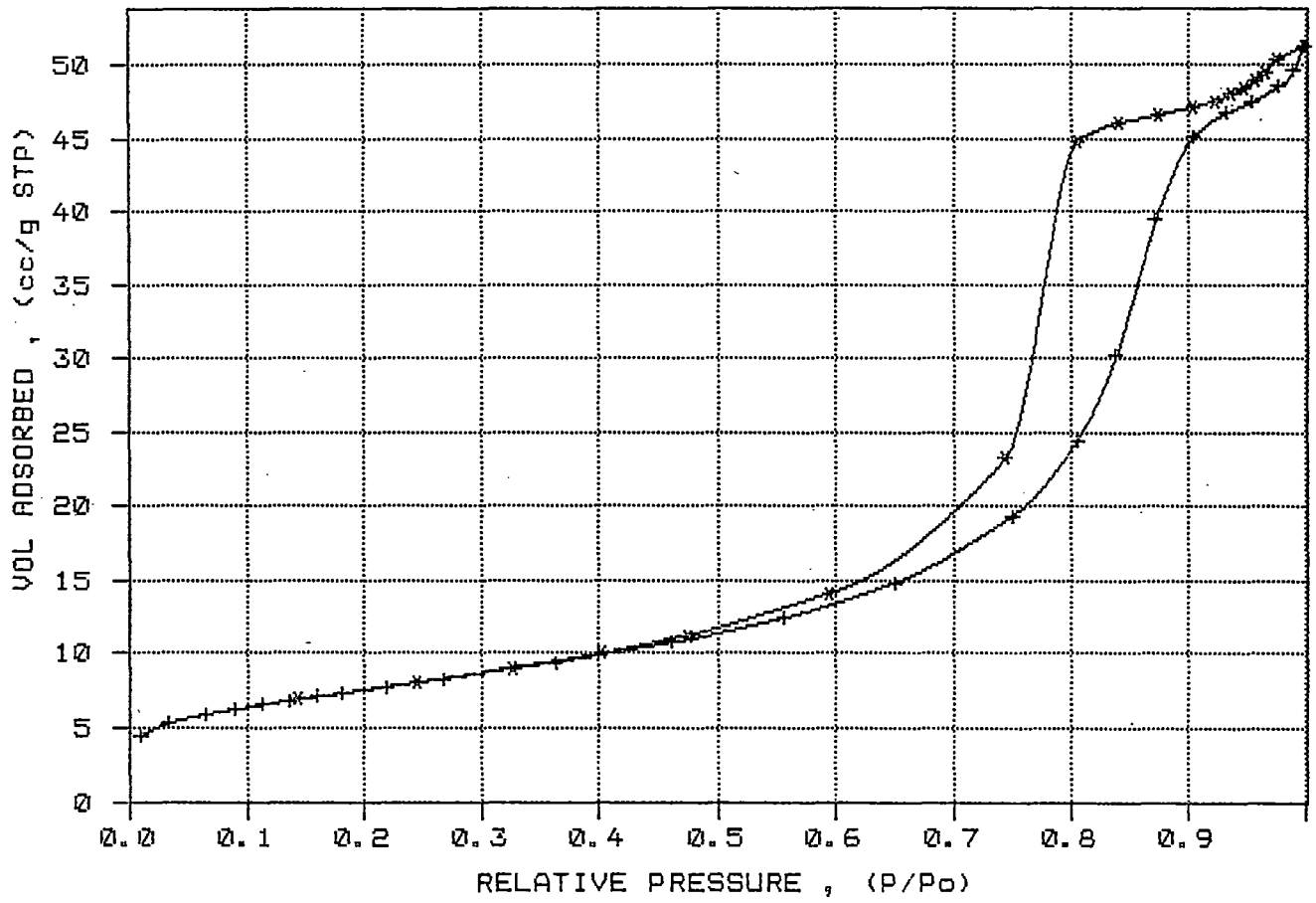

BET SURFACE AREA REPORT

BET SURFACE AREA:	27.3820	+/-	0.0596	sq. m/g
SLOPE:	0.157404	+/-	0.000342	
Y-INTERCEPT:	0.001576	+/-	0.000051	
C:	100.864426			
VM:	6.290086	cc/g STP		
CORRELATION COEFFICIENT:	9.99993E-01			

RELATIVE PRESSURE	VOL ADSORBED (cc/g STP)	1/ [VA(Po/P - 1)]
0.0640	5.8910	0.011606
0.0886	6.2431	0.015572
0.1350	6.8322	0.022847
0.1802	7.3500	0.029914
0.2188	7.7742	0.036017

BET PLOT

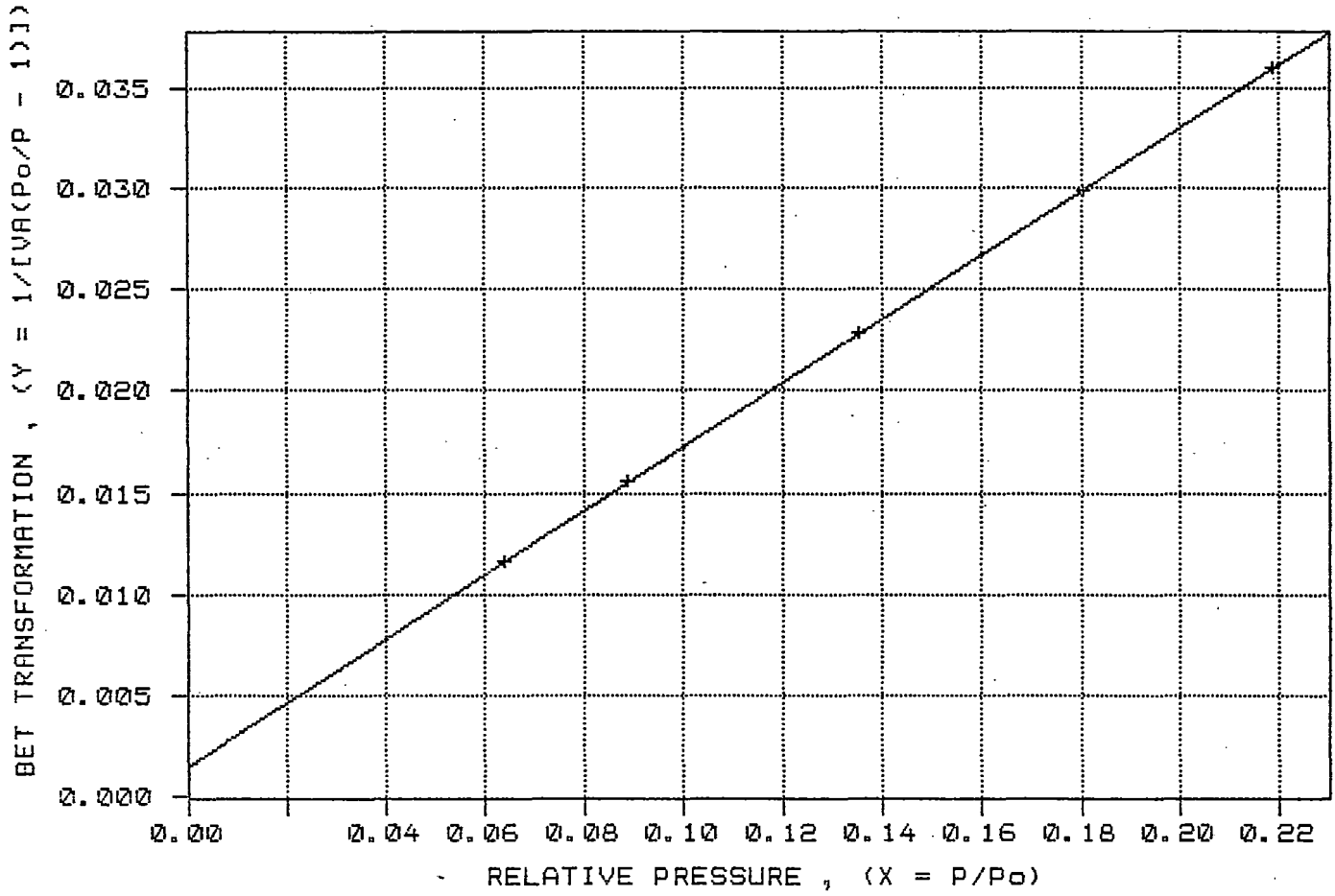

MICROPORE ANALYSIS REPORT

MICROPORE VOLUME:	0.000165	cc/g	
MICROPORE AREA:	0.9498	sq. m/g	
EXTERNAL SURFACE AREA:	26.4322	sq. m/g	
SLOPE:	1.708829	+/-	0.005236
Y-INTERCEPT:	0.106581	+/-	0.021727
CORRELATION COEFFICIENT:	9.99977E-01		

RELATIVE PRESSURE	STATISTICAL THICKNESS, (A)	VOL ADSORBED (cc/g STP)
0.0097	2.615	4.4858
0.0328	3.035	5.3143
0.0640	3.375	5.8910
0.0886	3.588	6.2431
0.1118	3.767	6.5443
0.1350	3.935	6.8322
0.1581	4.093	7.0947
0.1802	4.240	7.3500
0.2188	4.490	7.7742
0.2678	4.804	8.3225
0.3626	5.429	9.4308
0.4603	6.141	10.7437
0.5563	6.961	12.4280
0.6490	7.943	14.8507

THICKNESS VALUES USED IN THE LEAST-SQUARES ANALYSIS
WERE BETWEEN 3.500 AND 5.000 A .

$$t = \left[\frac{13.9900}{0.0340 - \log(P/Po)} \right]^{0.500}$$

SURFACE AREA CORRECTION FACTOR IS 1.000.

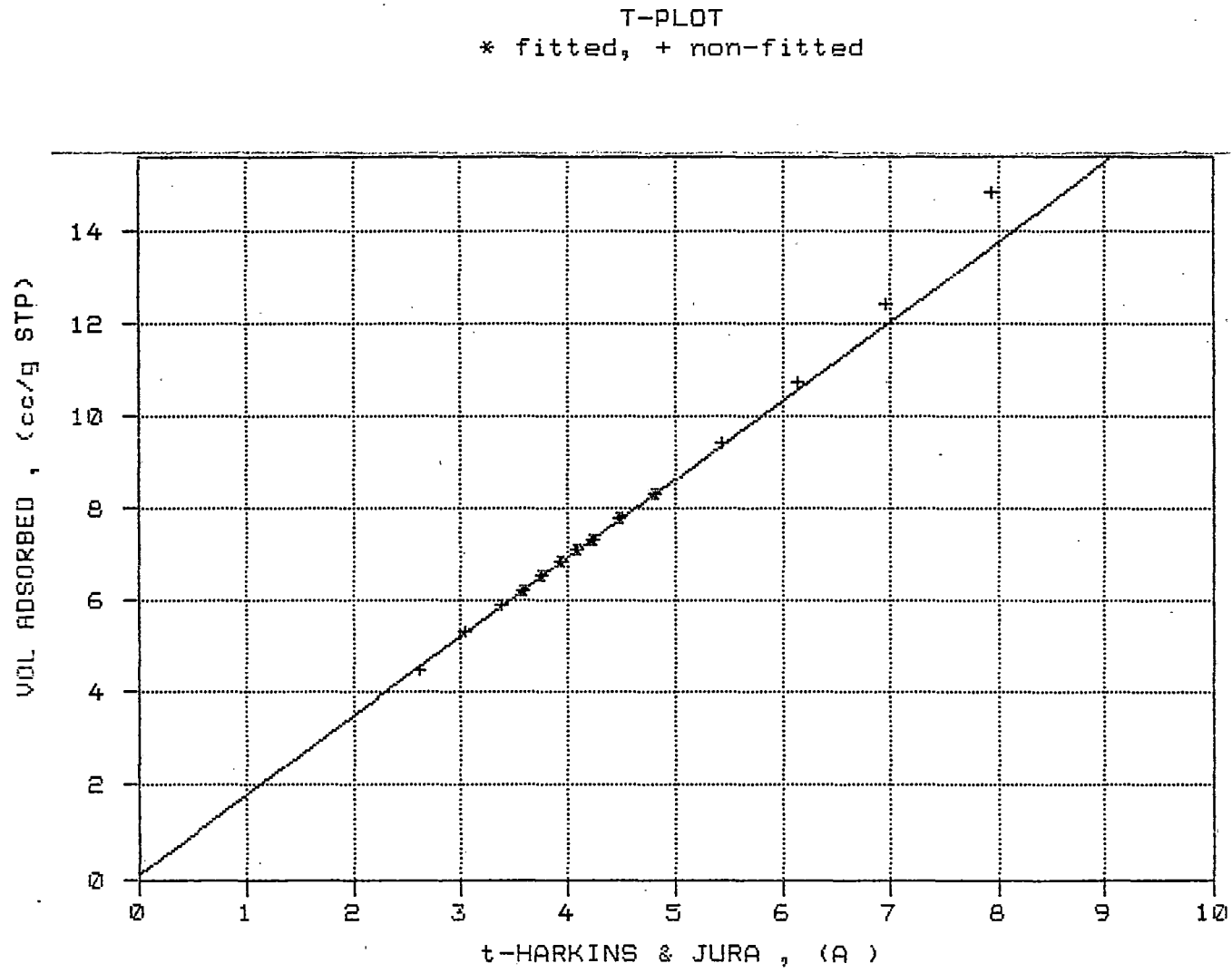

BJH ADSORPTION PORE DISTRIBUTION REPORT

PORE DIAMETER RANGE (A)	AVERAGE DIAMETER (A)	INCREMENTAL PORE VOLUME (cc/g)	CUMULATIVE PORE VOLUME (cc/g)	INCREMENTAL PORE AREA (sq. m/g)	CUMULATIVE PORE AREA (sq. m/g)
7306.2- 1746.5	2037.9	0.002796	0.002796	0.055	0.055
1746.5- 833.5	998.3	0.001837	0.004633	0.074	0.128
833.5- 441.1	524.0	0.001788	0.006421	0.136	0.265
441.1- 297.8	341.5	0.001351	0.007772	0.158	0.423
297.8- 212.6	240.6	0.002914	0.010685	0.484	0.908
212.6- 160.2	178.6	0.011153	0.021838	2.497	3.405
160.2- 127.2	139.6	0.018681	0.040520	5.351	8.756
127.2- 105.5	114.1	0.011822	0.052341	4.143	12.899
105.5- 82.0	90.5	0.010060	0.062401	4.444	17.343
82.0- 57.9	65.4	0.008505	0.070906	5.203	22.546
57.9- 44.7	49.4	0.003930	0.074836	3.184	25.730
44.7- 35.5	38.9	0.002248	0.077084	2.313	28.043
35.5- 28.6	31.2	0.001393	0.078477	1.788	29.832
28.6- 23.3	25.3	0.000954	0.079431	1.509	31.341
23.3- 18.0	19.8	0.000761	0.080192	1.539	32.880

dV/dlog(D) ADSORPTION PORE VOLUME PLOT

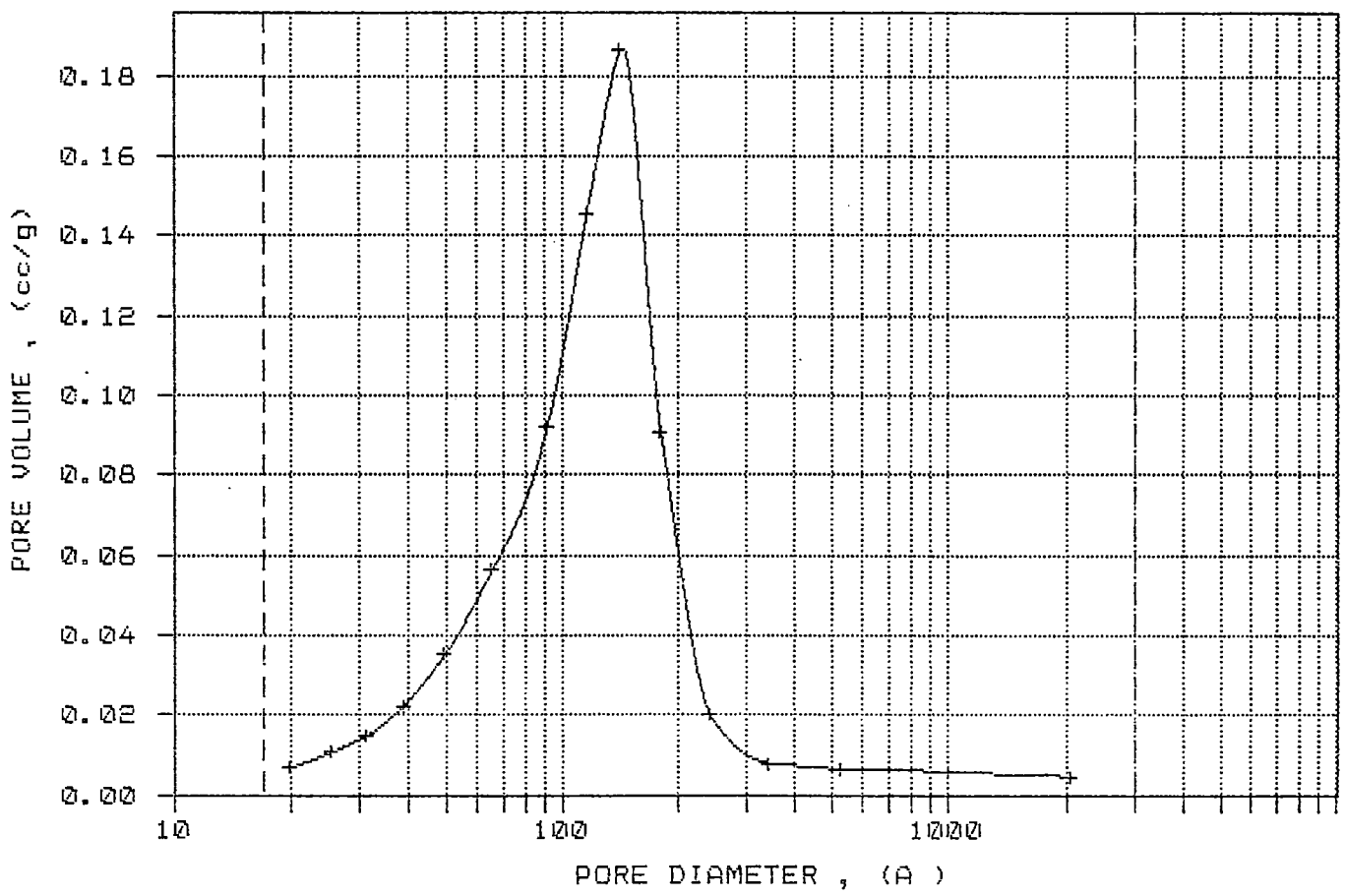

BJH DESORPTION PORE DISTRIBUTION REPORT

PORE DIAMETER RANGE (A)	AVERAGE DIAMETER (A)	INCREMENTAL PORE VOLUME (cc/g)	CUMULATIVE PORE VOLUME (cc/g)	INCREMENTAL PORE AREA (sq. m/g)	CUMULATIVE PORE AREA (sq. m/g)
768.2- 583.6	650.4	0.001356	0.001356	0.083	0.083
583.6- 469.3	513.7	0.001093	0.002448	0.085	0.168
469.3- 385.0	418.6	0.000850	0.003298	0.081	0.250
385.0- 315.7	343.2	0.000789	0.004087	0.092	0.342
315.7- 260.8	282.8	0.000733	0.004820	0.104	0.445
260.8- 209.5	229.4	0.000759	0.005579	0.132	0.578
209.5- 161.9	179.4	0.000928	0.006506	0.207	0.785
161.9- 126.5	139.7	0.001113	0.007620	0.319	1.103
126.5- 103.6	112.6	0.002435	0.010055	0.865	1.968
103.6- 78.1	87.0	0.047134	0.057188	21.670	23.638
78.1- 47.5	55.1	0.017156	0.074344	12.453	36.092
47.5- 34.8	39.0	0.003109	0.077454	3.187	39.278
34.8- 29.3	31.6	0.000777	0.078230	0.985	40.263
29.3- 24.6	26.5	0.000136	0.078367	0.206	40.468

dV/dlog(D) DESORPTION PORE VOLUME PLOT

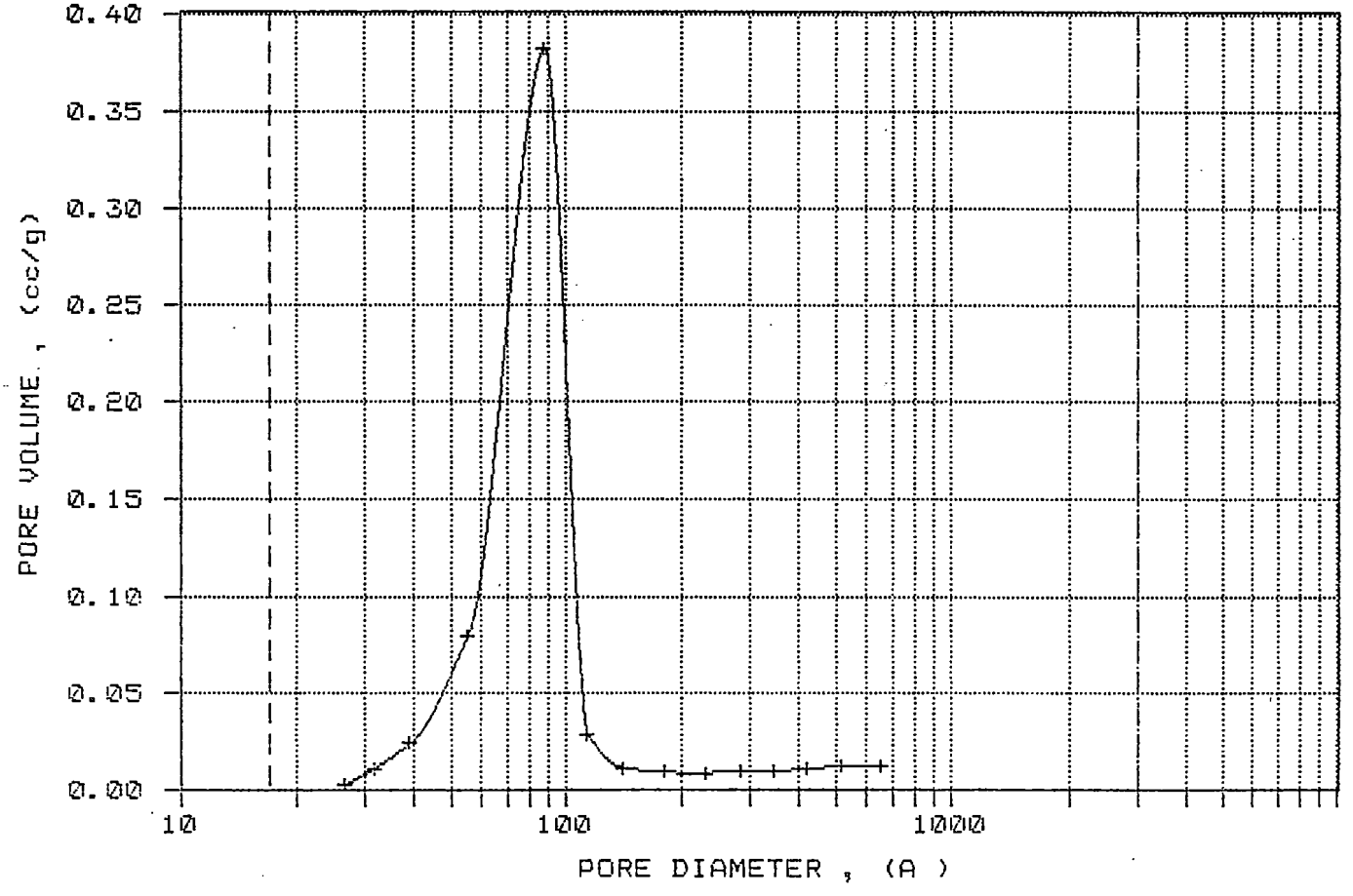

SUMMARY REPORT

AREA

BET SURFACE AREA:	27.3820	sq. m/g
SINGLE POINT SURFACE AREA AT P/Po 0.2188:	26.4395	sq. m/g
BJH CUMULATIVE ADSORPTION SURFACE AREA OF PORES BETWEEN 17.0000 AND 3000.0000 A DIAMETER:	32.8800	sq. m/g
BJH CUMULATIVE DESORPTION SURFACE AREA OF PORES BETWEEN 17.0000 AND 3000.0000 A DIAMETER:	40.4684	sq. m/g
MICROPORE AREA:	0.9498	sq. m/g

VOLUME

SINGLE POINT TOTAL PORE VOLUME OF PORES LESS THAN 1732.7573 A DIAMETER AT P/Po 0.9888:	0.076752	cc/g
BJH CUMULATIVE ADSORPTION PORE VOLUME OF PORES BETWEEN 17.0000 AND 3000.0000 A DIAMETER:	0.080192	cc/g
BJH CUMULATIVE DESORPTION PORE VOLUME OF PORES BETWEEN 17.0000 AND 3000.0000 A DIAMETER:	0.078367	cc/g
MICROPORE VOLUME:	0.000165	cc/g

PORE SIZE

AVERAGE PORE DIAMETER (4V/A BY BET):	112.1200	A
BJH ADSORPTION AVERAGE PORE DIAMETER (4V/A):	97.5571	A
BJH DESORPTION AVERAGE PORE DIAMETER (4V/A):	77.4597	A

APPENDIX N. TYPICAL RESULTS OBTAINED DURING CHEMISORPTION ANALYSIS.

Sample number: 4

Sample ID: GCSM19

Submitter ID: GC

Operator ID: GC

Report Title: Micromeritics Instrument Corporation

Sample wt: 0.6449 g

Type of data? automatically collected

Element	Description	Atomic Weight	Atomic Cross Sect Area (sq nm)	Stoich. Factor	% of Sample Weight
1) Pt	Platinum	195.090	0.0800	1.000	0.236

Run conditions set ID:

Fast evacuation? yes

Analysis temperature: 35.00 deg C
Analysis gas: Carbon Monoxide

Estimated free space: 18.0000 cc

Dose amount: 0.000 cc/g STP

Dose delay: 15 sec

Equil interval: 15 sec Pressure tolerance: 5.0 % 5.0
Repeat analysis? no mm Hg

Post analysis evac time: 15 min

Pressure table ID: GCTAB2

	Pressure	Vol Ads	Pressure	Vol Ads	Line Fit
1)	10.7572	0.3263	0.0000	0.0000	
2)	21.2037	0.5759	0.0000	0.0000	
3)	52.7498	1.3262	0.0000	0.0000	
4)	105.2405	2.5715	0.0000	0.0000	
5)	115.2215	2.8094	0.0000	0.0000	
6)	120.3413	2.9316	0.0000	0.0000	
7)	130.4258	3.1712	0.0000	0.0000	
8)	145.1645	3.5218	0.0000	0.0000	
9)	150.2843	3.6422	0.0000	0.0000	
10)	165.2299	3.9981	0.0000	0.0000	
11)	170.2463	4.1157	0.0000	0.0000	
12)	185.2437	4.4712	0.0000	0.0000	
13)	190.2083	4.5899	0.0000	0.0000	
14)	200.3444	4.8316	0.0000	0.0000	
15)	210.2220	5.0663	0.0000	0.0000	
16)	225.3745	5.4234	0.0000	0.0000	
17)	235.4589	5.6602	0.0000	0.0000	
18)	245.1813	5.8915	0.0000	0.0000	
19)	250.3011	6.0157	0.0000	0.0000	
20)	260.3338	6.2519	0.0000	0.0000	
21)	275.2278	6.6031	0.0000	0.0000	

22)	285.2087	6.8416	0.0000	0.0000	
23)	290.2251	6.9601	0.0000	0.0000	
24)	305.3259	7.3155	0.0000	0.0000	
25)	325.2879	7.7893	0.0000	0.0000	
26)	340.2852	8.1430	0.0000	0.0000	
27)	365.2119	8.7329	0.0000	0.0000	
28)	385.3807	9.2090	0.0000	0.0000	
29)	405.2910	9.6796	0.0000	0.0000	
30)	425.2530	10.1503	0.0000	0.0000	
31)	445.2667	10.6230	0.0000	0.0000	
32)	465.1769	11.0970	0.0000	0.0000	
33)	480.1743	11.4520	0.0000	0.0000	
34)	505.2043	12.0453	0.0000	0.0000	*
35)	520.2017	12.4016	0.0000	0.0000	*
36)	540.2154	12.8756	0.0000	0.0000	*
37)	565.1937	13.4659	0.0000	0.0000	*
38)	585.2075	13.9384	0.0000	0.0000	*
39)	605.1694	14.4108	0.0000	0.0000	*
40)	635.1641	15.1187	0.0000	0.0000	*
41)	665.2106	15.8282	0.0000	0.0000	*
42)	705.1863	16.7732	0.0000	0.0000	*

ANALYSIS DATA

PRESSURE (mmHg)	VOL ADSORBED (cc/g STP)	ELAPSED TIME (HR:MN)
10.7572	0.1132	0:09
21.7783	0.1189	0:13
53.5813	0.1308	0:16
104.1709	0.1455	0:19
115.4545	0.1501	0:23
121.3344	0.1526	0:26
130.2066	0.1560	0:30
145.8726	0.1616	0:33
145.4189	0.1615	0:36
168.1983	0.1678	0:40
164.7792	0.1670	0:43
179.8147	0.1707	0:46
189.2323	0.1736	0:50
203.9932	0.1783	0:53
219.3886	0.1816	0:56
222.5204	0.1821	1:00
217.7154	0.1812	1:03
237.0595	0.1850	1:07
260.1094	0.1906	1:10
260.1524	0.1906	1:13
263.9173	0.1915	1:17
289.3482	0.1970	1:20
292.8612	0.1977	1:23
291.8864	0.1975	1:27
328.7380	0.2035	1:30
335.4605	0.2044	1:34
369.3328	0.2091	1:37
385.6729	0.2112	1:40
409.8629	0.2141	1:44
418.1022	0.2151	1:47
435.6323	0.2176	1:50
467.5656	0.2256	1:54
479.7367	0.2287	1:57
504.0434	0.2349	2:01
522.2055	0.2399	2:04
543.8272	0.2443	2:08
567.0247	0.2478	2:11
581.2471	0.2498	2:14
611.2855	0.2536	2:18

ANALYSIS DATA

PRESSURE (mmHg)	VOL ADSORBED (cc/g STP)	ELAPSED TIME (HR:MN)
634.0444	0.2563	2:21
661.8911	0.2596	2:25
705.1860	0.2657	2:28

ISOTHERM PLOT
* first analysis data point
o repeat analysis data point

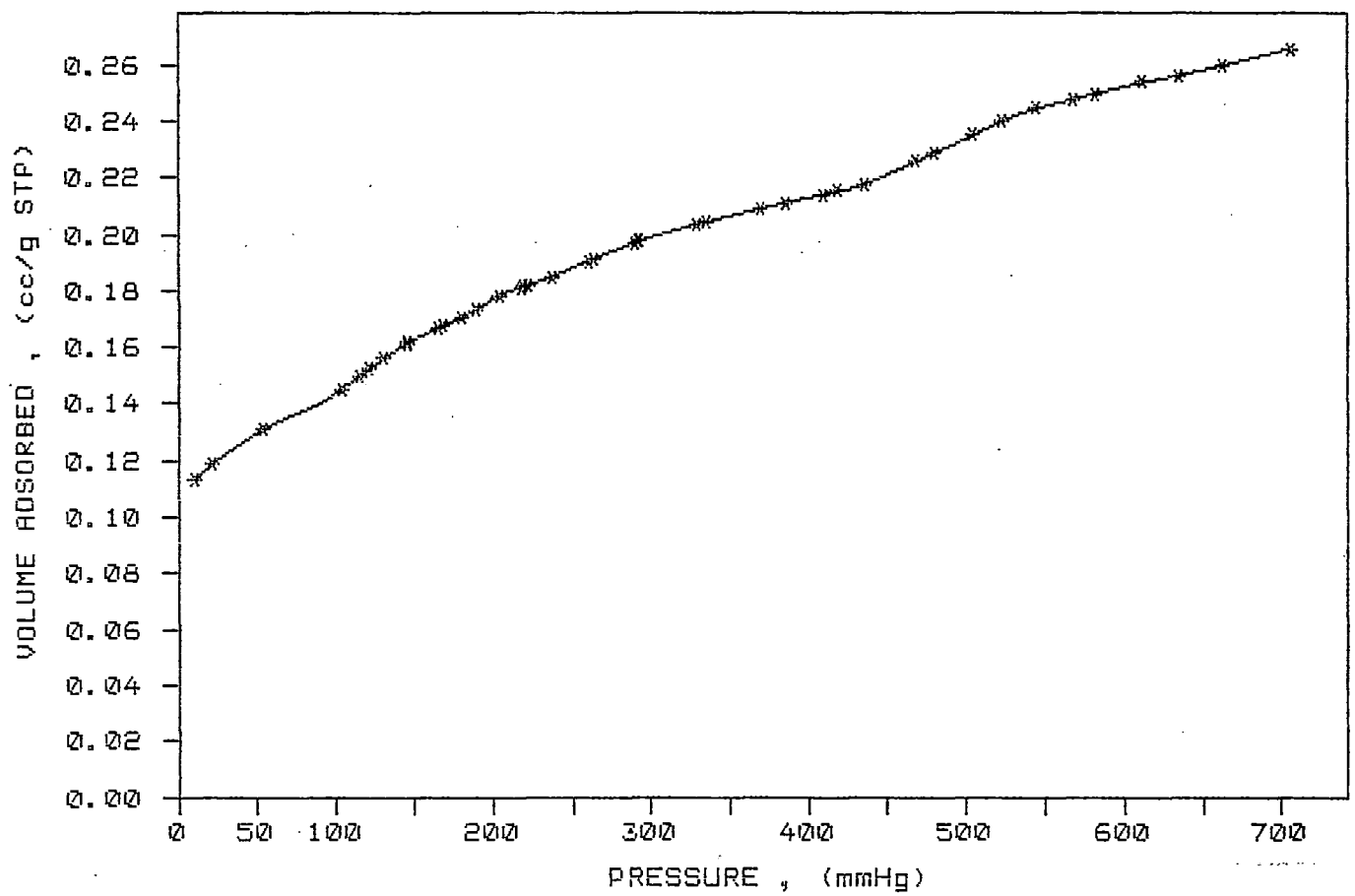

ANALYSIS REPORT

ELEMENT	% OF SAMPLE WEIGHT	ATOMIC WEIGHT	STOICHIOMETRY FACTOR	ATOMIC CROSS SECT AREA (sq nm)
Platinum	0.236	195.090	1.000	0.0800

ANALYSIS RESULTS

METAL DISPERSION:	60.5184 %	
METALLIC SURFACE AREA:	0.3532 sq m/g	
Y-INTERCEPT VOLUME ADSORBED:	0.164299 +/- 0.004232	cc/g STP
SLOPE:	0.000145 +/- 0.000007	
CORRELATION COEFFICIENT:	9.91705E-01	

ANALYSIS ISOTHERM

PRESSURE (mmHg)	VOL ADSORBED (cc/g STP)
10.7572	0.1132
21.7783	0.1189
53.5813	0.1308
104.1709	0.1455
115.4545	0.1501
121.3344	0.1526
130.2066	0.1560
145.8726	0.1616
145.4189	0.1615
168.1983	0.1678
164.7792	0.1670
179.8147	0.1707
189.2323	0.1736
203.9932	0.1783
219.3886	0.1816
222.5204	0.1821
217.7154	0.1812
237.0595	0.1850
260.1094	0.1906
260.1524	0.1906
263.9173	0.1915
289.3482	0.1970
292.8612	0.1977
291.8864	0.1975
328.7380	0.2035
335.4605	0.2044
369.3328	0.2091
385.6729	0.2112
409.8629	0.2141
418.1022	0.2151
435.6323	0.2176
467.5656	0.2256
479.7367	0.2287
504.0434	0.2349*
522.2055	0.2399*
543.8272	0.2443*
567.0247	0.2478*
581.2471	0.2498*
611.2855	0.2536*
634.0444	0.2563*
661.8911	0.2596*
705.1860	0.2657*

* included in calculation of line fit and difference data

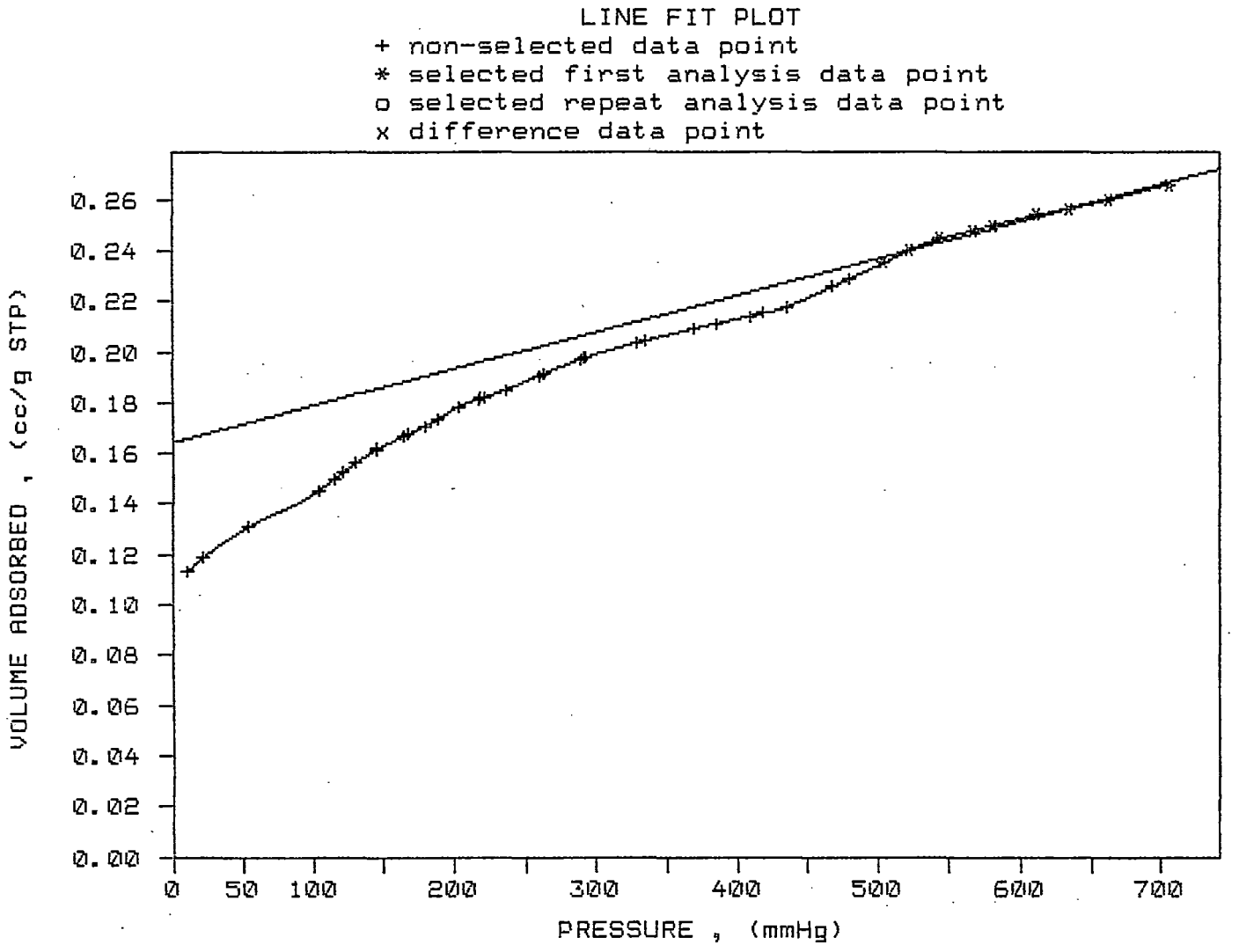
LINE FIT PLOT
+ non-selected data point
* selected first analysis data point
o selected repeat analysis data point
x difference data point
VOLUME ADSORBED , (cc/g STP)
0.26
0.24
0.22
0.20
0.18
0.16
0.14
0.12
0.10
0.08
0.06
0.04
0.02
0.00
0
50
100
200
300
400
500
600
700
PRESSURE , (mmHg)

APPENDIX O. SURFACE AND CO ACTIVITY PROPERTIES OF STANDARD COMMERCIAL EXHAUST CATALYST

Table O.1 Surface and CO activity properties of standard commercial exhaust catalyst.

Wash coat loading (%)	31
BET N_2 surface area (m^2/g)	14.55
BJH N_2 total pore volume (cm^3/g)	0.06
BJH average pore size (nm)	10.6
Pt dispersion (%)	45
Pt surface area (m^2/g metal)	45
Average Pt crystallite size (nm)	6.2
Activation energy (General method, kJ/mol)	86.2-100.5
CO oxidation rate [mol CO/(s m^3 catalyst)]	0.30
Pt surface area (m^2Pt/g catalyst)	0.22
Specific rate (g mol CO/(s m^2Pt m^3catalyst)]	1.36